Seed development and carbohydrates

Peter E. Wittich

Promotor: dr. M.T.M. Willemse
hoogleraar in de plantkunde
Laboratorium Plantencytologie en -morfologie

Co-promotoren: dr. A.A.M. van Lammeren
universitair hoofddocent
Laboratorium Plantencytologie en -morfologie

dr. ir.C.J. Keijzer
universitair docent
Laboratorium Plantencytologie en -morfologie

Seed development and carbohydrates

Peter E. Wittich

Proefschrift

ter verkrijging van de graad van doctor
op gezag van de rector magnificus
van de Landbouwuniversiteit Wageningen,
dr. C.M. Karssen,
in het openbaar te verdedigen
op dinsdag 19 mei 1998
des namiddags te vier uur in de Aula.

CIP-DATA KONINKLIJKE BIBLIOTHEEK, DEN HAAG

Wittich, P.E.

Seed development and carbohydrates
P.E. Wittich. - [S.I.: s.n.] Fig., Tab.
Thesis Landbouwuniversiteit Wageningen, - with ref. - with summary in Dutch.
ISBN 90-5485-855-9

Keywords: carbohydrate distribution, *Gasteria verrucosa*, invertase, phytomelan, seed development, sucrose synthase, *Zea mays*

Cover: Cryo-scanning electron micrograph of 10% sucrose dissolved in millipore water. First, the solution was frozen in liquid nitrogen, followed by sublimation of the water.

CONTENTS

STELLINGEN

1. Koolhydraattransport kan niet gesimuleerd worden door het transport van kleurstoffen (dit proefschrift).
2. Enzymhistochemie als techniek om de activitieit van enzymen in weefsels aan te tonen kan leiden tot andere conclusies over de relatie tussen plaats en functie van enzymen dan immunocytochemie (dit proefschrift).
3. De activiteit van zowel sucrosesynthase als van invertase heeft diffusie van sucrose, glucose, fructose en UDP-glucose tot gevolg (dit proefschrift).
4. Een vast patroon van koolhydraatverdeling en een variabel moment van zaadverspreiding zijn goede parameters voor een zaadontwikkelingsmodel (dit proefschrift).
5. Callose bepaalt de vorm van het phytomelanblok in de epidermiscellen van de *Gasteria verrucosa* zaadhuid (dit proefschrift).
6. De synthese van phytomelaneenheden vindt plaats aan het oppervlak van bolletjes (dit proefschrift).
7. Digitale beeldverwerking werkt in de hand dat resultaten mooier gepresenteerd worden dan ze in werkelijkheid waren (niet in dit proefschrift).
8. De Landbouwuniversiteit Wageningen behoort tijdens de dagen dat studenten afstuderen op elk gebouw feestelijk de vlag uit te hangen.
9. Afbeeldingen op de tempels van Khajuraho (India) laten zien dat er duizend jaar geleden minder taboes waren dan heden ten dage.
10. Bij sporten waarbij de lichaamslengte van deelnemers een discriminerende rol speelt zouden er verschillende klassen gecreëerd moeten worden, zoals er gewichtsklassen zijn bij de kracht- en vechtsporten.
11. De Nederlandse voorkeursspelling bepaalt dat een onderzoeker die werkt aan *Zea mays* de puntjes op de i moet zetten.
12. Het is onjuist te concluderen dat bij een promotie zes jaar na aanvang van het promotieonderzoek, een AIO of OIO twee jaar werkloos of werkeloos is geweest.

Stellingen behorende bij het proefschrift 'Seed development and carbohydrates'.

Peter E. Wittich
Wageningen, 19 mei 1998

Chapter

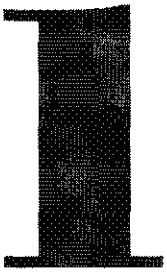

Seed development and carbohydrates: introduction

P.E. Wittich

Seeds and diaspores are the units to assure a next generation of seed plants. While plants invest energy to produce seeds, they follow various strategies in order to find a balance between the amount of energy which will be used for seed production, and successful offspring . These various strategies result in numerous types of seeds. Some species may develop seeds with large embryos, loaded with nutrients for the seedlings initial growth, while others produce seeds with an undifferentiated embryo and hardly any storage products.

Nutrients are required for the growth of seed and for storage product synthesis. Therefore the distribution and transport pathway of nutrients is closely related with the seed development strategy of a particular species. A plant may even use nutrient distribution to orchestrate its seed development. Sequential tissue development and polarity in the development of for instance the embryo, point to this direction. A more detailed knowledge on nutrient distribution in developing seeds is therefore necessary to understand the developmental biology of seeds. As a result this information may be very useful for plant breeders to enhance seed development of plants: for a better germination or a higher yield in storage products.

Carbohydrates are only one class of nutrients that is transported by the plant into the developing seeds. They are essential for cell metabolism, growth, and storage product synthesis. The present study is restricted to the distribution of sucrose and its breakdown products, since sucrose is the main carbohydrate transported into the seed of most plants.

OVULE AND SEED DEVELOPMENT

Two stages are important for seed development: ovule development (pre-fertilization), and seed development (post-fertilization). In both stages plants follow various pathways which influence the final seed structure.

Ovules develop from one or two sub-epidermal placental layers (Bouman 1984). The mature ovule consist of gametophytic tissue (embryo sac) and enveloping sporophytic tissues (raphe, funicle, chalaza, integument(s) and nucellus). The ovule will be supplied with nutrients via the funiculus, and remains attached to the placenta by it till the mature seed is ready for dispersal. Consequently, the differentiation of the sporophytic tissues will influence the development of the embryo sac, and after fertilization the further development of the embryo and endosperm.

The development of the female gametophyte, or embryo sac (including amongst others the egg cell), starts in the ovule. One of the ovular nucellar cells undergoes a meiotic division, resulting in four megaspores. Most often three of these haploid spores degenerate, while only one, the functional megaspore, undergoes further mitotic divisions, resulting in an embryo sac. The most common type of embryo sac development is the Polygonum type, which results in three antipodal cells, a central cell with two polar nuclei (which will fuse to form the diploid central cell nucleus), and the egg apparatus with two synergids, and a egg cell (Fig. 1) (Willemse and Van Went 1984).

The male gametophyte (or pollen grain) develops from the microspore mother cell in the anther. The microspore mother cell undergoes meiotic divisions and forms four haploid microspores. These cells are enclosed by a callose wall. After microspore mitosis the microgametophyte (pollen grain), is formed. The pollen grain consists of a vegetative and a generative cell. The generative cell divides into two sperm cells either in the pollen, or after germination in the pollen tube (Fig. 2) (Keijzer 1984, Knox 1984).

Figure 1: Development of the female gametophyte. **(a)** In an ovary one or more ovules can develop. The development of one ovule is follower here which shows a Polygonum type of embryo sac development. A megaspore mother cell **(b)** develops subsequently into **(c)** a tetrad (four megaspores), **(d)** a functional megaspore, **(e)** a two-nucleate, **(f)** a four-nucleate, **(g)** an eight-nucleate coenocytic cell, and finally into **(h)** an embryo sac. (Figure after Keijzer 1984)

Figure 2: Development of the male gametophyte. **(a)** Pollen develop in the locules of an anther. Cells of the sporogenous tissue develop into **(b)** a microspore mother cell which will form **(c)** a callosic wall, and give rise to **(d)** a tetrad (four microspores). These cells **(e)** form an exine and the callose dissolves. This results in **(f)** free microspores. In the microspores a vegetative and a generative cell **(g)** are formed, the latter migrating **(h)** from the pollen wall into the centre of the vegetative cell. In a few angiosperm families the generative cell divides into two sperm cells before pollen maturation, resulting in tricellular pollen grains. In the majority of families this division takes place after pollen germination, *i.e.* inside the pollen tube (Knox 1984). (Figure after Keijzer 1984)

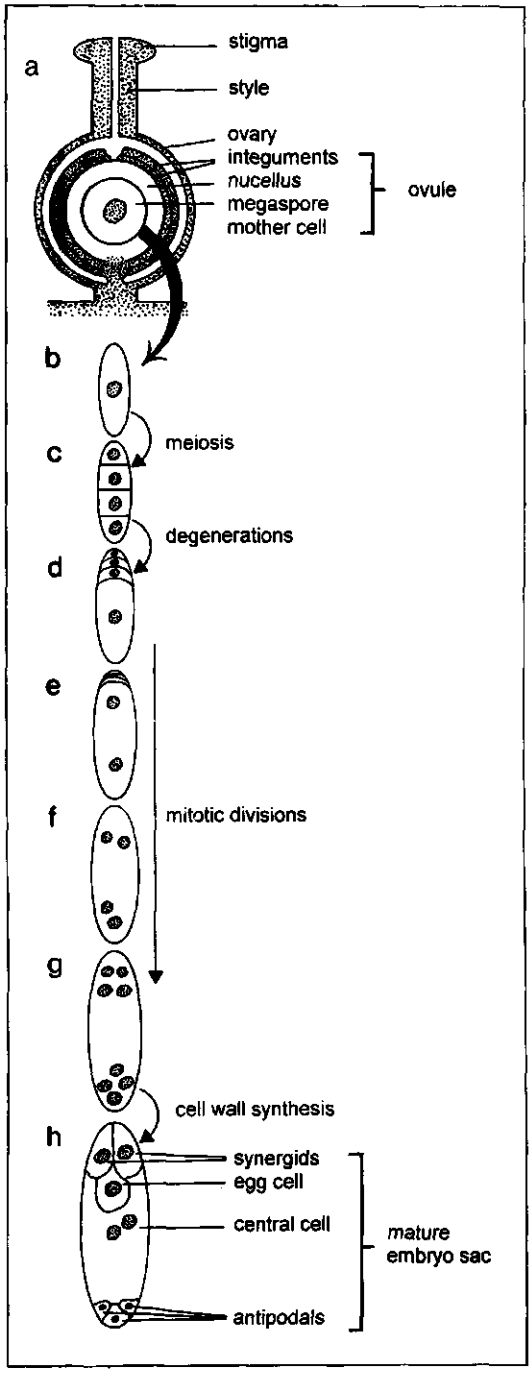

Figure 1

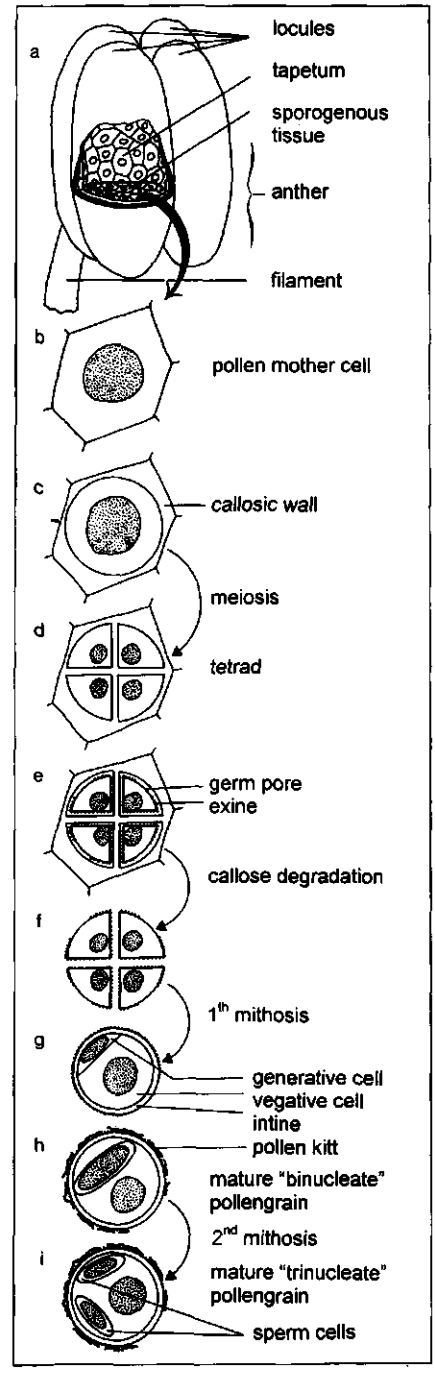

Figure 2

As a result of the meiotic origin, the haploid embryo sac in the ovule is genetically different from the enveloping sporophytic tissues. There are only some plasmodesmal contacts reported between the two plants, and these might be closed (Willemse and Van Went 1984). Consequently, the sporophyte nurses the developing gametophyte by supplying the needed nutrients via an apoplastic phase. During the development of pollen in the anther plasmodesmal contacts are only reported between sporophyte and microspore mother cells. The formation of the callose wall isolates the microspore mother cells, which become free from their nursing tissue (Bhandari 1984, Keijzer and Willemse 1988).

All angiosperms have double fertilization. This includes the fusion of the egg cell and one sperm cell to form the zygote, the start cell for the embryo, the new plant of the next generation. The second male sperm cell fuses with the central cell, and this results into a triploid central cell nucleus in the case of a Polygonum-type embryo sac. This cell gives rise to the endosperm, which can be considered as an organism (Favre-Duchartre 1984 and references herein). The endosperm often functions in the storage of nutrients, to be used by the embryo in a later stage during seed development or germination (Fig. 3). The sporophytic tissues supply the nutrients for these two organisms, the embryo and the endosperm, via an apoplastic phase (Thorne 1985). There is no symplastic contact between these organisms

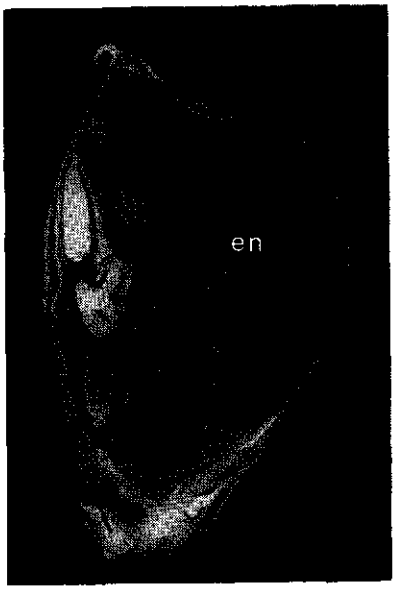

Figure 3. High concentration of stored starch in the endosperm (*en*) of the maize kernel, to be used by the embryo during germination. The embryo contains a lower amount of starch. Starch is stained (blue, here black) with IKI. (Mag.: 5.5 X)

CARBOHYDRATES DURING OVULE AND SEED DEVELOPMENT

Developing ovules and seeds are sinks; they show hardly any photosynthetic activity and are completely dependent on assimilates produced by the photosynthetic parts of the plant. Carbohydrates are transported symplastically via the phloem into the developing sporophytic ovule and seed tissues. They enter the apoplast between the sporophytic and gametophytic tissue by facilitated membrane transport, after which they are imported into the gametophytic tissue (Patrick 1997).

In most plants the main carbohydrate transported is sucrose, but also sorbitol and other hexoses are commonly found. The enzymes sucrose synthase and invertase break sucrose down into hexoses; sucrose synthase catalyzes the reversible reaction of sucrose and UDP into UDP-glucose and fructose, while invertase catalyzes the reaction of sucrose into glucose and fructose. These carbohydrates are used for respiration, cell wall synthesis, and storage (Amor *et al.* 1995, Chourey and Nelson 1976, Xu *et al.* 1989), but are also known to influence the regulation of genes (Xu *et al.* 1996) and the rate of cell divisions (Weber *et al.* 1997). Taking these functions of carbohydrates into consideration, it seems very important how the

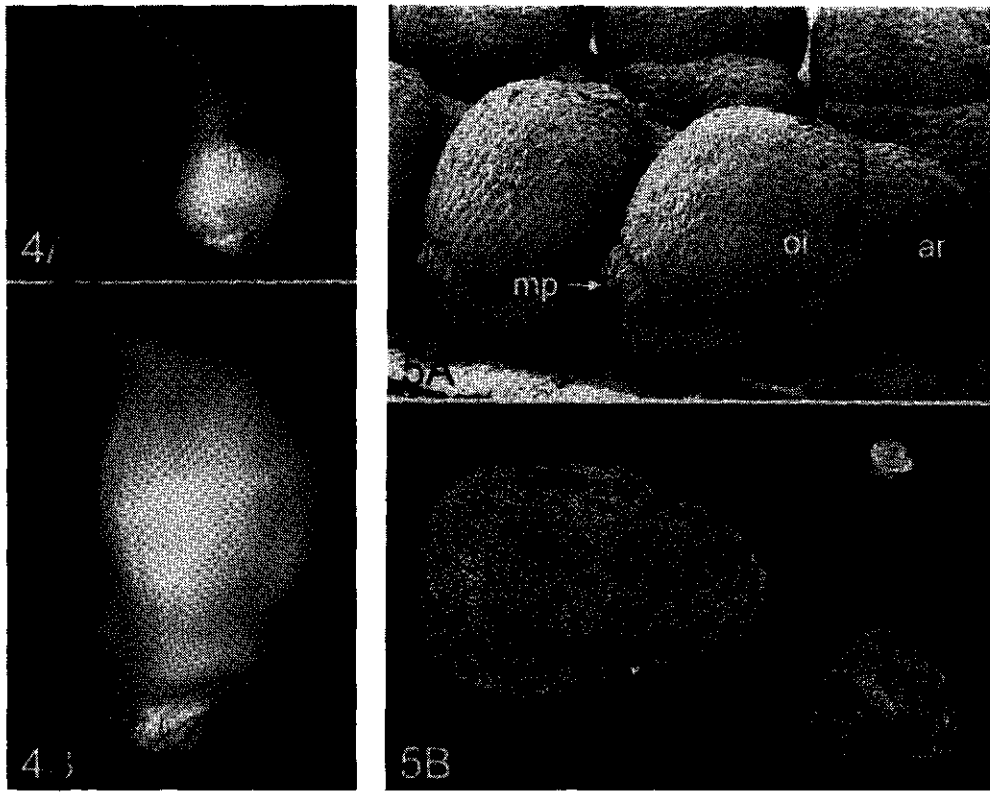

Figure 4. Maize ovary and seed. (Mag.: 4.7 X) **(A)** The ovary with mature ovule, ready for fertilization. **(B)** The seed, just before dehydration.

Figure 5. *Gasteria* ovule and seed. (Mag.: 100 X) **(A)** Ovules on the placenta (scanning electron microscopy). The inner integument forms the micropyle (*mp*), and is further enveloped by the outer integument (*oi*). An arillus (*ar*) grows from the basal part of the ovule. **(B)** The seed (Mag. 14 X). On the left a complete seed with the wing shaped arillus. On the lower right side a mature seed from which the arillus is removed manually. The surface is formed by the phytomelan layer. To give an impression of dimensions, in the upper right corner an ovule as in (A).

carbohydrates are supplied to the developing embryo sac, embryo, and endosperm by the sporophytic tissue, in other words, what kind of carbohydrates do these tissues receive, and does a polarity or a gradient exist in the pathway during the supply. Altering this transport during ovule and seed development might coincide with crucial changes in the development of embryo sac, embryo, or endosperm. Such correlations have already been demonstrated in the development in pea seeds, where apoplastic invertase hydrolyzes the sucrose only during the growth phase of the seed, while sucrose is directly imported into the seed during the storage phase (Weber *et al.* 1997).

The intention of the present study is to get a better perspective of the carbohydrate transport routes in developing ovules and seeds, and the possible consequences of changes in this transport for ovule and seed development.

PLANT MATERIAL

The study of carbohydrate distribution in developing seeds is performed on maize (*Zea mays* L.) and *Gasteria verrucosa* (Mill.) H. Duval. These plant species form different types of ovules and seeds, and are used in this study since they are expected to show different carbohydrate distribution pathways.

Maize forms anatropous crassinucellate ovules (Fig. 4A), and after fertilization endospermous seeds (kernels) (Fig. 4B). The central endosperm is mainly filled with starch, while the aleurone and sub-aleurone layers also store proteins.

Gasteria forms anatropous tenuinucellate ovules (Fig. 5A), and after fertilization also endospermous seeds (Fig. 5B). The endosperm stores lipids and proteins, and hardly any starch. Like the maize embryo, its embryo is monocotyledonous.

METHODS

To elucidate the relationships between development of the various regions of the seed and carbohydrate transport many techniques have been developed in the past (see also chapter 9). Dye tracers are used which show either apoplastic or symplastic transport, as well as radioactive labelled sugars which demonstrate the distribution of utilized and soluble carbohydrates. Inhibitors which block membrane transport are used in combination with the tracer techniques showing sites of membrane transport (Wang *et al.* 1995). More recent developments are NMR techniques to elucidate transport processes (Pope *et al.* 1993), and immunocytochemical methods to localize membrane transporters. In the near future the latter can be useful in combination with transgenic plants to prove the lack of these specific

transporters. Ultrastructural and histological studies may give indications about how the transport pathway can occur by showing the presence or absence of symplastic contacts (plasmodesmata), apoplastic barriers (cutin, lignin), or the presence of wall ingrowths (transfer walls, enhancing nutrient uptake capacity out of the apoplast). However, none of these techniques can show the actual transport of carbohydrates. Besides structural and histological analyses an additional approach is used in this study to collect circumstantial evidence for carbohydrate transport. Since the developing ovule and seed tissues are true sinks, and the strength of these sinks will influence the flow of carbohydrates over the various tissues, the sink strengths of cell and tissues can be used as indicators for the preferential direction of carbohydrate transport. The enzymes sucrose synthase and invertase are suggested to be indicators for sink strength by several authors, since sucrose has to be broken down into monosaccharides by sucrose synthase or invertase prior to further use (Ho *et al.* 1991, Sun *et al.* 1991). In maize and *Gasteria* the most common transported carbohydrate is sucrose, thus sucrose synthase and invertase activity can be used in combination with morphological data to deduce possible carbohydrate transport pathways.

EXPECTATIONS

The results of this study will give new insights in the distribution pattern of carbohydrates in maize and *Gasteria* ovules and seeds.

With the localization of sucrose synthase and invertase activity, possible carbohydrate transport pathways will be postulated. It is presumed that these enzymes play an important role in the diffusive carbohydrate transport by enhancing the diffusion gradients in the developing seeds.

Special attention will be given to the carbohydrate dependent development of phytomelan in the seed coat of *Gasteria*. Phytomelan is a black, chemical resistant cell wall material of a polyphenolic composition, which forms a protective layer around the seed. The remarkable process of wall synthesis has never been studied thoroughly.

The distribution of carbohydrates in the ovules and seeds studied will result in a proposal for a general model in which angiosperm plants regulate their carbohydrate investment via a determined sequence of seed tissue development. Initially the plant invests carbohydrates in the seed coat, followed by investment in the endosperm, and finally in the embryo. The different strategies of seed development by the various plant families follow this sequence. However, depending upon their energy supply and dispersal strategy, the development of endosperm and embryo is hampered during the development. This results in seeds which differ in endosperm and embryo development.

REFERENCES

Amor Y, CH Haigler, S Johnson, M Wainscott and DP Delmer (1995) A membrane-associated form of sucrose synthase and its potential role in synthesis of cellulose and callose in plants. Proc Natl Acad Sci USA 92: 9353-9357

Bhandari (1984) The microsporangium. In: Johri BM (ed) Embryology of angiosperms. Springer-Verlag, Berlin: 53-121

Bouman F (1984) The ovule. In: Johri BM (ed) Embryology of angiosperms. Springer-Verlag, Berlin: 123-157

Chourey PS and OE Nelson (1976) The enzyme deficiency conditioned by the *shrunken-1* mutations in maize. Biochem Genet 14: 1041-1055

Ho LC, A Lecharny and J Willenbrink (1991) Sucrose cleavage in relation to import and metabolism of sugars in sink organs. In: Bonnemain JL, S Delrot, WJ Lucas and J Dainty (eds) Recent advances in phloem transport and assimilate compartmentation. Ouest editions, Nantes: 178-186

Keijzer CJ (1984) Voortplantingsonderzoek, pijler voor plantenveredeling. Landbouwkundig Tijdschrift 96: 21-26

Keijzer CJ and MTM Willemse (1988) Tissue interactions in the developing locule of *Gasteria verrucosa* during microsporogenesis. Acta Bot Neerl 37: 493-508

Knox RB (1984) The pollen grain. In: Johri BM (ed) Embryology of angiosperms. Springer-Verlag, Berlin: 197-271

Patrick JW (1997) Phloem unloading: sieve element unloading and post-sieve element transport. Annu Rev Plant Physiol Plant Mol Biol 48: 191-222

Pope JM, D Jonas and RR Walker (1993) Applications of NMR micro-imaging to the study of water, lipid, and carbohydrate distribution in grape berries. Protoplasma 173: 177-186

Sun J, T Loboda, SS Sung and CC Black (1992) Sucrose synthase in wild tomato, *Lycopersicon chmielewskii*, and tomato fruit sink strength. Plant Physiol 98: 1163-1169

Thorne JH (1985) Phloem unloading of C and N assimilates in developing seeds. Ann Rev Plant Physiol 36: 317-343

Wang X-D, G Harrington, JW Patrick, CE Offler and S Fieuw (1995) Cellular pathway of photosynthate transport in coats of developing seed of *Vicia faba* L. and *Phaseolus vulgaris* L. II Principal cellular site(s) of efflux. J Exp Bot 46: 49-63

Willemse MTM and JL van Went (1984) The female gametophyte. In: Johri BM (ed) Embryology of angiosperms. Springer-Verlag, Berlin: 159-196

Weber H, L Borisjuk, and U Wobus (1997) Sugar import and metabolism during seed development. Trends in Plant Science 2: 169-174

Xu D-P, S-J S Sung, T Loboda, PP Kormanik, and CC Black (1989) Characterization of sucrolysis via the uridine diphosphate and pyrophosphate-dependent sucrose synthase pathway. Plant Physiol 90: 635-642

Xu J, WT Avigne, DR McCarty and KE Koch (1996) A similar dichotomy of sugar modulation and developmental expression affects both paths of sucrose metabolism: Evidence from a maize invertase gene family. Plant Cell 8: 1209-1220

Chapter

Localization of sucrose synthase activity in developing maize kernels by *in situ* enzyme histochemistry

P.E. Wittich[1] and **D. Vreugdenhil**[2]

[1]Laboratory of Plant Cytology and Morphology, Wageningen Agricultural University, Wageningen

[2]Laboratory of Plant Physiology, Wageningen Agricultural University, Wageningen

Journal of Experimental Botany (1998), in press

Summary. Sucrose synthase is usually localized by immunocytochemistry but this method does not show the actual activity of the localized enzyme. Here a histochemical assay is presented showing the activity of sucrose synthase by tetrazolium salt precipitation on sections of developing maize kernels. The advantages of the assay are a high sensitivity for low amounts of active sucrose synthase and independence of specific antibodies.

In this study the activity of endosperm sucrose synthase is shown to move gradually from the apical part of the endosperm to the basal endosperm during kernel development. This shift in sucrose synthase activity correlates well with the localization of starch synthesis during kernel development. The assay also shows the early loss of activity in the aleurone layer bordering the embryo, and a loss of activity in the apical aleurone during the final stage of kernel development while the enzyme was still found by immunocytochemistry. This is in contrast to a high sucrose synthase activity in the epithelium of the scutellum, where hardly any labelling was found with antibodies against maize sucrose synthase. Low sucrose synthase activities were found in the pericarp and pedicel parenchyma.

Possible functions of the high and low activity patterns in the developing maize kernels and differences between the enzyme assay and immunocytochemistry are discussed.

INTRODUCTION

The enzyme sucrose synthase (UDP-D-glucose:D-fructose 2-α-glucosyltransferase, EC 2.4.1.13) catalyses the reversible conversion of sucrose and uridine diphosphate (UDP) into fructose and UDP-glucose. Although the reaction is reversible, it is thought to be involved primarily in the breakdown of sucrose (Huber and Huber 1996, Kruger 1990). Two isozymes of sucrose synthase have been described in the kernels of maize (*Zea mays* L.): SS1 and SS2, encoded by the *Sh1* and *Sus1* genes, respectively (Echt and Chourey 1985). Chourey and Nelson (1976) showed that the cytoplasmic SS1 isozyme plays an important role in starch biosynthesis. It was demonstrated immunocytochemically that the SS1 isozyme is localized in the cytoplasm of endosperm starch storage cells (Chen and Chourey 1989, Heinlein and Starlinger 1989). The SS2 isozyme was found in high amounts in the cytoplasm of aleurone cells but also in the basal endosperm transfer cells and in developing embryos, especially in the plumule-radicle axis. The function of the SS2 isozyme in these regions is not known but might be related with the high metabolic activity in these cells (Chen and Chourey 1989, Heinlein and Starlinger 1989).

In addition to a function in starch biosynthesis, sucrose synthase can also play a role in the respiratory pathway (Xu *et al.* 1989), and during cell wall synthesis where the membrane-associated callose synthase and cellulose synthase use UDP-glucose as substrate (Delmer and Amor 1995). A membrane-associated form of sucrose synthase probably exists in a complex with the cellulose and callose synthases. The cellulose synthase seems to use UDP-glucose directly from the associated sucrose synthase, while callose synthase probably accepts UDP-glucose from the cytoplasmic and membrane-associated sucrose synthases (Amor *et al.* 1995, Delmer and Amor 1995). Recently the two isoforms SS1 and SS2 of sucrose synthase were also found in a membrane-associated form next to the cytoplasmic form in maize (Carlson and Chourey 1996).

Nolte and Koch (1993) showed that cytoplasmic sucrose synthase is also present in phloem companion cells of sucrose importing and exporting maize organs. However, its physiological significance in these companion cells remains unclear.

In this study an *in situ* histochemical enzyme assay was set up to localize the activity of sucrose synthase on sections of developing maize kernels. The assay distinguishes high and low sucrose synthase activities in cells and tissues, and the detected enzyme activity can be compared with the relative amounts of enzyme found by immunocytochemical localization methods.

Changes in sucrose synthase distribution and activity during kernel development will be discussed and related with its possible functions.

MATERIAL AND METHODS

Zea mays L. plants of the hybrid line (A188) were hand pollinated. Female inflorescences were collected at 0, 5, 10, 14, 19, 28 and 42 days after pollination (DAP).

Histochemical enzyme assay

Kernels were dissected from the middle part of the inflorescence. Longitudinal sections of 200 µm thickness were cut with a sledge microtome, or 1 mm thick sections were cut by hand. The sections were fixed in 2% paraformaldehyde with 2% polyvinylpyrrolidone 40 and 0.005 M dithiotreitol, pH 7.0, at 4°C for 1 hour. After fixation the sections were rinsed overnight in 250 ml water at 4°C. The water was refreshed at least 5 times to remove all soluble sugars from the sections.

Detection of enzyme activity in sections was done in 7 ml vials with 705 µl incubation medium, at 30°C for 30 minutes. The composition of the incubation medium was a modification of the protocol of Xu *et al.* (1986) who measured sucrose synthase activity spectrophotometrically by measuring the production of NADH. The incubation medium contained 5 µl 150 mM NAD, 5 µl (= 1U) phosphoglucomutase from rabbit muscle, 5 µl 3 mM glucose-1,6-biphosphate, 5 µl (= 1U) glucose 6-phosphate dehydrogenase from *Leuconostoc*, 5 µl (=1U) UDPG-pyrophosphorylase from beef liver, 280 µl 0.07% aq. nitro blue tetrazolium (NBT), 350 µl buffer and 50 µl substrate. The buffer consisted of 100 mM HEPES, 10 mM $MgCl_2$, 2 mM EDTA, 0.2% BSA, 2 mM EGTA at pH 7.4. The substrate contained 0.75 M sucrose, 15 mM UDP, and 15 mM pyrophosphate (PPi). Figure 1 shows the sequence of enzymatic reactions after sucrose degradation by sucrose synthase in the tissue, resulting in reduction of NBT and the subsequent precipitation of the blue product.

In the control reaction phosphoglucomutase, Glu 1,6-P_2, and PPi were omitted. In a second control reaction only sucrose was omitted.

After the incubation period the sections were rinsed with water to stop the enzyme reactions, and then stored in 15% ethanol at 4°C. The sections were studied with a Wild dissecting microscope and a Nikon Optiphot in bright field mode. Photographs were taken with a digital Panasonic wv-E550 Colour Video Camera.

The assay also worked on other plant material like sugar cane stems, young potato tubers and *Gasteria verrucosa* ovules (data not shown).

Immunocytochemistry

Slices of kernels with a thickness of 2 to 4 mm were fixed with 4% paraformaldehyde in 0.005 M phosphate buffer pH 7.2, dehydrated and embedded in butyl-methylmethacrylate. The resin was polymerized at -10°C with UV-lamps. Sections of 3 µm were labelled with antibodies

against sucrose synthase according to Baskin *et al.* (1992). The polyclonal antibodies were a gift from Dr. KE Koch and raised in rabbit against a mixture of maize SS1 and SS2 isozymes (Koch *et al.* 1992). The second antibody (Goat anti rabbit) was conjugated with Cy3. Photographs were taken with the digital Panasonic video camera, using a Nikon Labophot in epifluorescence mode.

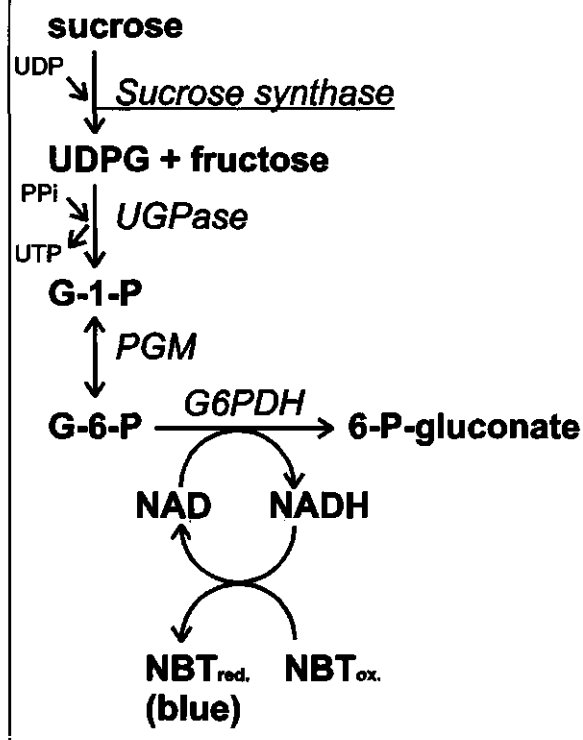

Figure 1 Reaction scheme of the sucrose synthase assay.
The sucrose synthase which is fixed in the tissue catalyzes the formation of UDP-glucose (UDPG) and fructose from sucrose and UDP. UDPG-pyrophosphorylase (UGPase) catalyzes the conversion of UDPG (plus pyrophosphate (PPi)) into glucose-1-P (G-1-P), which is in equilibrium with glucose-6-P (G-6-P) through the action of phosphoglucomutase (PGM). Glucose-1,6-biphosphate in the medium functions as a catalyst for the PGM. Glucose 6-phosphate dehydrogenase (G6PDH) catalyzes the subsequent reaction of NAD + G-6-P into NADH and 6-phosphate gluconate (6-P-gluconate). The produced NADH causes the reduction of the nitro blue tetrazolium (NBT) into the blue formazan salt which precipitates.

RESULTS

The localization and changes of sucrose synthase activity during kernel development were analyzed at regular time intervals between 0 to 28 DAP.

The sucrose synthases are fixed in the tissue by the paraformaldehyde and catalyze the production of UDP-glucose from the added sucrose and UDP. This UDP-glucose causes a cascade of enzyme reactions in the incubation medium which ends in the precipitation of a blue formazan salt at the site of sucrose synthase activity. Both control reactions did not result in any precipitation of formazan on the maize tissue (Fig.2-1).

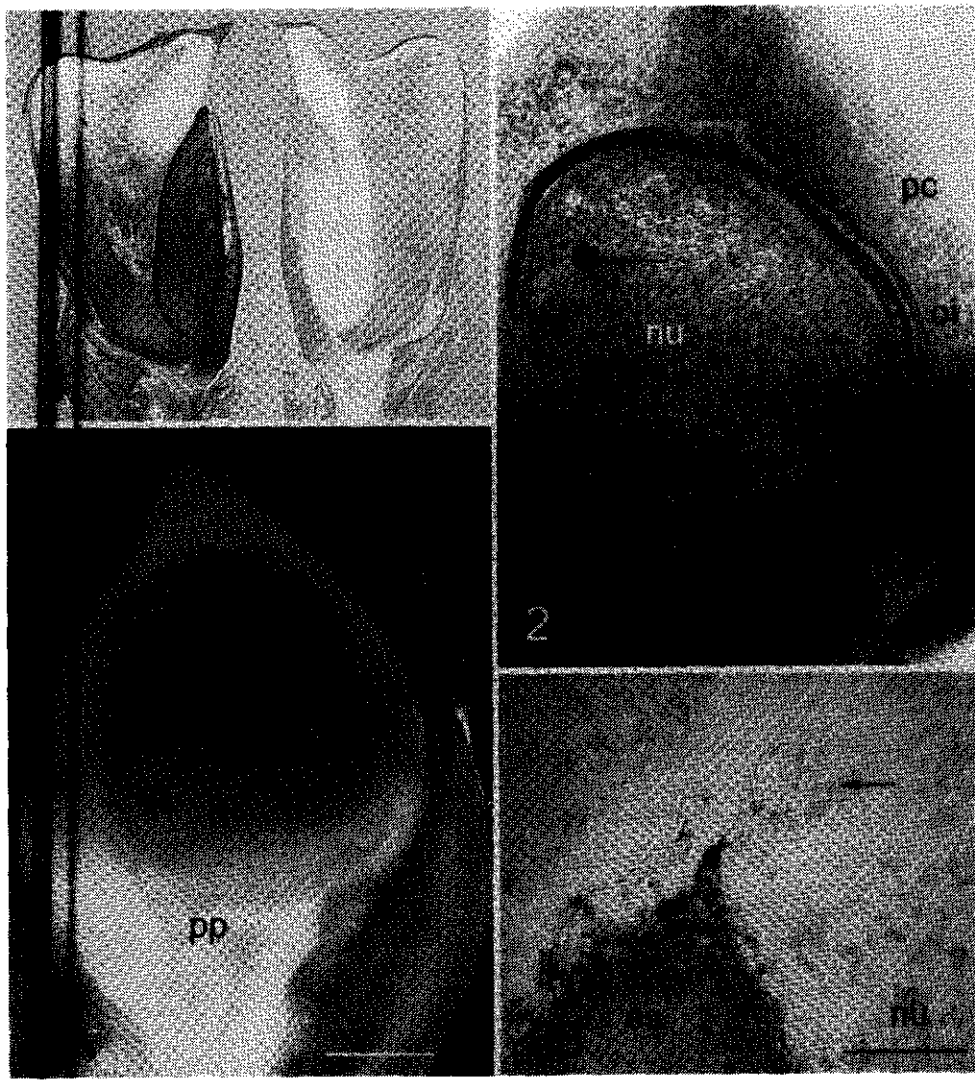

Figure 2 (1) Histochemical assay on sections of maize kernels showing sucrose synthase activity by the precipitation of a blue formazan precipitate (left) and no staining in the control reaction without phosphoglucomutase, glu 1,6-P_2 and PP_i (right). Both sections are consecutive sections of a kernel of 19 DAP. **(2)** Sucrose synthase activity in maize unfertilized ovule: High sucrose synthase activity in antipodal cells (arrow) and integuments. Bar = 200 μm. **(3A)** Sucrose synthase activity in maize kernel of 5 DAP: Endosperm (es) grows at the cost of nucellus (nu). High sucrose synthase activity in integuments and a gradient in pericarp. Bar = 700 μm. **(3B)** Detail of **(3A)**, showing activity in endosperm (es), low activity in nucellus (nu), and no activity in antipodal cells (arrow). Bar = 100 μm. Endosperm (es), inner integument (ii), nucellus (nu), outer integument (oi), pericarp (pc), pedicel parenchyma (pp).

Histochemical enzyme assay

At 0 DAP some sucrose synthase activity was found in the nucellus of the mature unfertilized ovule and a high activity in the antipodal cells of the embryo sac (Fig.2-2). The integuments also showed high sucrose synthase activity while the pericarp showed lower activity.

At 5 DAP the globular embryo did not show sucrose synthase activity (not shown). The endosperm grew at the cost of the disintegrating nucellus (Fig.2-3A). Relatively low sucrose synthase activities were found in both endosperm and nucellus. The epidermal cells of the endosperm showed a higher activity than the bordering tissues. Antipodal cells were still present but not stained any more by the enzyme assay (Fig.2-3B). Both the inner and outer integument showed high sucrose synthase activity. The middle pericarp showed low activity of this enzyme while the most apical and basal parts were negative. The pedicel did show low activity.

At 10 DAP the embryo showed sucrose synthase activity in all its tissues, with the highest activity in the epidermis of the scutellum (Fig.3-1). Sucrose synthase was very active in the apical part of the endosperm where starch granules appeared. The endosperm epidermis and integuments also showed a high activity, but there was no sucrose synthase activity in the nearly completely disintegrated nucellus. Some enzyme activity in the basal part of the pericarp and pedicel was detected.

At 14 DAP the embryo was almost fully developed. The differentiated epidermal cells of the scutellum exhibited a much higher sucrose synthase activity than the rest of the embryo (Fig.3-2). In the endosperm a high activity was found in the middle and apical parts (Fig.3-2) but in the endosperm cells above the embryo the sucrose synthase activity was diminishing. The aleurone layer showed high enzyme activity everywhere, also in the part bordering the embryo. Some activity was found in the pericarp. The integuments had degenerated and only unstained remnants persisted.

Figure 3 Sucrose synthase activity in maize kernels of 10 - 28 DAP. **(1)** 10 DAP: High activity in apical and epidermal endosperm, and in epidermis of the scutellum of the embryo (em). The nucellus (nu) shows no sucrose synthase activity. Bar = 2 mm. **(2)** 14 DAP: Diminishing activity in apical endosperm above the embryo (asterix) and high activity in middle and rest of the apical endosperm. Bar = 2 mm. **(3)** 19 DAP: Loss of sucrose synthase activity in apical endosperm (asterix), but still activity in aleurone (arrows). Bar = 2 mm. **(4)** 19 DAP: The embryo shows high activity in the differentiating epidermis of the scutellum (sc). Bar = 1 mm. **(5)** Detail of **(3)**, showing apical endosperm with activity only in the aleurone. Bar = 300 μm. **(6)** 19 DAP: Basal part of the kernel shows activity in the aleurone (arrows), except for the part that borders the embryo (arrow head). Bar = 700 μm. **(7)** 19 DAP: Activity in the phloem companion cells of the pedicel. Bar = 30 μm.
Closing layer (cl), embryo (em), nucellus (nu), placento-chalazal tissue (pc), pedicel parenchyma (pp), scutellum (sc), basal endosperm transfer cells (tc).

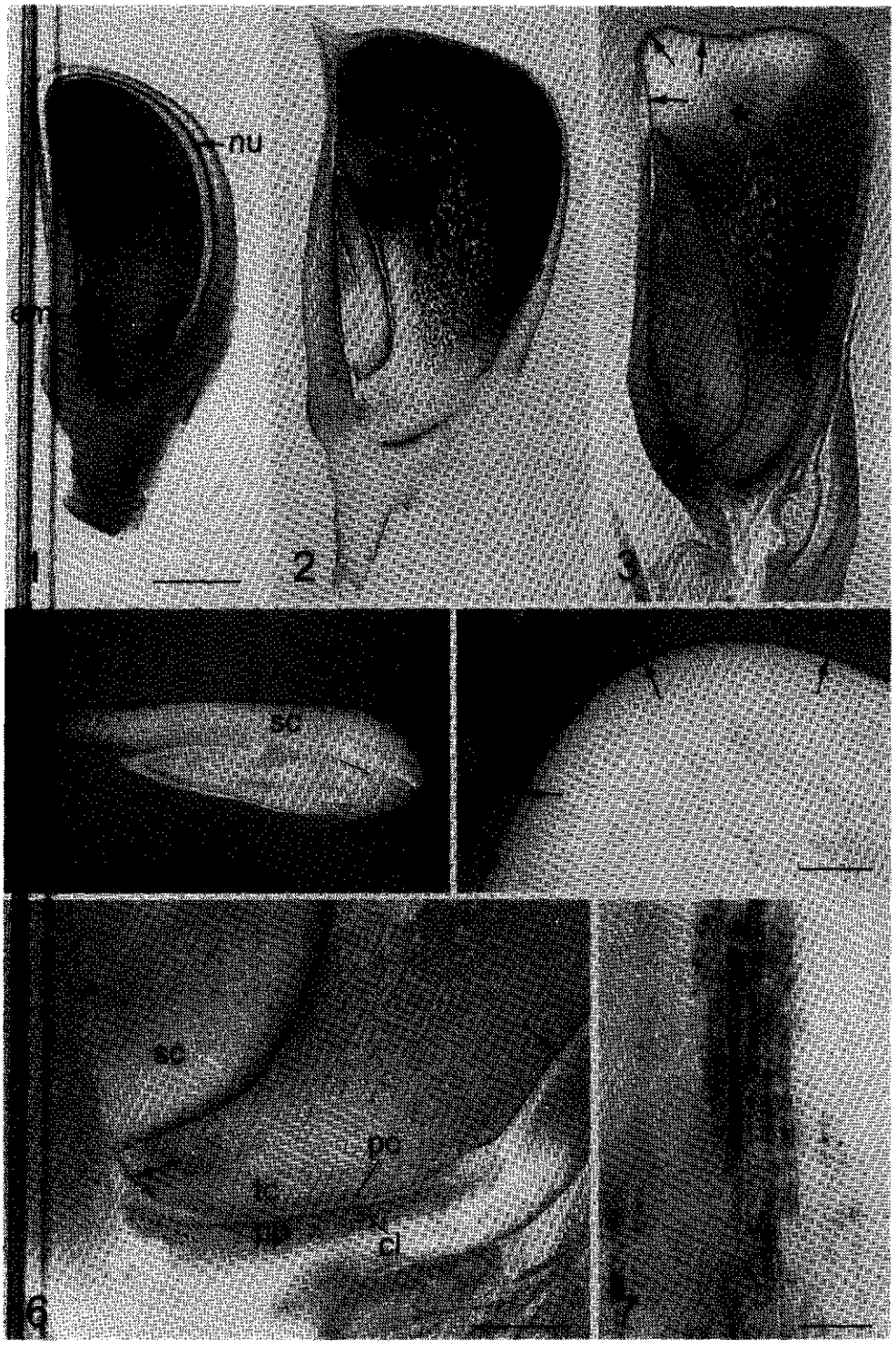
nu
em
2
3
sc
sc
pc
ic
ep
cl
6

At 19 DAP the embryo still showed a high activity in the differentiated epidermal cells of the scutellum (Fig.3-4). The activity of sucrose synthase had disappeared in the most apical part of the endosperm. At that moment the cells in that region were completely filled with starch. The aleurone cells, however, were still enzymatically active all around the endosperm (Fig.3-3 and Fig.3-5) except for the aleurone layer between the embryo and the nucellar cuticle (Fig.3-6). The activity of the sucrose synthase increased in the middle part of the endosperm and also became visible in the cells of the basal endosperm (Fig.3-3). The activity in the sub-aleurone cells in the centre of the kernel was similar to the activity in the bordering aleurone cells. The endosperm transfer cells and the closing layer showed little sucrose synthase activity. The placento-chalazal tissue between those two layers showed no activity. In the pedicel parenchyma, and the basal pericarp some enzyme activity was found (Fig.3-6).

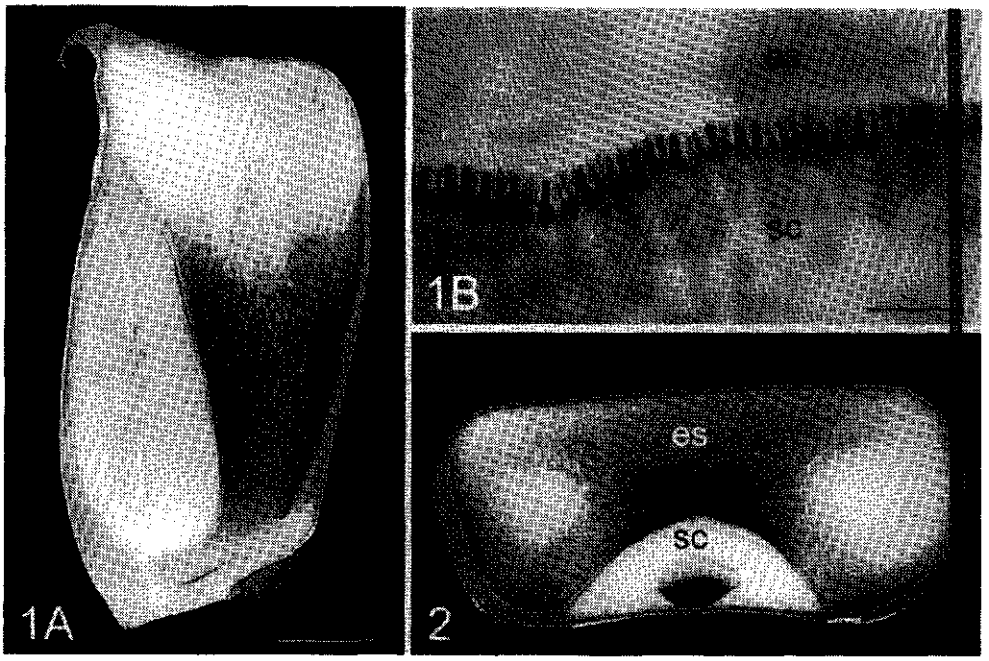

Figure 4 Sucrose synthase activity in maize kernels of 28 DAP: **(1A)** Activity in middle and basal endosperm, but not in apical endosperm. Almost no activity in apical aleurone cells. Bar = 2 mm. **(1B)** Detail of **(1A)**, showing high activity in epithelial cells of the scutellum. Bar = 300μm. **(2)** 28 DAP: Transversal section through middle of kernel. Activity diminishing started in two centres of endosperm (es). In the scutellum (sc) there is a hole where plumule used to be. Bar = 2 mm.
Endosperm (es), scutellum (sc)

At 28 DAP the embryo showed a similar enzyme activity pattern as found at 19 DAP with a high activity in the differentiated epidermal cells of the scutellum (Fig.4-1A and Fig.4-1B). In almost the entire apical part of the endosperm sucrose synthase activity had disappeared, but there was still a high activity in the middle and basal endosperm. The aleurone layer in the apical part of the kernel showed almost no activity while there was still activity in the basal part. A transversal section through the kernel just above the embryo axis showed that sucrose synthase activity diminished in two centres which were completely filled with starch (Fig.4-2). Hardly any sucrose activity was observed in the pericarp and in the pedicel parenchyma.
At 42 DAP no sucrose synthase activity was found in the maize kernel (not shown).
In all the developmental stages described, sucrose synthase activity was found in the companion cells of the pedicel phloem (Fig.3-7).

Immunocytochemistry
Most of the immunocytochemical results are coherent with the histochemical results presented above, and the immunocytochemical results of Chen and Chourey (1989) and Heinlein and Starlinger (1989). Only those results are presented which are deviating from the histochemical data or from the published immunocytochemical results.
At 5 DAP no labelling was found in the developing kernel while the enzymatic assay had shown sucrose synthase activity.
During the development of the kernel, immunolabelling was found in the aleurone layer that borders the embryo at 10 DAP, but no labelling was found here any more at 14 DAP (Fig.5-1A). The rest of the aleurone layer was labelled at 14 and 19 DAP. At 28 DAP there was not much labelling in the apical aleurone (Fig.5-2A) while the apical sub-aleurone and endosperm cells still showed some labelling. The middle and basal endosperm and aleurone showed better labelling at 28 DAP. Labelling was not found in the transfer cells at 19 DAP or any other stage with the antibody used. In the epithelium cells of the scutellum no abundant labelling was found (Fig.5-3A).

DISCUSSION

The histochemical enzyme assay clearly shows the activity of sucrose synthase on sections of maize kernels. It already showed sucrose synthase activities in 5 DAP kernels while immunocytochemical labelling did not yet show the presence of these enzymes. The control reactions which did not show formazan precipitation confirm the specificity for the sucrose synthase activity detection.
The sucrose synthase assay is a useful technique to compare with the invertase assay used on

maize by Doehlert and Felker (1987). The activity of invertase in maize kernels is localized in the base of the kernel and this enzyme is supposed to function in phloem unloading and carbohydrate uptake into the endosperm (Doehlert and Felker 1987). The sucrose degrading activity of both enzymes, sucrose synthase and invertase, are used as indicators for sink strength (Ho *et al.* 1991, Sung *et al.* 1989).

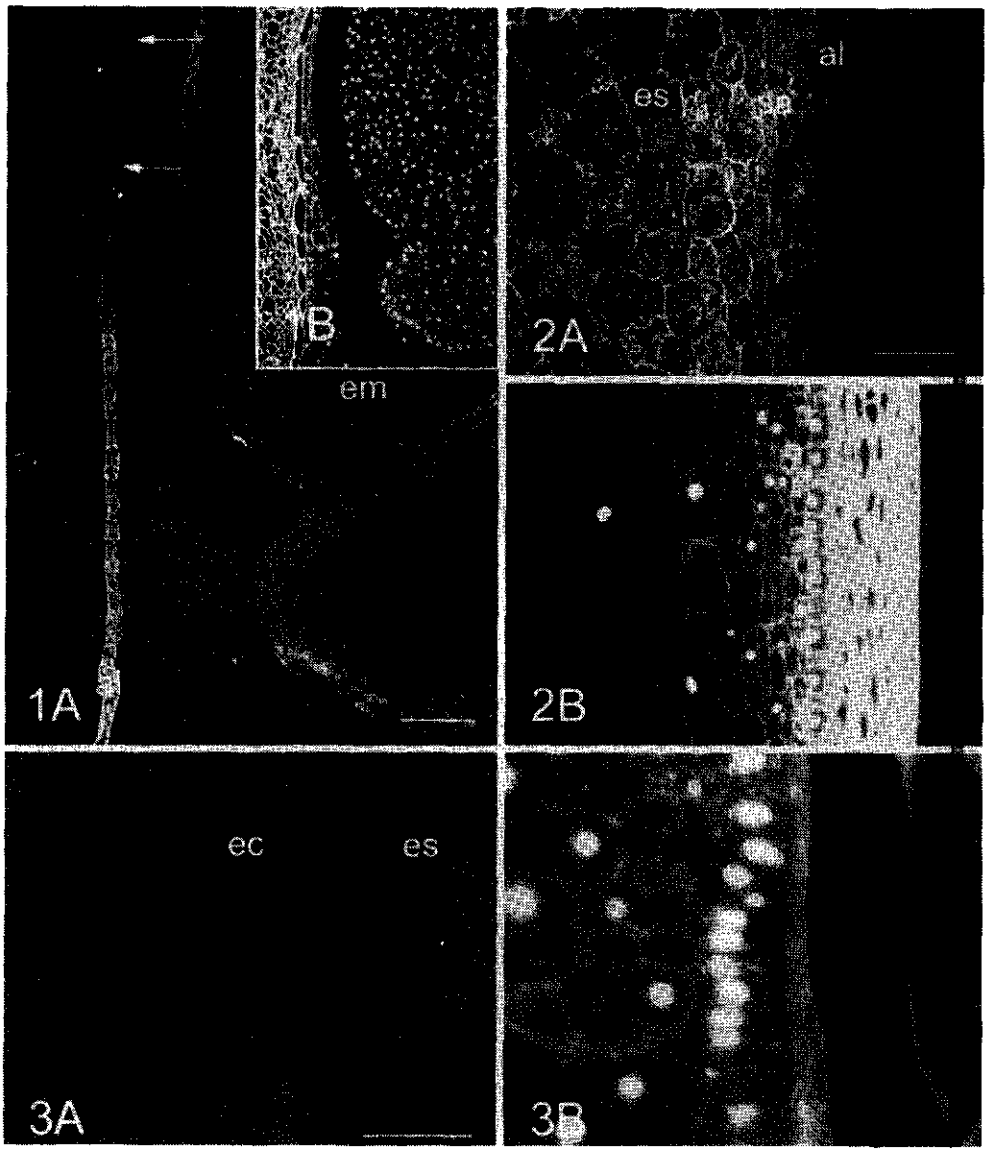

Integuments and nucellus

Low sucrose synthase activity at 5 DAP is found in many kernel tissues, *viz.*, the integuments, nucellus, and the basal part of the carpel. This is most likely the activity of the SS2 isozyme, since Chen and Chourey (1989) and Heinlein and Starlinger (1989) showed the presence of this isozyme immunocytochemically, in the same tissues.

At 10 and 14 DAP respectively, the nucellus and integuments no longer showed sucrose synthase activity. At that moment they were disintegrating and probably did not use UDP-glucose and fructose from sucrose any more for respiratory purposes. The nucellus was gradually replaced by the endosperm.

Antipodal cells

The function of the antipodal cells is not known but they are supposed to play a role in the nutrition of the embryo sac. Van Lammeren (1986) found high amounts of ribosomes and well developed dictyosomes in these antipodal cells shortly after fertilization. This points, together with the high sucrose synthase activity found in this study at mature embryo sac stage, to a metabolic high activity of the antipodal cells. The absence of the sucrose synthase activity at 5 DAP supports the hypothesis that the antipodal cells supply nutrients to the embryo sac before and shortly after fertilization.

Endosperm

In maize endosperm it was shown that the synthesis of starch is primarily mediated by sucrose synthase activity (Doehlert 1990). The sucrose synthase enzyme assay clearly showed this relation of the sucrose synthase with the starch synthesis in maize kernels. At 5 DAP low sucrose synthase was detected, but from the moment that abundant starch synthesis started in the apical part of the endosperm (10 DAP) a high activity of sucrose synthase was found in this region. During the following stages of development the highest activity of the enzyme moved towards the basal part of the endosperm. Meanwhile the activity diminished in the apical part of the endosperm where the cells were filled with starch. The inhibition of starch

Figure 5 Sucrose synthase immunocytochemistry on maize kernels. **(1A)** 14 DAP: Immunocytochemistry does not show sucrose synthase in aleurone layer (arrows) that borders the embryo. The aleurone basal of the embryo (al) shows immunolabelling. Bar = 100 μm. **(1B)** UV illumination of **(A)**, showing nuclei stained with DAPI. **(2A)** 28 DAP: No labelling for sucrose synthase in apical aleurone (al). The sub-aleurone (sa) and endosperm (es) show labelling. Bar = 100 μm. **(2B)** UV illumination of **(2A)**, showing nuclei stained with DAPI. **(3A)** 28 DAP: No labelling for sucrose synthase in epithelial cells (ec) of the scutellum. Bar = 30 μm. **(3B)** UV illumination of **(3A)**, showing nuclei stained with DAPI.

Aleurone (al), epithelial cells (ec), embryo (em), endosperm (es), sub-aleurone (sa).

synthesis seemed to be correlated with decreasing sucrose synthase activity. This shift of enzyme was also found by Heinlein and Starlinger (1989), using immunocytochemistry. Besides the major starch formation gradient from the apical part of the endosperm to the basal part there is also a minor gradient from the inner part with large starch granules towards the periclinal dividing cells near the endosperm surface with small granules (Randolph 1936, Kiesselbach 1949). This minor starch synthesis gradient was clearly found to be correlated with the sucrose synthase activity in the transversal section through the centre of the kernel of 28 DAP.

Aleurone

The aleurone cells showed high sucrose synthase activity, presumably by the SS2 isoform which was found in these cells by Chen and Chourey (1989). Heinlein and Starlinger (1989) found a high amount of sucrose synthase in the developing aleurone by immunocytochemistry, but at 23 DAP they found a shift of sucrose synthase to the sub-aleurone. Also from ultrastructural studies a shift of activity was suggested from the aleurone to the sub-aleurone (Kyle and Styles 1977), but our immunochemical study as well as the enzyme assay did not show such a shift of sucrose synthase activity nor a shift towards the sub-aleurone layer in the apical part of the endosperm. At 14 DAP, only in the middle and basal part of the endosperm the activity of the sub-aleurone cells became similar to the activity in the aleurone cells. The apical aleurone cells did show a longer period of sucrose synthase activity than the apical endosperm cells, but around 28 DAP activity and presence was lost. However, at 30 DAP Heinlein and Starlinger (1989) reported strongest signal of sucrose synthase in the aleurone, but this dissimilarity may be due to an other maize hybrid line that they used.

The function of sucrose synthase in the aleurone and sub-aleurone cells might be related to the synthesis of the protein bodies (aleurone bodies) since there is no starch synthesis in the aleurone cells, and there is a correlation between sucrose synthase and the endosperm protein zein described by Doehlert (1990).

Another function for the sucrose synthase in the aleurone cells could be the production of UDP-glucose for cell wall thickening, which occurs after 14 DAP. A third option is that the sucrose synthase in these cells resynthesizes sucrose for further transport into the endosperm, although *in vivo* the sucrose synthase activity is thought to be active primarily in the sucrose degrading direction (Huber and Huber 1996, Kruger 1990).

It is noteworthy that only until 10 DAP the embryo-bordering part of the aleurone layer showed sucrose synthase activity and presence. This points to a nutritive function of the aleurone towards the endosperm, since after 10 DAP this cell layer does not border endosperm cells anymore.

Basal endosperm transfer cells

The transfer cells showed some sucrose synthase activity at 19 DAP while immunocytochemical experiments in this study did not show any signal in the transfer cells. This lack of labelling may be caused by a too low enzyme concentration. Chen and Chourey (1989) found the SS2 isozyme already present at 12 DAP in the transfer cells, but Heinlein and Starlinger (1989) found only at 23 DAP a weak immunocytochemical signal of this enzyme in the transfer cells. Their results could be caused by the use of other antibodies and different maize lines.

Chen and Chourey (1989) postulate that the function of the sucrose synthase in these cells is resynthesis of sucrose after monosaccharides have entered the endosperm symplast, but the low sucrose synthase activity now found with the assay does not contribute to this hypothesis.

Embryo

The epidermal cells of the scutellum differentiate into a secretory epithelium with also absorbing characteristics. These cells showed high sucrose synthase activity, already before differentiation. Heinlein and Starlinger (1989) found a strong signal for the enzyme in these epidermal cells at 30 DAP, but immunocytochemical experiments in our study did not reveal a higher signal than in the other scutellar cells. In the epidermal cells the sucrose synthase may have a similar function in further transport of sugars into the embryo, as in the aleurone and transfer cells. Monosaccharides are supplied via the apoplast between embryo and endosperm to the scutellum. In the scutellum sucrose may be resynthesized by the sucrose synthase. Griffith *et al.* (1987) showed that glucose and fructose are preferred by maize embryos *in vitro*, and that embryos accumulate sucrose after monosaccharide uptake.

The sucrose synthase in the epidermal cells might also be related with the disintegration process of the endosperm surrounding the growing embryo. The differentiated epidermal cells are involved in excreting proteolytic and other digestive enzymes during germination (Kiesselbach 1949) and it is plausible that these enzymes are also excreted for digestion of the endosperm during this stage of kernel development. Randolph (1936) already concluded that the growing embryo seems to digest the endosperm.

Phloem

Sucrose synthase activity in the phloem complex during all developmental stages was probably in the companion cells where its presence is reported by Nolte and Koch (1993). A hypothesis on the physiological role of the sucrose synthase in these cells is the provision of energy for transport processes and/or provision of UDP-glucose for callose synthesis in the sieve plates (Geigenberger *et al.* 1993, Nolte and Koch 1993). In sugar cane stems sucrose synthase activity was found exclusively in the companion cells of the phloem (Wittich, unpublished).

Pedicel, placento-chalazal tissue and closing layer

In the pedicel parenchyma sucrose synthase was found by immunocytochemistry and by its activity. Here sucrose is unloaded from the phloem into the apoplast. Most of the sucrose is thought to be converted into glucose and fructose by invertase activity in pedicel and placento-chalazal tissue. A high invertase activity enhances the phloem unloading (Shannon and Dougherty 1972). However, the detected sucrose synthase activity was not very high in the pedicel parenchyma and might be needed only for respiratory purposes. At 19 DAP no activity was found in the placento-chalazal tissue, which at that time consisted of disintegrated cells. The closing layer lost its sucrose synthase activity after it had differentiated around 19 DAP.

Pericarp

In the pericarp sucrose synthase activity was mainly found in the basal part. This coincides with the region where most of the cell divisions take place during its growth (Randolph 1936). The apical part of the pericarp starts to disintegrate in an early stage (10 DAP) (Randolph 1936).

Conclusions on the assay

This study shows that the assay is a very sensitive method to visualize sucrose synthase activity, even more sensitive than immunocytochemistry. It is also shown that immunochemically localized enzymes do not necessarily have to be active in the sucrose cleavage direction forming UDP-glucose and fructose. Phosphorylation of sucrose synthase has been reported to activate the sucrose cleavage reaction, while the sucrose synthesis reaction is not sensitive for phosphorylation (Huber *et al.* 1996). Thus, the assay visualizes phosphorylated sucrose synthase activity.

An advantage of a histochemical assay over immunocytochemistry is that there is no need to raise specific antibodies. Immunocytochemical studies are often done with antibodies against enzymes from other plant species. These antibodies might not recognize the enzymes in the plant that is being studied. However, antibodies are still needed to discriminate between different enzyme isoforms, in this case SS1 and SS2.

The presented assay is easy to apply to most plant material and gives information on the activity of all cytoplasmic sucrose synthase isozymes. It is unlikely that the activity of the membrane-associated sucrose synthase is detected by this assay because according to the model of Delmer and Amor (1995) the UDP-glucose is directly used by cellulose synthase.

Using this assay in combination with immunocytochemistry, will give relevant data in future studies on sucrose synthase localization. This method might also be used to localize other enzymes, if the reaction catalyzed by the enzyme can be coupled to the production of NADH.

ACKNOWLEDGEMENTS

The authors thank KE Koch for the donation of the maize sucrose synthase antibodies, J van Dongen for his technical assistance, MTM Willemse and AAM van Lammeren for their valuable discussions and critically reading the manuscript, and S Massalt and AB Haasdijk for the artwork.

REFERENCES

Amor Y, CH Haigler, S Johnson, M Wainscott and DP Delmer (1995) A membrane-associated form of sucrose synthase and its potential role in synthesis of cellulose and callose in plants. Proc Natl Acad Sci USA 92: 9353-9357

Baskin TI, CH Busby, LC Fowke, M Sammut and F Gubler (1992) Improvements in immunostaining samples embedded in methacrylate: localization of microtubules and other antigens throughout developing organs in plants of diverse taxa. Planta 187: 405-413

Carlson SJ and PS Chourey (1996) Identification of plasma membrane-associated forms of maize sucrose synthase. Plant Phys 111: 99

Chen Y-C and PS Chourey (1989) Spatial and temporal expression of the two sucrose synthase genes in maize: immunohistological evidence. Theor Appl Genet 78: 553-559

Chourey PS and OE Nelson (1976) The enzymatic deficiency conditioned by the *shrunken-1* mutations in maize. Biochem Genet 14: 1041-1055

Delmer DP and Y Amor (1995) Cellulose biosynthesis. Plant Cell 7: 987-1000

Doehlert DC (1990) Distribution of enzyme activities within the developing maize (*Zea mays*) kernel in relation to starch, oil and protein accumulation. Physiol Plant 78: 560-567

Doehlert DC and FC Felker (1987) Characterization and distribution of invertase activity in developing maize (*Zea mays*) kernels. Physiol Plant 70: 51-57

Echt CS and PS Chourey (1985) A comparison of two sucrose synthetase isoenzymes from normal and *shrunken-1* maize. Plant Physiol 79: 530-536

Geigenberger P, S Langenberger, I Wilke, D Heineke, HW Heldt and M Stitt (1993) Sucrose is metabolised by sucrose synthase and glycolysis within the phloem complex of *Ricinus communis* L. seedlings. Planta 190: 446-453

Griffith SM, RJ Jones and ML Brenner (1987). *In vitro* sugar transport in *Zea mays* L. kernels. II. Characteristics of sugar absorption and metabolism by isolated developing embryos. Plant Physiol 84: 472-475

Heinlein M and P Starlinger (1989) Tissue- and cell-specific expression of the two sucrose synthase isozymes in developing maize kernels. Mol Gen Genet 215: 441-446

Ho LC, A Lecharny and J Willenbrink (1991) Sucrose cleavage in relation to import and metabolism of sugars in sink organs. In: Bonnemain JL, S Delrot, WJ Lucas and J Dainty (eds). Recent advances in phloem transport and assimilate compartmentation. Ouest editions, Nantes: 178-186

Huber SC and JL Huber (1996) Role and regulation of sucrose-phosphate synthase in higher plants. Ann Rev Plant Physiol Plant Mol Biol 47: 431-444

Huber SC, JL Huber, P-C Liao, DL Gage, RW McMichael, PS Chourey, LC Hannah and KE Koch (1997) Phosphorylation of serine-15 of maize leaf sucrose synthase. Occurrence in vivo and possible regulatory significance. Plant Physiol 112: 793-802

Kiesselbach TA (1949) The structure and reproduction of corn. University of Nebraska College of Agriculture

Agricultural Experiment Station Res Bull 161: 1-96

Koch KE, KD Nolte, ER Duke, DR McCarty and WT Avigne (1992) Sugar levels modulate differential expression of maize sucrose synthase genes. Plant Cell 4:59-69

Kruger NJ (1990) Carbohydrate synthesis and degradation. In: Dennis DT, DH Turpin (eds.) Plant physiology, biochemistry and molecular biology. Longman Scientific & Technical, Ellex: 59-76

Kyle DJ and ED Styles (1977) Development of aleurone and sub-aleurone layers in maize. Planta 137: 185-193

Nolte KD and KE Koch (1993) Companion-cell specific localization of sucrose synthase in zones of phloem loading and unloading. Plant Physiol 101: 899-905

Randolph LF (1936) Developmental morphology of the caryopsis in maize. J Agr Res 53: 881-916

Shannon JC and CT Dougherty (1972) Movement of ^{14}C-labeled assimilates into kernels of *Zea mays* L. II. Invertase activity of the pedicel and placento-chalazal tissues. Plant Physiol 49: 203-206

Sung S-JS, D-P Xu and CC Black (1989) Identification of actively filling sucrose sinks. Plant Physiol 89: 1117-1121

Van Lammeren AAM (1986) A comparative ultrastructural study of the megagametophytes in two strains of *Zea mays* L. before and after fertilization. Agricultural University Wageningen Papers 86-1: 1-37

Xu D-P, S-JS Sung, CA Alvarez and CC Black (1986) Phosphate-dependent sucrose metabolism and its activation by fructose 2,6-biphosphate in sucrose importing plant tissues. Biochem Biophys Res Comm 141: 440-445

Xu D-P, S-JS Sung, T Loboda, PP Kormanik and CC Black (1989) Characterization of sucrolysis via the uridine diphosphate and pyrophosphate-dependent sucrose synthase pathway. Plant Physiol 90: 635-642

Chapter 3

Localization of invertase activity by enzyme histochemistry, and invertase and sucrose synthase by immunocytochemistry, in developing maize kernels

P.E. Wittich

Summary. Sucrose synthase and invertase are the only two sucrose degrading enzymes, and are considered to be indicators for sink strength. The localization of these enzymes may give better insight on the distribution of sucrose in developing maize kernels. In this study both enzymes are localized in developing maize kernels by immunocytochemistry *in situ* (detection of proteins). Enzyme histochemistry was performed to detect invertase activity (localizing the active enzymes), while sucrose synthase histochemistry was already accomplished in a previous study.

Cell wall-bound invertase activity was found in the basal part of the kernel, and seems to play a role in the unloading of sucrose from the pedicel into the apoplast between sporophytic and gametophytic derived tissues by creating a sucrose gradient. Activity and presence of this enzyme was also found in the cell walls of the basal endosperm. It seems likely that all sucrose is hydrolyzed into glucose and fructose prior to uptake into the endosperm and embryo. Immunocytochemistry showed invertase appearing in the aleurone during ripening of the kernel, but activity was not demonstrated and speculations are made on a possible function. The activity of sucrose synthase shown in a previous study did not always match the immunocytochemical results. During kernel development sucrose synthase activity decreased in the apical endosperm while the enzyme was still detected immunocytochemically, and a high activity of sucrose synthase in the aleurone layer was not found correlated with a high enzyme concentration. Membrane-associated sucrose synthase was found against new formed cell walls, plasmodesmata, and pit fields, suggesting a function in callose synthesis.

INTRODUCTION

Invertase (β-D-fructofuranoside fructohydrolase, EC 3.2.1.26) and sucrose synthase (UDP-D-glucose:D-fructose 2-α-glucosyltransferase, EC 2.4.1.13) are the only two enzymes known which catalyse the breakdown of sucrose in plants. Invertase hydrolyses sucrose into glucose and fructose, sucrose synthase converts sucrose and uridinediphosphate (UDP) into UDP-glucose and fructose. These monosaccharides are used for the synthesis of cell components and respiratory purposes. Although the sucrose synthase activity is reversible, it is thought to work *in vivo* mainly in the degrading direction (Huber and Huber 1996, Kruger 1990). The hydrolysing activity of invertase is irreversible and requires double the net energy of the sucrose synthase pathway (Black *et al.* 1987). The activity of the two enzymes in sinks is considered to be an indicator for the sink strength of cells or tissues where these enzymes are active (Ho *et al.* 1991, Sung *et al.* 1989, 1994). Three forms of invertase are known (Avigad 1982): an acidic invertase which is ionically bound to the cell wall and also called cell wall invertase (Laurière *et al.* 1988), and two soluble invertases, a cytoplasmic neutral invertase and a vacuolar invertase which can be acidic or neutral (Ho *et al.* 1991).

In maize kernels soluble and cell wall invertases are present in the basal part (Doehlert and Felker 1987), having a rate limiting role in the kernel development (Shanker *et al.* 1995). Sucrose is transported towards the kernel via the phloem, unloaded symplastically in the pedicel parenchyma symplast, and finally unloaded in the pedicel apoplast (Felker and Shannon 1980). This unloading is passive and probably turgor mediated (Shannon *et al.* 1986). In the apoplast of the pedicel and basal endosperm sucrose is hydrolysed by invertase into glucose and fructose. The endosperm and embryo are symplastically isolated from the enveloping nucellus and placento-chalazal tissue, and the monosaccharides will be apoplastically transported into these tissues (Felker and Shannon 1980). Due to the invertase activity in the basal part of the kernel a continuous sucrose gradient is established between the phloem in the pedicel, and the endosperm, enhancing phloem unloading and carbohydrate transport (Doehlert and Felker 1987, Felker and Shannon 1980, Miller and Chourey 1992). The hydrolysis of sucrose by invertase is found to be a prerequisite for growth of the kernel. Only glucose and fructose seem to be utilized by the ovary (Miller and Chourey 1992, Zinselmeier *et al.* 1995) although the sucrose is not necessarily hydrolysed prior to uptake into the endosperm (Cobb and Hannah 1980, Schmalstig and Hitz 1987). Monosaccharides which are taken up into the cytoplasm of the endosperm are probably resynthesized into sucrose by the activity of sucrose phosphate synthase (SPS) in conjunction with sucrose phosphate phosphatase (SPS) and other enzymes (Chourey *et al.* 1995, Huber and Huber 1996). The activity of the invertase in the basal endosperm is also found to be correlated with the amount of lipids that are synthesized in the embryo (Doehlert 1990). Invertase activity is further known

to be correlated with monosaccharide storage (Konno *et al.* 1993) and cell elongation (Xu *et al.* 1995).

Until recently sucrose synthase was only known as a soluble cytoplasmic enzyme, but now also a membrane-associated form is found which is believed to be involved in cellulose and callose synthesis (Amor *et al.* 1995). The activity of the cytoplasmic sucrose synthases is correlated with the production of storage products like starch (Chourey and Nelson 1972, Doehlert 1990), probably the synthesis of callose (Delmer and Amor 1995), and respiratory processes (Xu *et al.* 1989). In maize kernels two isoforms of the cytoplasmic form are found, sucrose synthase 1 (SS1) and sucrose synthase 2 (SS2). SS1 is associated with starch formation and mainly found in the starch synthesizing endosperm cells. SS2 can be found in all kernel tissues (Chen and Chourey 1989, Heinlein and Starlinger 1989). Carlson and Chourey (1996) showed that in maize both SS1 and SS2 isoforms are also present in a membrane-associated form.

The studies on invertase and sucrose synthase found in literature were mostly done either by detecting the presence *in situ* by immunocytochemistry, or by enzyme activity measurements in tissue extracts. In this study histochemical techniques were used for the detection of the activity of these enzymes *in situ*, and as a comparison antibodies were used to localize the peptides. These two localization methods do not always give matching patterns. The differences between presence and activity of the enzymes will be related to the role of these enzymes in carbohydrate distribution in the kernel.

MATERIAL AND METHODS

The female inflorescences of *Zea mays* L. (hybrid line A188) plants were collected at 0, 5, 10, 14, 19, 28 and 42 days after pollination.

Detection of enzyme activity:

The protocol used for the detection of *invertase activity* on sections of maize kernels was according the protocol of Doehlert and Felker (1987). Approximately 1 mm thick sections of the kernels were made by hand, or 200 µm thick sections with a sledge microtome. Fresh sections were immediately fixed for 1 hour in 2% paraformaldehyde with 2% polyvinylpyrrolidone (PVP), pH7.0, at 4°C. After fixation sections were rinsed overnight in 250 ml water, and refreshed at least 5 times to remove the soluble carbohydrates. The sections were incubated in a medium for 30 minutes at 30°C. The incubation medium contained 0.024% nitro blue tetrazolium, 0.014% phenazine methosulfate, 25 units glucose oxidase and 1% sucrose in 0.38M sodium phosphate, pH 6.0. The reaction was terminated by rinsing the sections in water. The sections were stored in 15% ethanol at 4°C. In the control reaction sucrose was omitted. The dye in the control reaction stained the section pink (data not shown)

while glucose production by invertase activity caused precipitation of the blue formazan salt.
The procedure for the *sucrose synthase activity* assay is published in detail in chapter 2 (Wittich and Vreugdenhil 1998). In short, the UDP-glucose produced by the sucrose synthase activity causes via a cascade of enzymatic reactions (UDPglucose-pyrophosphorylase, phosphoglucomutase, and glucose-6-phosphate dehydrogenase) the oxidation and precipitation of nitro blue tetrazolium on the site of sucrose synthase activity. Sectioning and fixation of the sections was according the protocol for the invertase assay as described above. Results obtained with the sucrose synthase assay (Wittich and Vreugdenhil 1998, in this thesis chapter 2) are used in the present study for the discussion.
The sections were studied with a Wild dissecting microscope and a Nikon bright field microscope. Photographs were taken with a digital Panasonic wv-E550 Colour Video Camera.

Localization of the enzymes:
For immunocytochemical detection of invertase and sucrose synthase, 2 mm thick slices of kernels were fixed in 4% paraformaldehyde in 0.005M phosphate buffer, pH 7.2. The slices were rinsed twice in 0.1M phosphate buffer, dehydrated in ethanol series and infiltrated in gradient steps of butyl-methyl methacrylate (BMM) according to Baskin *et al.* (1992). The resin was polymerized at -10°C with two 8W Philips UV-lamps for 48 hours. Sections of 2-6 μm were made with a Reichert Ultramicrotome, stretched on water, and dried on microscope slides at 60°C for 1 hour.
The BMM was removed from the sections by washing the slides in pure acetone for 15 minutes. They were washed in phosphate buffered saline (PBS) and blocked with 0.1M hydroxyl ammonium chloride and 1% bovine serum albumine (BSA). The sections were incubated with the first antibody (see below) overnight at 4°C. The next day the sections were washed with 0.1% acetylated BSA in PBS and incubated for 2 hours at 30°C with a second antibody (goat anti rabbit) conjugated with the fluorescent dyes FITC or Cy3. The sections were then rinsed with PBS, and mounted with 1μg/ml DAPI (4,6-Diamidino-2-phenylindole) containing Citifluor. The sections were studied with a Nikon Labophot in epifluorescence mode. Photographs were taken on diapositive slides and digitalized afterwards.
For the invertase immunocytochemistry an antibody against soluble grape invertase was a gift from H.P. Ruffner (Ruffner *et al.* 1995), and an antibody against carrot cell wall invertase (Laurière *et al.* 1988), and two soluble invertases (Unger *et al.* 1992) from carrot were kindly provided by A. Sturm.
For immunocytochemistry on cytoplasmic sucrose synthase antibodies against the native and the denatured protein from broad bean were given by H. Ross (Ross and Davies 1992), and an antibody against the two isoforms of maize sucrose synthase was provided by KE Koch (Koch

et al. 1992). The antibody raised against the membrane-associated sucrose synthase from cotton was a donation of D.P. Delmer and Y. Amor (Amor *et al.* 1995).

RESULTS

At **5 DAP** (days after pollination) a gradient of invertase activity was observed in the basal part of the nucellus with highest activity in the placento-chalazal tissue (Fig.1-1). Invertase activity was also found in the pedicel parenchyma, where the phloem ends. A high activity was shown in the endosperm and the persisting antipodal cells. The invertase activity in the basal parts of the integuments and pericarp diminished towards the apical parts, like in the nucellus (Fig.1-1). Immunocytochemistry showed the presence of the invertases in the basal part of the nucellus and some in the epidermal cells of the endosperm. Labelling was also found in the pedicel parenchyma (Fig.1-2).

Labelling for cytoplasmic sucrose synthase showed a signal in the carpel, with more sucrose synthase in the inner and outer epidermal layers. The antibody raised against the denatured sucrose synthase of broad bean gave a stronger signal in these cells than the maize-derived antibody. In the top of the carpel, sucrose synthase was only found in the outer layer. In the base of the kernel the placento-chalazal tissue labelled, as did the phloem companion cells in the pedicel parenchyma (Fig.1-4). Membrane-associated sucrose synthase was found to label pit-fields in the epidermis of the endosperm, integuments and carpel, and in new formed cell walls of the nucellus and endosperm (Fig.1-3 and 1-5).

At **10 DAP** invertase activity was present in the basal cells of the endosperm and just reached the base of the embryo (Fig.2-1). The basal cells started to differentiate into endosperm transfer cells and showed high invertase activity (Fig.2-2). The embryo showed no invertase activity. The compressed cells of the nucellus along the side of the endosperm distal of the embryo, showed no invertase activity, but this layer continued into the chalazal part of the placento-chalazal tissue with low invertase activity. At the transition into placento-chalazal cells a bulge is formed. This bulge remained in all further developmental stages, but invertase activity in this area disappeared in later stages. The pedicel parenchyma and transport bundles showed high invertase activity. Between the placento-chalazal tissue and the pedicel parenchyma a layer of cells differentiated with less invertase activity than the pedicel cells below it (Fig.2-2). This layer becomes the closing layer in a later stage. Only the most basal part of the pericarp showed invertase activity. Invertase was found in the placento-chalazal

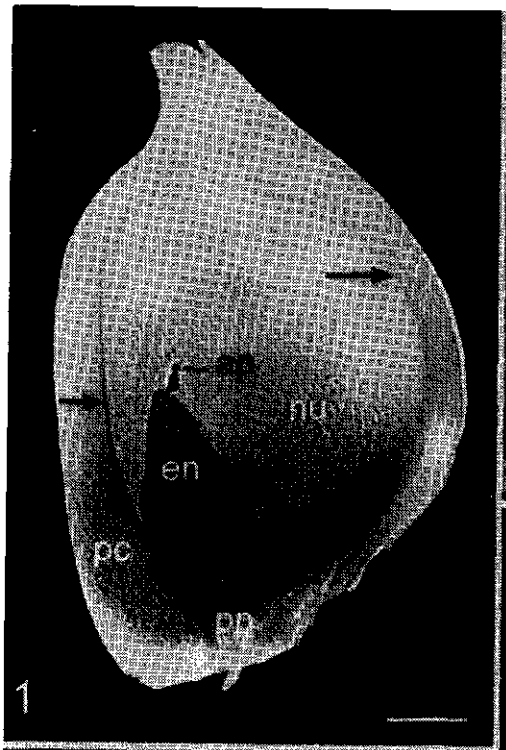
nu
en
pc
pp
1

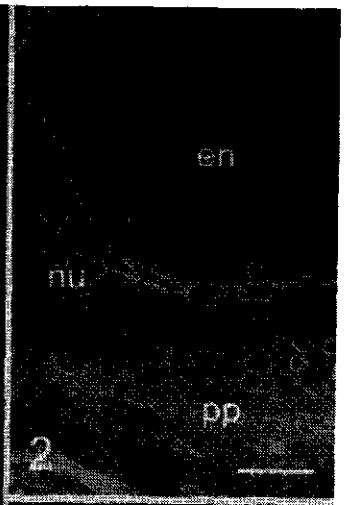
en
nu
pp
2


3A

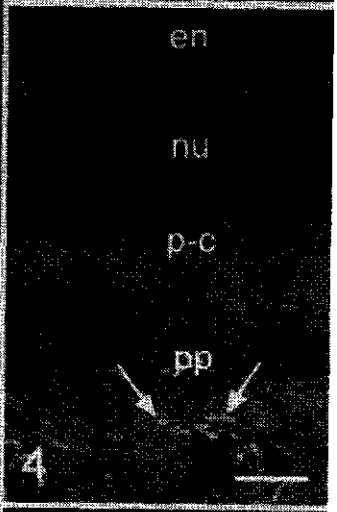
en
nu
p-c
pp
4

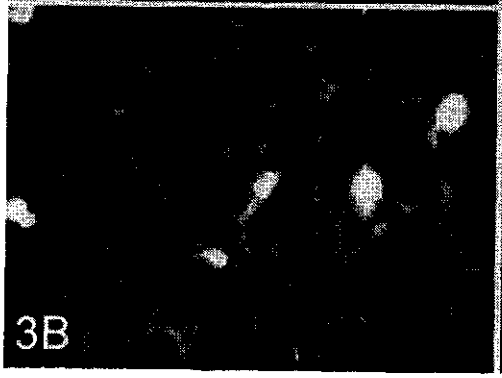
3B


nu
5

tissue mainly with the antibody against soluble acid invertase I of carrot (Fig.2-3), other invertase antibodies gave a less intense signal.

Immunocytochemistry on cytoplasmic sucrose synthases showed the presence of these enzymes in the top of the endosperm in a few layers below the epidermal layer. The endosperm epidermal layer, which will differentiate into the aleurone layer, was only labelled in the part that directly borders the pericarp (at the side of the embryo), and not in the part bordering the nucellus. The cytoplasm of the basal part of the differentiating closing layer was well labelled with the antibody against the denatured sucrose synthase of broad bean (Fig.2-6), and showed less strong labelling with the maize sucrose synthase antibody. Also the membrane-associated sucrose synthase antibody labelled this part of the closing layer. In the placento-chalazal tissue no cytoplasmic sucrose synthase was found. The antibody against the denatured sucrose synthase of broad bean also labelled some new cell walls in the endosperm. The antibody against membrane-associated sucrose synthase labelled the new cell walls of the endosperm and embryo (Fig.2-4). The cell walls of the differentiating endosperm epidermis labelled very well, as will be shown at 14 DAP (Fig.3-8). This antibody labelled also the numerous pit-fields, especially in the basal endosperm (Fig.2-7). The basal endosperm cells that had differentiated into transfer cells did not contain cytoplasmic sucrose synthase, only membrane-associated sucrose synthase (Fig.2-5).

At **14 DAP** no invertase activity was seen in the growing embryo. The embryo was partly embedded in the basal endosperm which showed high invertase activity. At this stage the closing layer and pedicel parenchyma with the transport tissues were still positive (Fig.3-1).

Invertase immunocytochemistry showed the presence of this enzyme against the walls of the endosperm transfer cells (Fig.3-2). In the apical endosperm the cytoplasm of starch storing cells was labelled, and sometimes also the cytoplasm of aleurone cells (Fig.3-3). Some label was found in the pedicel parenchyma against the closing layer.

Immunochemistry showed the presence of cytoplasmic sucrose synthase in the embryo, and in the apical cells of the endosperm (Fig.3-4). In the aleurone and sub-aleurone layer distal from

Figure 1: Maize kernels of 5 DAP

(1) Invertase activity in kernel stained dark blue. Bar = 1.5 mm. **(2)** Immunolabelling of basal nucellus (*nu*) and pedicel parenchyma (*pp*) of the kernel with the antibody raised against soluble acid invertase II. Bar = 100 µm. **(3A)** Immunolabelling on new cell walls in nucellus with the antibody against membrane-associated sucrose synthase of cotton. Bar = 30 µm. **(3B)** UV illumination of (3A), showing nuclei stained with DAPI. **(4)** Immunolabelling of basal part of the placento-chalazal tissue (*p-c*) and phloem companion cells (arrows) with the antibody raised against denatured soluble sucrose synthase of broad bean. Bar = 100 µm. **(5)** Immunolabelling in epidermis of nucellus (*nu*) and inner integument (*ii*) with the antibody against membrane-associated sucrose synthase of cotton. Bar = 20 µm.

ap = antipodal cells, en = endosperm, ii = inner integument, nu = nucellus, p-c = placento-chalazal tissue, pc = pericarp, pp = pedicel parenchyma

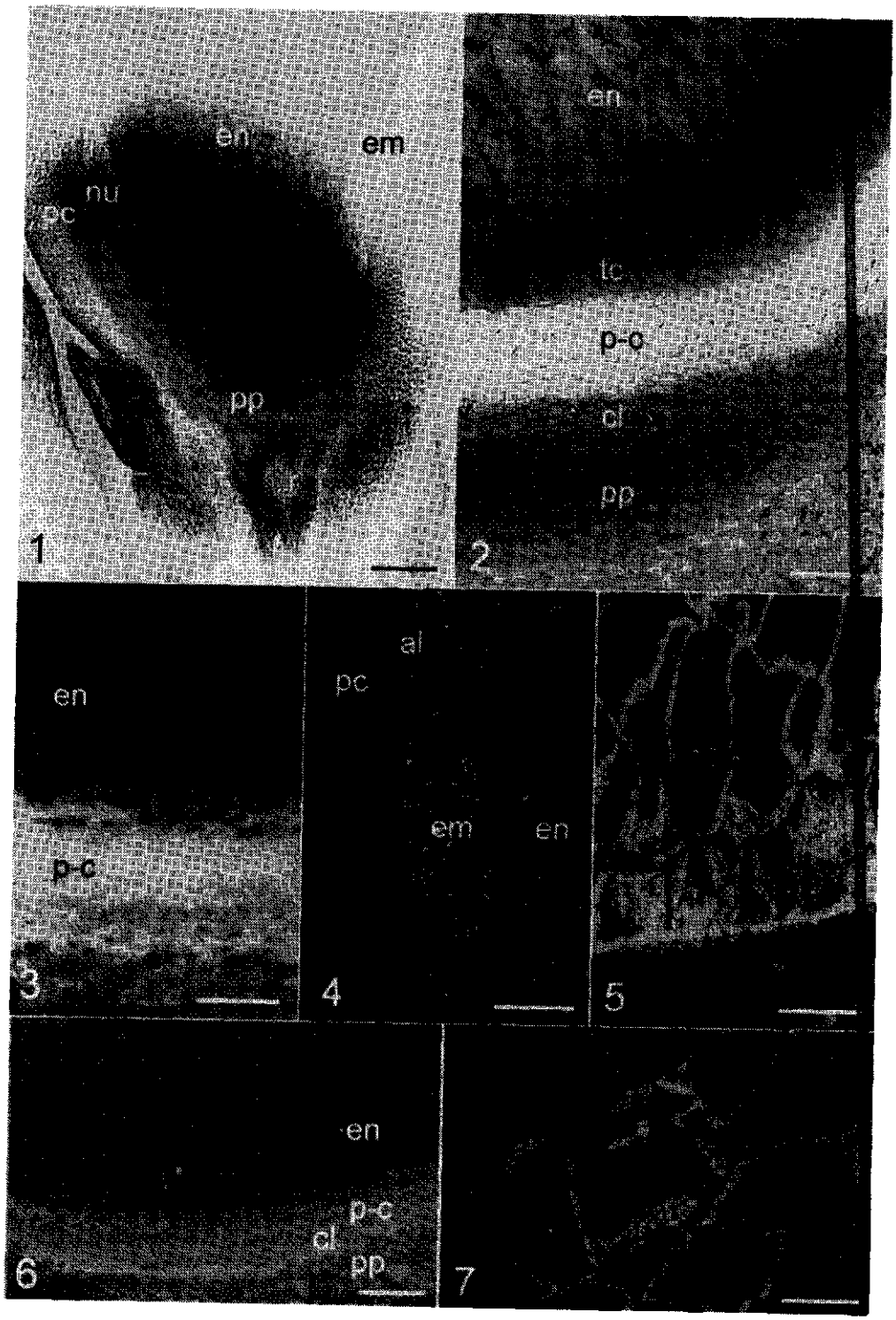
en
em
nu
pc
pp
1
en
tc
p-c
cl
pp
2
en
p-c
3
al
pc
em
en
4
5
en
p-c
cl
pp
6
7

the embryo strong labelling was found (Fig.3-5) while in the apical layers above the embryo the strongest labelling was found in the sub-aleurone cytoplasm. In these cells also densely labelled granular structures were observed (Fig.3-6). The part of the aleurone that borders the embryo contained little or no sucrose synthase while the aleurone basal of the embryo did label very well (Fig.3-7). The pericarp showed no labelling. The membrane-associated sucrose synthase was present in new cell walls of the embryo and endosperm, especially in the cell walls near the periphery of the endosperm, and in the aleurone layer (Fig.3-9). Also in some walls of the pericarp membrane-associated sucrose synthase was observed. The pedicel parenchyma labelled also very well for this form of sucrose synthase.

At **19 DAP** the basal part of the scutellum had grown closer towards the basal endosperm transfer cells and was bordered by endosperm cells with high invertase activity. The activity in the closing layer and more profound in the pedicel parenchyma and pericarp had decreased (Fig.4-1).

Immunocytochemistry with the grape invertase antibody revealed that the invertase enzyme was present not only in the transfer cells, as showed by the other invertase antibodies as well, but also in the bordering endosperm cells (Fig.4-4) and in some endosperm cells that will disintegrate later to make space for the embryo (Fig.4-2). Remarkable was the labelling by the grape invertase antibody of an excretion product of the primary root between coleorhiza and scutellum (Fig.4-3). In the closing layer much invertase was found, but no invertase was observed in the pedicel.

Cytoplasmic sucrose synthase was found to be present in most of the apical and central endosperm cells, and in the aleurone. No sucrose synthase was found immunocytochemically in the aleurone layer bordering the embryo. Unlike the maize sucrose synthase antibody, the antibody against denatured sucrose synthase of broad bean showed some labelling in the

Figure 2: Maize kernels of 10 DAP

(1) *Invertase activity (dark stained) in base of the kernel. Bar = 500 µm.* **(2)** *Detail of (1), showing high activity in transfer cells (tc) and pedicel parenchyma (pp), and low activity in closing layer (cl).* Bar = 80 µm. **(3)** Immunolabelling with the antibody raised against soluble acid invertase I of carrot gives a signal in the placento-chalazal tissue (*p-c*). Bar = 40 µm. **(4)** Cell walls in endosperm (*en*) and embryo (*em*) labelled with antibody against membrane-associated sucrose synthase of cotton. Bar = 200 µm. **(5)** Walls of basal endosperm transfer cells labelled with the antibody against membrane-associated sucrose synthase of cotton. Bar = 40 µm. **(6)** Immunolabelling of differentiating closing layer (*cl*) with an antibody against denatured sucrose synthase of broad bean. Bar = 100 µm. **(7)** *Pit fields in endosperm cell walls labelled with the antibody against membrane-associated sucrose synthase of cotton.* Bar = 40 µm.

ca = carpel, cl = developing closing layer, em = embryo, en = endosperm, nu = nucellus, p-c = placento-chalazal tissue, pp = pedicel parenchyma, tc = transfer cell

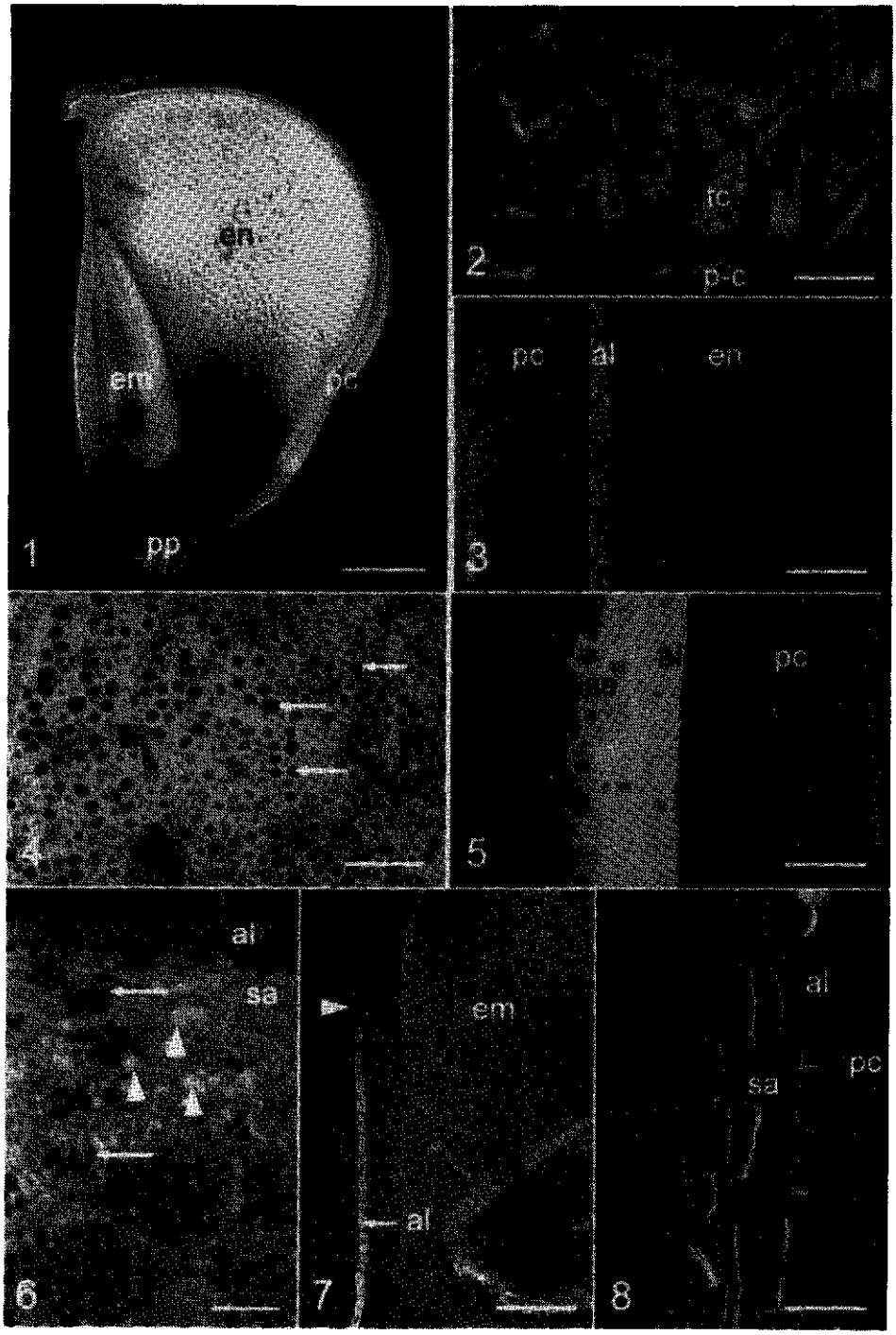
en
em
pc
1
pp
2
tc
p-c
pc
al
en
3
4
pc
5
al
sa
6
em
al
7
al
pc
sa
8

embryo cells, especially in the primary root and coleorhiza, as will be shown at 28 DAP (Fig.5-5). Membrane-associated sucrose synthase was predominantly found in the embryo and, at a lower level, in the scutellum. The membranes of the endosperm transfer cells were labelled, like the membranes of the periphere endosperm and endosperm cells near the embryo (Fig.4-5).

At **28 DAP** the results of the invertase histochemistry and immunocytochemistry were similar as described for 19 DAP (Fig.5-1). The only difference with 19 DAP was found with the use of the grape invertase antibody. This grape antibody also gave a strong labelling in the aleurone cells (Fig.5-2).

The labelling on cytoplasmic sucrose synthase showed the presence of sucrose synthase in some apical and middle endosperm cells while their bordering cells often did not label much (Fig.5-3). The aleurone was almost negative, only the antibody against denatured sucrose synthase of broad bean showed more label in the basal aleurone. The broad bean antibody also showed labelling in the coleorhiza of the embryo, and in seminal roots (Fig.5-5). The antibody against membrane-associated sucrose synthase was found to label plasmodesmata and pit fields in nearly all endosperm cell walls, but especially in the radial aleurone walls (Fig.5-4 and Fig.5-6).

At **42 DAP** the invertase results showed a similar activity pattern in the base of the kernel as described for 19 DAP. Immunolabelling for invertase or sucrose synthase was not performed. The sucrose synthase assay did not show any activity of the enzyme (not shown).

The results obtained by histochemical and immunocytochemical experiments on invertase and sucrose synthase are summarized in Figure 6.

Figure 3: Maize kernels of 14 DAP

(1) Invertase activity (dark stained) in basal part of the kernel. Bar = 2 mm. **(2)** Immunolabelling of basal endosperm transfer cells with the antibody raised against carrot cell wall invertase. Bar = 40 μm. **(3)** Immunolabelling of aleurone (*al*) and endosperm (*en*) cells, apical of embryo, with the antibody against grape soluble invertase. Bar = 40 μm. **(4)** Strong label in cytoplasm around starch granules (arrows) with the antibody against denatured sucrose synthase of broad bean. Bar = 40 μm. **(5)** The antibody against denatured sucrose synthase of broad bean labelled aleurone (*al*) and sub-aleurone (*sa*) distal of embryo. Bar = 15 μm. **(6)** The antibody raised against maize sucrose synthase gave stronger labelling of sub-aleurone (*sa*) cytoplasm than aleurone (*al*) cytoplasm in cells apical of embryo. Granule like structures labelled strong in sub-aleurone cells (arrow-heads). Bar = 25 μm. **(7)** The antibody raised against maize sucrose synthase labelled aleurone basal of embryo (*al*), but not the part that borders the embryo (arrow-head). Bar = 100 μm. **(8)** Aleurone (*al*) and sub-aleurone (*sa*) cell walls labelled with the antibody raised against membrane-associated sucrose synthase of cotton. Bar = 40 μm.

al = aleurone, em = embryo, en = endosperm, p-c = placento-chalazal tissue, pc = pericarp, pp = pedicel parenchyma, sa = sub-aleurone, tc = transfer cell

DISCUSSION AND CONCLUSIONS

Sucrose synthase and invertase are localized in this study to determine where sink tissues are present with high and low sink strength. This information can help to understand carbohydrate movement during kernel development.

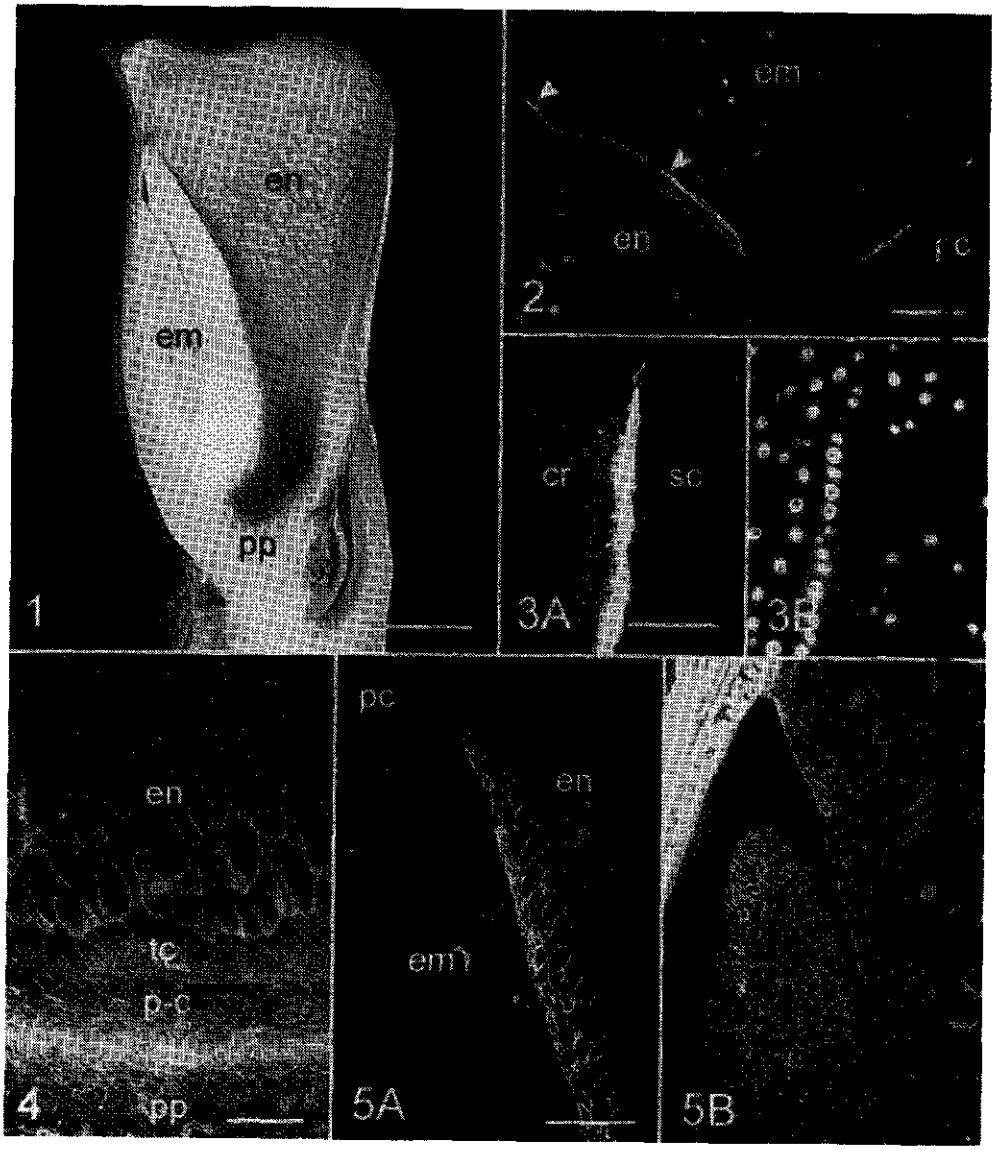

SPOROPHYTIC TISSUE:

Nucellus

At 5 DAP the chalazal part of the nucellus showed activity of invertase while also a gradient of sucrose synthase activity was found in the basal nucellus towards the apical part (Fig.6). In the present study, invertase could be detected by immunocytochemistry, but cytoplasmic sucrose synthase could not be found by this method (Fig.6). Apparently the histochemical localization of sucrose synthase activity is more sensitive for low enzyme concentrations than the immunocytological localization technique (Wittich and Vreugdenhil 1998). A function for the soluble invertase might be in the growth and carbohydrate import activity of the nucellus during this first week of kernel development (Xu *et al.* 1996).

The membrane-associated sucrose synthase was found in some new cell walls of the nucellus, showing that there are still cell divisions in the nucellus at this stage. In the new formed nucellus walls also callose was found (not shown). This supports the suggestion by Amor *et al.* (1995) that the membrane-associated sucrose synthase is correlated with both cellulose synthesis and callose synthesis in the cell wall. They also reported sucrose synthase being located at the cell plate of *Zinnia* where callose is synthesized. In this study the antibody against membrane-associated sucrose synthase also labelled plasmodesmata and pit fields. At these places callose was found too (not shown), indicating again that the membrane-associated sucrose synthase is correlated with callose synthesis. Carlson and Chourey (1996) reported that they found both forms of maize sucrose synthase, SS1 and SS2, also in membrane-associated forms. It is likely that the cotton antibody used in the present study label both these membrane-associated sucrose synthase isozymes in the maize kernel.

After 5 DAP the nucellus disintegrated and was consumed by the growing endosperm.

Figure 4: Maize kernels of 19 DAP

(1) Invertase activity (dark stained) in basal tissues kernel. Bar = 2 mm. **(2)** Disintegrating endosperm cells (arrowheads) bordering the embryo (*em*) labelled with the antibody raised against soluble invertase of grape. Bar = 100 µm. **(3A)** The antibody against soluble invertase of grape labelled excretion product of primary root. Bar = 150 µm. **(3B)** UV-illumination of (3A) showing DAPI image of nuclei. **(4)** Immunolabelling of most basal cells of kernel with the antibody raised against soluble invertase of grape, but most intense labelling in basal endosperm cells (*en*) and closing layer (*cl*). Bar = 100 µm. **(5A)** Endosperm walls (en) near the apical part of the embryo (*em*) labelled with the antibody against membrane-associated sucrose synthase of cotton. Bar = 200 µm. **(5B)** UV-illumination of (5A) showing nuclei and cell walls.

cr = coleorhiza, em = embryo, en = endosperm, p-c = placento-chalazal tissue, pc = pericarp, pp = pedicel parenchyma, sc = scutellum, tc = transfer cell

Placento-chalazal tissue

The placento-chalazal tissue, between the nucellus and the pedicel parenchyma, started to disintegrate around 10 DAP and had lost all invertase and sucrose synthase activity at 14 DAP. From the immunocytochemical results described in the present study it seems that in the placento-chalazal tissue mainly soluble invertase is present.

During further kernel development this layer functions as a large apoplastic space between pedicel parenchyma and endosperm through which all the carbohydrates for the endosperm have to be transported, and might even function as a storage buffer for sugars (Schel *et al.* 1984). It is remarkable that the placento-chalazal tissue did not show cell wall invertase activity after disintegration, while the closing layer at the chalazal side of the placento-chalazal tissue did show this activity after disintegration.

Pedicel

In the pedicel the vascular bundles divide and terminate. Above the "cup" of vascular tissue are a few layers of thin-walled pedicel parenchyma cells. The cells of the pedicel parenchyma and/or the lower placento-chalazal tissue gradually form a closing layer of compressed and dead cells (Felker and Shannon 1980). From the pedicel symplast sucrose is unloaded into the apoplast. This unloading might be via simple or facilitated diffusion.

The invertase activity data from this study are in coherence with results from Doehlert *et al.* (1988), showing that invertase maintains its activity in the pedicel throughout the development of the kernel from 5 DAP, till 30 DAP (Fig.6), although it decreased in activity during maturation of the kernel. Immunocytological localizations suggest that the activity that is shown results from the cell wall invertase. This cell wall invertase is isoform-1

Figure 5: Maize kernels of 28 DAP)

(1) Invertase activity (dark stained) in basal part of kernel. Bar = 800 μm. **(2A)** Immunolabelling in apical aleurone cells (*al*) with the antibody raised against soluble invertase of grape. Bar = 40 μm. **(2B)** UV-illumination of (2A) showing nuclei and cell walls. **(3)** Apical endosperm cells labelled with the antibody against denatured sucrose synthase of broad bean. The cytoplasm of some cells labelled strong while others were almost negative (asterix). Bar = 100 μm. **(4A)** Plasmodesmata in walls of endosperm cells (*en*) and aleurone (*al*) in the middle of the kernel, labelled with the antibody against membrane-associated sucrose synthase of cotton. Bar = 40 μm. **(4B)** UV-illumination of (4A) showing nuclei and cell walls. **(5)** The antibody against denatured sucrose synthase of broad bean labelled the seminal roots (*sr*). Bar = 200 μm. **(6A)** The antibody against membrane-associated sucrose synthase of cotton labelled plasmodesmatal openings against the radial walls of apical aleurone cells (*al*). Bar = 80 μm. **(6B)** UV-illumination of (6A) showing nuclei and cell walls.

al = aleurone, en = endosperm, pc = pericarp, pp = pedicel parenchyma, sc = scutellum, sr = seminal root

(CWI-1)(Cheikh and Jones 1995). The sucrose hydrolyzing activity is likely to play a role in enhancing the phloem unloading, although Cheng *et al.* (1996) could not detect a clear function for this invertase isoform. They suggest that the cell wall invertase isoform 2 (CWI-2) in the basal endosperm is critical for transport of sucrose into the endosperm.

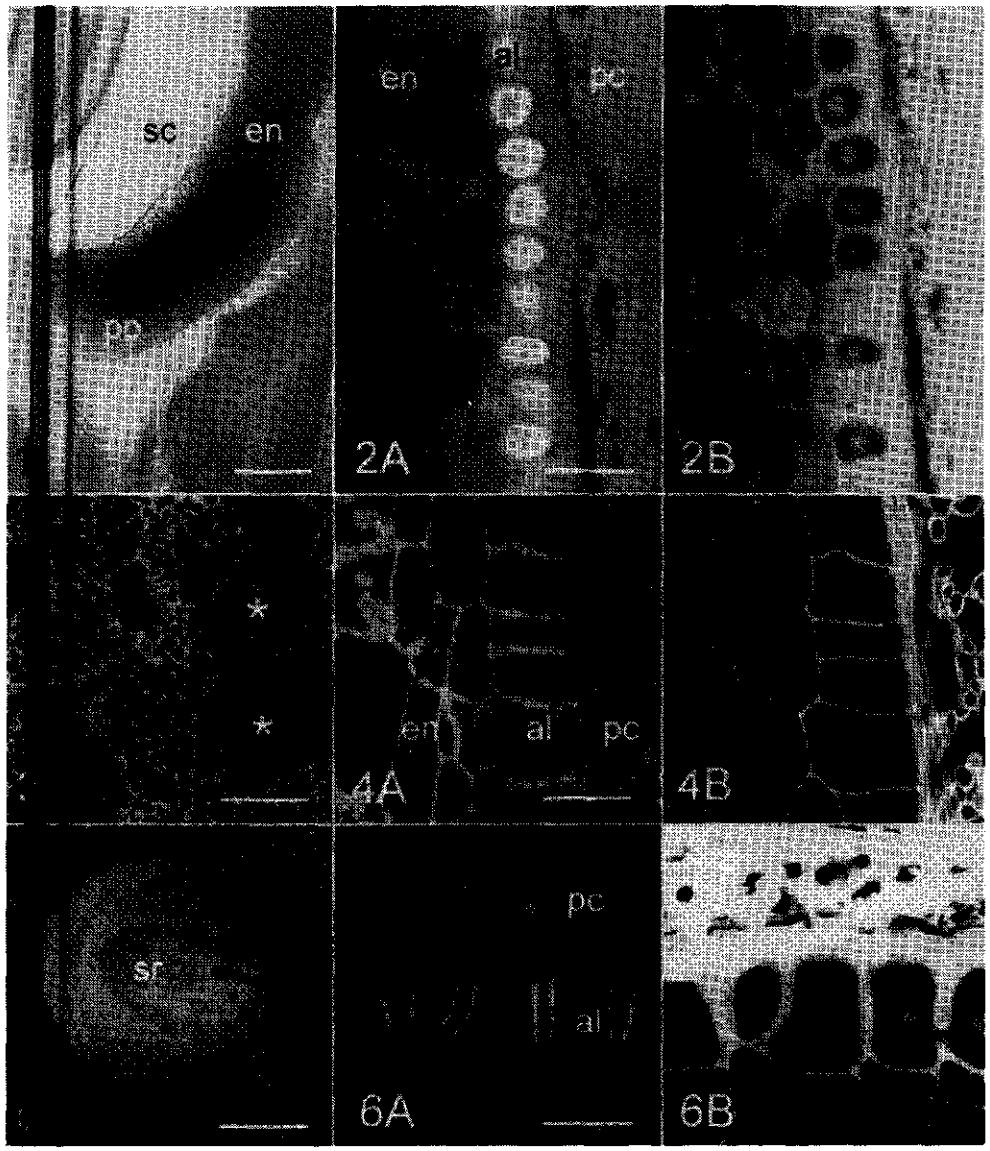

Closing layer

The closing layer started to develop between the placento-chalazal tissue and the pedicel parenchyma as early as 10 DAP. This was shown by the deviating invertase activity as compared to the pedicel parenchyma and placento-chalazal tissue. Invertase activity remained in this layer during all stages of kernel development. According to the results of Cheikh and Jones (1995) this should be invertase isoform CWI-1. Using enzyme extraction methods Cheikh an Jones (1995) concluded that the activity of the CWI-1 invertase in pedicel and closing layer increased gradually between 12 and 30 DAP. This increase could not be confirmed with the activity results presented in this study. From their results also only cell wall invertase was expected in the closing layer at 19 DAP, but labelling of these cells with the antibody against soluble grape invertase may be explained by the non-specificity of the antibody.

Immunocytochemistry showed cytoplasmic sucrose synthase to be present in the pedicel parenchyma cells which differentiate into the closing layer before 19 DAP. Sucrose synthase activity was found in these cells until 19 DAP (Wittich and Vreugdenhil 1998). This suggests that sucrose synthase is still present at 19 DAP, but the concentration is too low to detect with immunocytochemical methods. After 19 DAP the cell degenerate.

The sucrose synthase that was found in the pedicel and closing layer during this study might be needed for respiratory uses. Chen and Chourey (1989) determined that these are SS2 sucrose synthases.

Figure 6

A. Sucrose synthase histochemistry results on developing maize kernels, (as published elsewhere: Wittich and Vreugdenhil 1998, in this thesis chapter 2), showed locally a high activity of the enzyme in the endosperm. The activity in the embryo bordering aleurone cells was lost at 14 DAP, while the aleurone cells which border the inner endosperm cells had lost their activity at 28 DAP. A lower activity of sucrose synthase was found in the pedicel, basal part of the carpel, endosperm and embryo. Only, the epithelium of the scutellum showed a high enzyme activity.

B. Cytoplasmic sucrose synthase was localized by immunocytochemistry, detecting a high concentration of this enzyme in the pedicel and basal part of the carpel at 5 and 10 DAP.

C. Invertase histochemistry showed a high activity in the basal part of the kernel. Only in the placento-chalazal tissue enzyme activity was gradually lost after 10 DAP. At 5 DAP the nucellus showed some activity.

D. Invertase was localized by immunocytochemistry. All localized isoforms are summarized together in this figure. In the basal part of the kernel the labelling coincided with the detected activity.

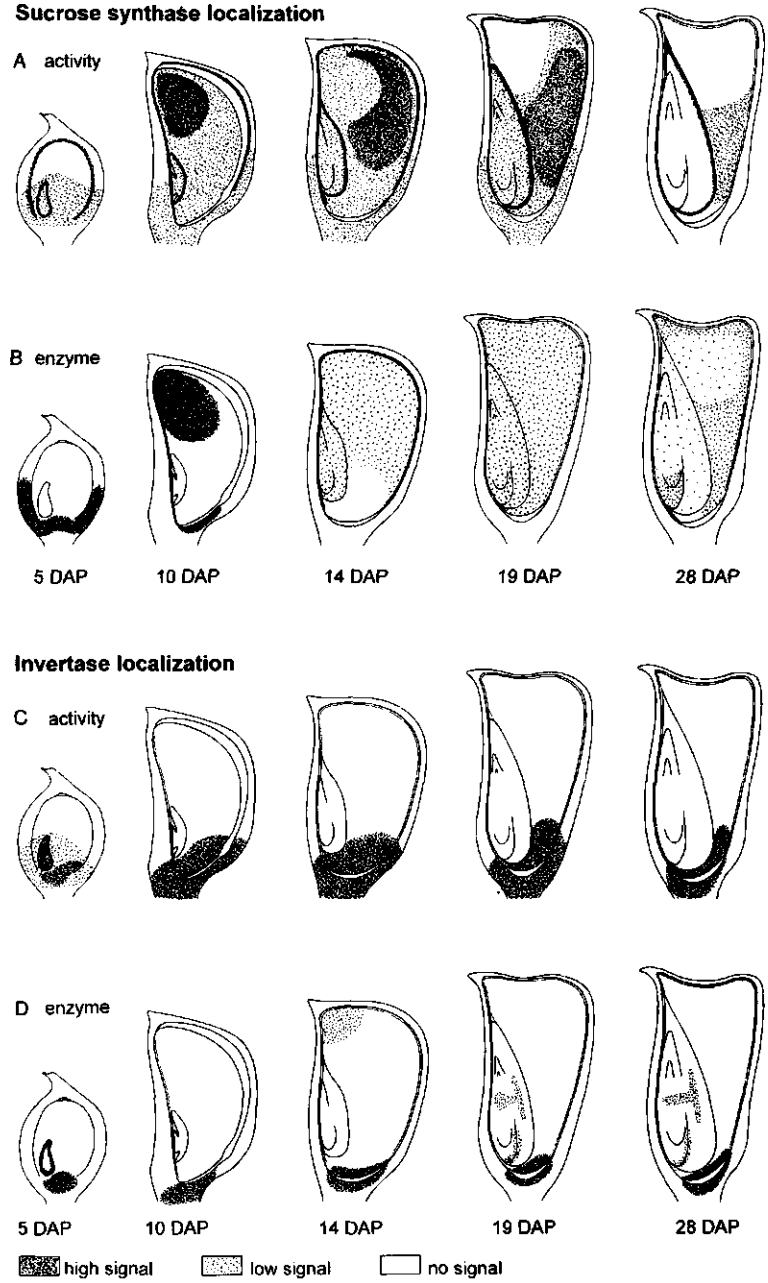

Figure 6: Summary of sucrose synthase and invertase localization results.

GAMETOPHYTIC DERIVED ORGANISMS:

Endosperm

At 5 DAP invertase activity was found in all endosperm cells, but from 10 DAP on the activity was found only in the basal part of the endosperm (Fig.6). This basal endosperm invertase activity seemed to increase till 14 DAP, as the kernel had grown to its maximum size. The histochemical assay indicated a rather constant apoplastic invertase activity in the basal endosperm after 14 DAP.

The transfer cells at the base of the endosperm started to differentiate at 10 DAP and showed invertase activity on the cell wall ingrowths. These ingrowths enhance the uptake capacity of the cell by enlarging the membrane surface (Davis *et al.* 1990, Pate and Gunning 1972). Immunocytochemistry showed that the wall-bound carrot invertase antibody labelled the membrane bordering part of the transfer cell walls, as was also shown by Cheng *et al.* (1996). In the present study it is shown that the soluble carrot invertase antibodies labelled also the cell wall borders in the two-cell thick layer of endosperm transfer cells. The carrot antibodies apparently label the cell wall invertase of maize, but do not recognise the soluble isoforms. The grape invertase antibody labelled besides the endosperm transfer cell walls also the non-transfer basal endosperm cells. These cells showed also invertase activity in the histochemical assay. Hence, the grape invertase antibody is the best alternative antibody for labelling maize invertases when maize invertase antibodies are not available.

In this study the total volume of basal endosperm cells with invertase activity increased till 14 DAP. These findings are coherent with the increasing amount of invertase found in this tissue by Zinselmeier *et al.* (1995). The activity of invertase in the basal endosperm suggests that not all the sucrose which is unloaded from the phloem, is hydrolysed in the pedicel and closing layer. It seems that a lot of the sucrose still has to be hydrolysed in the basal endosperm cells before it can be imported into the symplast of the endosperm cells. By using other methods, Zinselmeier *et al.* (1995) found that probably all the sucrose has to be hydrolysed prior to uptake into the endosperm symplast, although some sucrose can be taken up by the endosperm (Cobb and Hannah 1986, Schmalstig and Hitz 1987). The glucose and fructose uptake into the endosperm symplast is probably via hexose symporters (Patrick 1997). The activity of the invertase in these basal endosperm cells also helps to maintain the sucrose gradient from pedicel towards the endosperm, enhancing the phloem unloading and transport of sucrose towards the endosperm.

After uptake of the monosaccharides into the symplast of the basal endosperm cells sucrose is probably resynthesized (Chourey *et al.* 1995, Griffith *et al.* 1986, Shannon 1972, Shannon *et al.* 1986). The sucrose is transported further through the symplast towards the apical endosperm cells, where it is utilized for the synthesis of starch, lipids and proteins, for

respiratory purposes, and for cell wall synthesis. A considerable symplastic transport capacity of these basal endosperm cells is indicated by the large number of pit fields found in the cells walls by labelling of membrane-associated sucrose synthase.
In this study cytoplasmic sucrose synthase was found to be present immunocytochemically in the apical endosperm at 10 DAP (Fig.6), a few cell layers inwards from the epidermis. The enzymes localized are of the SS1 isoform of sucrose synthase and related to starch synthesis (Chen *et al.* 1989, Chourey and Nelson 1976, Heinlein and Starlinger 1989). The activity of these enzymes is also shown by enzyme histochemistry, occurring first in the apical endosperm, moving gradually towards the basal endosperm, and increasing from the periphery to interior endosperm (Fig.6) (Wittich and Vreugdenhil 1998). Although by histochemical localization the activity in the apical endosperm decreased after these cells were filled with starch, immunocytochemistry showed that the protein is still present. It is concluded that these enzymes are probably inactivated (Wittich and Vreugdenhil 1998).

The epidermis of the endosperm started to differentiate into aleurone cells at the moment that the nucellus between the endosperm and integument remnants disintegrated. This started (at 10 DAP) at the side of the embryo. These differentiated epidermal cells labelled well for cytoplasmic sucrose synthase which is likely the SS2 isoform (Chen and Chourey 1989). However, a few days later the amount of sucrose synthase in the single aleurone layer between embryo and nucellar remnants decreased. Histochemistry showed loss of sucrose synthase activity in these cells while in the rest of the aleurone activity was found till 19 DAP (Fig.6) (Wittich and Vreugdenhil 1998). The loss of activity might be related to the fact that these cells do not border endosperm cells. As a result there is likely only a limited supply of sucrose via the bordering aleurone cells. This may cause a low sucrose concentration in these cells and no need for high sucrose synthase activity. On the other hand these cells do not have a function in the development of the endosperm, which might be the reason for low sucrose synthase activity. At 28 DAP the sucrose synthase activity (Wittich and Vreugdenhil 1998) and its presence was lost in most parts of the aleurone. Only in the basal aleurone cells the enzyme persisted, but apparently not active any more.
The activity of this SS2 isoform of sucrose synthase in aleurone and sub-aleurone (Chen and Chourey 1989) is suggested to be related with the synthesis of protein granules, lipid synthesis, or wall thickening of these cells (Heinlein and Starlinger 1989, Wittich and Vreugdenhil 1998). Sucrose can be transported symplastically via the endosperm, or via the neighbouring aleurone cells, to the apical aleurone cells, where they will be utilized by the sucrose synthase. Aleurone cells have many plasmodesmatal contacts as was shown by the localization of membrane-associated sucrose synthase. But via these pathways, and via the apoplast, also

monosaccharides might be transported to the aleurone cells. There the monosaccharides may be used for resynthesis of sucrose by sucrose synthase. Thus, it remains not clear from the present study whether *in vivo* the sucrose synthase is active in the direction of sucrose synthesis, or in sucrose breakdown.

In the present study no change in strongest immunolabelling signal for sucrose synthase was found from aleurone to the sub-aleurone, as Heinlein and Starlinger (1989) reported at the moment of morphological differentiation of these cell layers at 23 DAP. During differentiation the aleurone cells become cuboidal shaped while the sub-aleurone cells flatten.

Interesting is the strong labelling of the aleurone cytoplasm with the grape invertase antibody at 28 DAP when the layer is fully developed. The invertase assay shows that these enzymes are not functional. However, it is possible that they become activated during seed imbibition.

Embryo

The embryo is simplastically isolated from the endosperm and it is known that the sugars absorbed by the embryo are monosaccharides rather than sucrose (Griffith *et al.* 1987). The embryo takes up the monosaccharides from the cavity between embryo and endosperm (Doehlert *et al.* 1988) of which the basal part borders invertase-active endosperm cells. It is likely that all the sucrose is already hydrolysed in the endosperm apoplast before it enters the cavity, although some sucrose may leak through. This way the symplast of the endosperm plays no direct role in the nutrient supply to the embryo.

In the embryo no invertase activity was detected by the histochemical assay, confirming earlier results by Doehlert and Felker (1987) and Miller and Chourey (1992). Immunocytochemistry with the grape invertase antibody showed that the primary root and adventitious roots excrete a substance that contains invertase. This invertase might play a role during seed imbibition since it is not active during seed development as was shown by the histochemical assay (Fig.6).

Sucrose synthase histochemistry showed low activity of the enzyme in all tissues of the embryo and a high activity in the epithelium of the scutellum (Fig.6) (Wittich and Vreugdenhil 1998). Immunochemistry did not confirm the presence of high levels of cytoplasmic sucrose synthase in the epithelium. However, Heinlein and Starlinger (1989) reported high amounts of SS2 sucrose synthase in the epithelium of the scutellum as these cells differentiate at 30 DAP, and in the plumule-radicle axis. In the present study the epithelial cells differentiate already at 14 DAP. This may explain the earlier activity that was found. Relatively higher amounts of sucrose synthase in the embryo could be detected only in and around the roots. Chen and Chourey (1989) detected a much lower signal in the scutellar region than in the coleoptile, primordial leaves and coleorhiza at 16 DAP. The sucrose degradation by sucrose synthase is probably for the energy supply for these growing organs.

Since the embryo accumulates sucrose and not monosaccharides, resynthesis of sucrose is expected by SPS (Griffith *et al.* 1986), like described for the endosperm.

MEMBRANE-ASSOCIATED SUCROSE SYNTHASE

The membrane-associated sucrose synthase was found with immunocytochemistry during all developmental stages of the kernel. The antibody labelled new cell walls, especially in the embryo, and in the periphery of the endosperm.

Next to the membrane-associated sucrose synthase also callose was found (not shown). This suggests that the membrane-associated sucrose synthase is correlated with callose synthesis in the secondary wall as postulated by Amor *et al.* (1995). They also report sucrose synthase being located at the cell plate of *Zinnia* where callose is synthesized.

In this study the antibody also labelled plasmodesmata and pit fields. They were found abundant in the basal endosperm, in the disintegrating endosperm cells bordering the basal part of the embryo, and in the radial cell walls of the aleurone. At all these locations callose was found present, suggesting that the membrane-associated sucrose synthase is correlated with callose synthesis.

Carlson and Chourey (1996) reported both isoforms of maize sucrose synthase, SS1 and SS2, also in a membrane-associated form. It is likely that the cotton antibody used in the present study labels both these membrane-associated sucrose synthase isoforms in the maize kernel.

ACKNOWLEDGEMENTS

I would like to thank MTM Willemse, AAM van Lammeren and D Vreugdenhil for reading this chapter critically , and S Massalt, AB Haasdijk and PA van Snippenburg for the artwork. My gratitude goes to DP Delmer, KE Koch, H Ross, HP Ruffner, A Sturm, for giving me the antibodies for this research, and J van Dongen for his technical assistance.

REFERENCES

Amor Y, CH Haigler, S Johnson, M Wainscott and DP Delmer (1995) A membrane-associated from sucrose synthase and its potential role in synthesis of cellulose and callose in plants. Proc Natl Acad Sci USA 92, 9353-9357

Avigad G (1982) Sucrose and other disaccharides. In Plant carbohydrates. I. Intracellular carbohydrates. Loewus FA and W Tanner (eds). Encyclopedia of Plant Physiology 13a. New Series. Springer-Verlag, Berlin: 217-347

Baskin TI, CH Busby, LC Fowke, M Sammut and F Gubler (1992) Improvements in immunostaining samples embedded in methacrylate: localization of microtubules and other antigens throughout developing organs in plants of diverse taxa. Planta 187: 405-413

Carlson SJ an PS Chourey (1996) Identification of plasma membrane-associated forms of maize sucrose synthase. Plant Physiol 111: 99

Cheikh N and RJ Jones (1995) Heat stress effects on sink activity of developing maize kernels grown in vitro. Physiol Plant 95: 59-66

Chapter

4

Carbohydrates in developing ovules of *Gasteria verrucosa* (Mill.) H. Duval: sucrose synthase and invertase localization and activity

P.E. Wittich

Summary. The development of the anatropous ovule of *Gasteria verrucosa* is studied with respect to the degradation of carbohydrates. Histochemical assays are used to visualize the activity of the two sucrose degrading enzymes sucrose synthase and invertase. The results indicate where sucrose is metabolized in the ovule, and a distribution pattern for sucrose can be deducted. Besides the enzyme histochemical localization, immunocytochemical localizations are performed for sucrose synthase and invertase. This technique is more isoform-specific and can also localize inactive enzymes.

The developing megaspores of *Gasteria* use sucrose for the callose synthesis around the tetrad, as is monitored by immunolabelling on membrane-associated sucrose synthase. Sucrose synthase seems to be involved in the resynthesis of sucrose from the degradation of callose and the three non-functional megaspores. Cytoplasmic sucrose synthase shows sucrose degrading activity in the nucellus, integuments, and arillus during their growing phase, while not much activity was found in the mature ovule. The invertase activity was only detected in the mature ovule. The stored glucose in the nucellus and integuments only partly coincides with the invertase activity. Glucose is localized in typical ring shaped patterns in the nucellus around the embryo sac, and may influence late embryo sac development and early seed development.

After the tetrad stage the nucellus starts to form an hypostase at the chalazal side of the developing embryo sac. This hypostase seems to alter the nutrient pathway towards the embryo sac from chalazal to more micropylar directed. This change in nutrient flow may be important for the polarized development of the embryo sac.

INTRODUCTION

Gasteria verrucosa (Mill.) H. Duval forms an anatropous ovule with a two cell layer thick inner integument and a three cell layer thick outer integument. The ovule is tenuinucellar and forms a cup-shaped hypostase of lignified cell walls during the final stages of ovule development (Willemse 1981). The embryo sac develops according to the *Polygonum* type.
During early developmental stages of megasporogenesis a nutrient flow exists from the chalaza to the micropylar tissues. Till the dyad stage nutrients are more or less equally distributed throughout the ovule. Lignification of the hypostase may change this nutrient flow in the nucellus (Willemse 1981). In the central-chalazal part of the nucellar tissue high amounts of proteins, amino acids, lipids, peroxidases and phosphatases are found after the dyad stage, and in the megaspore high amounts of starch and lipids (Willemse and Bednara 1979). Changes in the nutrient flow and development of the nucellar tissue can partly explain the polarity in the development of the embryo sac. This polarity is the result of tissue interaction between megagametophyte and the ovule as part of the sporophyte (Willemse 1981).

Developing ovules and seeds of *Gasteria* do not contain any photosynthetically active tissues. Therefore they are true sinks, absorbing nutrients which are supplied via the placental tissue. In most plants sucrose is the main carbohydrate that is transported through the phloem into a sink tissue. To utilize sucrose for cell growth, maintenance and synthesis of storage products, most of the sucrose has to be hydrolysed. The two enzymes responsible for the sucrose breakdown are invertase (β-D-fructofuranoside fructohydrolase, EC 3.2.1.26) and sucrose synthase (UDP-D-glucose:D-fructose 2-α-glucosyltransferase, EC 2.4.1.13). Invertase catalyses the hydrolysis of sucrose into glucose and fructose, and sucrose synthase a reversible reaction of sucrose and uridine diphosphate (UDP) into UDP-glucose and fructose. The activity of both enzymes is often used as an indicator for sink strength (Ho *et al.* 1991, Sun *et al.* 1989, 1994).
The activity and function of sucrose synthase and invertase during ovule development is not well studied, more is known about their function during seed development. Neither much is known of the carbohydrate distribution in developing ovules, but Willemse and Franssen-Verheijen (1988) demonstrated zones with high glucose concentrations around the hypostase and micropylar nucellar cells in mature unfertilized *Gasteria* ovules. In the present study the activity and presence of sucrose synthase and invertase during ovule development of *Gasteria* is demonstrated on sections. The results are discussed in the context of carbohydrate distribution during ovule development.

MATERIAL AND METHODS

Plants of a self-incompatible hybrid population of *Gasteria verrucosa* (Mill.) H. Duval were grown in the greenhouse at temperatures between 18 and 25°C. Flower buds of different developmental stages were collected and the ovaries were dissected.

Invertase histochemistry:

Invertase activity localization was performed according the protocol of Doehlert and Felker (1987). Fresh ovaries were sectioned, 1mm thick by hand, or 200μm thick with a sledge microtome. The sections were fixed for 1 hour in 2% paraformaldehyde with 2% polyvinylpyrrolidone and 0.005M dithiotreitol, pH 7.0, at 4°C. After fixation the sections were rinsed in 50ml water over at least 10 hours, and refreshed at least 5 times. The sections were incubated in an incubation mixture of 0.024% nitro blue tetrazolium, 0.014% phenazine methosulfate, 25 units glucose oxidase and 1% sucrose in 0.38M sodium phosphate (pH 6.0), for 30 minutes at 30°C. After terminating the reaction by rinsing the sections in water, the sections were stored in 15% ethanol at 4°C. In the control reaction sucrose was omitted from the incubation mixture. The unreacted nitro blue tetrazolium stained the tissue pink while glucose production by invertase activity resulted indirect in the precipitation of a blue formazan salt.

Sucrose synthase histochemistry:

For the localization of sucrose synthase activity, ovaries were sectioned 200 μm thick with a sledge microtome, fixed and rinsed as described above for the invertase histochemistry. The incubation mixture was according to the protocol of Wittich and Vreugdenhil (1998). After incubation, the sections were rinsed with water and stored in 15% ethanol.

The sections were studied using a Wild dissecting microscope and a Nikon Optiphot, in bright field mode. Photographs were taken with a digital Panasonic wv-E550 Colour Video Camera.

Immunocytochemistry:

For localising the presence of invertase and sucrose synthase by immunocytochemistry, ovaries were fixed in 4% paraformaldehyde in 0.005M phosphate buffer, pH 7.2. They were rinsed two times in 0.1M buffer, dehydrated in ethanol series and infiltrated in gradient steps of butyl-methyl methacrylate (BMM) according to Baskin *et al.* (1992). Polymerization occurred in Eppendorf capsules, at minus 10°C with 2x 8W UV-lamps (Philips) on 15cm distance. Sections of 3 μm were made with a Reichert Ultramicrotome, stretched on water and dried on microscope slides at 60°C for 1 hour. The BMM was removed by rinsing in acetone for 15 minutes. The sections were washed in phosphate buffered saline (PBS) and blocked with 0.1M hydroxylamoniumchloride and 1% bovine serum albumine (BSA). Incubation with the first

antibody was overnight at 4°C. The sections were washed with 0.1% acetylated BSA in PBS and incubated with a second antibody which was labelled with the fluorescent dye FITC or Cy3, for 2 hours at 30°C. After rinsing with PBS, the sections were mounted with DAPI containing Citifluor. A Nikon Labophot with appropriate filter sets was used to study the sections. Photographs were taken on diapositive slides and digitized afterwards.

For the invertase immunocytochemistry an antibody against soluble grape invertase was given by H.P. Ruffner (Ruffner *et al.* 1995), an antibody against a synthetic invertase polypeptide part with high homologies with various plant species and with soluble and wall-bound invertase was kindly provided by A.H. Kingston-Smith (Kingston-Smith and Pollock 1996), and antibodies against carrot cell wall invertase (Laurière *et al.* 1988), and two carrot soluble invertases (Unger *et al.* 1992) were donated by A. Sturm. For immunocytochemistry on cytoplasmic sucrose synthase an antibody against the two isoforms of maize sucrose synthase was given by KE Koch (Koch *et al.* 1992), and antibodies against the native and the denatured protein from broad bean were a donation by H. Ross (Ross and Davies 1992). An antibody raised against the membrane-associated sucrose synthase from cotton was provided D.P. Delmer and Y. Amor (Amor *et al.* 1995). Localization of callose was performed with an antibody against β-1,3 oligosaccharides (Genosys Biotechnologies) (Northcote *et al.* 1989).

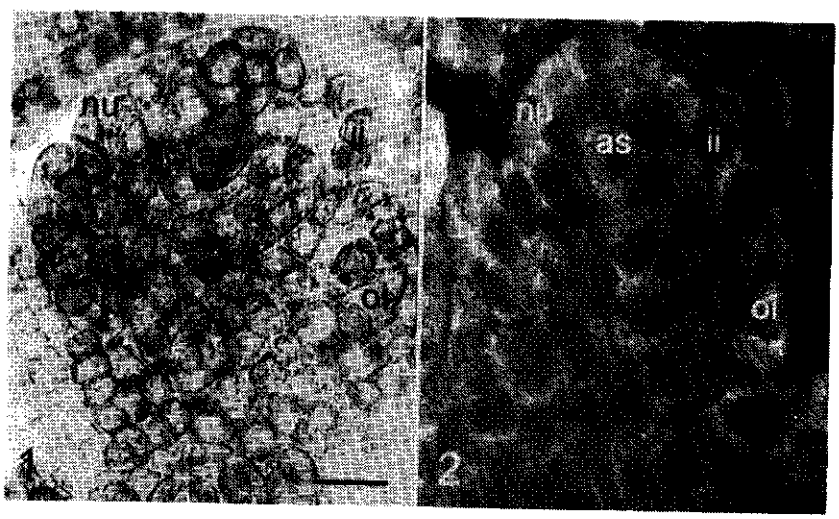

Figure 1: Archespore stage. **(1)** Sucrose synthase activity in archespore (*as*), nucellus (*nu*) and developing inner integuments (*ii*) and outer integuments (*oi*) shown by the precipitation of formazan (dark granules). Bar = 30 μm.. **(2)** Immunolabelling in archespore (*as*), nucellus (*nu*) and developing inner integuments (*ii*) and outer integuments (*oi*) with an antibody against denatured broad bean cytoplasmic sucrose synthase. Magnification as in (1).
as = archespore, ii = inner integument, nu = nucellus, oi = outer integument

Glucose staining:

Dissected ovules were stained for glucose by the method of Okamoto *et al.* (cited in Gabe 1976). Fresh ovules were fixed for 24 hours at 4°C in methyl alcohol saturated with barium hydroxide, and rinsed three times in absolute alcohol. Then the ovules were transferred into a alcohol-silver nitrate solution, and incubated in full illumination. After 30 minutes they were rinsed with absolute ethanol, reduced by an ethanol-formalin solution, and rinsed with ethanol. The ovules were further cleared with a clearing solution (Herr 1971) and studied using a Nikon Labophot with Nomarski optics. Some ovules were freeze-fixed in liquid nitrogen and sectioned with a cryo-microtome. The sections were studied with the same microscope.

In an experiment to confirm the specificity of this staining method (not shown) also sucrose, fructose, sorbitol, mannitol, and maltose reacted with the silver nitrate, but slower, thus less intense than glucose. Glucose-6-phosphate did not react. For the sake of convenience only glucose will be discussed in this report.

RESULTS

Sucrose synthase and invertase in developing ovules:

At the archespore stage of the ovule development sucrose synthase was found active in all tissues. The archespore showed a similar cytoplasmic activity as the enveloping nucellar cells (Fig.1-1). Immunochemistry showed a matching localization pattern for the cytoplasmic sucrose synthase (by the antibody against denaturated broad bean sucrose synthase) with the sucrose synthase localization pattern as revealed by the histochemical assay (Fig.1-2).

At the archespore stage no invertase activity was found in the ovule, nor any specific labelling was found with the different invertase antibodies.

At the tetrad stage sucrose synthase activity was found in the cells of the nucellus and outer integument. The megaspore cells did not show any activity (Fig.2-1), and the inner integument showed only a little activity (Fig.2-2). During degeneration of the micropylar megaspores high sucrose synthase activity was often found in the degenerating cells only (Fig.2-3). Immunochemistry showed an equal signal of cytoplasmic sucrose synthase in all ovular cells.

The antibody raised against the membrane-associated sucrose synthase labelled the megaspore membranes bordering the separating callose walls before tetrad degeneration (Fig.2-4). This antibody also labelled many radial walls of the nucellus and integuments (inner integument especially), cells which are still dividing during this developmental stage (Fig.2-5). The callose antibody labelled also these newly formed cell walls and the callose enveloping the tetrad cells (Fig.2-6). Neither invertase activity, nor its presence was detected by the assay and antibodies respectively in the ovule at the tetrad stage.

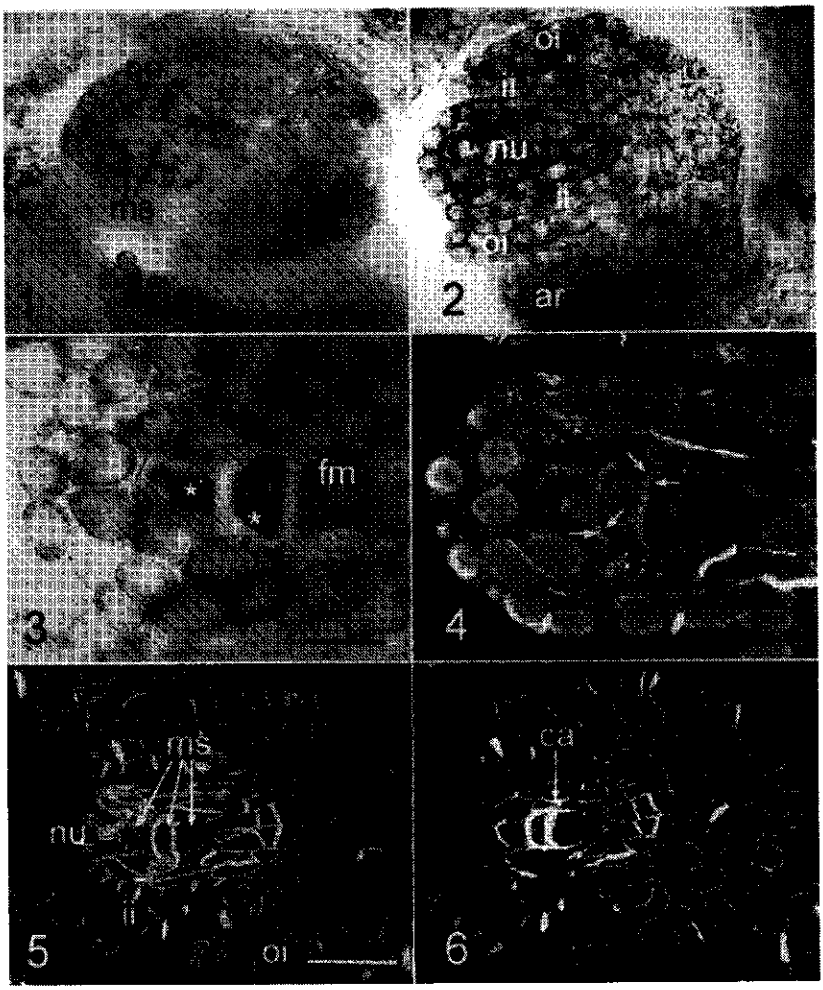

Figure 2: Tetrad stage. **(1)** Ovule at tetrad stage showing sucrose synthase in nucellus (*nu*), but not in megaspore cells (*ms*). Bar = 50 μm. **(2)** Hardly any sucrose synthase activity in inner integument (*ii*). Same ovule as in Fig.2-1, different focus plane. Magnification as (1). **(3)** High sucrose synthase activity in degenerating megaspore cells (asterix). Bar = 20 μm. **(4)** Double exposure showing immunolabelling signal against separating tetrad callose walls with membrane-associated sucrose synthase antibody (arrows), and staining of nuclei by DAPI. Magnification as (3). **(5)** Lower magnification of (4), showing strong labelling of many radial walls in nucellus (*nu*), outer- (*oi*) and inner integuments (*ii*) with membrane-associated sucrose synthase antibody. Bar = 50 μm. **(6)** Immunolabelling of different section of same ovule as in Fig.2-5 labelled with an antibody against callose, gives similar localization pattern as labelling with membrane-associated sucrose synthase antibody: labelling of radial walls in nucellus and integuments, but especially the callose around the megaspore cells (*ca*). Magnification as (5).
ca = callose, fm = functional megaspore, ii = inner integument, ms = megaspore, nu = nucellus, oi = outer integument

During the coenocytic stage of ovule development sucrose synthase activity was found in the cytoplasm of the coenocyte (Fig.3-1). The epidermis of the nucellus which envelopes the coenocyte showed also sucrose synthase activity but not in the hypostase, which is nearly fully developed (Fig.3-1 and 3-2). The micropylar part of the inner integument shows low activity (Fig.3-1).

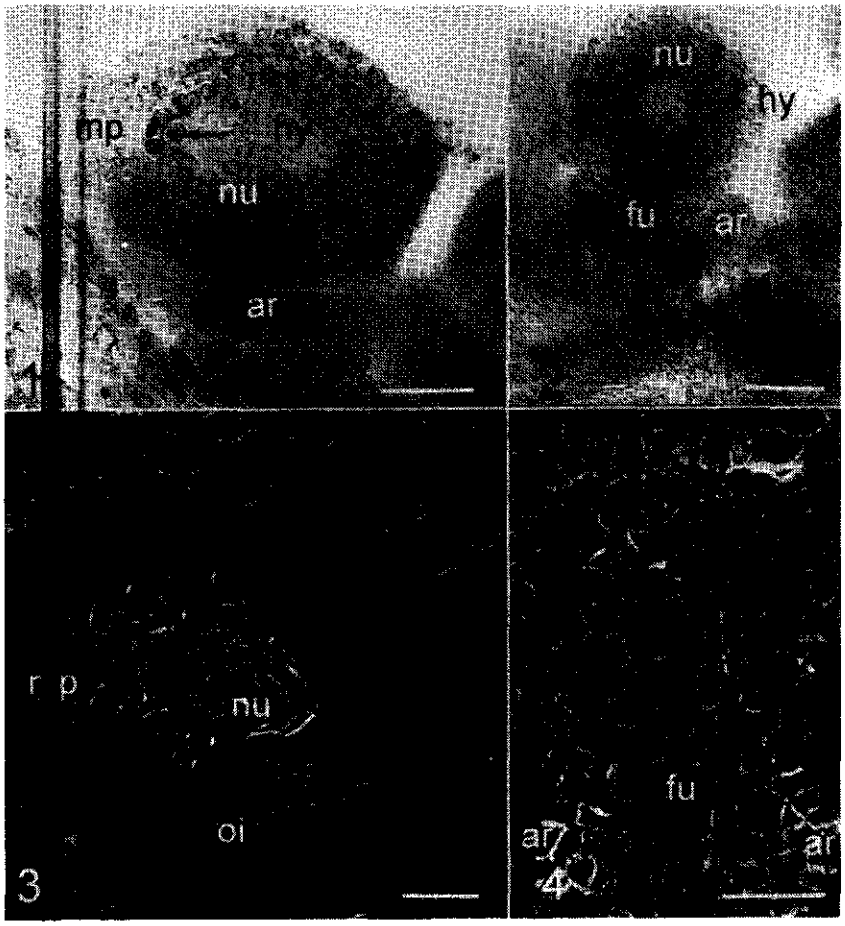

Figure 3: Coenocytic embryo sac stage. (1) Two or four nucleate embryo sac showing sucrose synthase activity in cytoplasm (*arrow*) and nucellus (*nu*), but not in hypostase (*hy*) and mycropylar part of the inner integument (*mp*). Bar = 100 µm. **(2)** Transversal section through funicle (*fu*) and hypostase (*hy*) showing no sucrose synthase activity in hypostase. Bar = 100 µm. **(3)** Membrane-associated sucrose synthase antibody labels walls of nucellus (*nu*) and micropylar part of inner integument (*ii*), but hardly in outer integument (*oi*). Bar = 50 µm. **(4)** Initiation of arillus (*ar*) at base of funiculus (*fu*) in tangential section, shown by labelling with membrane-associated sucrose synthase antibody. Bar = 50 µm.

ar = arillus, fu = funiculus, hy = hypostase, mp = micropyle, nu = nucellus, oi = outer integument

Membrane-associated sucrose synthase antibody labelled profoundly new nucellar walls and inner integumental walls around the micropyle (Fig.3-3). The initiation of the arillus at the base of the funiculus was also marked by this antibody (Fig.3-4).

During the coenocytic stage no invertase was found by histochemical and immunocytochemical methods in the ovule.

In mature ovules with fully developed embryo sacs sucrose synthase was found active in and around the egg apparatus, and in the cytoplasm of the chalazal part of the central cell (Fig4-1).

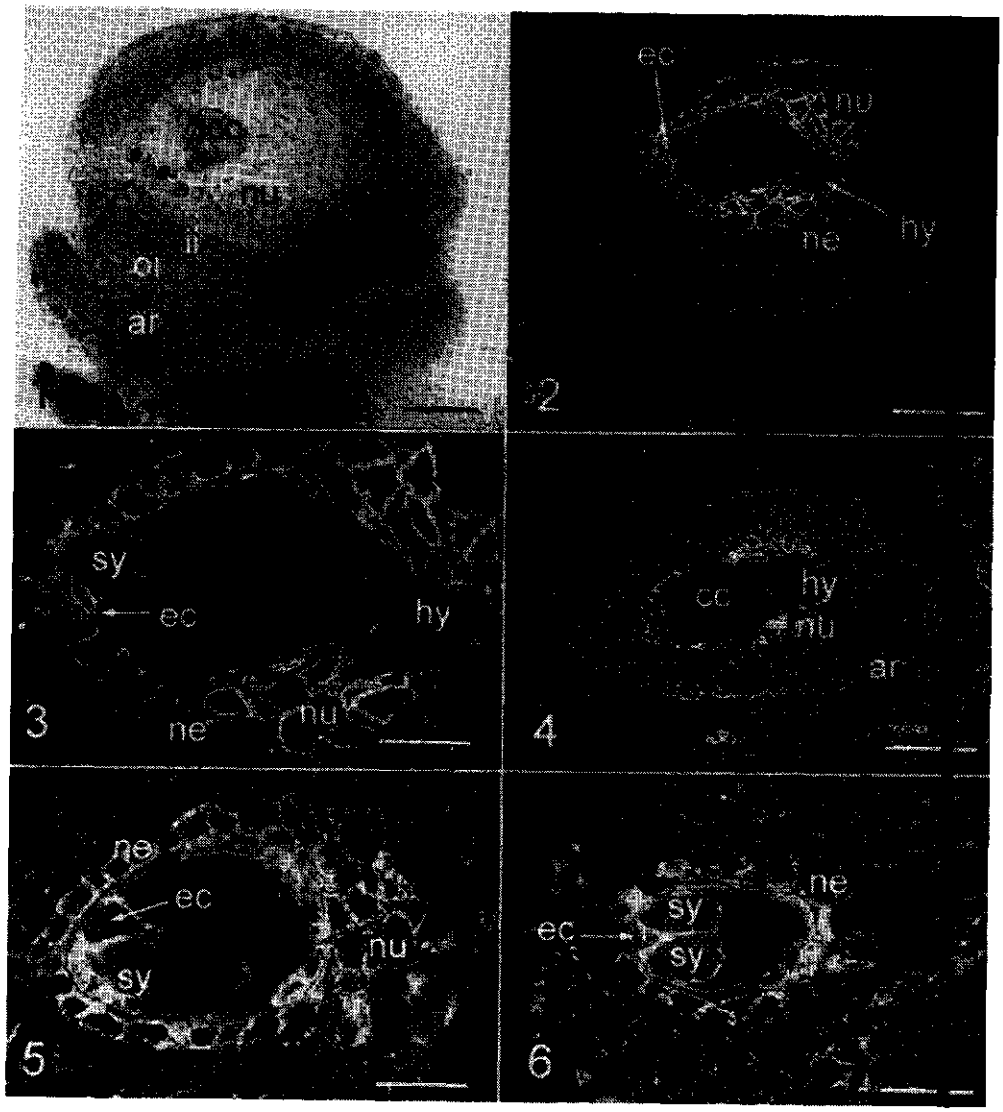

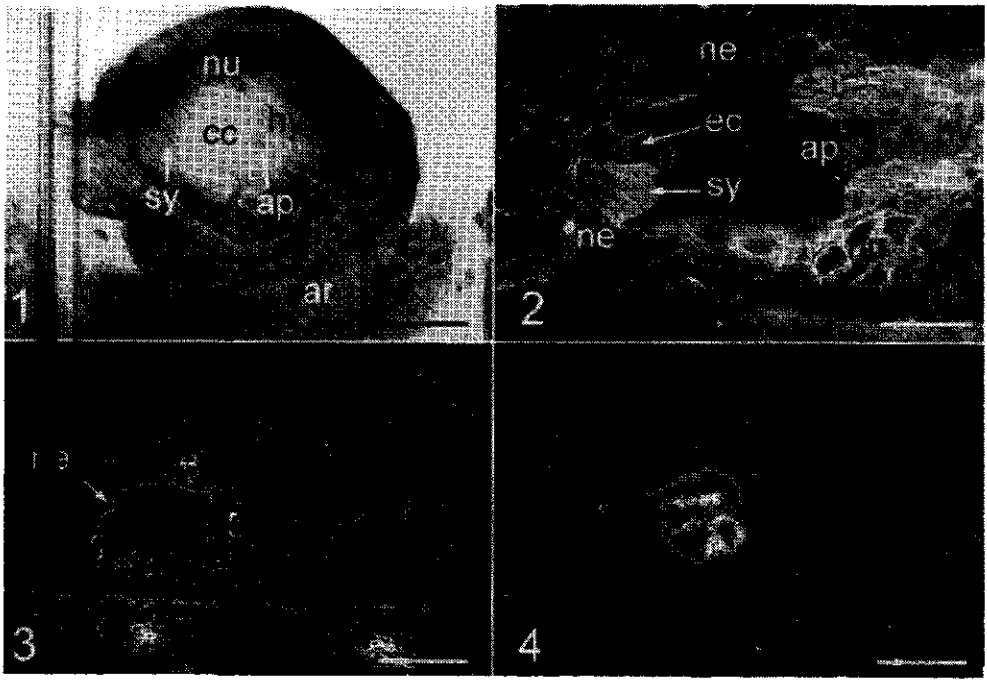

Figure 5: Mature embryo sac stage - invertase. (1) Invertase activity in cytoplasm synergids (*sy*), antipodal cells (*ap*), nucellus (*nu*) and arillus (*ar*) of mature ovule, but not in central cell (*cc*) and hypostase (*hy*). Bar = 100 µm. **(2)** Immunolabelling with grape invertase antibody in synergids (*sy*) and chalazal nucellus (*nu*), but not in the nucellar epidermis (*ne*) and egg cell (*ec*). Bar = 40 µm. **(3)** Immunolabelling of nucellar epidermis (*ne*) with carrot cell wall invertase antibody. Bar = 100 µm. **(4)** Immunolabelling of filiform apparatus with antibody against synthetic invertase part. Bar = 40 µm.

ap = antipodal cell, ar = arillus, ec = egg cell, hy = hypostase, ne = nucellar epidermis, nu = nucellus, sy = synergid

Figure 4 (previous page): Mature embryo sac stage - sucrose synthase and callose. (1) Sucrose synthase activity in cytoplasm of the central cell (*cc*) of a mature embryo sac. Higher sucrose synthase activity in integuments (*ii*)(*oi*), and arillus (*ar*) than in nucellus (*nu*). Bar = 150 µm. **(2)** Immunolabelling of egg cell (*ec*) and nucellus (*nu*) with antibody against denatured broad bean cytoplasmic sucrose synthase: nucellus (*nu*) shows no labelling in hypostase (*hy*) and chalazal epidermis (*ne*). Bar = 100 µm. **(3)** Detail of (2), showing labelling in egg cell (*ec*). Bar = 40 µm. **(4)** Membrane-associated sucrose synthase antibody labels plasmodesmata in nucellus (*nu*) and arillus (*ar*) cell walls. The hypostase (*hy*) is negative. Bar = 100 µm. **(5)** Immunolabelling with callose antibody shows callose in and around egg cell (*ec*) and synergid (*sy*), and in plasmodesmata of the nucellus (*nu*). Bar = 40 µm. **(6)** Tangential section through egg apparatus labelled with callose antibody, showing labelling in egg cell (*ec*) and synergids (*sy*). Bar = 40 µm.

ar = arillus, cc = central call, ea = egg apparatus, ec = egg cell, hy = hypostase, ii = inner integument, ne = nucellar epidermis, nu = nucellus, oi = outer integument, sy = synergid

In the nucellus and inner integument sucrose synthase activity was found, but often a higher amount of activity was observed in the outer integument and arillus (Fig.4-1).
Cytoplasmic sucrose synthase was found by immunocytochemistry in the chalazal nucellus, of which the hypostase and the epidermal cells did not label. Labelling was also found in the egg cell (Fig.4-2 and 4-3).
Membrane-associated sucrose synthase was localized near the cell walls of the nucellar cells (Fig.4-4), labelling plasmodesmata. The cells of the hypostase were negative. In the arillus also much membrane-associated sucrose synthase was found.
Abundant callose was found immunocytochemically in the egg apparatus, especially around the egg cell, and in plasmodesmata in the nucellar cell walls (Fig.4-5 and 4-6).
Abundant invertase activity was found in the cytoplasm of the synergids of the fully developed embryo sac. Also the antipodal cells showed invertase activity while the central cell did not show much activity (Fig.5-1). Abundant activity was found in the nucellar cells, except for the hypostase cells where almost no activity was found. The integuments, funiculus and arillus showed also invertase activity. Immunocytochemistry with the grape invertase antibody localized invertase in the synergids, but hardly any in the egg cell or other parts of the embryo sac (Fig.5-2). This antibody did not label invertases in the nucellar epidermis but did label the chalazal nucellar cells. Labelled invertase was present in the cytoplasm of the hypostase. The antibody raised against a synthetic part of acid invertase and the carrot cell wall invertase showed labelling in the nucellar epidermis (Fig.5-3), the synthetic invertase antibody also labelled the filiform apparatus (Fig.5-4).

Sucrose synthase and invertase in ovary:
At the stage of mature ovules the histochemical assays showed activity of invertase and sucrose synthase in the carpels. Immunocytochemistry showed a high concentration of invertase in the pericarp when ovules were in the two nucleate coenocytic stage, but the epidermal cells of these carpels did not label for invertase (Fig.6-1). However, the epidermal

Figure 6: Carpels. (1) Immunolabelling of carpel parenchyma cells (*pa*) with antibody against carrot soluble invertase (iso-enzyme II). The epidermal cells do not label (arrows). Bar = 200 μm. **(2)** Immunolabelling of nectar gland cells (*ng*) with synthetic invertase antibody. Bar = 40 μm. **(3)** Sucrose synthase activity in epidermal cells (arrows), nectar gland cells (*ng*) and transport tissue (*tt*) of carpels. Bar = 300 μm. **(4)** Invertase activity in transport tissue of the carpel. Bar = 50 μm..
ng = nectar gland cell, pa = parenchyma cells, tt = transport tissue

cells showed sucrose synthase activity, while the carpel parenchyma did not (Fig.6-3). Using antibodies, invertase and sucrose synthase were found abundant in the cytoplasm of septal nectar gland cells (Fig.6-2) which were also found very active (Fig.6-3). The cells bordering these nectar glands also labelled for sucrose synthase but not for invertase. Vascular bundles showed the presence of both invertase and sucrose synthase activity (Fig.6-3 and 6-4).
The placental papillar cells developed already at the tetrad stage of the ovule. At the mature ovule stage they were fully developed and showed cytoplasmic activity of invertase and sucrose synthase (Fig.7-1 and 7-2). Immunocytochemistry results were in agreement with these activity localizations (Fig.7-3). At the ovule tetrad stage invertase was also found by immunocytochemistry in the placental fluid (Fig.7-4), which is excreted by the placental papillar cells (Willemse and Wittich 1998). In the later developmental stages this fluid was probably rinsed away during the fixation.

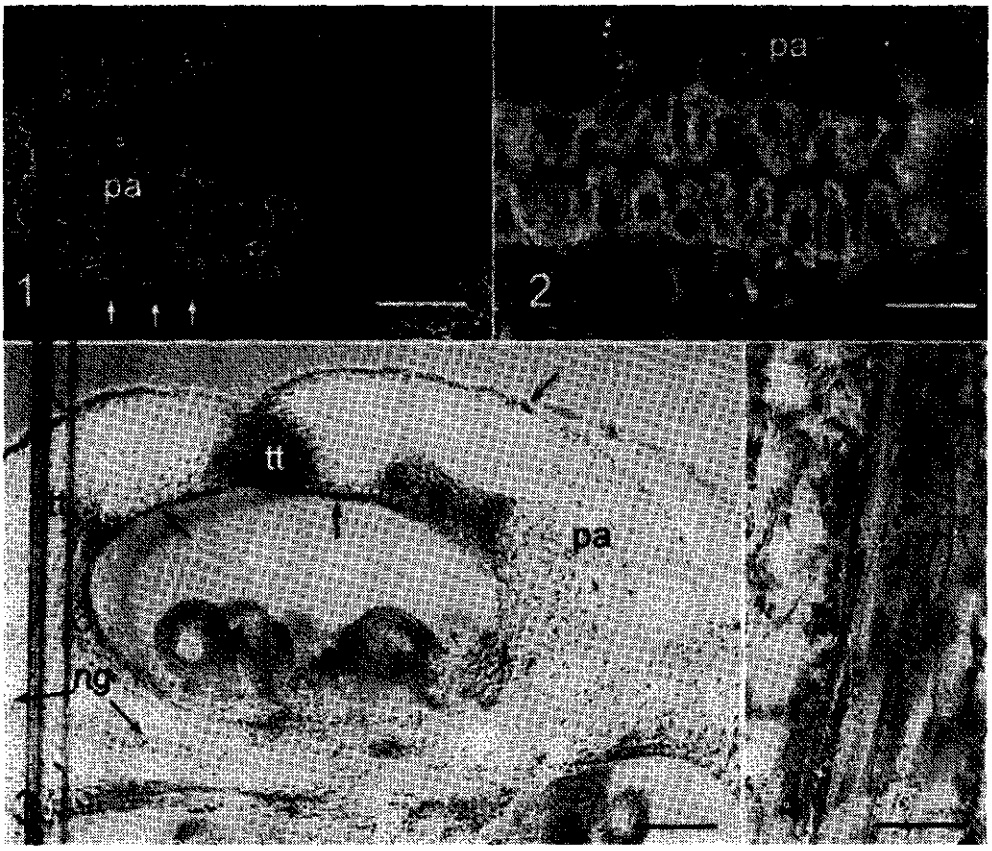

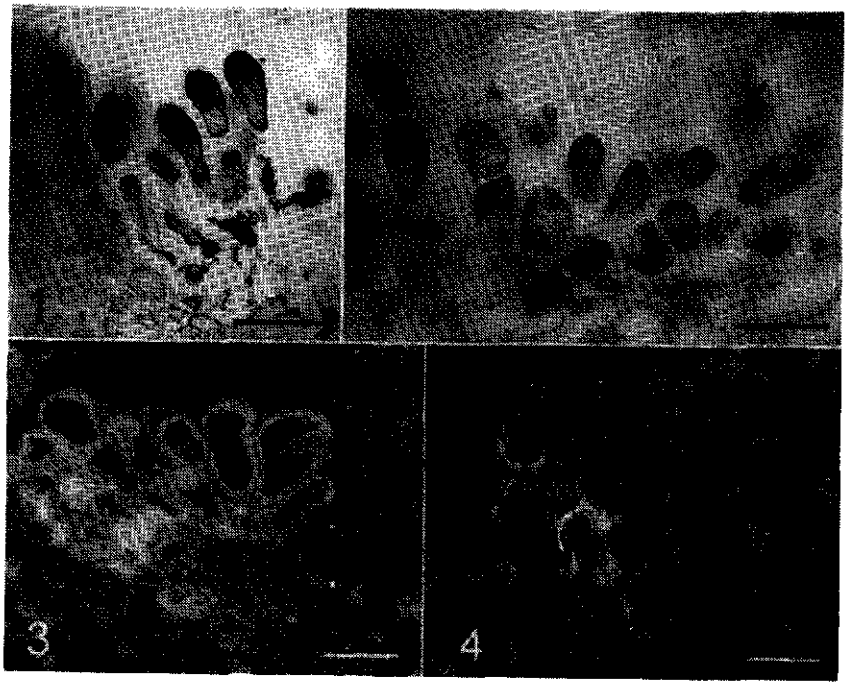

Figure 7: Papillar cells. (1) Invertase activity in placental papillar cells. Bar = 50 μm. **(2)** Sucrose synthase activity in placental papillar cells. Bar = 50 μm. **(3)** Immunolabelling of placental papillar cells with an antibody against grape invertase. Bar = 40 μm. **(4)** Immunolabelling of placental fluid with grape invertase antibody (from Willemse and Wittich 1998). Bar = 30 μm.

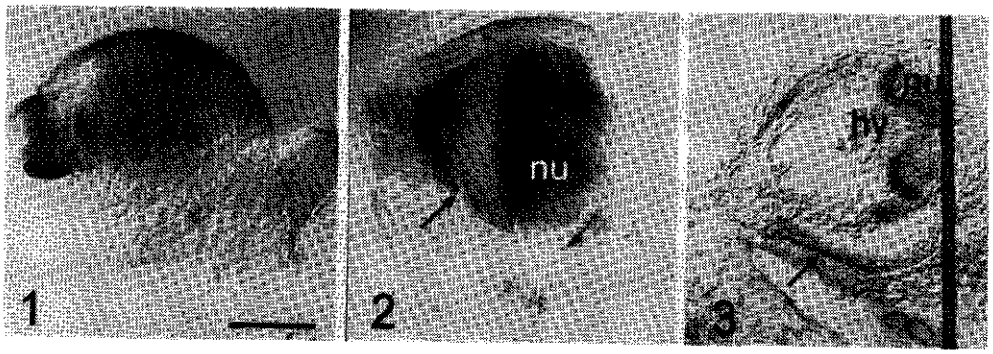

Figure 8: Glucose staining. (1) Staining for glucose in all tissues of ovule of two nucleate coenocytic stage. Bar = 100 μm. **(2)** Glucose distribution in mature ovule: staining in chalazal nucellus (*nu*) and micropylar part inner integument (*arrow*). Magnification as in (1). **(3)** Cryo section through mature ovule after staining for glucose (as shown in (2). Magnification as in (1).
hy = hypostase, nu = nucellus

Distribution of soluble sugars in ovules:

Using the staining procedure of Okamoto and co-workers (cited in Gabe 1976) for glucose detection (and probably other saccharides), a brown precipitate was found during all developmental stages of the ovule: from the two nucleate coenocytic ovule on, a gradient pattern was built up, resulting in the ring-shaped localizations found at the fully developed ovule (Fig.8-1, 8-2 and 8-3). A high glucose concentration was found in the chalazal nucellar cells (with the hypostase excluded), in the micropylar nucellus cells, and in some mid parts of the inner integuments.

DISCUSSION

Development from megaspore to embryo sac

The results obtained from using the immunocytochemical and histochemical methods are summarized in Figure 9.

Sucrose synthase activity was found in the cytoplasm of the archespore and tetrad cells before the three micropylar megaspores degenerated. The function of sucrose synthase here, and in general, is providing energy for cell maintenance and growth. In the tetrad stage the cytoplasmic sucrose synthase will likely also supply UDP-glucose for the callose synthesis, since it is suggested that UDP-glucose can be supplied by both, the cytoplasmic and the membrane-associated sucrose synthase (Amor *et al.* 1995). The activity of the cytoplasmic sucrose synthase in the degenerating megaspores might very well be related to the breakdown of the cell for recycling purposes, *i.e.* nutrition of the functional megaspore (Willemse and De Boer-De Jeu 1981). In the *Gasteria* ovule the membrane-associated sucrose synthase also seems to be involved in the callose synthesis around the non-functional megaspores in the tetrad, since it is found against the callose walls between the megaspore cells. It is probably located on the plasma membrane. The corresponding labelling for callose and membrane-associated sucrose synthase around the egg cell also implies the association of sucrose synthase with callose synthesis. From the immunolabelling results with membrane-associated sucrose synthase antibody it seems that at the micropylar part of the egg cell a cell wall is formed, probably consisting of callose and cellulose. At the chalazal side of the egg apparatus usually no cell wall is deposited (Franssen-Verheijen and Willemse 1990), which is coherent with the result that no labelling was found at this side. Willemse and Franssen-Verheijen (1988) reported the deposition of callose at the micropylar side of the filiform apparatus before fertilization which maintained after fertilization. From the present results it is not clear whether this callose is involved in the cell wall development or if it forms a special callose layer which

is involved in the functioning of the filiform apparatus or pollen tube guidance.

It is unlikely that the activity of the membrane-associated sucrose synthase can be localized by the histochemical assay. The hypothetical model presented by Delmer and Amor (1995) indicates that this membrane-bound form of sucrose synthase delivers the produced UDP-glucose directly to the cellulose synthase, without loss of UDP-glucose into the cytoplasm. The histochemical assay can only detect free UDP-glucose. It is suggested that for callose synthase a similar association might exist with this membrane-bound sucrose synthase (Delmer and Amor 1995).

Invertase activity only appears in the embryo sac stage. Its activity and presence was found in the cytoplasm of the mature synergid, and might be related with the carbohydrate composition in the micropylar exudate, which is produced by the synergids (Franssen- Verheijen and Willemse 1993, Willemse and Wittich 1998).

The antipodal cells might have a function in the nutrition of the young central cell, and degenerate often during embryo sac maturation (Stiffler 1925, Willemse and Kapil 1981). The activity of invertase that was found in these cells might be related to the nutritional function in favour of the central cell. Given this explanation, it is strange that in the mature ovule the carbohydrates have to be supplied to the antipodal cells via this very central cell since the hypostase hinders the transport from the chalazal side.

Figure 9

In developing *Gasteria* ovule stages (archespore stage, tetrad stage, two nucleate coenocytic stage and mature embryo sac stage, respectively) the localization patterns and intensity of sucrose synthase activity and invertase histochemistry and immunocytochemistry, and glucose staining is shown.

A. Cytoplasmic sucrose synthase activity was high in the growing arillus and outer integument in the mature embryo sac stage. During the development of the hypostase sucrose synthase activity decreased till almost zero in these differentiating nucellar cells.

B. Immunocytochemistry showed the distribution of cytoplasmic sucrose synthase, with a rise in concentration in a part of the nucellus during the mature embryo sac stage.

C. The presence of membrane-associated sucrose synthase shown by immunocytochemistry. The antibody labelled new cell walls in arillus (last two stages), integuments (especially inner integument in tetrad and coenocytic stage) and nucellus (in these same stages). Labelling of the nucellus during the mature embryo sac stage represents labelling of the many plasmodesmata in the cell walls.

D. Invertase histochemistry showed only activity during the mature embryo sac stage, with a high activity in the nucellar cells enveloping the embryo sac and hypostase.

E. Invertase immunocytochemistry showed the enzyme presence only during the mature embryo sac stage.

F. Staining results for glucose by the method of Okamoto *et al.* (Gabe 1976), with high concentrations in parts of the nucellus and inner integuments during embryo sac development.

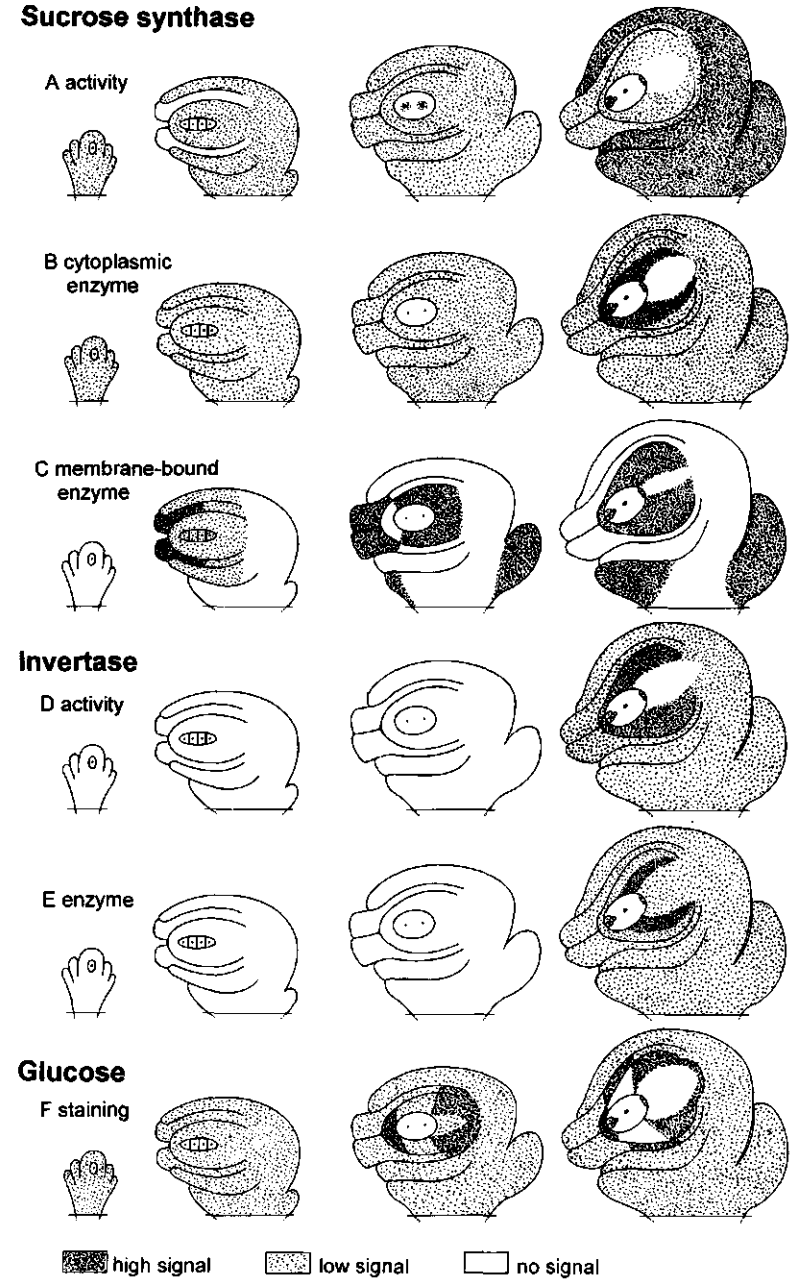

Figure 9: Summary of sucrose synthase, invertase, and glucose localization results.

Development of nucellus

At the mature stage of the ovule the nucellus stops to grow and only needs UDP-glucose for respiration. This loss of activity in the nucellus is also found in the pattern of sucrose synthase activity. However, immunocytochemistry showed a high concentration of sucrose synthase in the nucellar tissue, higher than in the bordering cells. Deducting from the histochemical assay these enzymes are probably not very active.

The membrane-associated sucrose synthase antibody and the callose antibody labelled new transverse cell walls in the nucellus during ovule development. In these new walls between two cells first callose and later cellulose are being synthesized. The membrane-associated sucrose synthase might be associated with both synthases. In the nucellus enveloping the embryo sac of the mature ovule the labelling of many plasmodesmata was found. The membrane-associated sucrose synthase seems to be involved in the callose synthesis in plasmodesmata. This localization shows also clearly the abundant number of plasmodesmata, suggesting a huge potential symplastic transport route in the nucellar cells around the embryo sac.

The high invertase activity in the nucellus could be important for the supply of nutrients to this tissue as well as to the embryo sac. Sucrose can be transported completely symplastic into the nucellus, but has to be unloaded into the apoplast of the nucellus before uptake into the embryo sac since there are hardly any plasmodesmata between nucellus and gametophyte. The only plasmodesmata found are some between nucellus and antipodals (Franssen-Verheijen and Willemse 1990). It is possible that the embryo sac prefers the uptake of monosaccharides instead of sucrose, but by breaking down the supplied sucrose into glucose and fructose not only the embryo sac can be nursed, but also a steeper sucrose concentration gradient is created which enhances the transport of sucrose into the nucellus. Phenomena like these are found in several studies on seed development where breakdown of sucrose by invertase is required for endosperm and embryo growth (Weber *et al.* 1997, and references herein).

The detected loss of invertase activity in the *Gasteria* hypostase could be expected, since there is probably not much apoplastic and symplastic transport through these cells due to the wall lignification and suberination, and the few plasmodesmal contacts. The development of the hypostase is thought to alter the pathway of nutrient transport and thus seems to prevent nutrient supply to the embryo sac via the antipodals. Immunolabelling with the grape invertase antibody surprisingly labelled the hypostase cells and surrounding chalazal nucellar cells which did not show much invertase activity. The other used invertase antibodies labelled the epidermal nucellar cells which had shown high invertase activity. An explanation for this discrepancy could be the specificity of the antibodies. The grape invertase antibody might

detect the presence of a denaturated invertase, or a different invertase isoform (than the isoforms which are detected by the other invertase antibodies). The activity of this different isoform might be very low or completely absent.

Development integuments and arillus

Sucrose synthase seemed to have diminished drastically in the inner integument at the tetrad stage, but was again present during further development although sometimes with a lower activity than in the outer integument and arillus. Again, the activity is probably related with growth and respiratory purposes. Immunocytochemistry did not show the presence of the enzymes. This could be due to a different isoform of the enzyme which cannot be detected by the used antibodies, but also an effect of a too low enzyme concentration.

In the integuments and arillus the membrane-associated sucrose synthase was found present near the plasmodesmata showing potential symplastic transport routes, and new cell walls. From these results it becomes clear that the integuments continue with cell divisions during the ovule development, and that the arillus undergoes rapid growth by cell divisions which start at the base of the funiculus during the coenocytic stage of the ovule.

Activity of invertase in the integuments and arillus was found only at the mature stage of the ovule. A function for this invertase activity might be found in the growth and swelling of these tissues after the coenocytic stage, especially of the arillus. Immunocytochemistry could not detect these invertases, which may indicate that there is a low concentration of enzyme present in these tissues, or a different invertase isoform.

Carpels and nectar cells

The epidermis of the carpel remained growing and dividing during the ovary development. The sucrose synthase activity found in these cells is likely related to these processes. Invertase activity is apparently not required in these cells.

The septal nectar gland cells produce a product containing aromatic compounds, proteins and sugars. The high invertase activity found in these cells might be involved in the ratio [sucrose] to [glucose] + [fructose] in the nectar, while the sucrose synthase activity in the nectar cells and bordering parenchyma cells might be related with protein synthesis. Sucrose synthase may also supply energy for the probably high respiratory costs in these cells. Also the bordering parenchyma cells of the epidermal nectar gland cells show high sucrose synthase activity, perhaps supporting the nectar cells.

Placental papillar cells

Already during the tetrad stage of the ovule, activity of both invertase and sucrose synthase was found in the placental papillar cells. These cells produce the placental fluid which contains sucrose, glucose and fructose as main carbohydrate components (Willemse and Wittich 1998). The activity of the two sucrose degrading enzymes may also play a role in the carbohydrate composition of the placental fluid (invertase), protein synthesis (sucrose synthase) and respiratory costs for cell maintenance and excretion activities (sucrose synthase).

Glucose distribution

During the *Gasteria* ovule development, cytoplastic sucrose synthase seems to play a constant role in supplying growing tissues with UDP-glucose. Invertase however, is only detectable active in the mature ovule and especially in the nucellus. The suggested function in hydrolyzing sucrose into glucose and fructose for embryo sac nutrition matches the results obtained with the glucose staining patterns during this stage: a high concentration of glucose in the nucellus and to a lesser extent in the bordering tissues. However, the typical glucose localization pattern can not completely be explained by the invertase activity distribution, especially not during early developmental stages where invertase activity was not found. It is possible that there is a low invertase activity during this stage of development, but too low to be detected by the assay. However, it should also be taken into account that the detected stain is not glucose and fructose alone, since there were indications that the staining method is not very specific. This may cause the difference between the sugar staining and the invertase localization.

Glucose was not found in the hypostase. This is, apart from the absence of invertase activity, a signal that the nutrient transport pathway to the embryo sac is altered by the development of the hypostase: from directly via the chalazal side of the embryo sac, now via the micropylar side. This change may have an important influence on the development of the embryo sac and early seed development.

The used techniques of enzyme localization by their activities (histochemistry) and by using antibodies (immunocytochemistry) were both essential in this study. The enzyme activity assay shows the activity of all enzyme isoforms, with the possible exception of membrane-associated sucrose synthase, and is in the case of the sucrose synthase assay also proven to be more sensitive than immunocytochemistry. The assay is also very useful when (plant-)specific antibodies are not available, as was in this study. However, (plant-)aspecific antibodies in this study showed their value in localizing enzymes which were inactive, or enzymes which product did not become available for the assay (membrane-associated sucrose synthase), or enzymes for which the assay was not sensitive enough (invertase assay).

ACKNOWLEDGEMENTS

I would like to thank MTM Willemse, AAM van Lammeren, and CJ Keijzer for reading this manuscript critically, S Massalt for the photography, and AB Haasdijk and PA van Snippenburg for the artwork. For sending me antibodies for this research my gratitude goes to DP Delmer, AH Kingston-Smith, KE Koch, H Ross, HP Ruffner, and A Sturm.

REFERENCES

Amor Y, CH Haigler, S Johnson, M Wainscott and DP Delmer (1995) A membrane-associated from sucrose synthase and its potential role in synthesis of cellulose and callose in plants. Proc Natl Acad Sci USA 92, 9353-9357

Baskin TI, CH Busby, LC Fowke, M Sammut and F Gubler (1992) Improvements in immunostaining samples embedded in methacrylate: localization of microtubules and other antigens throughout developing organs in plants of diverse taxa. Planta 187, 405-413

Delmer DP and Y Amor (1995) Cellulose biosynthesis. Plant Cell 7, 987-1000

Doehlert DC and FC Felker (1987) Characterization and distribution of invertase activity in developing maize (*Zea mays*) kernels. Physiol Plant 70, 51-57

Franssen-Verheijen MAW and MTM Willemse (1990) The ovule of *Gasteria verrucosa* at receptivity of the stigma: an ultrastructural study. Acta Bot Neerl 39: 53-63

Franssen-Verheijen MAW and MTM Willemse (1993) Micropylar exudate in *Gasteria* (Aloaceae) and its possible function in pollen tube growth. Am J Bot 80, 253-262

Gabe M (1976) Histological techniques. Masson, Paris

Herr JM (1971) A new clearing squash technique for the study of ovule development in angiosperms. Am J Bot 58, 785-790

Ho LC, A Lecharny and J Willenbrink (1991) Sucrose cleavage in relation to import and metabolism of sugars in sink organs. In:: JL Bonnemain, S Delrot, WJ Lucas and J Dainty (Eds). Recent advances in phloem transport and assimilate compartmentation. Ouest editions, Nantes, 178-186

Kingston-Smith AH and CJ Pollock (1996) Tissue level localization of acid invertase in leaves: an hypothesis for the regulation of carbon export. New Phytol 134, 423-432

Koch KE, KD Nolte, ER Duke, DR McCarty and WT Avigne (1992) Sugar levels modulate differential expression of maize sucrose synthase genes. Plant Cell 4, 59-69

Laurière CM, A Laurière, A Sturm, L Faye and MJ Chrispeels (1988) Characterization of ß-fructosidase, an extracellular glycoprotein of carrot cells. Biochimie 70, 1483-1491

Northcote DA, R Davey and J Lay (1989) Use of antisera to localize callose, xylan and arabinogalactan in the cell-plate, primary and secondary walls of plant cells. Planta 178, 353-366

Ross HA and HV Davies (1992) Purification and characterization of sucrose synthase from the cotyledons of *Vicia faba* L. Plant Physiol 100, 1008-1013

Ruffner HP, M Hürlimann and R Skrivan (1995) Soluble invertase from grape berries: purification, deglycosylation and antibody specificity. Plant Physiol Biochem 33, 25-31

Stiffler EG (1925) Development of embryo sac in *Gasteria, Cyrtanthus,* and *Velthemia.* Bot Gaz 79, 207-216

Sung SS, WJ Sheih, DR Geiger and CC Black (1994) Growth, sucrose synthase, and invertase activities of developing *Phaseolus vulgaris* L. fruits. Plant Cell Env. 17, 419-426

Sung SJS, DP Xu and CC Black (1989) Identification of actively filling sucrose sinks. Plant Physiol 89, 1117-1121

Unger C, J Hofsteenge and A Sturm (1992) Purification and characterization of a soluble β-fructofuranosidase from *Daucus carota*. Eur J Biochem 204, 915-921

Weber L, L Borisjuk and U Wobus (1997) Sugar import and metabolism during seed development. Trends in Plant Sci 2, 169-174

Willemse MTM (1981) Polarity during megasporogenesis and megagametogenesis. Phytomorph 31, 124-134

Willemse MTM and J Bednara (1979) Polarity during megasporogenesis in *Gasteria verrucosa*. Phytomorph 29, 156-165

Willemse MTM and MJ De Boer-De Jeu (1981) Megasporogenesis and early megagametogenesis. Acta Soc Bot Pol 50, 111-120

Willemse MTM and MAW Franssen-Verheijen (1988) Ovular development and pollen tube growth in the ovary of *Gasteria verrucosa* (Mill.) H. Duval as condition for fertilization. Sexual reproduction in higher plants. Eds: M Cresti, P Gori and E Pacini. Springer-Verlag, Berlin. 357-362

Willemse MTM and RN Kapil (1981) Antipodals of *Gasteria verrucosa* (Liliaceae) - An ultrastructural study. Acta Bot Neerl 30, 25-32

Willemse MTM and PE Wittich (1998) Pollination and fertilization in *Gasteria verrucosa* (Mill.) H. Duval: Interaction between pollen tube and ovary. In: Reproductive Biology 96 Conference Book In Press

Wittich PE and D Vreugdenhil (1998) Localization of sucrose synthase activity in developing maize kernels by in situ enzyme histochemistry. J Exp Bot: In Press

Chapter

5

Carbohydrates in developing seeds of *Gasteria verrucosa* (Mill.) H. Duval: sucrose synthase and invertase localization and activity

P.E. Wittich

Summary. The development of *Gasteria verrucosa* seeds seems to follow a pattern of growth in which the distribution of carbohydrates is first directed to the developing arillus and seed coat, then to the developing endosperm, followed by carbohydrate investment in the developing embryo and storage products. This distribution pattern is deducted from a localization study on sucrose synthase and invertase. These two enzymes break down imported sucrose, and are in that perspective used as markers for carbohydrate transport since diffusion is expected to be induced towards cells and tissues with high sucrose hydrolysing activities. Structural analysis showed the development of the phytomelan layer in the seed coat, preceded by the deposition of callose. Immunocytochemistry revealed that sucrose synthase is involved in the callose synthesis and breakdown, while invertase may only play a role in the latter. During seed coat development the helobial endosperm shows nuclear divisions, but remains coenocytic. When the phytomelan is formed, the endosperm starts to form cell walls. The chalazal chamber remains coenocytic and seems to function in the uptake of nutrients for the micropylar cells. Import of nutrients into the endosperm is also expected to occur via the entire endosperm outer surface.

INTRODUCTION

Gasteria verrucosa (Mill.) H. Duval is a member of the family Asphodelaceae and thus forms anatropous ovules with helobial endosperm after fertilization (Dahlgren *et al.* 1985, Schnarf and Wunderlich 1938). Cellularization of the micropylar chamber occurs after a long nuclear period but the chalazal chamber remains coenocytic and is still present in the mature seeds. After cellularization the endosperm becomes filled with storage products like starch, lipids, and proteins. For the synthesis of these storage products the required nutrients are provided by the phloem, which terminates in the chalazal tissue. From this tissue the nutrients are transported further into the integuments, or via the nucellus into the developing endosperm and embryo. Before fertilization, the embryo sac is symplastically isolated from the nucellus (in this thesis, chapter 4). Usually also after fertilization plasmodesmal contacts are neither present between endosperm and surrounding tissues, nor between the endosperm and zygote. The lack of plasmodesmata implies that nutrients have to pass an apoplastic phase between maternal tissue and endosperm or zygote. This apoplastic transport is well studied in legume seeds and cereal grains (Patrick and Offler 1995). Sucrose is in most plants the main carbohydrate which is transported via the phloem into the developing seed. In sink tissues sucrose is hydrolysed by sucrose synthase or invertase, after which it is used for cell maintenance, cell growth or the synthesis of storage products.

In maize kernels invertase activity (β-D-fructofuranoside fructohydrolase, EC 3.2.1.26) in the pedicel tissue plays a crucial function in nutrition of endosperm and embryo. The invertase hydrolyzes the unloaded sucrose, thus maintaining a sucrose gradient between phloem and pedicel which enhances the sucrose unloading. Hydrolysis may also be a prerequisite for uptake into the endosperm (in this thesis, chapter 3). Besides a function in phloem unloading, invertase might be involved in lipid synthesis and storage of carbohydrates. But in general invertase activity is considered to be related with cell growth and expansion (Weber *et al.* 1997). Invertase is known in a wall-bound acidic isoform, a cytoplasmic neutral isoform, and neutral and acid vacuolar isoforms (Ho *et al.* 1991).

The second, and only other, enzyme that breaks down sucrose prior to its use is sucrose synthase (UDP-D-glucose:D-fructose 2-α-glucosyltransferase, EC 2.4.1.13). This enzyme is found in a cytoplasmic form and a membrane-associated form, both creating sucrose gradients by their activity and thus enhancing sucrose transport. Sucrose synthase catalyzes a reversible reaction of sucrose and uridinediphosphate (UDP) into UDP-glucose and fructose, but is thought to work only in the degrading direction *in vivo* (Huber and Huber 1996, Kruger 1990). Cytoplasmic sucrose synthase supplies UDP-glucose for respiration (Xu *et al.* 1989), cell wall synthesis (Amor *et al.* 1995), starch synthesis (Chourey and Nelson 1976) and protein synthesis (Doehlert 1990). The membrane-associated form of sucrose synthase is involved in

the synthesis of cellulose and probably callose (Amor *et al.* 1995, Delmer and Amor 1995).
In this study the morphological development of the *Gasteria* seed is described first, followed by the analysis of sucrose transport from the phloem into the developing seed tissues. For the latter, sucrose synthase and invertase are localized during seed development. This enzyme localization is performed by histochemical detection of their activity *in situ*, as well as by immunolocalization of the enzyme-proteins. Because the sucrose degrading activity of sucrose synthase and invertase is considered to be an indicator for the sink strength of cells and tissues (Ho *et al.* 1991, Sung *et al.* 1989, 1994) the localization patterns are used to deduct a alternating carbohydrate distribution pattern during seed development.

MATERIAL AND METHODS

Plants of a self incompatible hybrid population of *Gasteria verrucosa* (Mill.) H. Duval, were grown under greenhouse conditions of 16 hours light and a temperature between 18 and 25°C. Flowers were pollinated and seeds were collected at various days after pollination (DAP).

Enzyme histochemistry

Collected ovaries and seeds were longitudinally sectioned by hand, and processed as follows. The sections were fixed in 2% paraformaldehyde with 2% polyvinylpyrrolidone (PVP-40) and 0.005M dithiotreitol, pH7.0, at 4°C. After rinsing in water the sections were incubated in an assay mixture for sucrose synthase activity (Wittich and Vreugdenhil 1998; in this thesis chapter 2) or an assay mixture for invertase activity as described by Doehlert and Felker (1987). In short, sucrose synthase activity was detected by the production of UDP-glucose from sucrose via a cascade of the enzymatic reactions of phosphoglucomutase, glucose-6-phosphate dehydrogenase and UDPglucose-pyrophosphorylase, resulting in the oxidation and precipitation of nitro blue tetrazolium on the site of sucrose synthase activity (in this thesis, chapter 2, 3 and 4). The invertase incubation medium contained nitro blue tetrazolium, phenazine methosulfate, glucose oxidase and sucrose, causing precipitation of nitro blue tetrazolium at the site of glucose production by invertase (in his thesis, chapter 3 and 4). To stop the incubation, the sections were rinsed with water and stored in 15% ethanol.
Sections were studied with a dissecting microscope (Wild) and Nikon Optiphot in bright field mode. Photographs were taken with a digital Panasonic wv-E550 Colour Video camera.

Immunocytochemistry

Seeds were fixed for immunocytochemistry in 4% paraformaldehyde in 0.005M phosphate buffer, pH7.2. After rinsing in buffer and dehydration in alcohol, the sections were infiltrated with butyl-methyl methacrylate (BMM) according to Baskin *et al.* (1992). Polymerization in

eppendorf capsules was at minus 10°C with 8W Philips UV lamps on 15 cm distance. On a Reichert Ultramicrotome 3 µm thick sections were made, stretched on water and dried on microscope slides at 60°C.

The BMM was removed by rinsing the slides in acetone for 15 minutes. The slides were washed in phosphate buffered saline (PBS; 137mM NaCl, 13 mM KCl, 7.3mM KH_2HPO_4 and 8mM $NaHPO_4$) and blocked with 0.1M hydroxylamoniumchloride and 1% bovine serum albumine (BSA). After the first incubation with the specific antibody overnight at 4°C, the sections were washed with 0.1% acetylated BSA in PBS and incubated with a second antibody which was labelled with FITC or Cy3, for 2 hours at 30°C. The sections were mounted in Citifluor containing 1 µg/ml DAPI, after rinsing with PBS.

With a Nikon Labophot and appropriate UV filters the sections were studied. Digital images were recorded with the Panasonic Video camera.

Antibodies:

For the invertase immunocytochemistry several antibodies were applied: an antibody against soluble grape invertase, which was a gift from H.P. Ruffner (Ruffner *et al.* 1995); two antibodies against synthetic parts of invertase polypeptides of various plants, donated by A.H. Kingston-Smith (Kingston-Smith and Pollock 1996); and a cell wall-bound invertase antibody and two soluble invertase antibodies from carrot, donated by A. Sturm (Laurière *et al.* 1988, Unger *et al.* 1994).

The immunocytochemistry for sucrose synthase was performed with two antibodies against the native and the denatured cytoplasmic protein from *Vicia faba*, donated by H. Ross (Ross and Davies 1992); with an antibody against a mixture of both isoforms of maize cytoplasmic sucrose synthase, given by K.E. Koch (Koch *et al.* 1992); and with an antibody raised against the membrane-associated sucrose synthase from cotton, which were kindly provided by D.P. Delmer and Y. Amor (Amor *et al.* 1995).

Callose was detected by using an antibody against β-1,3-glucans (Genosys, described by Northcote *et al.* (1989)), and detected by staining the labelled sections with 0.005% aniline blue (Eschrich and Currier 1964).

Histochemistry

Seed development was studied on Technovit and Unicryl embedded material. The seeds were fixed in 3% glutaraldehyde in 0.1M phosphate buffer, pH7.2, dehydrated in ethanol series, and embedded in Technovit 7100 (Kulzer) or Unicryl (BioCell). Toluidine blue was used as a general stain (O'Brien *et al.* 1965). Carbohydrates were stained red with the periodic acid-Schiff's (PAS) reagent (Jensen 1962), and proteins blue with amido black in 7% acetic acid (Schneider 1981). The Nikon Optiphot and Panasonic camera were used for photography.

RESULTS

Seed development

Seven hours after pollination the first pollen tubes penetrated the micropyle of ovules, and double fertilization took place (see also Willemse and Franssen-Verheijen 1988). After the first division of the endosperm nucleus cytokinesis took place, resulting in a micropylar and a chalazal cell. The micropylar cell enlarged in volume by vacuolization, while the nucleus repeatedly divided at the periphery, forming a coenocytic micropylar chamber (Fig.1-1). During the nuclear phase of the endosperm the embryo showed little growth. At 8 DAP it was only consisting of four cells (Fig.1-2), and developed according to the *Onagrad* type, Lilium variation (Johansen 1950). The arillus had grown during the first 5 DAP, and formed a wing shaped envelope around the outer integument which was tree cell layers thick, and the inner integument which was two cell layers thick (Fig.1-1).

At about 11 DAP the outer integument started to deposit callose in the outer epidermis, while nuclear divisions continued in the coenocytic endosperm (Fig.1-3). In the chalazal cell (chamber) three or four hypertrophied nuclei were found (Fig.1-4). At 17 DAP the callose in the outer integument was broken down (Fig.1-5 and Fig.1-6), followed by phytomelan synthesis in the space left by the dissolved callose.

At the onset of the callose breakdown, aveoli appeared in the coenocytic micropylar endosperm chamber, marking the beginning of cellularization (Fig.1-5 and Fig.1-7). By this time the single nucellar layer enveloping the endosperm degenerated at the micropylar side. During phytomelan synthesis in the seed coat, the endosperm cellularization went slowly (Fig.2-1), but cellularization was finished at the moment that embryo growth increased (Fig.2-2). The chalazal chamber remained coenocytic with big nuclei, and showed cell wall ingrowths at its chalazal side (Fig.2-3). The hypostase was compressed due to the growth of the endosperm.

The first storage products in the endosperm were found as starch by the end of cellularization at 20 DAP. A layer of the nucellus remained functional at the chalazal side, while the inner integument started to degenerate (Fig.2-4). In the next 7 days proteins and lipids accumulated in the endosperm, embryo, and the outer integument, while the arillus degenerated, leaving a protective seed coat (Fig.2-5 and 2-6). The fruit released its mature seeds at about 40 days after pollination.

Sucrose synthase activity and immunocytochemistry

During the early cellularization phase of the endosperm at 5 DAP, sucrose synthase activity was mainly found in the apical part of the arillus, the micropylar nucellus, and in the chalazal chamber (Fig.3-1). At 7 DAP sucrose synthase activity was found in most tissues, but almost

not in the cells of the inner integument and hypostase. Again the apical part of the arillus showed high activity, as did the young embryo and the micropylar nucellus (Fig.3-2). Immunolabelling was not found at this stage.

At 14 DAP the activity of sucrose synthase had diminished in the arillus and most parts of the integuments. However, high activity was found in the outer epidermal cells of the outer integument (Fig.3-3). This activity was observed during callose synthesis and callose degradation, after which the activity disappeared. The activity was mainly localized in the cytoplasm bordering the block of callose that was synthesized during that stage. Immunolabelling with the antibody against native sucrose synthase of broad bean, showed symplastic sucrose synthase only in the cytoplasm of these epidermal cells during the period of callose synthesis and degradation (Fig.5-1 and 5-4), but not when the callose was completely dissolved (Fig.5-10). The antibody against membrane-associated sucrose synthase labelled the block of callose at the moment that synthesis took place (Fig.5-2 and 5-3), but not when the callose was broken down (Fig.5-5 and 5-6). During callose breakdown, the dissolved callose was labelled (Fig.5-5, 5-11 and 5-12). The antibody against the denatured broad bean sucrose synthase, however, labelled both, the cytoplasm as described for the native antibody, as well as the callose and break down product, as described for the membrane-associated sucrose synthase (Fig.5-7 and 5-13). The antibody against callose (Fig.5-8 and 5-14) always showed the labelling of callose as did the staining with aniline blue, but more intense.

During the stages of callose presence in the integumental cells, membrane-associated sucrose synthase was also found against walls of the chalazal nucellus cells and aveolar walls in the coenocytic endosperm (Fig.3-4 and 3-5). These walls also labelled with the callose antibody (Fig.3-6), but are thin since the aniline blue staining gave a very weak signal (not shown).

Figure 1: Gasteria seed development: coenocytic endosperm. Sections stained with toluidine blue. **(1)** Coenocytic endosperm divided into a chalazal chamber (*cc*) and a micropylar chamber (*mc*). Plasmolysis is due to the embedding protocol (8 DAP). Arrows indicate the tonoplast. Technovit (8 DAP), Bar = 0.2 mm. **(2)** Four celled embryo (*em*) and filiform apparatus (*fa*). Tonoplast (*tp*) is close to embryo due to plasmolysis. Technovit (8 DAP), Bar = 40 μm. **(3)** Coenocytic endosperm showing nuclei (arrows) in the periphere cytoplasm. The transport tissue of the funiculus (*ti*) terminates in the chalazal tissue. Technovit (11 DAP), Bar = 200 μm. **(4)** Detail of **(3)**; Chalazal chamber with three nuclei, and the remnants of the hypostase (*hy*). Bar = 50 μm. **(5)** Formation of aveoli (*av*) in the micropylar chamber endosperm after callose breakdown in the outer epidermis of the outer integument (*oe*). Unicryl (17 DAP), Bar = 60 μm. **(6)** Detail of **(5)**; Callose is broken down (asterix) in the outer epidermis of the outer integument. Bar = 20 μm. **(7)** Detail of **(5)**; Aveoli (*av*) in the coenocytic endosperm against the wall which borders the nucellus (*nu*). Bar = 40 μm. ar = arillus, av = aveoli, cc = chalazal chamber, fa = filiform apparatus, hy = hypostase, ii = inner integument, mc = micropylar chamber, nu = nucellus, oe = outer epidermis outer integument, oi = outer integument, tp = tonoplast

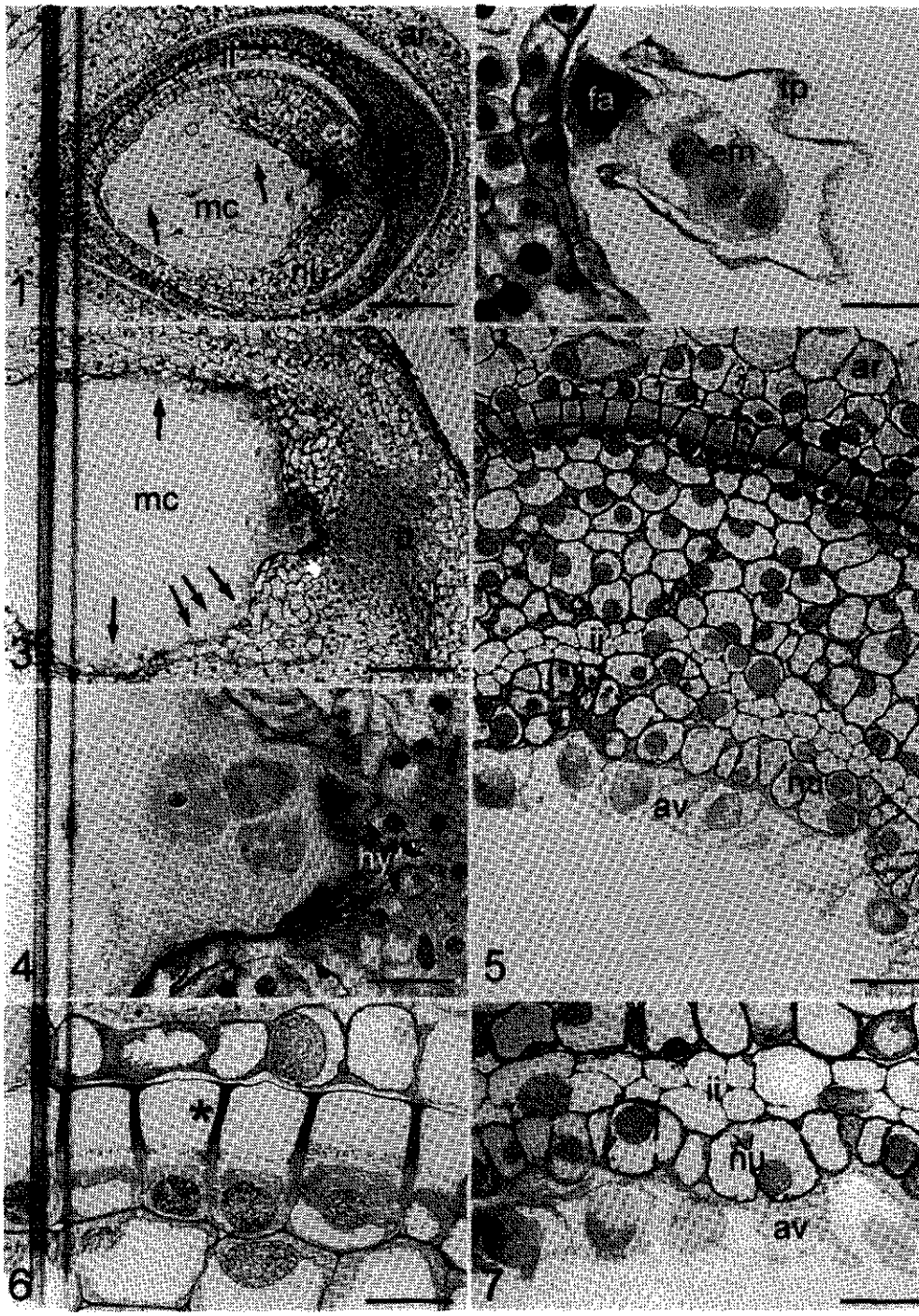
ii
ar
mc
nu
1
fa
sp
em
mc
3
ar
ny
4
ii
nu
av
5
*
6
ii
nu
av
7

At 20 DAP the endosperm sucrose synthase activity was found in the cellularized endosperm, while the seed coat showed hardly any activity (Fig.3-7). The embryo also showed activity (Fig.3-8) but immunocytochemistry did not show labelling for cytoplasmic sucrose synthase in any tissue of the seed. The membrane-associated sucrose synthase antibody labelled new cell walls between probably recently divided endosperm cells (Fig.3-9). At 28 DAP sucrose synthase activity was still found in embryo and endosperm, but the enzyme was not localized by immunolabelling.

Invertase activity and immunocytochemistry.

Invertase activity was not detected until complete cellularization of the endosperm. From 20 DAP till at least 28 DAP, activity was found in endosperm and embryo during production of proteins and lipids (Fig.4-1). During this period invertase activity was also found in the nucellus and some activity was found in the integuments. Immunocytochemistry with the antibody against soluble invertase of carrot, showed the presence of invertases in the nucellus layer around the fertilized embryo sac already at 2 DAP (Fig.4-2). Although the nucellus was not labelled strongly at 7 DAP (Fig.4-3), signal was found in the chalazal nucellus through further development till 20 DAP. Also the synthetic invertase antibodies and the grape invertase antibody gave the same localization in the nucellus (Fig.4-4 and Fig.4-5). At 7 DAP only the parenchyma cells of the arillus showed labelling with the carrot soluble invertase antibody (Fig.4-3), a signal which disappeared during later stages.

Figure 2: Gasteria seed development: endosperm cellularization and filling. **(1) to (4), and (6)** are stained with toluidine blue, **(5)** is stained with PAS and Amido black. **(1)** Slow cellularization of the micropylar chamber endosperm (*mc*) during phytomelan synthesis in the outer epidermis of the outer integument (*oe*). Unicryl (18 DAP), Bar = 150 μm. **(2)** Endosperm cellularization in micropylar chamber (*mc*) finished before the embryo (*em*) increased its growth. Technovit (24 DAP), Bar = 200 μm. **(3)** Coenocytic chalazal chamber (*cc*) with big nuclei (arrows) and wall ingrowths at the chalazal side were also remnants of the compressed hypostase were found (*hy*). Technovit (24 DAP), Bar = 100 μm. **(4)** Starch (black granules) is the first storage product in the endosperm (*es*), but starch is not synthesized in a high amount. The inner integument (*ii*) is degenerated. A layer of nucellus (*nu*) remains functional in chalazal part of the ovule. Technovit (22 DAP), Bar = 100 μm. **(5)** Accumulation of proteins (arrows) and lipids (arrowheads) in endosperm cell. In this particular case, the lipids were not washed out during the fixation and embedding procedure in Unicryl. The lipids showed a brown colour. (36 DAP), Bar = 20 μm. **(6)** Endosperm cells with big nuclei (*n*), protein storage (arrows) and vacuoles (arrowheads) which probably contained lipids but are now empty due to the embedding procedure. The nucellus (*nu*) in this chalazal part is still viable, while the integuments (*in*) and arillus (*ar*) are degenerated. The phytomelan (*ph*) in the outer epidermis of the outer integument is very brittle. Unicryl (27 DAP), Bar = 30 μm.

ar = arillus, cc = chalazal chamber, hy = hypostase, ii = inner integument, em = embryo, es = endosperm, mc = micropylar chamber, n = nucleus, nu = nucellus, oe = outer epidermis outer integument, oi = outer integument, ph = phytomelan

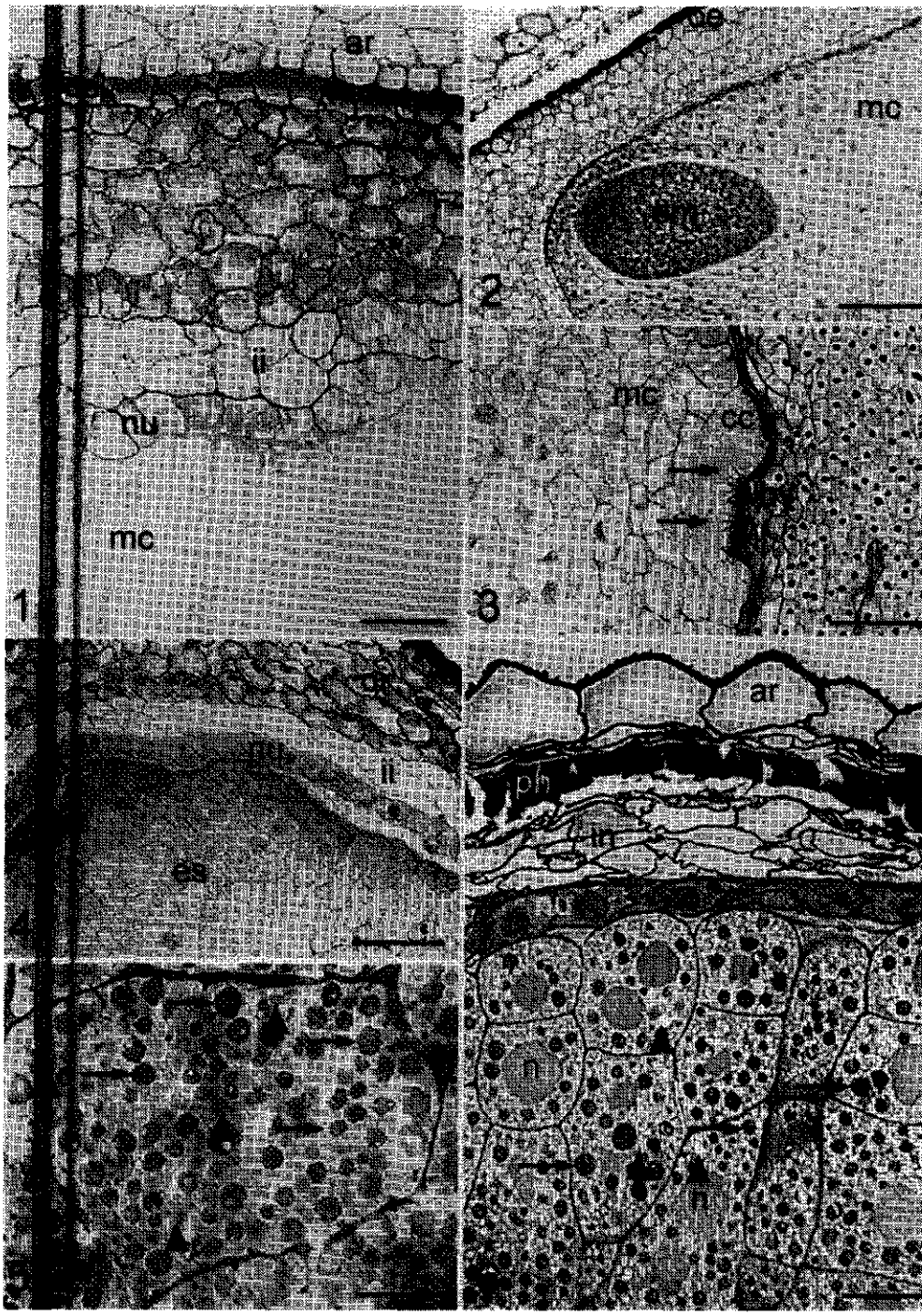
ar
ii
nu
mc
1
oe
mc
2
mc
cc
3
ar
ph
in
ii
n
n

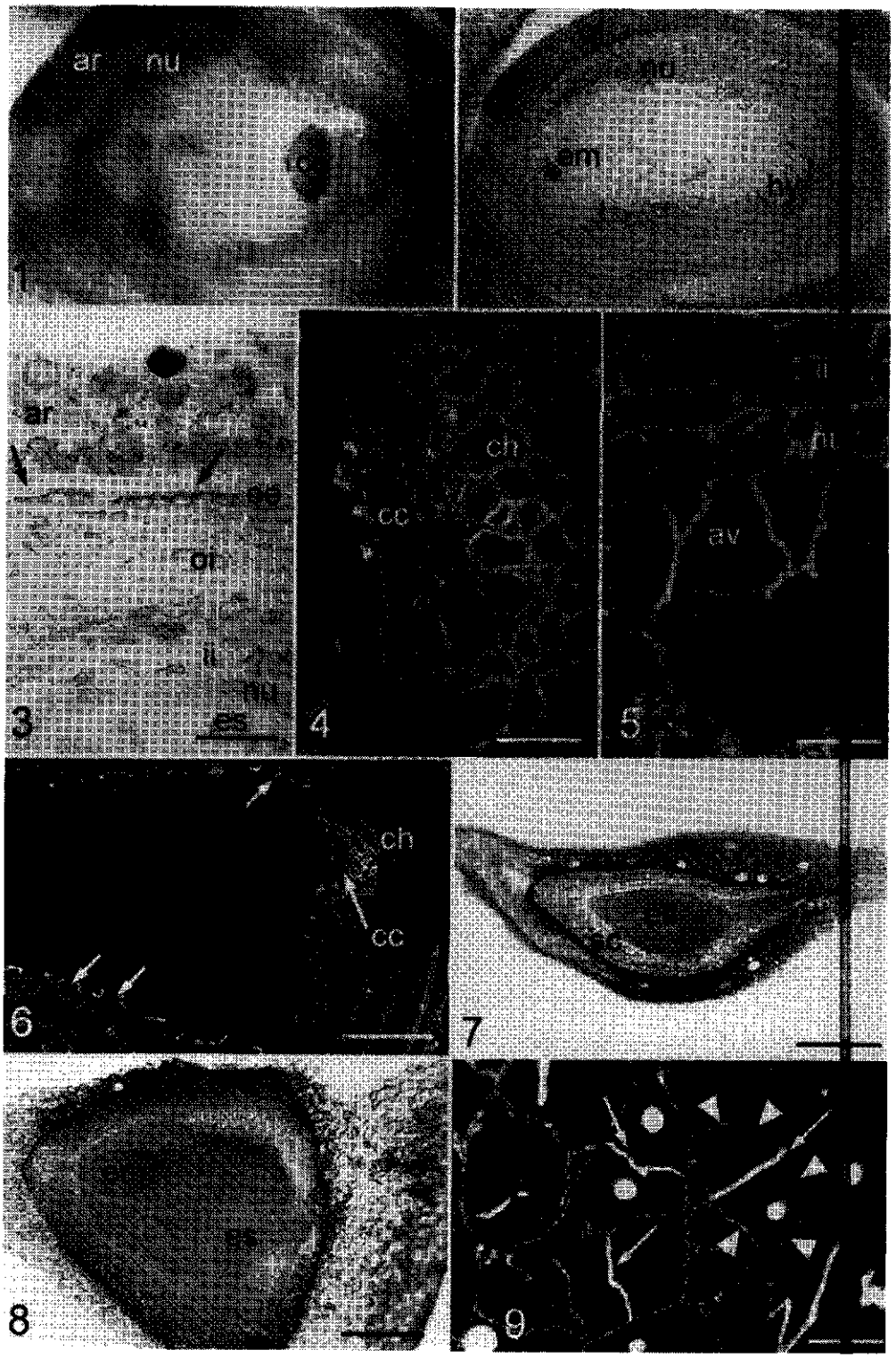
ar
nu
1
nu
em
hy
ar
cc
or
il
nu
es
3
ch
cc
4
nu
av
5
ch
cc
6
7
8
9

During the stage of endosperm filling, the carrot soluble invertase antibody seemed to label cytoplasm and plastids, especially in the cells bordering the embryo (Fig.4-6).
Remarkable results were found during the callose synthesis and degeneration in the outer integument prior to the phytomelan development. The block of callose was labelled with the grape invertase antibody during its synthesis (not shown), but during the breakdown the label was found in the apoplastic solution outside the callose (Fig.5-9 and 5-15).

Figure 3 (previous page): Sucrose synthase activity and presence during seed development. **(1)** Sucrose synthase activity in chalazal chamber (*cc*), in the micropylar nucellus (*nu*), and in the arillus (*ar*), shown by using the sucrose synthase histochemical assay (5 DAP). Bar = 100 μm. **(2)** Sucrose synthase activity in the embryo (*em*), nucellus (*nu*), outer integument (*oi*) and arillus (*ar*), while almost no activity is shown in the inner integument (*ii*) and hypostase (*hy*) (7 DAP). Bar = 200 μm. **(3)** Sucrose synthase activity in the cytoplasm of the outer epidermis cells of the outer integument (*oe*) while callose (arrows) is being synthesized in these cells. In arillus (*ar*) and integuments (*oi* and *ii*) sucrose synthase activity is diminished (14 DAP). Bar = 100 μm. **(4)** The antibody against membrane-associated sucrose synthase labels the walls of chalazal cells (*ch*) (14 DAP). Bar = 20 μm. **(5)** The antibody for membrane-associated sucrose synthase labels the walls of aveoli (*av*) (14 DAP). Bar = 40 μm. **(6)** Labelling with callose antibody shows a signal on chalazal cell walls (*ch*) and aveoli walls (arrows) (14 DAP). Bar = 200 μm. **(7)** Sucrose synthase activity in cellularized endosperm (*es*), while seed coat (*sc*) shows not much activity. Tangential section (20 DAP). Bar = 500 μm. **(8)** Sucrose synthase activity in embryo (*em*) and endosperm (*es*). Longitudinal section (20 DAP). Bar = 500 μm. **(9)** Membrane-associated sucrose synthase antibody labels new cell walls (arrows) in endosperm (20 DAP). In older cell walls plasmodesmata are labelled (arrowheads). Nuclei are stained with DAPI (double exposure). Bar = 40 μm.
ar = arillus, av = aveoli, cc = chalazal chamber, ch = chalazal cells, em = embryo, es = endosperm, hy = hypostase, ii = inner integument, nu = nucellus, oe = outer epidermis outer integument, oi = outer integument, sc = seed coat

Figure 4 (next page): Invertase activity and presence during seed development. **(1)** Invertase activity in endosperm (*es*) and embryo (*em*) during the endosperm filling with proteins and lipids, shown by using the invertase histochemical assay (20 DAP). Bar = 500 μm. **(2)** Carrot soluble invertase antibody labels nucellus (*nu*) (2 DAP). Bar = 40 μm. **(3)** Carrot soluble invertase antibody labels invertase in chalazal nucellus (*nu*) weak, and parenchyma cells of the arillus (*ar*) strong (7 DAP). Bar = 100 μm. **(4)** Grape soluble invertase antibody labels the nucellus (*nu*), while the rest of the tissue is negative (15 DAP). Bar = 100 μm. **(5)** Grape soluble invertase antibody labels the chalazal nucellar cells (*nu*) (20 DAP). Bar = 100 μm. **(6A)** Carrot soluble invertase antibody labels cytoplasm and plastids in the endosperm (*es*) bordering the embryo (*em*) (28 DAP). Bar = 200 μm. **(6B)** UV illumination of **(6A)**, showing DAPI-staining of nuclei.
ar = arillus, ch = chalazal cells, ea = egg apparatus, em = embryo, es = endosperm, ii = inner integument, nu = nucellus, oi = outer integument, sc = seed coat

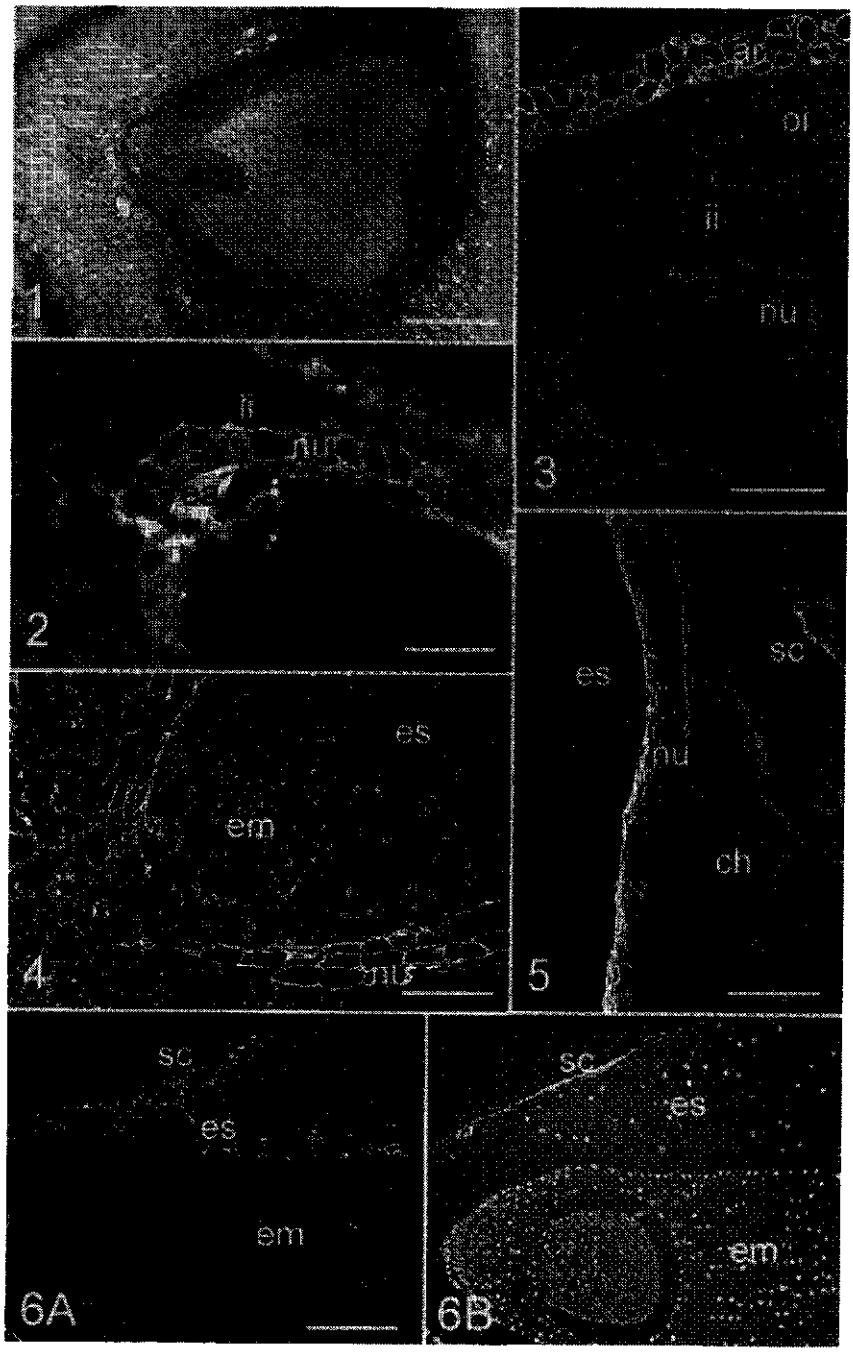
1
ii
nu
2
ii
nu
3
or
ii
nu
4
es
em
nu
5
es
sc
nu
ch
6A
sc
es
em
6B
sc
es
em

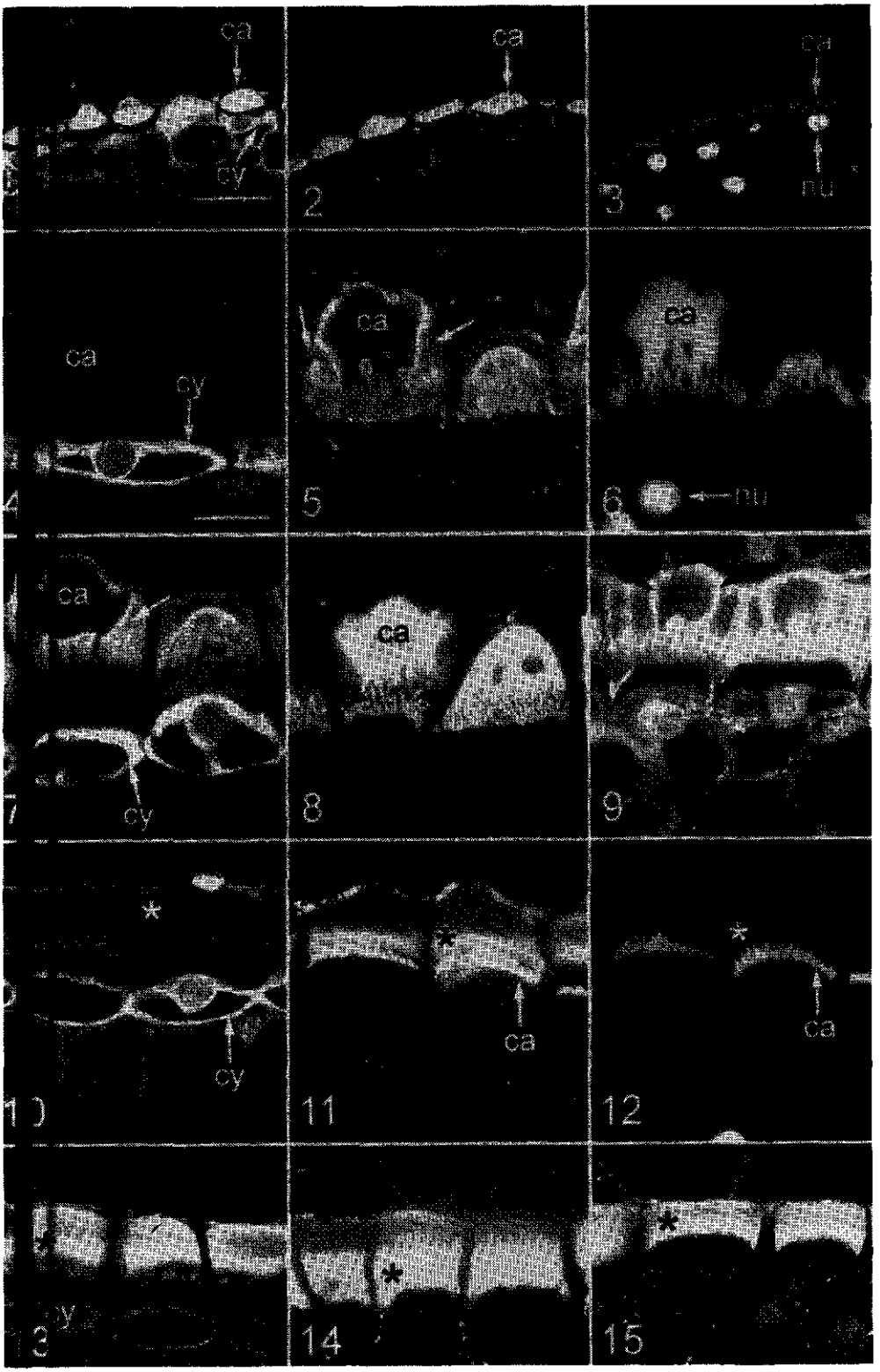
ca
cy
2
3
nu
4
5
6
7
8
9
10
11
12
13
14
15

DISCUSSION AND CONCLUSIONS

In Figure 6 the results obtained with the enzyme activity assays and the immunocytological results are summarized schematically. They point to four steps in seed development.

(1) Ovule expansion

First after fertilization the nucleate helobial endosperm expands, together with the rest of the ovule. Invertase is present in the nucellus, but the activity is probably too low to detect by the assay or perhaps even absent. Also in other experiments it was concluded that the invertase assay is not sensitive enough to detect low invertase activities (In this thesis chapter 3). Activity of invertase in the nucellus might be needed to break down the sucrose into monosaccharides which can be transported into the nucleate endosperm. Invertase activity could also create a sucrose gradient from phloem to nucellus, enhancing the phloem unloading. During the first five days after pollination the arillus expands dramatically and finally envelopes the entire ovule. Sucrose synthase activity in the arillus during its growth, might provide the carbohydrates for cell growth. Sucrose synthase activity in the micropylar nucellus and chalazal chamber may function in the nutrition of the micropylar chamber.

Figure 5 (previous page): Callose synthesis, callose breakdown and dissolved callose in the outer integument of the outer epidermis.

(1) to (3): Callose synthesis at 12 DAP. All figures magnification as in **(1)**. **(1)** Immunolabelling of the callose (*ca*) and cytoplasm (*cy*) with an antibody against native sucrose synthase of broad bean. Bar = 75 μm. **(2)** Immunolabelling of callose (*ca*) with an antibody against membrane-associated sucrose synthase. **(3)** Aniline blue (callose) and DAPI (nuclei) staining of section shown in **(2)**.

(4) to (9): Callose breakdown at 15 DAP. All figures magnification as in **(4)**. **(4)** Immunolabelling of the cytoplasm (*cy*) with an antibody against native sucrose synthase of broad bean. Bar = 20 μm. **(5)** Immunolabelling of the dissolved callose (arrows) around the callose block (ca) with an antibody against membrane-associated sucrose synthase. **(6)** Aniline blue (callose) and DAPI (nuclei) staining of section shown in **(5)**. **(7)** Immunolabelling of the dissolved callose (arrows) around the callose block and the cytoplasm with an antibody against denatured broad bean sucrose synthase. **(8)** Immunolabelling of the dissolving block callose with antibody against β-1,3-glucans. **(9)** Immunolabelling of the dissolved callose (arrows) around the callose block with antibody against grape invertase.

(10) to (15): Completely dissolved callose block at 18 DAP. All figures magnification as in **(4)**. **(10)** Immunolabelling with the antibody against native sucrose synthase of broad bean gives no signal in the dissolved callose (asterix). **(11)** Immunolabelling of the dissolved callose (asterix) with the antibody against membrane-associated sucrose synthase. **(12)** Aniline blue (callose) and DAPI (nuclei) staining of section shown in **(11)**. **(13)** Immunolabelling of the dissolved callose (asterix) with an antibody against denatured sucrose synthase of broad bean. **(14)** Immunolabelling of the dissolved callose (asterix) with an antibody against β-1,3-glucans. **(15)** Immunolabelling of the dissolved callose (asterix) with an antibody against soluble invertase of grape.

ca = callose, cy = cytoplasm, nu = nucleus

(2) Callose in the seed coat

The phytomelan layer develops after ovule expansion, and is preceded by the callose synthesis in the outer epidermis of the outer integument (Wittich and Graven 1995; in this thesis chapter 6). Immunolabelling suggests the presence of invertase in the epidermal callose, but activity was not detected. Sucrose synthase activity is present in the cytoplasm of the integumental epidermis during callose synthesis and degradation. The supply of UDP-glucose for callose synthesis might be completely provided by this cytoplasmic sucrose synthase. However, apoplastic sucrose synthase, as was detected by the membrane-associated sucrose synthase antibody, might also supply UDP-glucose for the callose synthesis. No activity of the apoplastic sucrose synthase was shown by the assay, but when a complex of sucrose synthase and callose synthase exists (Amor *et al.* 1995), the UDP-glucose will be directly used by the callose synthase, and be not released into the cytoplasm or apoplastic fluid. Thus the activity of apoplastic and membrane-associated sucrose synthase can not be detected by the assay. A same model of UDP-glucose supply is also expected for the sucrose synthase-cellulose synthase complex (Amor *et al.* 1995, This thesis: Chapter 2). The fact that the denatured sucrose synthase labels two different epitopes (for cytoplasmic sucrose synthase and membrane-associated sucrose synthase) may indicate that the antibody for membrane-associated sucrose synthase labels denatured sucrose synthase. However, it is hard to speculate on a possible function of the (denatured) sucrose synthase, and the invertase, in the block of callose. If callose is broken down by endoglucanases, there might be a function for sucrose synthase and invertase in the breakdown of the glucan polymers into smaller polymers or monosaccharides. It is not likely that sucrose is resynthesized from callose by the sucrose synthase, because that process requires UDP-glucose and fructose, while the callose breakdown product is most likely glucose. On the other hand, the apoplastic enzymes might also be inactivated and have no particular use here.

The block of callose determines the size of the phytomelan deposition, but seems also to function as temporary storage of carbohydrates for the synthesis of phytomelan or a new cellulose wall between phytomelan and plasma membrane (Wittich and Graven 1995; in this thesis chapter 6). The layer of phytomelan around the seed integument also determines the final volume of the seed, and might protect the endosperm against dehydration, pathogens, and mechanical pressure form the outside.

(3) Endosperm cellularization

At the time that callose in the outer integument is almost completely broken down, the cellularization of the endosperm starts with the formation of aveoli. After completion of phytomelan synthesis, the endosperm cellularization increases. Also the embryo slowly starts its growth. Invertase was found in the nucellus by immunocytochemistry during cytokinesis,

and its (low) activity was detected by the assay. This activity is probably needed for providing monosaccharides for uptake by the embryo and endosperm and to create a sucrose gradient towards the phloem, thus enhancing the phloem unloading. The degeneration of the micropylar nucellus may mark the loss of nutrient transport into the endosperm via the micropylar side, resulting in uptake into the endosperm only via the chalazal side. Cytoplasmic sucrose synthase is not present in high concentrations, but the membrane- associated sucrose synthase is present against the new aveolar walls and cell walls of the chalazal nucellus. Cytoplasmic sucrose synthase is not present in high concentrations, but the membrane-associated sucrose synthase is present against the new aveolar walls and in new cell walls after divisions of endosperm cells. This membrane-associated sucrose synthase seems to be related with the callose synthesis and/or cellulose synthesis which takes place in new cell walls.

Antibodies against callose and membrane-associated sucrose synthase gave a strong signal in the chalazal nucellar cells, they probably labelled the callose of plasmodesmata. The high concentration of plasmodesmata in these cells indicate a strong capacity for symplastic transport towards the chalazal endosperm. This, together with the cell wall ingrowths found in the chalazal chamber, point towards a function of the chalazal chamber in the uptake of nutrients into the endosperm. This is prevented in early stages by the hypostase, which is almost completely degenerated during endosperm cellularization.

The maturation of the seed coat starts by the degeneration of the inner integumental cells. The degradation products might be transported towards the endosperm and used there for growth and storage.

Figure 6

Schematic presentation of enzyme-histochemical and immunocytochemical results on developing *Gasteria* seeds. The first row represents the stage of ovule expansion, with coenocytic endosperm and a growing arillus. The second row represents the stage of callose deposition in the outer epidermis of the outer integument. The third row represents the stage of initiation of endosperm cellularization by the formation of aveoli at the moment that callose in the outer integument is dissolved, while in the fourth row cellularization is completed. The fifth row represents the stage where the endosperm becomes filled with storage products.

Column 1: Invertase activity is detected in the nucellus after endosperm cellularization and in the endosperm during the storage synthesis.

Column 2: Invertase immunocytochemistry shows presence of the enzyme first in nucellus and arillus, followed by presence in the callose of the outer integument (before phytomelan synthesis), and finally in the endosperm around the embryo.

Column 3: Sucrose synthase activity is localized in growing tissues; first in the nucellus and arillus, then in the callose synthesizing cells of the outer integument (before phytomelan synthesis), and finally in cellularizing and filling endosperm.

Column 4: Sucrose synthase immunocytochemistry shows only high amounts of sucrose synthase in the outer epidermis of the outer integument during callose synthesis and breakdown (leading to phytomelan).

(4) Endosperm storage

During cellularization of the endosperm there is some starch synthesis, but after completion of the cellularization synthesis of lipids and proteins starts in endosperm and embryo, whereas no further starch synthesis takes place from that time. Increased invertase activity in the nucellus is probably related with a higher supply of monosaccharides to the strong endosperm sink. The

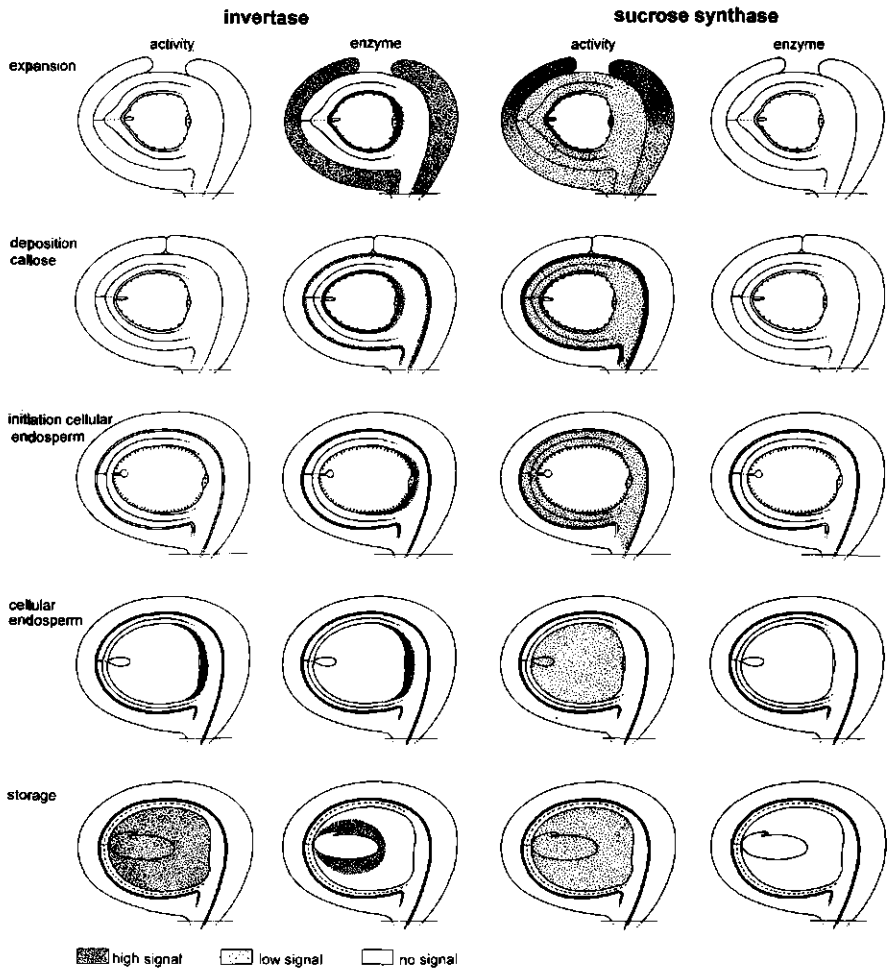

Figure 6: Summary of invertase and sucrose synthase localization results.

high invertase activity in the endosperm cells might be related with lipid synthesis (Slack and Browse 1984), while sucrose synthase activity might provide UDP-glucose for protein synthesis as was found by Doehlert (1990) for the synthesis of zein in maize. The high activity of invertase in both nucellus and endosperm indicates that sucrose is present in both tissues. It is possible that not all sucrose is hydrolysed prior to uptake into the endosperm, however, it is also possible that sucrose is re-synthesized in the endosperm by the activity of sucrose phosphate synthase and other enzymes (Chourey *et al.* 1996, Huber and Huber 1996). The latter seems not to be a very economical way for the plant to provide the endosperm with carbohydrates since invertase and sucrose synthase in the endosperm have to break down the sucrose again, but it may enhance the diffusion of carbohydrates through the tissues by creating a cascade of gradients. A similar pathway is found in maize kernels (Chourey *et al* 1996, Wittich and Vreugdenhil 1998; in this thesis chapter 2).

A function of the chalazal chamber during endosperm development might be found in the uptake of nutrients into the endosperm. From the results it seems that this chamber remains coenocytic, although results on the chalazal chamber in mature seeds is lacking. Cell wall ingrowths into the chalazal side of the chamber indicate an increased import capacity. Also other studies pointed to a haustorial or nutritive function of the chalazal chamber (Vijayaraghavan and Prabhakar 1984). This nutritive function makes the import of nutrients into the endosperm via the chalazal side possible again, after it was prevented by the hypostase in the ovule before fertilization (In this thesis chapter 4). However, the nutrient import capacity of the transfer walls does not seem sufficient to supply the entire endosperm with nutrients via the chalazal chamber if it is compared with the basal transfer cells of maize (In this thesis chapter 4). It seems likely that nutrient uptake takes place along the whole endosperm surface because nucellus tissue remains present during endosperm formation, and along the chalazal side of the endosperm even during endosperm filling. Also no explicit gradients of starch, lipid, or protein synthesis takes place during this endosperm filling like those found during maize endosperm filling (Wittich and Vreugdenhil 1998; in this thesis chapter 2).
During the endosperm filling, the cytoplasm of the outer integument and arillus degenerates after loosing its sucrose synthase and invertase activity.

The role for invertase in the nucellus of *Gasteria* seems to be providing monosaccharides for uptake into the endosperm and embryo, and by its activity also enhancing the phloem unloading. During the switch of endosperm cellularization to endosperm filling there is no decrease of invertase activity. In *Vicia faba* this switch to storage functions correlated with a decrease in invertase activity in the seed coat, and the gain in the embryo's ability to import

sucrose directly for storage (Weber *et al* 1997, and references herein). However, in *Gasteria* hexoses may still be needed for the synthesis of lipids as storage products and thus a decrease in activity is not to be expected.

The cytoplasmic sucrose synthase is shown to be related with cell growth and callose synthesis during *Gasteria* seed development, especially in the outer integument. It is present in the growing tissues and disappears afterwards. The vacuolar and/or cytoplasmic invertase, and sucrose synthase seem to be needed for synthesis of storage products.

In conclusion, during the seed development the plant seems to direct its energy in the form of carbohydrates to distinct tissues. These tissues appear to develop almost completely before the carbohydrate flow will be directed to an other tissue. First the carbohydrates are used for arillus formation (sucrose synthase activity) and a little for nucleate helobial endosperm development (sucrose synthase activity in chalazal chamber, but low invertase activity in nucellus). Then most of the carbohydrates are used for callose synthesis prior to phytomelan synthesis (sucrose synthase activity). After the phytomelan layer has determined the seeds final volume like a scaffold, the seed is ready for endosperm cellularization and the accumulation of storage products (invertase and sucrose synthase activity). Whereas supplies are transported via the nucellus into the chalazal part of the endosperm (invertase activity in nucellus), the reduced hypostase does not function as a barrier anymore in this stage. During the accumulation of storage products in the endosperm, the cells of the seed coat and arillus degenerate. This may be due to starvation, since the endosperm consumes all the nutrients.

ACKNOWLEDGEMENTS

For sending me the antibodies I would like to thank DP Delmer, AH Kingston-Smith, KE Koch, H Ross, HP Ruffner, and A Sturm. For reading the manuscript and giving their comments I would like to acknowledge MTM Willemse, AAM van Lammeren and CJ Keijzer, for the drawings AB Haasdijk and PA van Snippenburg, and for the photo plates S Massalt.

REFERENCES

Amor Y, CH Haigler, S Johnson, M Wainscott and DP Delmer (1995) A membrane-associated from sucrose synthase and its potential role in synthesis of cellulose and callose in plants. Proc Natl Acad Sci USA 92: 9353-9357

Baskin TI, CH Busby, LC Fowke, M Sammut and F Gubler (1992) Improvements in immunostaining samples embedded in methacrylate: localization of microtubules and other antigens throughout developing organs in plants of diverse taxa. Planta 187: 405-413

Chourey PS, W-H Cheng, EW Taliercio and KH Im (1996) Genetic aspects of sucrose metabolizing enzymes in developing maize seed. In: Madore MA and WJ Lucas (eds) Carbon partitioning and sucrose-sink interactions.

American Society of Plant Physiologists, Rockville: 239-245

Chourey PS and OE Nelson (1976) The enzymatic deficiency conditioned by the *shrunken-1* mutations in maize. Biochem Genet 14: 1041-1055

Dahlgren RMT, HT Clifford and PF Yeo (1985) The families of the monocotyledons. Structure, evolution, and taxonomy. Springer-Verlag Berlin, Heidelberg, New York, Tokyo.

Delmer DP and Y Amor (1995) Cellulose biosynthesis. The Plant Cell 7: 987-1000

Doehlert DC (1990) Distribution of enzyme activities within the developing maize (*Zea mays*) kernel in relation to starch, oil and protein accumulation. Physiol Plant 78: 560-567

Doehlert DC and FC Felker (1987) Characterization and distribution of invertase activity in developing maize (*Zea mays*) kernels. Physiol Plant 70: 51-57

Eschrich W and HB Currier (1964) Identification of callose by its diachrome and fluorochrome reactions. Stain Techn. 39: 303-307

Jensen WA (1962) Botanical histochemistry. FWH Freeman and Company, San Francisco

Johansen DA (1950) Plant embryology. Embryology of the spermatophyta. Chronica Botanica Company, Waltham

Ho LC, A Lecharny and J Willenbrink (1991). Sucrose cleavage in relation to import and metabolism of sugars in sink organs. In: Recent advances in phloem transport and assimilate compartmentation. JL Bonnemain, S Delrot, WJ Lucas and J Dainty (eds), Ouest editions, Nantes: 178-186

Huber SC and JL Huber (1996) Role and regulation of sucrose-phosphate synthase in higher plants. Annu Rev Plant Physiol Plant Mol Biol 47: 431-444

Kingston-Smith AH and CJ Pollock (1996) Tissue level localization of acid invertase in leaves: an hypothesis for the regulation of carbon export. New Phytol 134: 423-432

Koch KE, KD Nolte, ER Duke, DR McCarty and WT Avigne (1992) Sugar levels modulate differential expression of maize sucrose synthase genes. Plant Cell 4: 59-69

Kruger NJ (1990) Carbohydrate synthesis and degradation. In: Plant Physiol, biochemistry and molecular biology. DT Dennis and DH Turpin (eds.) Longman Scientific & Technical. Ellex: 59-79

Laurière CM, A Laurière, A Sturm, L Faye and MJ Chrispeels (1988) Characterization of ß-fructosidase, an extracellular glycoprotein of carrot cells. Biochimie 70: 1483-1491

Northcote DH, R Davey and J Lay (1989). Use of antisera to localize callose, xylan and arabinogalactan in the cell-plate, primary and secondary walls of plant cells. Planta 178: 353-366

O'Brien TP, Feder N and ME McCully (1965) Polychromatic staining of plant cell walls by toluidine blue O. Protoplasma 59: 368-373

Patrick JW and CE Offler (1995) Post-sieve element transport of sucrose in developing seeds. Austr J Plant Physiol 109: 579-585

Ross HA and HV Davies (1992) Purification and characterization of sucrose synthase from the cotyledons of *Vicia faba* L. Plant Physiol 100: 1008-1013

Ruffner HP, M Hürlimann and R Skrivan (1995) Soluble invertase from grape berries: purification, deglycosylation and antibody specificity. Plant Physiol Biochem 33: 25-31

Schnarf K and R Wunderlich (1938) Zur vergleichenden Embryologie der *Liliaceae - Asphodeloideae*. Flora 133: 297-327

Schneider H (1981) Plant anatomy and general botany. In: Clark G (ed) Staining procedures. Williams and Wilkins, Baltimore: 315-333

Slack CR and JA Browse (1984) Synthesis of storage lipids in developing seeds. In: Murray (ed), Seed physiology, Vol 1. Academic Press, Sidney: 209-244

Sung S-JS, D-P Xu and CC Black (1989) Identification of actively filling sucrose sinks. Plant Physiol 89: 1117-1121

Sung SS, WJ Sheih, DR Geiger and CC Black (1994) Growth, sucrose synthase, and invertase activities of developing *Phaseolus vulgaris* L. fruits. Plant Cell Env 17: 419-426

Unger C, M Hardegger, S Lienhard and A Sturm (1994) cDNA cloning of carrot (*Daucus carota*) soluble acid β-fructofuranosidases and comparison with the cell wall isoenzyme. Plant Phys 104: 1351-1357

Vijayaraghavan MR and K Prabhakar (1984) The endosperm. In: Embryology of angiosperms. BM Johri (ed), Springer-Verlag, Berlin: 319-376

Willemse MTM and MAW Franssen-Verheijen (1988) Ovular development and pollen tube growth in the ovary of *Gasteria verrucosa* (Mill.) H. Duval as condition for fertilization. Sexual reproduction in higher plants. M Cresti, P Gori and E Pacini (eds), Springer-Verlag, Berlin: 357-362

Wittich PE and P Graven (1995) Histochemical study of the development of the phytomelan layer in the seed coat of Gasteria verrucosa (Mill.) H. Duval. Protoplasma 187: 72-78

Wittich PE and P Graven (1998) Callose deposition and breakdown, followed by phytomelan synthesis in the seed coat of *Gasteria verrucosa* (Mill.) H. Duval. Protoplasma 201: 221-230

Wittich PE and D Vreugdenhil. (1998) Localization of sucrose synthase activity in developing maize kernels by in situ enzyme histochemistry. J Exp Bot: in press

Xu D-P, S-JS Sung, T Loboda, PP Kormanik and CC Black (1989) Characterization of sucrolysis via the uridine diphosphate and pyrophosphate-dependent sucrose synthase pathway. Plant Physiol 90: 635-642

Chapter

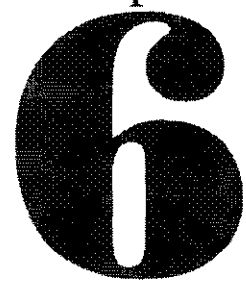

Histochemical study of the development of the phytomelan layer in the seed coat of *Gasteria verrucosa* (Mill.) H. Duval

P.E. Wittich[1] and P. Graven[2]

[1]Department of Plant Cytology and Morphology, Wageningen Agricultural University, Wageningen

[2]Hugo de Vries-Laboratory, University of Amsterdam, Amsterdam

Protoplasma (1995) 187: 72-78

Summary. In this study we document the development of the phytomelan layer in the outer epidermis of the outer integument of *Gasteria verrucosa.* Phytomelan has been described as a black, melanin-like substance which is chemically very inert. Using histochemical techniques we show that phytomelan development in the cell wall can be divided into three stages. The first stage is deposition of a callosic layer against the tangential wall, with simultaneous thickening of the adjacent parts of the radial walls. The second stage is the conversion of this callosic wall, which we call a tertiary wall, into a non-callosic inner and outer layer. The inner layer stains predominantly for cellulose and a little for pectin. The outer layer is of unknown composition, since it did not react with the stains that were used. In the third stage the outer tertiary layer becomes black, the phytomelan. The callosic wall deposited in the first developmental stage seems to function as a carbohydrate source and as a mould for the tertiary cell wall. The conversion of the callose in the second stage might be the result of penetration of substances which react with callose. All the components for phytomelan seem to be present in the outer layer before the conversion. Phenolics might be involved in this second conversion.

INTRODUCTION

The ovule of *Gasteria verrucosa* (Mill.) H. Duval (Asphodelaceae, subfamily Alooideae) is anatropous and has a two cell thick inner integument and a three cell thick outer integument. Like most Asphodelaceae (Huber 1969) *Gasteria* develops a phytomelan layer in the outer epidermis of the outer integument. After formation of the phytomelan layer the cytoplasm of the other integumental cell layers degenerates. The remaining cell walls become slightly compressed. A funicular arillus envelops the lower half of the mature ovule and expands after fertilization into a wing shaped structure enclosing the entire ovule. This arillus is generally four cells thick and dehydrated in mature seeds.

In the monocotyledons phytomelan seem to be most common in (and perhaps restricted to) the seeds of the order Asparagales (Dahlgren and Clifford 1982). Development of a phytomelan layer is shown in drawings of *Asparagus officinalis* by Robbins and Borthwick (1925) and of *Muscari commosum* and *M. racemosum* by Wunderlich (1937). In *A. officinalis* the phytomelan layer seems to comprise epidermal cells containing phytomelan deposits, while in *M. commosum* and *M. racemosum* it seems to be a continuous layer, covering the epidermal cells like a cuticle.

Takhtajan (1985) characterized the seed coat of the order Asparagales as a melanin cork: a black pigment formed by melanization, phytomelanin, that is stored in cells. Dahlgren and Clifford (1982) described phytomelan as opaque, brittle and charcoal-like. It is known that phytomelan is chemically very inert and has a carbon : hydrogen : oxygen ratio of 3.7 : 2.1 : 1.0 (Dafert and Miklauz 1912), we know of no chemical study of phytomelan that characterizes it as a type of melanin. In general, melanins are high molecular weight compounds formed by enzymatic oxidation of phenolics. They are difficult to study because they are resistant to chemical degradation (Thomson 1976).

Possible functions of the phytomelan layer in the seed coat are protection against fungal and microbial invasion, and prevention of deterioration, dehydration and radiation (Netolitzky 1926, Dahlgren and Rasmussen 1983). According to Takhtajan (1985) the phytomelan layer has a mechanical function in the seed coat. The phytomelan layer is used in plant systematics as an identification character. It has never been studied well enough to know what phytomelan is, how it is deposited in the seed coat, and whether it is of the same composition and structure in all the plant families which contain it. In this study we use histochemical techniques to investigate the development of the phytomelan layer in the seed coat of *Gasteria*.

MATERIAL AND METHODS

Plants of a self-incompatible hybrid population of *Gasteria verrucosa* (Mill.) H. Duval were grown in the greenhouse at 16 h light periods between 18 and 25°C. Flowers were cross-pollinated in November and December 1993. Seeds were collected every day from 14 days after pollination (DAP) until 20 DAP and then 22, 25, 29, 38 and 45 DAP (mature seed).

The seeds were hand sectioned into 1 mm thick slices and fixed for 45 min in 3% glutaraldehyde in 0.1 M phosphate buffer, pH 7.2 at room temperature. After dehydration in an alcohol series the material was embedded in Technovit 7100 (Kulzer), in polyethylene glycol (PEG) (Merck), or, after dehydration through a tertiary butyl alcohol series in paraplast (Brunschwig Chemie). Technovit sections (7 μm) were used directly for staining. PEG sections (5 μm) were transferred with PEG 6000 (Merck) to poly-l-lysine (Sigma) coated slides and rinsed with water before staining. Paraplast sections (5 μm) were deparafinized through a xylol, tertiary butyl alcohol, alcohol and water series. Fresh seeds were embedded in Tissue-Tek (Miles), frozen at -20°C and sectioned with a Micron CR 50-H Bio-Med cryostat.

The sections were stained for (a) callose with 1.5% resorcin blue in 0.5% NH_4OH or 0.005% aniline blue (Eschrich and Currier 1964), (b) cellulose with zinc chlor-iodide (Jensen 1962) or 1% congo red (Locquin and Langeron 1983), (c) pectin with 0.1% ruthenium red (Jensen 1962), (d) lignin with satured phloroglucinol in 20% HCl (Jensen 1962), (e) lignin and some polyphenols which stain green with the polychromatic stain toluidine blue (0.025%, pH 4.0) (Feder and Wolf 1965, O'Brien *et al.* 1965), (f) carbohydrates with periodic acid-Schiff's reagent (PAS) (Jensen 1962), omitting the oxidation reaction with periodic acid for controls, (g) proteins with 1% amido black in 7% acetic acid (Schneider 1981), and (h) cutin, suberin and fats with saturated Sudan IV in 95% ethanol (Schneider 1981). The cellulose stains and the ruthenium red may also stain some hemicelluloses and oxidized cellulose (Jensen 1962, Fry- Wyssling 1976), while a negative reaction not necessarily mean that the component being stained for is absent. It may have been extracted during embedding. It is also possible that the stain can not reach binding sites because they are covered with other wall material, or that

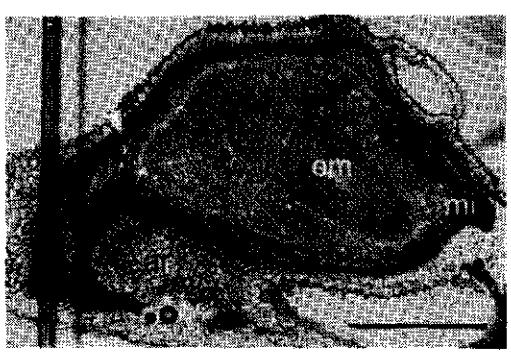

Figure 1 A 20 μm cryosection of a mature seed. The phytomelan layer (arrowhead) envelopes the ovule. Openings in the phytomelan layer at the micropyle (*mi*) and hilum (*hi*) are not visible. An arillus (*ar*) covers the integuments. *em* Embryo; bar : 500 μm. Bright field.

large numbers of binding sites must be present for staining to be detected (Jensen 1962).
The sections were photographed using bright field, polarizing light, differential interference contrast, or UV microscopy.
In order to remove the wall matrix paraplast sections of 22 DAP seeds were mounted on glass slides coated with Kaiser's glycerol gelatin (Merck), deparafinized, and boiled for 15 or 45 min in a mixture of 30% hydrogen peroxide and glacial acetic acid (1 : 1 v/v). When the material has been treated long enough only cellulose microfibrils remain (Willemse 1972, Desphande 1976, Emons 1988). The treated sections were stained for cellulose by zinc chlor-iodide.

RESULTS

Between 14 and 25 DAP wall material is deposited against the existing secondary wall of the outer epidermal cells of the outer integument. Because this material differs from that of the secondary walls, we use the term "tertiary wall". The formation of phytomelan in this tertiary wall results in a black epidermal layer enveloping the developing ovule (Fig. 1) except at the micropylar opening and the hilum.

Figure 2 PAS stained Technovit sections, A-D, x 975, bright field. **A** Stage 1: thickening of the radial secondary wall (*sw*) of the outer epidermal cells of the outer integument, and deposition of the PAS positive tertiary wall (*tw*). *cy* Cytoplasm. **B** Stage 2: conversion of the tertiary wall material into PAS negative material (arrows). *ar* Arillus. **C** The tertiary wall after first conversion: an PAS positive inner layer (*il*) and a PAS negative outer layer (*ol*). **D** Stage 3: second conversion (darkening) of the outer tertiary layer. The inner tertiary layer and secondary walls are PAS positive. The outer tertiary layer is PAS negative and converts into phytomelan. *cl* Cell lumen.

Figure 3 Stage 1: deposition of the tertiary wall. **A-C** Paraplast sections and **D** PEG section. A-D, x 975, differential interference contrast. **A** Zinc chlor-iodide stains the cellulosic radial secondary walls (*sw*) during the deposition of the callosic tertiary wall (*tw*) **B** Local pectin staining (arrow) by ruthenium red in the radial secondary wall at the end of the deposition of the callosic tertiary wall. **C** Pectin staining of the entire radial secondary wall after callose deposition. **D** Resorcin stains the tertiary wall (*tw*) blue, indicating the presence of callose.

Figure 4 Stage 2: first conversion of the tertiary wall. **A** PEG section, **B-D** paraplast sections. A-D x 975, differential interference contrast (A and D) and bright field (B and C). **A** Resorcin blue staining shows callose patterns (*ca*) during the first conversion of the tertiary wall. **B** Amido black staining reveals proteins in the inner tertiary layer (*il*). *ol* Outer tertiary layer. **C** Zinc chlor-iodide stains the cellulose in the inner layer. **D** The end of the first conversion; the cellulose stain congo red in combination with polarised light showing cellulose fibrils in the secondary wall and cellulose isotropy in the tertiary inner layer. A cell lumen (*cl*) remains after degeneration of the cytoplasm.

Figure 5 Second conversion of the tertiary wall. **A-D** Paraplast sections. x 975. **A** At the start of the second conversion the outer layer (*ol*) stains green with toluidine blue, indicating the presence of phenolics. *il* Inner layer, *cl* cell lumen. **B** Zinc chlor-iodide stains the cellulose of the inner layer. The outer layer is darkening. **C** Toluidine blue stains the brown outer layer green. **D** Zinc chlor-iodide stains the cellulosic inner layer (arrow). The outer layer is fully converted into phytomelan.

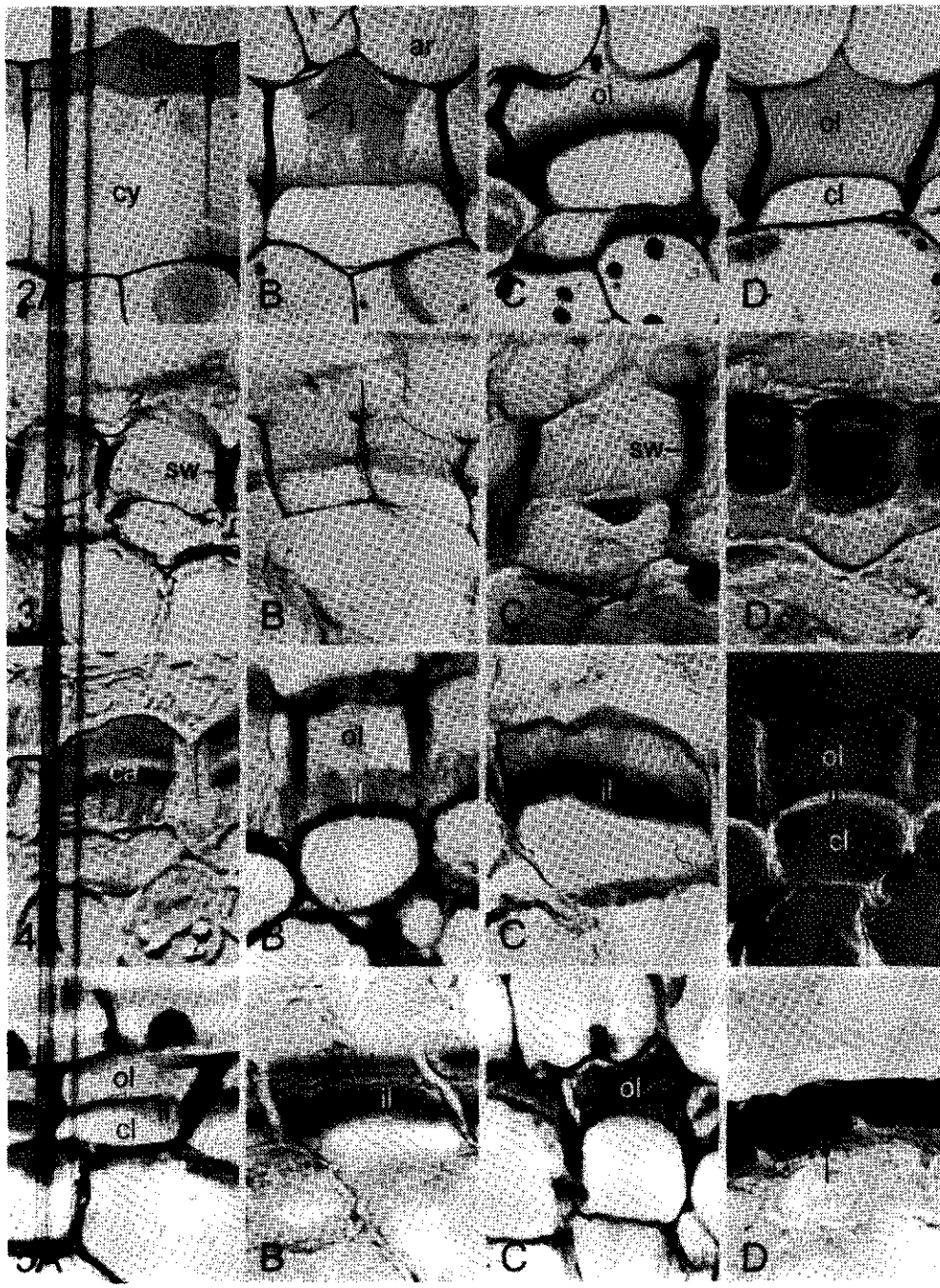
cy
ar
ol
cl
sw
ol
cl
ol
cl
ol
cl

Based on morphological changes we distinguish three developmental stages. The first stage (14-16 DAP) is the thickening of the radial secondary walls and the deposition of a tertiary wall against the outer secondary tangential wall (Fig. 2A). The second stage (17-19 DAP) is the conversion of the tertiary wall (Fig. 2B) into a two layered structure, an inner and an outer (Fig. 2C). The inner layer is PAS positive while the outer layer is PAS negative. In the third stage (20-25 DAP) the material of the outer layer is converted into phytomelan (Fig. 2D).

Stage 1 (14 - 16 DAP): deposition of the tertiary wall

During the first developmental stage the radial secondary walls thicken and the tangential tertiary wall is deposited. Radial secondary wall thickening starts at the outer tangential side of the wall. About two thirds of the wall thickens and can be stained for cellulose (Fig. 3A), but not for pectin or lignin. Staining for pectin develops in the radial secondary wall when the thickening is completed, initially on the tangential side (Fig. 3B, C). A tertiary wall is deposited against the outer tangential secondary wall, between the thickened radial walls. The callose stains aniline blue and resorcin blue both stain this tertiary wall (Fig. 3D). PAS also produces a positive reaction (Fig. 2A) but the PAS control and stains for cellulose, pectin, lignin, phenolics, proteins, and fatty substances do not react.

Stage 2 (17 - 19 DAP): first conversion of the tertiary wall.

In the second stage the callose wall is transformed (Fig. 4A) into two non-callosic layers. Just before this occurs proteins in the inner tangential layer of the callose wall, against the plasma membrane, become stainable. Protein staining is more distinct when the callose is being modified (Fig. 4B). After conversion of the callosic tertiary wall the inner tertiary layer can be stained for cellulose (Fig. 4C, D), slightly for pectin, but no longer for callose or proteins. The border between the inner and outer layer is not very distinct (Fig. 2C) and the inner layer near the plasma membrane shows isotropy of the cellulose with polarized light (Fig. 4D). The conversion of the outer callosic layer starts at its inner tangential and radial borders, resulting in a distinctive pattern (Fig. 2B and 4A). After conversion the outer tertiary layer can not be stained with cellulose, pectin, lignin, phenolic, carbohydrate (Fig. 2C), protein, or lipid stains. The secondary walls show no differences after conversion of the tertiary wall. At the end of this first conversion the cytoplasm of these epidermal cells degenerates leaving a lumen (Fig. 4D).

Stage 3 (20 - 25 DAP): second conversion of the tertiary wall

In the third stage the outer layer of the tertiary wall gradually becomes brown (Fig. 2D and 5A-C) and eventually black (Fig. 5D). The darkening outer tertiary layer can not be stained for cellulose, pectin, lignin (by phloroglucinol), carbohydrates, proteins, or fatty substances. Only

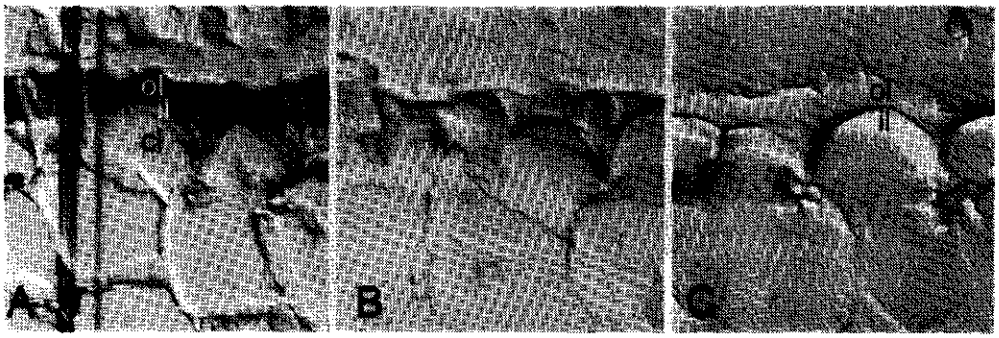

Figure 6 Sections (22 DAP) treated with hydrogen peroxide-glacial acetic acid. A-D, x 975, differential interference contrast. **A** 0 min. Dark brown outer tertiary layer (*ol*), inner tertiary layer (*il*), and cell lumen (*cl*). **B** 15 min. The outer layer is partly dissolved. **C** 45 min. Persistent secondary walls (*sw*) and inner layer; the outer layer seems to be dissolved.

toluidine blue stains the darkening wall green (Fig. 5A, C), indicating the presence of phenolics. The outer tertiary layer shows neither UV autofluorescence nor polarization effects. At about 25 DAP the outer tertiary layer is fully developed and black (Fig. 5D), masking any staining reactions. The inner tertiary layer does not show any differences after the second stage.

During the treatment of 22 DAP seed sections with hydrogen peroxide-glacial acetic acid the dark brown outer tertiary wall layer pales and seems to disappeared after 45 min treatment (Fig. 6). The persistent inner tertiary wall and the secondary walls stains for cellulose (data not shown).

DISCUSSION

As far as we know development of the phytomelan has never been studied by histochemical techniques. Drawings with little detail of seed coat development have been published by Robbins and Borthwick (1925) and Wunderlich (1937). Wunderlich (1937) stated that for *Muscari commosum* and *M. racemosum* "the lumina of the epidermal cells of the outer integument becomes almost completely filled with a dark brown substance". In *Gasteria* the phytomelan layer consists of outer integumental cells whose lumina are partly replaced by a tertiary wall of phytomelan.

Stage 1: deposition of the tertiary wall

From 14 DAP until 16 DAP deposition of a callosic tertiary wall occurs. In the outer epidermis of the outer integument two thirds of the radial secondary walls thickens, starting at the outer

tangential side. The thickening walls stain for cellulose but not for pectin. However, it can not be concluded that pectin is absent from the radial walls; other wall components might cover the pectin, or there may be too little pectin present to visualize the staining. When the secondary radial wall thickening is complete, pectin staining becomes visible, starting on the outer tangential side of the walls; the radial wall stains for pectin but no longer for cellulose. The treatment of 22 DAP seed sections with hydrogen peroxide-glacial acetic acid showed that cellulose is still present in the radial walls. Increased pectin or other wall components seem to prevent cellulose staining in these walls. The radial secondary walls do not seem to change any more during subsequent tertiary wall development.

A tertiary wall is deposited against the outer tangential secondary wall, between the thickened parts of the radial secondary walls. The tertiary wall seems to consists of callose and is probably synthesized by plasma membrane-bound callose synthase (Delmer *et al.* 1993). The callosic tertiary wall stains with PAS, but not with any of the other stains. PAS staining might be the result of the presence of other carbohydrates besides callose, since PAS does not stain β-1,3-glucans (such as callose) (Gabe 1976). The tertiary wall finally occludes about two thirds of the original cell lumen.

Stage 2: first conversion of the tertiary wall

Between 17 and 19 DAP the first conversion of the callosic tertiary wall takes place, resulting in an outer layer bordering the secondary tangential wall, and an inner layer against the plasma membrane. Just before conversion of the callosic tertiary wall can be detected, proteins in the inner layer of the callose become stainable. This inner layer converts into a layer which stains for cellulose and slightly for pectin. The border between the inner tertiary layer and the outer layer is not very distinct and cellulose isotropy suggest that cellulose near the plasma membrane is crystalline. The proteins in the inner layer are only stainable during the conversion and therefore may be involved in the formation of cellulose and pectin. Although it is known that cellulose synthase is localised at the plasma membrane (Delmer 1987, Emons 1991), it seems that cellulose and pectin are formed inside the tertiary callosic wall. The callose is probably the carbohydrate source for the cellulose formation. Meier *et al.* (1981) showed that callose might function as an intermediate in the cellulose biosynthesis in cotton fibres. The callose in the outer part of the tertiary wall undergoes a remarkable pattern of conversion. A substrate seems to penetrate the callosic wall via the plasma membrane and radial walls, and interferes with the callose. The consistency of the callose apparently permits this penetration and reaction. The penetrating substance might come from the cytoplasm. The outer layer of the callosic tertiary wall seems to be used during this first conversion as a source of carbohydrates, since there is a distinct border between the newly-formed PAS negative

material and callose during the conversion. The callosic wall also seems to serve as a mould for the converted tertiary wall, because the thickness of the callosic wall determines the thickness of the tertiary wall after conversion. Such functions for callose are known from microspore development; the breakdown products of the callosic wall around microspore tetrads are a source of carbohydrates for further microspore development (Keijzer and Willemse 1988) and the callosic tetrad wall can function as a mould for the pollen wall (Waterkeyn and Bienfait 1970, Willemse 1971). However, in this study the callosic wall seems to function simultaneously as a mould and source for the new tertiary wall. The composition of the converted outer layer remains unknown because it does not stain for cellulose, pectin, lignin, phenolics, carbohydrates, or fatty substances. It is also possible that there is nothing to be stained, if during conversion the callosic wall is broken down by enzymes into mono- and disaccharides. Such saccharides cannot be fixed by glutaraldehyde and will be rinsed away during the embedding procedure.

Stage 3: second conversion of the tertiary wall

Starting at 20 DAP a second conversion occurs in the outer layer of the tertiary wall. The whole layer slowly becomes brown and later black (the phytomelan). This darkening process, and the degeneration of the cytoplasm, suggest that the elements required for this conversion are already present in the tertiary layer. The composition of phytomelan remains unclear, because only toluidine blue stained the outer tertiary layer. The green stain obtained with toluidine blue indicates the presence of phenolics (Feder and Wolf 1965). This suggests that phytomelan is a type of melanin, because phenolics are involved in melanin synthesis (Thomson 1976). The treatment of sections with hydrogen peroxide-glacial acetic acid followed by cellulose staining, produced no reaction indicating the presence of cellulose.

The phytomelan layer around the seed appears to be discontinuous: black tertiary wall material (phytomelan) is separated by radial secondary walls. Phytomelan is chemically very inert and impermeable to water (Werker and Fahn 1975). But breaks in the phytomelan layer at the micropylar opening and hilum, plus its discontinuous nature, raises questions about its function in protecting the seed against fungal and microbial invasion. It is possible that it protects against rapid dehydration and radiation while the micropylar opening and hilum might be important for water uptake prior to germination. The construction of the phytomelan layer, i.e., stiff phytomelan within a softer secondary wall network, gives this mechanical layer (Takhtajan 1985) more flexibility.

Further studies are in progress to obtain more information on the ultrastructure of the phytomelan layer, and the synthesis and macromolecular composition of the phytomelan.

ACKNOWLEDGEMENTS

We wish to thank Dr. F. Bouman, Dr. A.M.C. Emons, and Dr. M.T.M. Willemse for the valuable discussions and critically reading the manuscript; G. van Geerenstein for culturing the plants; S. Massalt, P.A. van Snippenburg and A. Haasdijk for preparing the photographs for publication. This study was partly supported by the Life Sciences Foundation (SLW) which is subsidized by the Netherlands Organization for Scientific Research (NWO).

REFERENCES

Dafert FW and Miklauz R (1912) Untersuchungen über die kohleähnliche Masse der Kompositen (Chemischer Teil). Denkschr Akad Wiss Wien Math Naturw Kl 87: 143-152

Dahlgren RMT and Clifford HT (1982) The monocotyledons. A comparative study. Academic Press, London

Dahlgren RMT and Rasmussen FN (1983) Monocotyledon evolution, characters and phylogenetic estimation. Evol Biol 16: 255-395

Delmer DP (1987) Cellulose biosynthesis. Annu Rev Plant Physiol 38: 250-259

Delmer DP, M Volokita, M Solomon, U Fritz, W Delphendahl and W Herth (1993) A monoclonal antibody recognizes a 65 kDa higher plant membrane polypeptide which undergoes cation-dependent association with callose synthase in vitro and co-localizes with sites of callose deposition in vivo. Protoplasma 176: 33-42

Desphande BP (1976) Observations on the fine structure of plant cell walls. I. Use of permanganate staining. Ann Bot 40: 433-437

Emons AMC (1988) Methods for visualizing cell wall texture. Acta Bot Neerl 37: 31-38

Emons AMC (1991) Role of particle rosettes and terminal globules in cellulose synthesis. In: Haigler CH and Weimer PJ (eds) Biosynthesis and biodegradation of cellulose. Marcel Dekker, New York, pp 71-98

Eschrich W and HB Currier (1964) Identification of callose by its diachrome and fluorochrome reactions. Stain Technol 39: 303-307

Feder N and MK Wolf (1965) Studies on nucleic acid metachromasy II. Metachromatic and orthochromatic staining by toluidine blue of nucleic acid in tissue sections. J Cell Biol 27: 327-336

Fry-Wyssling A (1976) The plant cell wall. Gebrüder Borntraeger, Berlin [Handbuch der Pflanzenanatomie, vol III/4, 3rd edn]

Gabe M (1976) Histological techniques. Masson, Paris

Huber H (1969) Die Samenmerkmale und Verwandtschaftsverhältnisse der Liliifloren. Mitt Bot Staatssaml München VIII: 219-538

Jensen WA (1962) Botanical histochemistry. FWH Freeman and Company, San Francisco

Keijzer CJ and Willemse MTM (1988) Tissue interactions in the developing locule of *Gasteria verrucosa* during microsporogenesis. Acta Bot Neerl 37: 493-508

Locquin MV and Langeron M (1983) Handbook of microscopy. Butterworths, London

Meier H, L Buchs, AJ Buchala and T Homewood (1981) (1→3)-β-Glucan (callose) is a probable intermediate in biosynthesis of cellulose of cotton fibres. Nature 289: 821-822

Netolitzky F (1926) Anatomie der Angiospermen-Samen. Gebrüder Borntraeger, Berlin [Handbuch der Pflanzen Anatomie, vol X]

O'Brien TP, Feder N and McCully ME (1965) Polychromatic staining of plant cell walls by toluidine blue O.

Protoplasma 59: 368-373

Robbins WW and Borthwick HA (1925) Development of the seed of *Asparagus officinalis*. Bot Gaz 80: 426-438

Schneider H (1981) Plant anatomy and general botany. In: Clark G (ed) Staining procedures. Williams and Wilkins, Baltimore, pp 315-333

Takhtajan A (1985) Anatomia seminum comparativa, vol I, Liliopsida seu monocotyledons (in Russian). Nauka, Leningrad

Thomson RH (1976) Miscellaneous pigments. In: Goodwin TW (ed) Chemistry and biochemistry of plant pigments, vol 1. Academic Press, London, pp 597-623

Waterkeyn L and A Bienfait (1970) On a possible function of the callosic special wall in *Ipomoea purpurea* (L.) Roth. Grana 10: 13-20

Werker E and A Fahn (1975) Seeds anatomy of *Pancratium* species of three different habitats. Bot Gaz 136: 396-403

Willemse MTM (1971) Morphological and quantitative changes in the population of cell organelles during microsporogenesis of *Pinus sylvestris* L. III. Morphological changes during the tetrad stage and in the young microspore. A quantitative approach to the changes in the population of cell organelles. Acta Bot Neerl 20: 498-523

Willemse MTM (1972) Changes in the autofluorescence of the pollen wall during microsporogenesis and chemical treatments. Acta Bot Neerl 21: 1-16

Wunderlich R (1937) Zur vergleichenden Embryologie der Liliaceae - Scilloideae. Flora 132: 48-90

Chapter

Callose deposition and breakdown, followed by phytomelan synthesis in the seed coat of *Gasteria verrucosa* (Mill.) H. Duval

P.E. Wittich[1] and **P. Graven**[2]

[1]Laboratory of Plant Cytology and Morphology, Wageningen Agricultural University, Wageningen

[2]Hugo de Vries-Laboratory, University of Amsterdam, Amsterdam

Protoplasma (1998) 201, 3-4: in press

Summary. In the seed coat of *Gasteria verrucosa* the deposition of phytomelan takes place during seed development in three stages. Phytomelan is a black cell wall material which is chemically very inert. First the radial walls and part of the transverse cell wall of the outer epidermis of the outer integument become thickened by exocytosis of dictyosome vesicles. Callose is deposited at the tangential plasma membrane against those walls. After the callose deposition about two thirds of the original cell volume is filled with callose. During the second stage the callose is broken down, probably into glucose monomers or small polymers. At the same time cellulose is deposited at the outer tangential plasma membrane, forming a wall between the dissolving callose and the plasma membrane. In the third phase small granules appear in the solution of dissolved callose, which grow out and finally fuse to form a block of phytomelan, consisting of spherical 15 nm units. Remarkable is the function of the callose: it determines the size of the phytomelan block, and it probably functions as carbohydrate source for the phytomelan synthesis and/or for the cellulose inner layer. In this study transmission electron microscopy and cryo scanning electron microscopy are used to study the three developmental stages of the formation of the phytomelan layer.

INTRODUCTION

Phytomelan is found in the seed coat of members of the Asparagales (Dahlgren and Clifford 1982) and in the fruit of some Compositae (Hanausek 1907, Hegnauer 1962-1990). A member of the Asparagales is *Gasteria verrucosa* (Mill.) H. Duval (Asphodeliaceae). In *Gasteria* phytomelan is formed in the seed coat by the outer epidermal cells of the outer integument. The epidermis becomes a black layer, consisting of phytomelan blocks bordered by thickened radial and transverse secondary cell walls (Fig.1) (Wittich and Graven 1995). Phytomelan is a brittle, coal-like substance, rich in carbon (Dahlgren and Clifford 1982), and is chemically very inert (Dafert and Miklauz 1912). It is also described as a black pigment that is stored in cells, forming a continuous melanin cork (Takhtajan 1985).

Using light microscopy and histochemistry, Wittich and Graven (1995) showed that in the development of the phytomelan layer three stages can be distinguished (Fig.2). They showed that the first stage involves thickening of the radial and transverse secondary cell walls of the outer epidermal cells of the outer integument, followed by deposition of a callose tertiary wall against the outer tangential secondary wall, and finally accumulation of pectin in the radial and transverse secondary walls. At the end of this first stage about two thirds of the original cell lumen is occupied by callose. It was shown that in the second stage the callose tertiary wall converts into an inner layer and an outer layer. The inner tertiary layer consists of cellulose and some pectin, the composition of the outer tertiary layer remained unknown (Wittich and Graven 1995). In the third stage the outer tertiary wall layer converts into the black phytomelan. Histochemical stains showed that phenolics are involved in the synthesis of the phytomelan. The callose that is deposited during the first developmental stage functions probably as a source for carbohydrates and as a template of the phytomelan (Wittich and Graven 1995).

In this paper the ultrastructural development of the phytomelan layer is studied using electron microscopical techniques. The results are discussed in relation to histochemical data from the previous study (Wittich and Graven 1995).

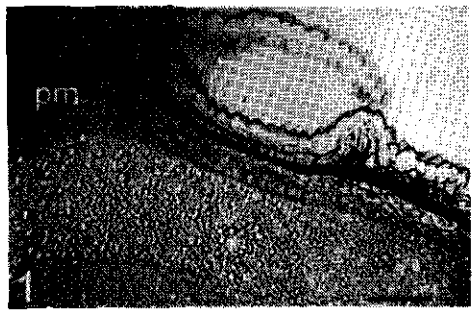

Figure 1: A 20 µm cryosection of the seed coat of *Gasteria verrucosa*. The epidermal cells are filled with phytomelan (*pm*). Bar = 50 µm.

Stages of phytomelan development based on histochemistry

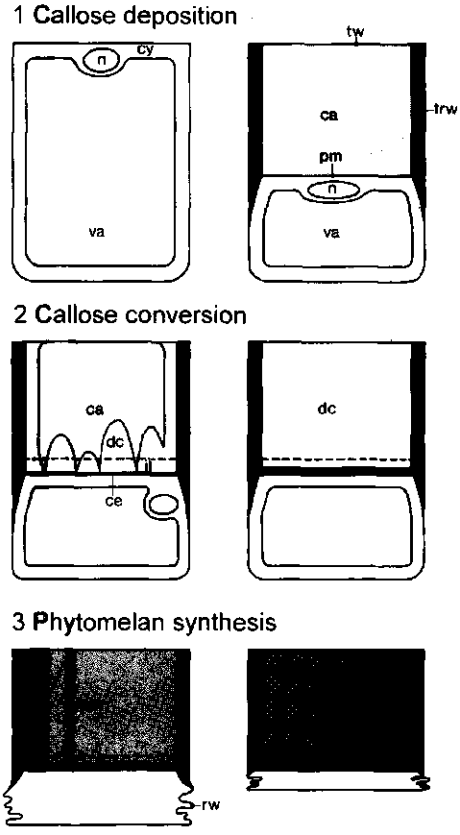

Figure 2: Schematic presentation of the phytomelan development in the outer epidermal cells of the outer integument of *Gasteria verrucosa*; based on histochemical study (Wittich and Graven 1995). **(1)** Callose deposition between the thickened part of the radial (and transverse) walls (*trw*), the outer tangential plasma membrane (*pm*), and the outer tangential wall (*tw*). The callose replaces approximately two thirds of the total volume of the cytoplasm (*cy*) and vacuole (*va*). *n* = Nucleus. **(2)** Callose conversion, starting from the outside. The block callose becomes dissolved (*dc*). From the plasma membrane the inner tertiary layer develops (*il*), consisting of a cellulose gradient (*ce*) with the highest cellulose concentration near the plasma membrane. **(3)** Phytomelan (*pm*) synthesis in the outer tertiary layer after complete degeneration of the cytoplasm. During the phytomelan synthesis the thin radial (and transverse) walls (*rw*) fold.

Material and methods

Plants of a self-incompatible population of *Gasteria verrucosa* (Mill.) H. Duval were grown in the greenhouse at a day length of 16 hours and a temperature between 18 and 25°C. Flowers were cross-pollinated and seeds were collected every day starting at 14 days after pollination (DAP) till 20 DAP and on 22, 25, 29, 38, and 45 DAP.

Electron microscopy

Seeds were dissected by hand into 1-2 mm thick sections to enhance penetration of solvents. They were fixed in 3% glutaraldehyde in 0.1 M phosphate buffer (pH 7.2) for 45 minutes at room temperature. The material was washed in the buffer, postfixed for 2 hours in 1%

buffered osmium tetroxide, and dehydrated in an ethanol series.
For transmission electron microscopy (TEM), the material was embedded in Epon 812 (Merck). Ultrathin sections were poststained with lead citrate and uranyl acetate and examined with a Jeol 1200 TEM. In some cases postfixation with osmium tetroxide and staining with lead citrate/uranyl acetate was omitted to observe autocontrast.
For scanning electron microscopy (SEM), ethanol dehydrated material was critical point dried over CO_2, mounted on a stub and a new cut surface was made with a razor blade. The specimen was sputter-coated with palladium/gold and examined using a Jeol JSM-6300F SEM.
For cryo-SEM fresh seeds were mounted on a stub with Tissue Tek, frozen in liquid propane, and inside an Oxford Instruments CT 1500 HF cryo-transfer unit freeze-fractured (at -120°C). After studying the fracture surface in the Jeol 6300F SEM (cooled at 170°C), the material was freeze dried for 20 minutes at -90°C in the cryo-transfer unit and sputter-coated with 4-5 nm palladium-gold.
Polysaccharides were stained for TEM and SEM according the PATAg technique described by Thiéry (1967), and modified as follows. The material was fixed as described above with 3% glutaraldehyde, but not postfixed with osmium tetroxide. Ultrathin sections for the TEM were mounted on golden grids prior to the PATAg staining, while for SEM, PATAg staining was performed on critical-point-dried material. The grids and critical point dried materials were oxidized for 30 minutes with 1% periodic acid, three times 10 minutes washed in water, placed for 20 hours in thiocarbahydrazide, three times 10 minutes washed in 15% acetic acid, two times placed for 10 minutes in 5% acetic acid, followed by two times 2% acetic acid and 10 minutes in water, 40 minutes treated with 1% silverproteinate, and finally washed in water.
After air drying, the SEM material was coated with carbon and examined with a Jeol 6300F SEM, using an Autrata backscatter detector.

RESULTS

Callose deposition (stage 1): 14 - 16 DAP

At 14 DAP, after full elongation of the outer epidermal cells of the outer integument, a large part of the secondary radial (and transverse) walls and a small part of the outer tangential wall start to thicken (Fig.3). The excreted radial wall material is fine granular and heterogeneous. The plasma membrane against the thickening radial walls undulates. In the cytoplasm dictyosomes and RER are abundant and sometimes starch is present.

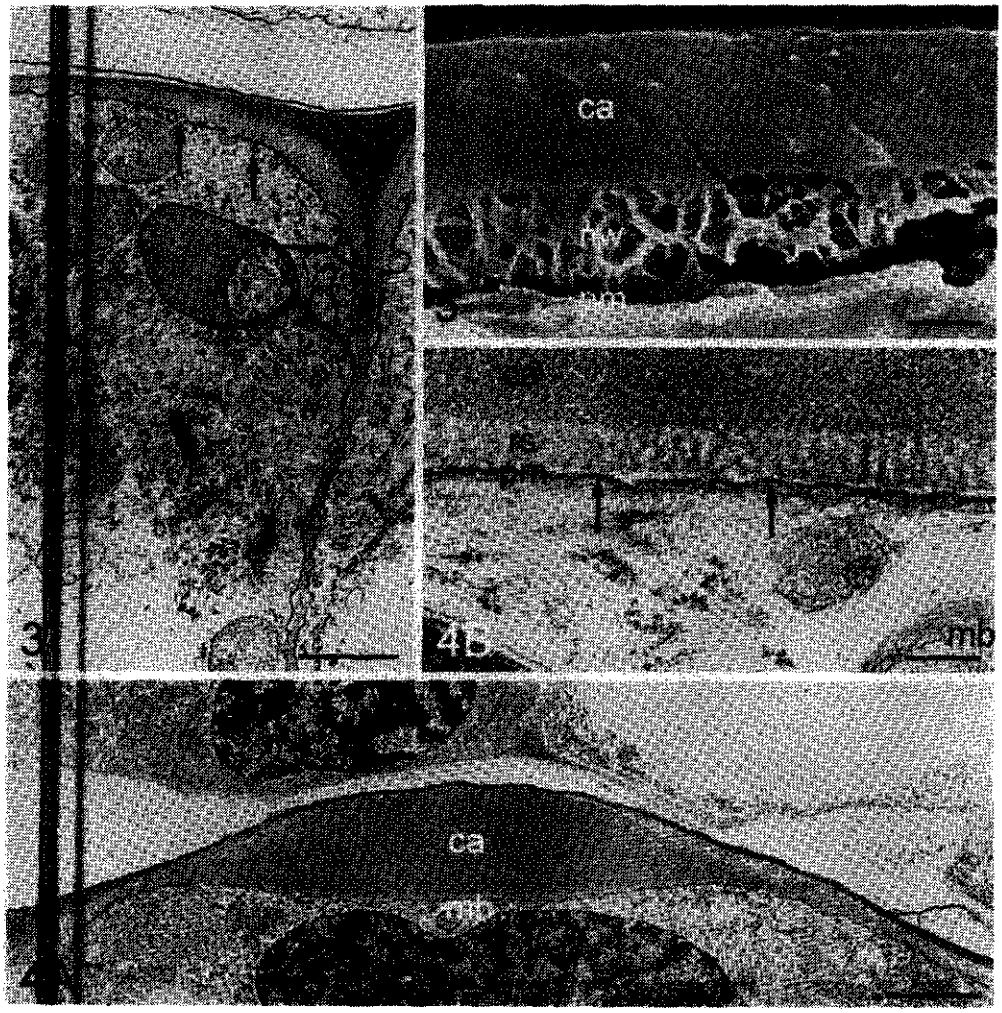

Figure 3. 14 DAP; undulating plasma membrane along the thickening of the radial wall and part of the tangential wall (arrows), TEM. Bar = 1 μm.

Figure 4. 15 DAP; deposition of callose against the exterior tangential wall, TEM. **A** Callose (*ca*) and multivesicular body (*mb*). Bar = 3 μm. **B** Detail of **A**; at several places (arrows) rod-like structures (*rs*) connect the plasma membrane (*pm*) with the callose (*ca*). Bar = 200 nm.

Figure 5. 15 DAP; callose deposition, cryo-SEM. Homogeneous callose (*ca*) during early deposition and rod-like or network-like structures (*nw*) at plasma membrane (*pm*). Shrinkage (artefact) caused separation of plasma membrane from network-like structures. Bar = 500 nm.

At 15 DAP a tertiary wall of fine granular material is deposited against the outer tangential secondary wall (Fig.4A). This tertiary wall was histochemically shown to consist of callose (Wittich and Graven 1995). The plasma membrane remains connected with the callose tertiary wall by small perpendicular rods (Fig.4B). Fine electron-dense spots can be found in the callose. In the cytoplasm multi-vesicular bodies appear. Also the cryo-SEM shows a homogeneous callose against the outer tangential wall but a more network-like structure toward the membrane (Fig.5).

At 16 DAP the secondary radial wall thickening has continued and the callose tertiary wall has increased in size at the cost of the cell volume (Fig.6A). In the heterogeneous, thickened radial wall the contents of dictyosome vesicles are still visible (Fig.6B). The callose deposition has continued till the end of the thickened part of the radial walls, but unlike the TEM images the cryo-SEM shows a homogenous center of the callose block, whereas its tangential sides show a network-like structure (Fig.7).

Breakdown of callose (stage 2): 17 - 19 DAP

At 17 DAP the radial (and transverse) wall thickening has completed. At the border of the radial walls with the callose tertiary wall, a thin layer of electron dense material is visible (Fig.8). The consistency of the callose tertiary wall seems to be homogeneous and two thirds of the original cell volume are filled by it. The rod-like structures have disappeared and the wall directly borders the plasma membrane. The cisterns of stacked RER slightly dilatates (Fig.9A) and the area between the RER strands become filled with dark-stained granular material (Fig.9B), resulting in large pools of the latter (Fig.8A and Fig.9C). At this time this dark stained granular material can also be found outside the plasma membrane, in the periplasmic space (Fig.9D). At the end of 17 DAP as well as at 18 DAP the previous cisterns of the (R)ER have started to swell (Fig.9D). Some number of the plastids have become hypertrophied (Fig.9C,D).

At 18 DAP sometimes an osmophilic network is found in the corners of the callose. Here the fine granular callose is not present anymore (Fig.10A,B).

Figure 6. 16 DAP; continued radial wall thickening and callose deposition, TEM. **A** Callose (*ca*) against thickened part of radial wall (*trw*). Bar = 3 μm. **B** Detail of thickening part of radial wall with undulating plasma membrane (*upm*), Golgi vesicles (arrows), dictyosome (*d*) and abundant ribosomes (*r*). Bar = 600 nm.

Figure 7. 16 DAP; deposition of callose, cryo-SEM. Freeze-etched homogeneous callose (*ca*) and network-like structures (*nw*) near shrunken plasma membrane (*pm*). cy Cytoplasm: bar = 1 μm.

Figure 8. 17 DAP; end of callose deposition, TEM. Callose (*ca*) bordered with a thin electron-dense material (arrows) against the radial (*rw*) and tangential secondary walls (*tw*). The ER in the cytoplasm (*cy*) is very active. Bar = 10 μm.

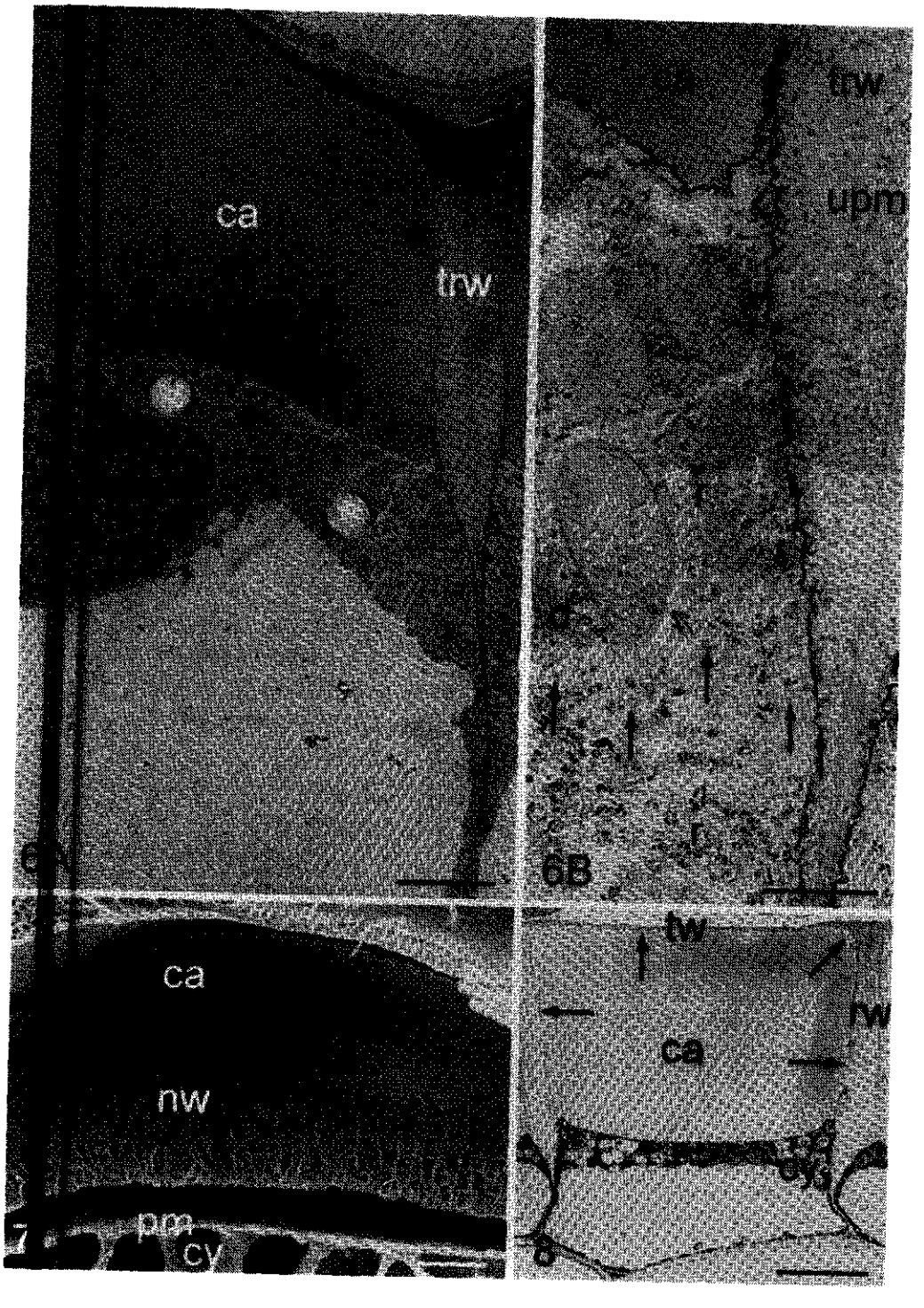
ca
tnw
6A
tnw
upm
6B
ca
nw
pm
cy
tw
nw
ca
cy
6

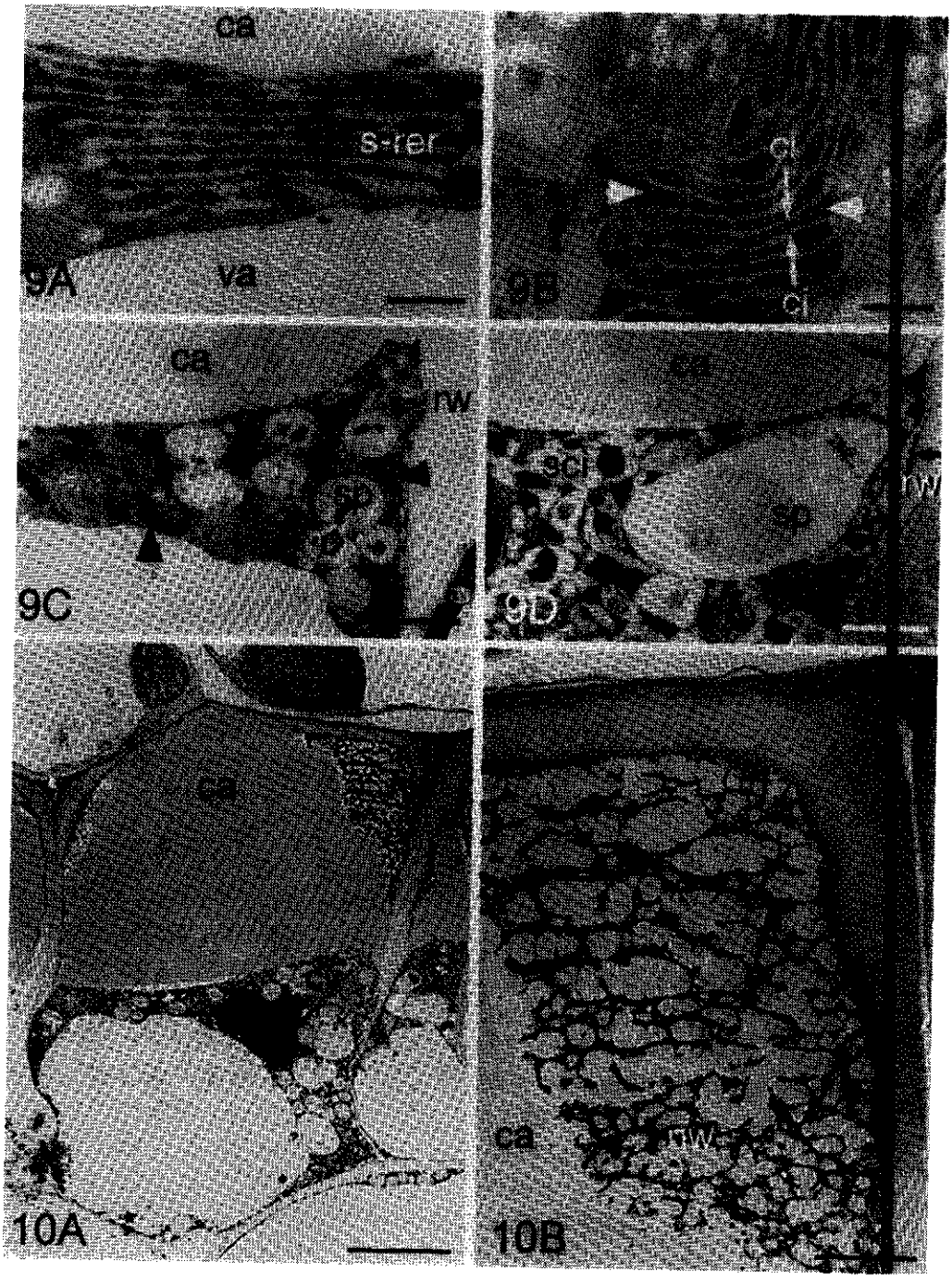
ca
s-rer
va
9A
ci
ci
9B
ca
rw
sp
9C
sci
sp
rw
9D
ca
ca
rw
10A
10B

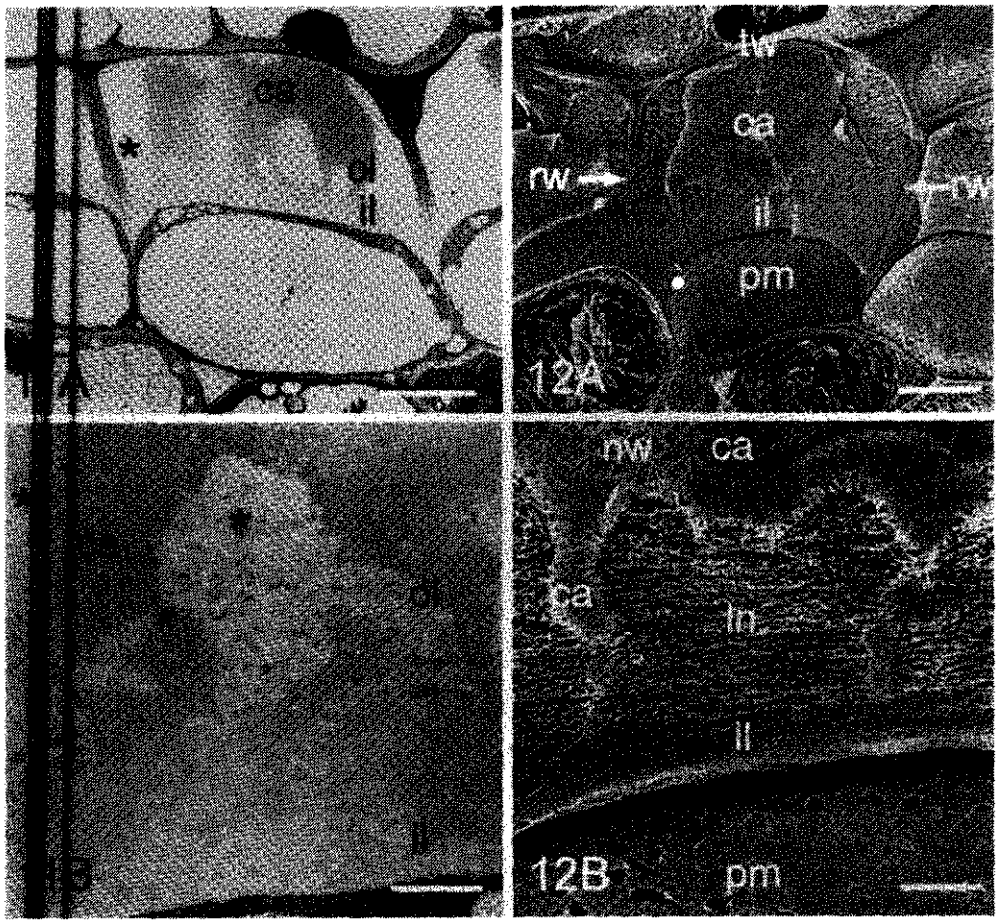

Figure 11. 19 DAP; breakdown of callose, TEM. **A** Breakdown of callose (*ca*) in outer layer (*ol*) while a cellulose inner layer (*il*) develops. Asterisk = dissolved callose; bar = 10 μm. **B** Detail of callose conversion. Bar = 1 μm.

Figure 12. 19 DAP; breakdown of callose, cryo-SEM. **A** Block of callose (*ca*) in a lumen of the outer layer. Inner layer (*il*), radial walls (*rw*) and tangential wall (*tw*) form the construction for the substrate in this lumen. This cell is broken along the plasma membrane surface (*pm*). Bar = 10 μm. **B** Detail of **A**. A network (*nw*) in the callose (*ca*) seems to longer resist the breakdown. Around the callose a layered network (*ln*) of probably smaller, soluble poly- and monosaccharides. The inner layer (*il*) cannot be clearly distinguished. Bar = 1.5 μm.

Figure 9 17 DAP; activity in the cytoplasm, TEM. **A** The stacked rough endoplasmatic reticulum (*s-rer*). *ca* Callose, *va* vacuole; bar = 400 nm. **B** Production by the s-rER of an osmiophilic product (arrowhead), stored between the cisterns (*ci*). Bar = 400 nm. **C** Pools of osmiophilic product (arrowhead) and swollen plastids (*sp*). Bar = 2 μm. **D** Osmophilic product in the periplasmic space (arrows), swollen plastids (*sp*) and ER cisterns (*sci*). Bar = 1.5 μm.

Figure 10. 18 DAP; network structures in the top corners of the callose, TEM. **A** Network (*nw*) replacing the granular callose (*ca*) and activity in cytoplasm (*cy*). Bar = 7.5 μm. **B** Detail of network and callose. Bar = 1.5 μm.

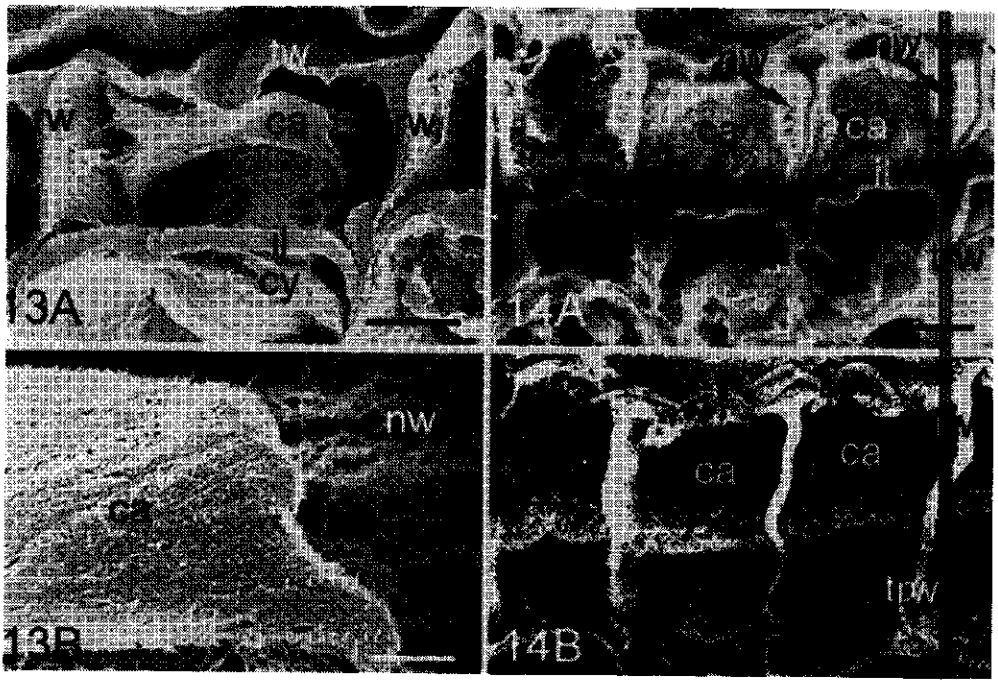

Figure 13. 19 DAP; breakdown of callose, critical-point-dried material, SEM. **A** Partly dissolved block of callose (*ca*) in the outer layer, between the tangential wall (*tw*), inner layer (*il*) and radial walls (*rw*). *cy* Cytoplasm; bar = 4 μm. **B** Detail of **A**, a network (*nw*) persists longer than the rest of the callose. Bar = 800 nm.

Figure 14. 19 DAP; breakdown of callose, SEM after PATAg staining and critical point drying. **A** SEM image; callose (*ca*) and in its corners a network (*nw*). *il* Inner layer, *trw* thin radial walls; bar = 10 mm. **B** Backscattered electron image of **A**; silver staining by the PATAg reaction on thickened radial walls (*rw*) and to a lesser extent on the thin radial walls (*trw*), tangential walls and the inner layer. No staining on callose and network.

Figure 15. 20 DAP; early phytomelan synthesis, TEM. **A** Small, black phytomelan globules in the outer layer (*ol*), and the cellulose inner layer (*il*). The cytoplasm has disappeared, a lumen remains (*lu*). *ar* Cell of arillus; bar = 5 μm. **B** Detail of **A**; electron-dense globules of phytomelan. Bar = 400 nm.

Figure 16. 22 DAP; phytomelan synthesis, TEM. Growing phytomelan globules with electron-dense borders. Bar = 400 nm.

Figure 17. 22 DAP; phytomelan synthesis, TEM. PATAg staining of growing phytomelan globules. *rw* Radial wall; bar = 800 nm.

Figure 18. 22 DAP; phytomelan synthesis, SEM. **A** Growing globules in the outer layer, comparable with Fig.13**B**. In the lumen (*lu*) of the cell similar globules are present. *rw* Radial wall, *tw* secondary tangential wall, *il* inner layer; bar = 2.5 μm. **B** High magnification of the growing globules. Their border consists of 15 nm units (arrows). Bar = 200 nm.

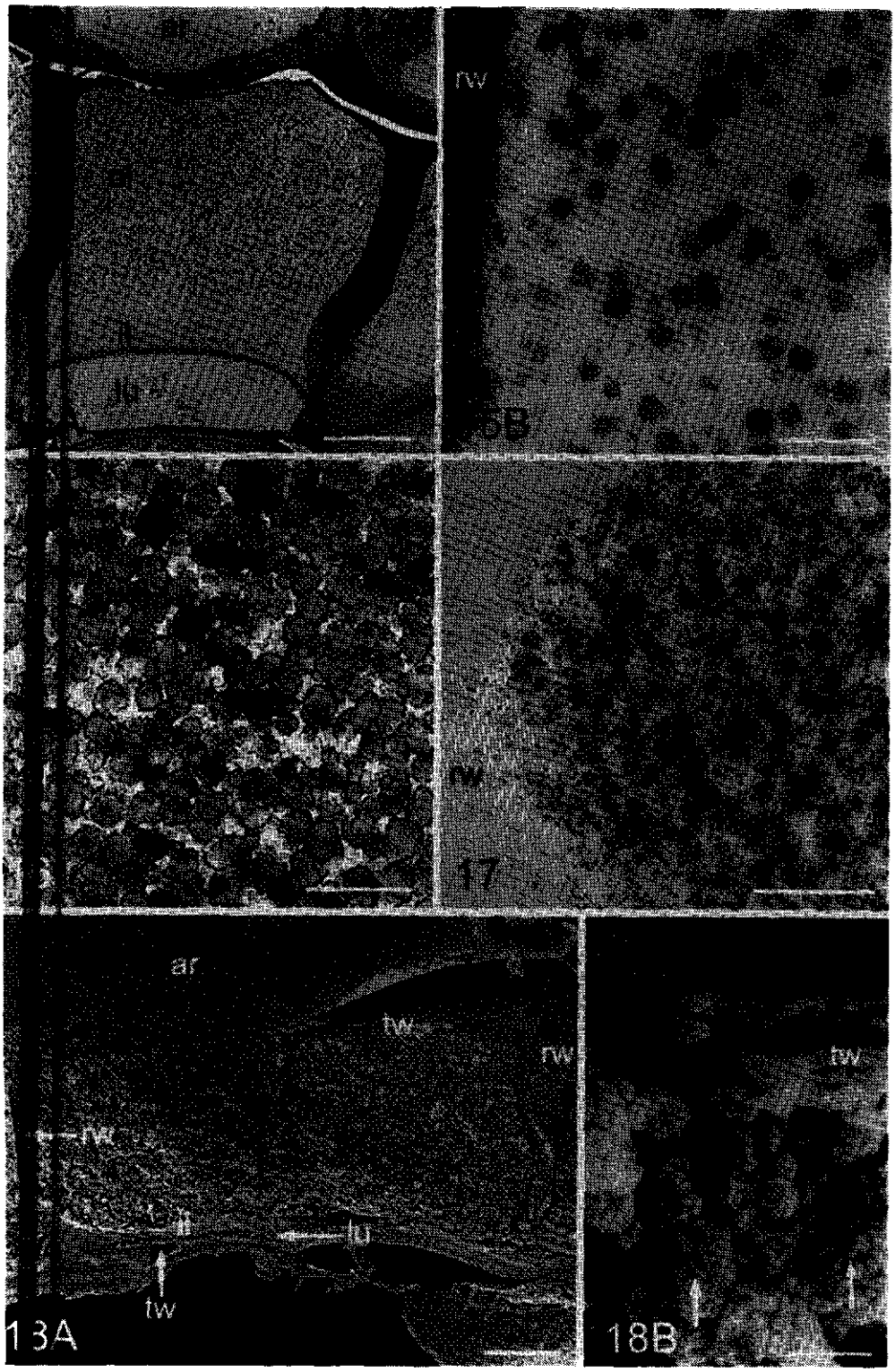
lu
rw
5B
rw
17
ar
tw
rw
iw
lu
tw
13A
tw
18B

At 19 DAP the callose tertiary wall has started to convert. TEM shows at the outer side of the tertiary wall the conversion of the fine granular homogeneous structure into a layer of electron transparent material (Fig.11A) with fine electron-dense dots (Fig.11B). SEM reveals that the callose dissolves, resulting into a network-like structure (Fig.12). The critical-point-dried material did not preserve the network-like structures very well (Fig.13). During this callose-breakdown an inner tertiary layer is deposited between the plasma membrane and the dissolving callose. This inner layer is cellulosic, as was shown by histochemistry (Wittich and Graven 1995), and seems to consist of fine granular and fibrillar material (Fig.11A). This cellulose layer cannot be clearly distinguished from the callose in the cryo-SEM (Fig.12B). PATAg staining on SEM material shows that the callose is faintly positive, the network-like structures are negative, and the radial walls positive (Fig.14). The cytoplasm seems to be partly restored; some mitochondria, multivesicular bodies, and free ribosomes are present (Fig.11).

Phytomelan synthesis (stage 3): 20 - 25 DAP

Starting at 19 DAP, and more expressive at 20 DAP, the secondary radial (and transverse) wall has become electron dense (Fig.11A and Fig.15A) and the thin part of the secondary radial wall that does not border the tertiary wall has folded. In the outer tertiary layer numerous electron-dense globules have appeared, being smaller at the border with the inner layer (Fig.15A and Fig.15B). The cell contents has disappeared (Fig.15A). At 20 DAP the outer tertiary layer of the tertiary wall contains larger globules bordered with fine granular electron-dense material (Fig.16). This border is electron dense, also without osmium fixation and lead citrate/uranyl acetate staining (not shown). The control reaction of the PATAg staining technique (without the peroxidase reaction) shows staining of the

Figure 19 24 DAP; fusion of the phytomelan globules in the outer layer, TEM. *il* Inner layer, *lu* lumen, *rw* radial wall, *tw* exterior tangential wall; bar = 2 μm.

Figure 20. 25 DAP; phytomelan at the end of the globule fusion, TEM. **A** Electron-dense material disappears towards the borders of the phytomelan (*pm*). *il* Inner layer, tw exterior tangential wall, *rw* radial wall; bar = 2 μm. **B** Detail of **A**; high magnification of the lamellar pattern in the phytomelan and electron-transparent fibril-like structures (arrows). Bar = 100 nm.

Figure 21. 29 DAP; mature phytomelan, TEM. Homogeneous mature phytomelan (*pm*) is bordered by electron-dense material against the radial walls and an electron-dense inner layer (*il*). The cell lumen (*lu*), result of the cytoplasm degeneration, is also filled with phytomelan. Bar = 7.5 μm.

Figure. 22. 29 DAP; mature phytomelan, SEM. **A** Breaking surface indicating the hardness of the block of phytomelan (*pm*). The lumen (*lu*) is also filled with phytomelan. *ar* Arillus cell, *rw* radial wall, *tw* tangential wall; bar = 6 μm. **B** Detail of **A**; phytomelan consisting of spherical units of ca. 15 nm diameter. Bar = 200 nm.

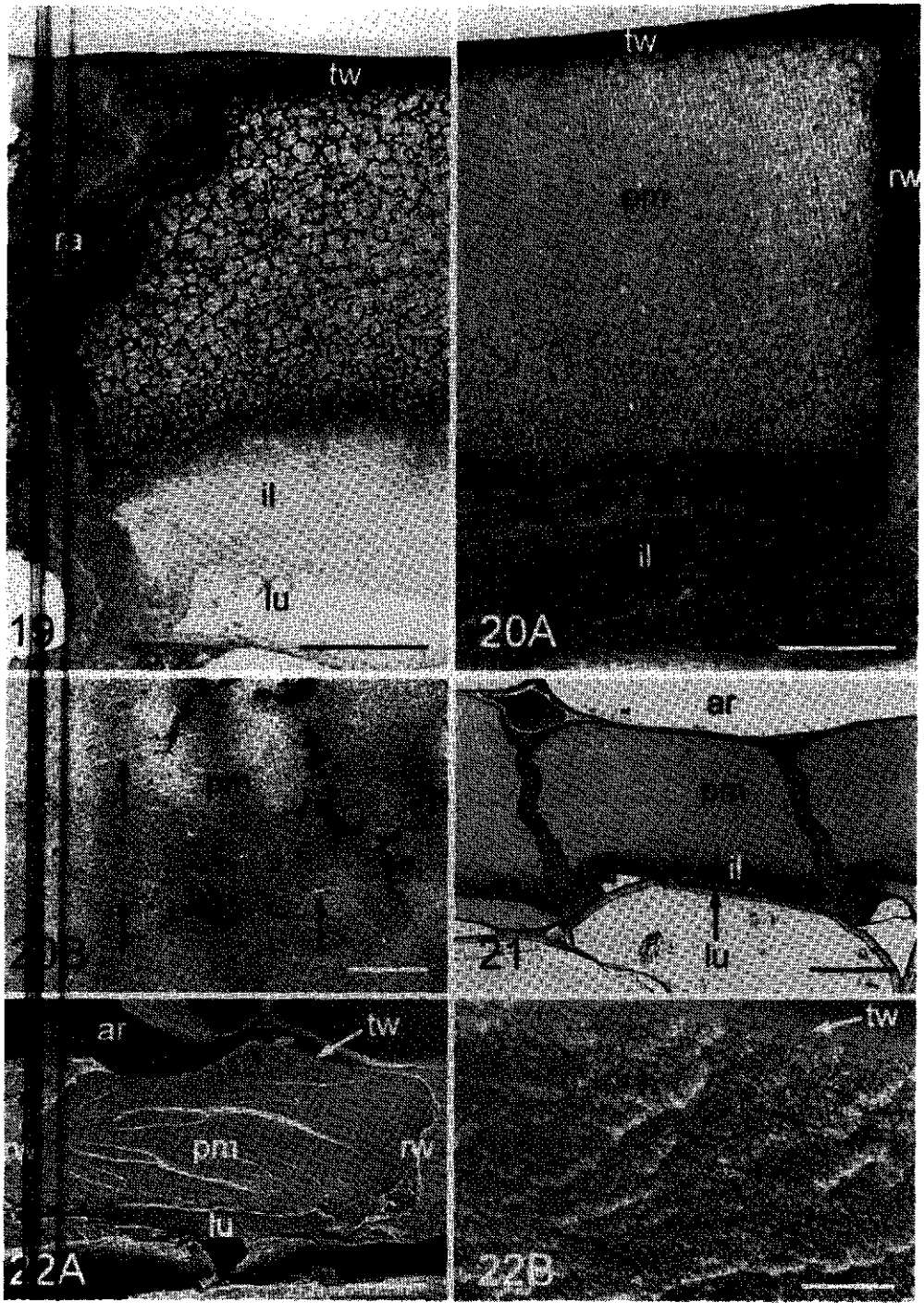
tw
il
lu
19
tw
rw
il
20A
ar
il
lu
21
ar
tw
pm
rw
lu
22A
tw
22B

globules in the TEM, indicating the presence of aldehyde groups in or at the globules (Fig.17). SEM reveals that the border of these growing globules consists of small units with a diameter of 15 nm (Fig.18). The cellulose inner tertiary layer has become more electron dense. Often are in the cell lumen also globules found (Fig. 18).

Till about 25 DAP the globules in the outer layer of the tertiary wall increase in size and fuse (Fig.19, Fig.20A). The electron-dense globule-bordering material can still be observed around, and sometimes inside the fused complexes while the inner layer starts to show a more distinct border with the outer layer (Fig.19). The outer layer of the tertiary wall becomes homogeneous and the electron-dense globule-bordering material disappears into the direction of both the secondary wall and the inner tertiary layer (Fig.20A). The latter becomes more compact and electron dense. In the globule complexes fine, fully electron transparent fibril-like structures have appeared (Fig.20B).

Finally at 29-45 DAP the outer layer of the tertiary wall is homogeneous and is bordered at its radial walls with electron-dense material (Fig.21). This homogeneous layer is the phytomelan. SEM studies show a very fine structure of 15 nm units on the cut surface of the phytomelan layer (Fig.22) while TEM studies show a regular lamellar pattern in this layer (Fig.20A). The border between the outer phytomelan layer and the inner tertiary layer is faint. The inner layer is darker stained near the interior cell side and has a border of a less electron-dense zone (Fig.21).

The previous cell lumen is also filled with the same material as the tertiary wall consists of, *i.e.* phytomelan (Fig.22A).

DISCUSSION

Callose deposition (stage 1)

From 14 till 17 DAP the template of the phytomelan layer is constructed (Wittich and Graven 1995). The outer epidermal cells of the outer integument thicken their radial and transverse cell walls and deposit callose between these thickened walls, against the outer tangential secondary wall.

The thickening of the secondary radial and transverse walls start at the outer side of the cell. About two thirds of the wall length thicken as does a small part of the tangential secondary wall. Both, the presence of dictyosomes and the undulating plasma membrane indicate that exocytosis of dictyosome vesicles is probably involved in this thickening. Using histochemical methods for light microscopy Wittich and Graven (1995) already showed that the newly synthesized wall material strongly stains for cellulose.

Callose is deposited as a tertiary wall against the outer tangential secondary wall. It is known that callose is synthesized by a membrane-bound β-glucan synthase, using UDP-glucose as substrate (Fincher and Stone 1981, Meikle et al. 1991, Delmer et al. 1993). The rod-like structures on the membrane (seen in the TEM) only appear during the callose synthesis, therefore they might be involved in the latter process. SEM also reveals structures connecting the callose with the membrane. However, these structures are more network-like and also appear sometimes at the outer tangential side of the homogeneous callose, indicating that they are part of the callose which accordingly might be more heterogeneous than it appears on the TEM images.

The callose deposition ends when the callose-synthesizing part of the membrane reaches the end of the thickened part of the radial and transverse secondary wall. The final size of this block of callose determines the size of the block of phytomelan that will be synthesized in a later stage. This is the template function of the callose (Wittich and Graven 1995).

After the callose tertiary wall has completely been deposited, TEM often shows an increase of electron density in the radial walls, starting near the outer tangential wall. This is probably due to the increase of pectins, as demonstrated by histochemical methods (Wittich and Graven 1995).

Callose breakdown (stage 2)

At about 18 DAP dark granular material is produced and accumulated between the stacked ER. This seems to be produced by the ER itself, stored, and later excreted into the periplasmatic space.

One day later, at 19 DAP, the tertiary wall converts into two different layers, an inner and an outer tertiary layer. The callose breakdown starts both at the radial (and transverse) and the membrane-bordering side of the callose tertiary wall. At that time the electron-dense material that is produced by the ER has disappeared and might be related to callose breakdown. On the other hand the electron-dense material produced by the ER might be phenolic since it is known that phenolics are very osmiophilic (Scalet et al. 1989), and Wittich and Graven (1995) show that phenolics seem to be involved in the phytomelan synthesis.

It is most likely that the callose in the seed coat is broken down into small soluble glucose polymers and monomers by apoplastic enzymes. By using our methods these soluble sugars are not fixed chemically, which can explain the electron transparency of the outer tertiary layer for the TEM. This might be the reason that in our light microscopical study the converted callose could not be stained by histochemical methods (Wittich and Graven 1995); the soluble sugars were rinsed out. The cryo-SEM did show a network-like structure

after callose breakdown, which was expected since soluble sugars are supposed to remain present after freeze drying. However, it has to be considered that the network-like structures consist of other water soluble components than sugars, which cannot be chemically fixed in aqueous solutions. The soluble sugars which result from the callose degradation are probably used for the phytomelan synthesis.

The inner tertiary layer is synthesized during the callose disintegration. It is a layer that contains cellulose and pectin (Wittich and Graven 1995) and is shown here as an electron-transparent layer with electron-dense inclusions and no distinct border with the outer layer. Also SEM and cryo-SEM did not clearly show the presence of cellulose. Cellulose is usually synthesized at the plasma membrane (Emons 1991, Delmer and Amor 1995) but based on the TEM images it cannot be excluded that in this case cellulose is synthesized in the dissolving callose. Furthermore it is possible that the soluble sugars from the callose breakdown are (also) used for the cellulose synthesis. A precursor role of callose for cellulose may be possible (Ryser 1985).

Phytomelan synthesis (stage 3)

Starting at 20 DAP a conversion in the outer layer of the tertiary wall takes place. Phytomelan is synthesized in the apoplast, probably in a pool of soluble sugars as shown above, with phenolics (Wittich and Graven 1995), and perhaps other substrates. On light microscopical level the transparent wall becomes slowly dark brown and eventually black. During this process TEM and SEM show growing globules in this wall layer, which fuse as they contact each other. The contents of these globules is phytomelan, which is an aggregation of 15 nm units. The border of the globules is of an electron-dense granular material, also when osmium staining is omitted. This is probably the site where the synthesis takes place of phytomelan units. The synthesis might be either enzymatic or autolytic . The nature of the electron transparent fibril-like structures in the phytomelan remains unclear. They might be cellulosic, but histochemical methods did not reveal the presence of cellulose in the phytomelan (Wittich and Graven 1995), while SEM only shows a very fine (15 nm) granular structure. This granular structure seems to cause the lamellar pattern that was found on the phytomelan TEM sections.

The cytoplasm of these epidermal cells degenerates during the early stage of phytomelan synthesis and the remaining cell lumen is compressed a little later due to the pressure of the expanding endosperm. This results in partly folded radial (and transverse) walls and a small lumen that is sometimes filled with phytomelan too. The phytomelan formation in this cell lumen lacks the preceding deposition of callose but does show the same globular structures as observed during the second conversion of the outer tertiary layer. Thus it does not seem

to be a prerequisite to have a callose stage as template or carbohydrate source at that very site prior to phytomelan synthesis. Perhaps there is no need for a callose template because the size of this second phytomelan layer is not important anymore. Carbohydrates for the synthesis of this phytomelan may also be provided by the bordering dissolved block of callose, or by neighbouring parenchyma cells.

ACKNOWLEDGEMENTS

The authors wish to thank Dr. C.J. Keijzer for his assistance with the cryo-SEM work, and together with Dr. M.T.M. Willemse for the valuable discussions and critically reading the manuscript; P.A. van Snippenburg, A. Haasdijk and S. Massalt for preparing the photographs and drawings. P.E. Wittich is a member of The Graduate School Experimental Plant Sciences. P. Graven is supported by the Life Sciences Foundation (SLW), which is subsidized by the Netherlands Organization for Scientific Research (NWO).

REFERENCES

Dafert FW and R Miklauz (1912) Untersuchungen über die kohleähnliche Masse der Kompositen (Chemischer Teil). Denkschr Akad Wiss Wien Math Naturwiss Kl 87: 143-152

Dahlgren RMT and HT Clifford (1982) The monocotyledons: a comparative study. Academic Press, London

Delmer DP and Y Amor (1995) Cellulose biosynthesis. Plant Cell 7: 987-1000

Delmer DP, M Volokita, M Solomon, U Fritz, W Delphendahl and W Herth (1993) A monoclonal antibody recognizes a 65 kDa higher plant membrane polypeptide which undergoes cation-dependent association with callose synthase in vitro and co-localizes with sites of high callose deposition in vivo. Protoplasma 176: 33-42

Emons AMC (1991) Role of particle rosettes and terminal globules in cellulose synthesis. In: Haigler CH, PJ Weimer (eds) Biosynthesis and biodegradation of cellulose. Marcel Dekker, New York: 71-98

Fincher GB and BA Stone (1981) Metabolism of noncellulosic polysaccharides. In: Tanner W, FA Loewus (eds) Plant carbohydrates II: extracellular carbohydrates. Springer-Verlag, Berlin, 68-132 [Pirson A, MH Zimmermann (eds) Encyclopedia of plant physiology. NS, vol 13B]

Hanausek TF (1907) Die Kohleschicht in Pericarp der Kompositen. Sitz Ber Akad Wiss Wien 116: 1-30

Hegnauer R (1962-1990) Chemotaxonomy de Pflanzen, vol. 1-9. Birkhäuser, Basel

Meikle PJ, KF Ng, E Johnson, NJ Hoogenraad and B Stone (1991) The β-glucan synthase from *Lolium* multiflorum. J Biol Chem 266: 22569-22581

Ryser U (1985) Cell wall biosynthesis in differentiating cotton fibres. Eur J Cell Biol 39: 236-256

Scalet M, E Crivellato and F Mallardi (1989) Demonstration of phenolic compounds in plant tissues by an osmium-iodide postfixation procedure. Stain Technol 64: 273-280

Takhtajan A (1985) Anatomia seminum comparativa, vol I, liliopsida seu monocotyledons (in Russian). Nauka, Leningrad

Thiéry J-P (1967) Mise en évidence des polysaccharides sur coupes fines en microscopie électronique. J Microsc 6:

987-1018

Wittich PE and P Graven (1995) Histochemical study of the development of the phytomelan layer in the seed coat of Gasteria verrucosa (Mill.) H. Duval. Protoplasma 187: 72-78

Chapter

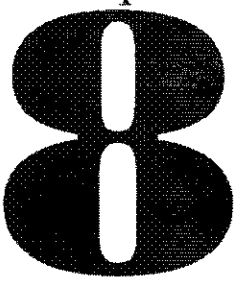

Characterization of phytomelan in the seed coat of *Gasteria verrucosa* (Mill.) H. Duval

P. Graven[1,4], P.E. Wittich[2], F. Bouman[1], G. Nachtegaal[3] and A.P.M. Kentgens[3]

[1]Hugo de Vries-Laboratory, University of Amsterdam, Kruislaan 318, 1098 SM Amsterdam, [2]Laboratory of Plant Cytology and Morphology, Wageningen Agricultural University, Arboretumlaan 4, 6703 BD Wageningen, [3]SON National HF-NMR Facility, Toernooiveld 1, 6525 ED Nijmegen, [4]FOM Institute for Atomic and Molecular Physics, Kruislaan 407, 1098 SJ, Amsterdam, The Netherlands

Summary. Phytomelan in seed coats of Asparagales is black tertiary cell wall material, which is chemically inert. It is a taxonomical important character in seed coats of Asparagales and fruits of Compositae.

Histochemical tests and pyrolysis mass spectrometry of phytomelan from the seed coat of *Gasteria verrucosa* demonstrated that catechol is one of the precursors of phytomelan. Solid state ^{13}C NMR experiments showed that this phytomelan has an aromatic structure with organic substituents, is rich in carbon, and because it contains no nitrogen, it is not a melanin as known from the animal kingdom or in fungi. Phytomelan shows much similarity with catechin-like green tea polyphenols and flavanoids, but is more polymerized.

INTRODUCTION

The term melanin is often used to describe deep brown or black naturally occurring pigments which are not tannins. Melanins constitute a group of pigments widespread in the animal and plant kingdom. Three classes can be distinguished: the eumelanins and phaeomelanins in the animal kingdom, and the allomelanins (including fungi) or catechol melanins in the plant kingdom (Nicolaus 1968). However, the term "phytomelan" is more often used then "allomelanins" to describe melanins in plants, but not for fungal melanins. The term "phytomelan" was introduced by Dafert and Miklauz (1912), and means nothing more then "black of plants". Dafert and Miklauz (1912) have studied the coal-like substance chemically on behalf of Hanausek, who studied pigments in the pericarp of a large amount of Compositae (Hanausek 1902, 1907, 1908a, 1908b, 1911a, 1911b, 1912, 1913). Phytomelan is an opaque, brittle, coal-like substance which is rich in carbon, and lacks nitrogen completely (Dafert 1932; Huber 1969; Dahlgren and Clifford 1982; Dahlgren and Rasmussen 1983; Dahlgren *et al.* 1985). The difference between phytomelan, and the fungal and animal melanins is the lack of nitrogen in plant melanins (Nicolaus 1968). However, the chemical composition of these melanins is difficult to study. Nicolaus (1968) stated in his study of natural melanins: "A lot of physico-chemical methods, which have contributed to the elucidation of the structure of many natural substances, cannot be used as structural tools in melanin chemistry".

Huber (1969), and Dahlgren and Clifford (1982) have pointed out the significance of the occurrence of phytomelan in seed coats for the circumscription of several families. Phytomelan is only known in seeds of taxa of the Asparagales, but this is not verified with certainty in seeds of any other order (Dahlgren *et al.* 1985). Hanausek (1907) and Hegnauer (1962-1990) described the localization and distribution of phytomelan in the family of the Compositae. Phytomelan encrusted seeds are not mentioned in this family, but it has been found in the fruit walls, receptacular bracts, involucral bracts, and rhizomes of some of the taxa. It is striking that no author has ever made the link between phytomelan in Compositae and the families of the Asparagales. Furthermore, phytomelan is mentioned to be present in the seeds of some taxa of the Orchidaceae (Rasmussen, personal communication). In table 1, a comparison is made of families with phytomelan containing seed coats, based on the classification of several authors.

In most capsule-fruited Asparagales phytomelan accumulates in the outer epidermis of the testa of the seeds, but lacks in most berry-fruited taxa of this order (Netolitzky 1926; Dahlgren and Clifford 1982; Dahlgren and Rasmussen 1983; Dahlgren *et al.* 1985). The thickness of the phytomelan layer varies considerably between the families and genera. Depending on the thickness of the black phytomelan layer, the taxa with a phytomelan layer can be divided into three groups. The groups vary in a range from less than 10 μm thickness, from 10 to 40 μm,

and 70 to 180 μm, (Huber 1969; Dahlgren and Clifford 1982). The development of the *Asparagus officinalis* seed coat, with epidermal phytomelan layer, has been described by Robbins and Borthwick (1925). This seed coat is compressed and decreases in thickness during the different stages of development. In a mature seed coat, hardly any other structural layer than phytomelan can be observed due to the shrinkage of the integumental cells and compression by the enlarging endosperm.

The phytomelan layer is in some cases described as an unreal seed coat when the development of the seed coat was not known and in the mature seed only a black layer remained, (Rode 1913; Robbins and Borthwick 1925). According to Netolitzky (1926), the content of the epidermal cells of certain seed coats are visible as big colored bodies (*viz.* phytomelan). In many of the Liliaceae (the Asparagales, according to Dahlgren and Rasmussen (1983), and Dahlgren *et al.* (1985)) the whole cell lumen is completely filled with a brittle, brown, dark violet, or black body. This is in the beginning radial striped, and can be a part of the cell wall. Lohde (1875) mentions a bar-like structure in the outer wall just under the cuticle in *Hemerocallis* and *Allium*. Also a cuticle-like phytomelan layer is described for *Muscari commosum* and *M. racemosum* (Wunderlich 1937).

Wittich and Graven (1995, 1998) have shown that phytomelan develops in three stages in the outer epidermis of the outer integument in the seed coat of *Gasteria verrucosa*. The first stage is the deposition of a callosic layer against the outer tangential wall, with simultaneous thickening of adjacent parts of the radial walls. The second stage is the conversion of the callosic wall, or tertiary wall, into a cellulosic inner layer and a lumen, probably filled with soluble carbohydrates. During the third stage the lumen becomes a black layer as a result of phytomelan synthesis. Electron microscopy has shown that the synthesis occurs at the borders of growing phytomelan globules. These globules consists of 15 nm units, and will finally fuse to form a homogeneous phytomelan layer (Wittich & Graven 1998).

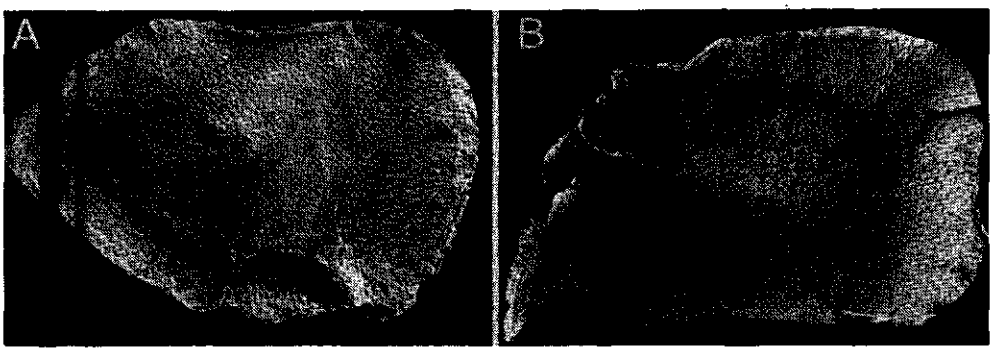

Figure 1: *Gasteria verrucosa* (Mill.) H. Duval (SEM) **A** Mature seed. **B** Germinating seed. (A and B x 27)

Table 1: Families with phytomelan consisting seed coats according to Huber (1969), Dahlgren and Clifford (1982), Dahlgren, Clifford and Yeo (1985), and Takhtajan (1985).

Dahlgren, Clifford and Yeo (1985)		Dahlgren and Clifford (1982)		Huber (1969)			Takhtajan (1985)
Asparagales	**Phytomelan presence in**	**Asparagales**	**Phytomelan presence in**	**Asparagoid Liliiflores**	**Phytomelan presence in**	**(µm)**	**Liliales**
Agavaceae	All	Agavaceae	All genera studied	Agavaceae *Agavae *Yuccae	*Hosta* except *Samuela*	6 5-10 8-20	Agavaceae (incl. Funkiaceae)
Alliaceae	All	Alliaceae	All	Alliaceae		10-28	-
Amaryllidaceae	In most taxa with dehydrated seeds	Amaryllidaceae	Most genera	Amaryllidaceae (incl. Ixioliriaceae)	 *Ixiolirion*	4-10 5-10	Amaryllidaceae (incl. Ixioliriaceae)
Antheriaceae	Most genera, except *Tricoryne*	-	-	Antheriaceae *Johnsoniae *Simethidae	*Alania, Borya* *Simethis*	14-40 60-160	-
Aphyllantaceae	All (*Aphyllanthes*)	Aphyllantaceae	*Aphyllanthes*	Agapanthaceae	*Agapanthus, Tulbaghia*	< 10	Aphyllanthaceae
Asparagaceae	All	Asparagaceae	*Asparagopsis, Asparagus, Myrsiphillum*	Asparagaceae	*Asparagopsis, Asparagus, Myrsiphilum*	10-16	Asparagaceae
Asphodelaceae	All (including *Gasteria*)	Asphodelaceae (incl. Asteliaceae, Antheriaceae, Aloëaceae, and Ixioliriaceae)	All	Asphodelaceae		14-30	Asphodelaceae
Asteliaceae	All (*Cordyline, Astelia, Cohnia, Milligania*)	-	-	Asteliaceae *Asteliae *Cordylinae	 *Astelia* *Cordyline*	 100-160 60-120	Dracaeanaceae (incl. Asteliaceae)
Funkiaceae	All	Funkiaceae	*Hosta*	-	-	-	-
Hemerocallidaceae	All (*Hemerocallis*)	Hemerocallidaceae	*Hemerocallis*	Hemerocalidaceae	*Hemerocallis*	16-40	Hemerocallidaceae
Herreriaceae	All (*Herreria*, ***Herreriopsis***)	Herreriaceae	*Herreria*	Herreriaceae	*Herreria*	8	Herreriaceae

Hyacinthaceae	The seeds have a **rather thick** phytomelan crust in *Massonia*, *Hyacinthoides* (*Endymion*) and *Hyacinthus*, but more often rather thin, or lacking, in *Chionodoxa*, *Puschkinia* and a few *Scilla* species	Hyacinthaceae	Most genera	Hyacinthaceae	All, Except *Endymion*, *Hyacinthus* (*Hyacinthella*), and *Massonia* No phtyomelan: *Chionodoxa*, *Puschkinia*, and some species of *Scilla*	4-10 12-15	Liliaceae
Hypoxidaceae	All	Hypoxidaceae	All genera studied	Hypoxidaceae		100-180	Hypoxidaceae
Ixioliriaceae	All (*Ixiolirion*)	-	-	-	-	-	-
Luzuriagaceae	*Geitonoplesium*, *Eustrephus*, and perhaps *Behnia*	Philesiaceae	*Geitonoplesium*, *Eustrephus*	Luzuriagaceae *Geitonopleisae	*Eustrephus* *Geitonoplesium*	6-10 70-100	Philesiaceae
Phormiaceae (incl. Dianellaceae)	All	Phormiaceae Dianellaceae	*Phormium*, *Xeronema*; *Dianella*, *Stypandra*	Phormiaceae Dianellaceae	*Phormium*	 14-100	Phormiaceae
Tecophilaeaceae	All, except *Walleria*	Tecophilaeaceae	Most genera but not *Walleria*	Tecophilaeaceae (incl. Cyanastraceae)	*Cyanella* Except in *Walleria* and *Cyanastrum*	2-3	?
Xanthorrhoeaceae	All (*Xanthorrhoea*)	Xanthorrhoeaceae	*Xanthorrhoea*	Xanthorrhoeaceae	*Xanthorrhoea*	16-40	Xanthorrhoeaceae
		Commelinales*					
		Commelinaceae	*Commelina*				
		Haemorodales*					
		Haemodoraceae	*Wachendorfia*				
		Zingiberales*	Certain taxa				

* According to Dahlgren and Clifford (1982), it is possible that phytomelan might be present in the seed coats of these orders

About the chemical composition of phytomelan is not much known, except the ratio of 2:1 of the hydrogen and oxygen content. This ratio may be caused by dehydration of carbohydrates (Dafert and Miklauz 1912; Dafert 1932; de Vries 1948; Hegnauer 1962-1990). Dafert and Miklauz (1912) made an attempt to study the chemistry of phytomelan in Compositae. They isolated a black residue of the fruits after treatment with Wiesner mixture. This mixture of sulphuric acid, saturated with chromic salt (Wiesner 1867), destroys every macromolecular component in the seed coat or fruit wall except the black residue. This residue had a ratio of carbon, hydrogen and oxygen of 3.7:2.1:1.0, while cellulose and coal had a ratio of 1.2:2.0:1.0 and 5.0:3.5:1.0, respectively (Dafert and Miklauz 1912). Dafert and Miklauz (1912), and later authors, concluded that the phytomelan is rich in carbon, lacks nitrogen and is chemically inert. In this study an attempt is made to elucidate the chemical composition of the phytomelan in the seed of *Gasteria verrucosa* (Fig. 1), by using various modern analytic techniques, in order to understand synthesis and the functions of phytomelan.

MATERIAL AND METHODS

Plant material

Various developmental stages of the seed of *Gasteria verrucosa* (Asphodelaceae), according to Wittich & Graven (1995), were studied. Further, mature seeds of *Camassia leichtinii* (Liliaceae), *Chlorophytum amairiense* (Asphodelaceae), *Hemerocallis aurantiaca* and *H. flava* (Hemerocallidaceae), *Asparagus officinale* (Asparagaceae), *Eustrephus laifolia* (Philesiaceae), *Dianella caerulea* (Dianellaceae), *Hypoxis nitida* (Hypoxidaceae), *Hosta* sp. (Funkiaceae) and *Vanilla pilifera* (Orchidaceae) were used, as well as the fruit of *Arnica montana* (Compositae), and developmental stages of the *Helianthus annuus* fruit (Compositae).

Germination

For germination, seeds of *Gasteria verrucosa*, *Chlorophytum amairiense* and *Cordyline haageana* were placed on a wet paper filter in petri dishes at room temperature.

Analytical pyrolysis mass spectrometry and pyrolysis gas chromatography mass spectrometry (PyMS)

Samples of the seed coats of all the taxa were treated with a Wiesner-mix for seven days (Wiesner 1867; Dafert and Miklauz 1912) followed by extensive washing with demineralized water. Samples of *Gasteria verrucosa* were also treated in a 1M NaOH, 2 M NaOH, or 4 M NaOH, H_2O_2 and $NaHClO_3$ solution.

For Pyrolysis Mass Spectrometry (PyMS) the following material was homogenized in a few drops of water using a small glass mortar and a glass pestle: a) the fruit wall of *Arnica montana*, b) treated and untreated samples of mature seed coats of several species, c) untreated samples of three developmental stages of the *Gasteria verrucosa* seed coat. The stages of the *Gasteria verrucosa* seed coat are according to Wittich and Graven (1995): a not colored epidermis in which the callose is dissolved into soluble carbohydrates (second stage), a light brown colored epidermis in which the phytomelan synthesis has started (start of the third stage), a completely dark brown-black colored outer epidermis (the end of the third stage). A small drop of the suspension was placed on a Pt/Rh wire and dried in vacuum. Analyses were performed on a JEOL JMS-SX102 Mass Spectrometer by means of electron impact (EI, 16 eV). The untreated samples were also analyzed by chemical, ammonia, ionization (CI).
Pyrolysis gas chromatography mass spectrometry (PyGC/MS) under (70eV) EI conditions was conducted on a Finnigan INCOS 50 quadrupole mass spectrometer connected to a HP 5890 series II gas chromatograph. About 5 mg of a suspension of a sample was applied to a ferromagnetic wire with a Curie-point temperature of 610 °C. The GC oven was kept at 30 °C during pyrolysis and subsequently programmed to 320 °C at a rate of 6 °C min^{-1}. The fragments were flushed towards a 25 m CPSILS-5 CB fused silica capillary column (i.d. 0.32; film thickness 1.2 mm) using He as carrier gas (flow 30 cm s^{-1}).

Chemical treatment
Seeds were treated with several chemicals, as listed in table 2, in order to test the chemical resistance of the phytomelan.

Solid-State ^{13}C-NMR Spectroscopy
For ^{13}C-NMR experiments 10 mg phytomelan layer of *Gasteria verrucosa* seeds was isolated by manual preparation. High-resolution solid-state NMR spectra were obtained on a Bruker AM spectrometer (carbon frequency 125.7 MHz) equipped with a Bruker solid-state accessory. Furthermore, measurements were conducted on a DMX-300 (7.05 T) and a AM-500 (11.7 T). Spectra were recorded using a 4 mm BB-H-Bruker MAS Probe and a broadband Doty HX probehead with a 5 mm double air bearing magic angle spinning (MAS) assembly. Spinning speeds varying from 5-8 kHz were employed. Cross-Polarization (CP) spectra were obtained with a 2 ms contact time and a repetition rate of 4 s. The proton and carbon 90° pulse width was 6.5 ms. Single Pulse Excitation spectra were obtained with a repetition rate of 10 s. For the CP spectra approximately 22000 FID's were accumulated, for SPE spectrum 32000. Spectra were referenced with respect to TMS using adamantane as a secondary reference.
Standard measurements on a Bruker AM spectrometer were conducted in order to find out if any information could be obtained from the phytomelan with ^{13}C-NMR.

A ^{13}C measurement was conducted on the AM-500 with proton disconnecting with a rf-field of 43 kHz to determine the resonances and the quantitative analyses.
Complementary AM-500 cp-mass spectra are added at different spinning velocities to determine the isotropic values of standard chemicals catechin, ellagic acid, and tannic acid, in order to determine the resemblance of these controls with phytomelan.
On the AM-500 dipolar dephasing experiments were conducted to ascribe the different C-atoms.
On the DMX-300 ^{13}C CP-mas measurements were conducted with the expectation that higher rf-fields (100 kHz) and higher spinner velocities, which can be used on this machine, will improve the resolution of the spectra.

Scanning Electron Microscopy
Seeds and fruits were treated in the Wiesner mix for several weeks, or dissected and fixed in FAA (formalin, alcohol, acetic acid; 9:1:1), dehydrated in acetone, incubated in tetramethyl-silane for 4h and air dried (Dey *et al.* 1989). The seeds were sputter-coated with gold/palladium and examined with an ISI-DS130 Dual Stage scanning electron microscope (SEM) at 9 kV.
For X-ray elemental analysis *Gasteria verrucosa* seeds during the second stage of phytomelan development (= not colored); seeds during the start of the third stage (= just coloring brown), and seeds during the end of the third stage of phytomelan development (= darkish colored) were intersected transversely with a cryo microtome, mounted with carbon cement on aluminum stubs, and air dried under low humidiation at room temperature. The specimens were carbon sputter-coated and examined in a CAMSCAN SEM (at 20 kV), fitted with a backscatter detector (KE Developments, Cambridge, England), and a LINK energy dispersive X-ray analyzer.

Fourier-transform infrared (FTIR) spectroscopy
Fourier-transform infrared (FTIR) spectroscopy on seeds of *Gasteria verrucosa* and *Chlorophytum amairiense* was performed on a Nicolet 510P spectrometer using the diffuse reflectance method. The instrument resolution was 2 cm^{-1}.

Thin layer Röntgen diffraction analyses
Phytomelan of *Gasteria verrucosa* was ashed or grinded and analyzed on silica in a thin layer Philips horizontal Röntgen diffraction meter PW 1380 in combination with an analyses system PW 1375. The CuK radiation was 1.65 kW (HV generator PW 1011). The divergention slit was 0.25°. As Goniometer a PW 1371 and a flat LiF monochromator crystal were used. The standard theta value was 1°.

Lightmicroscopy and histochemistry

Hand cut sections of different developmental stages of the seed coat of *Gasteria verrucosa* were stained for phenolics (Table 3), for cutin (neutral fats and fatty acids) with Sudan IV (Gerlach 1969), for lignin with phloroglucinol/HCl (Gahan 1984; Krisnamurhty 1988), for protein with Coomassie Brilliant Blue (Gahan 1984; Krisnamurhty 1988), for pectin and hemicellulose with ruthenium red (Gahan 1984; Krisnamurhty 1988), for cellulose with zinc-chlor-iodide (Gahan 1984; Krisnamurhty 1988), and with toluidine blue as a general stain (Feder and O'Brien 1968). Mature fruits of *Arnica montana* and developmental stages *of Helianthus annuus* fruits were stained with periodic acid-Schiff's reagent (PAS) (Gahan 1984) and contra stained with toluidine blue (Feder and O'Brien 1968). All samples were examined in a Zeiss microscope.

As marker for water entry, seeds were incubated in an aqueous solution of eosin. The appearance of the color was examined under a binocular.

RESULTS AND DISCUSSION

The main problem in the study of melanins, and thus also of phytomelan, is the chemical inertness, because phytomelan is insoluble. The chemical inertness is demonstrated in the fossil record where the phytomelan layer of a Compositae fruit is still present (Fig. 2) (Wijninga 1996). Also chemical treatments of seed coats showed the inertness (Table 2). From the Compositae only the phytomelan layer in the fruit wall remains in fossils. Phytomelan of seed coats of Asparagales is hard to find in the fossil record due to the minuscule size of this tertiary cell wall.

Phytomelan and non-phytomelan containing seeds can be distinguished with the Wiesner mix.Only seeds of *Camassia leichtinii* (Liliaceae) and *Vanilla pilifera* (Orchidaceae) did not contain phytomelan in the seed coat. The dark brown layer in these seeds probably consists of condensed tannins instead, whereas seeds of phytomelan containing taxa showed remnants of the chemical inert phytomelan. In figure 3 phytomelan in the seed coat of *Gasteria*

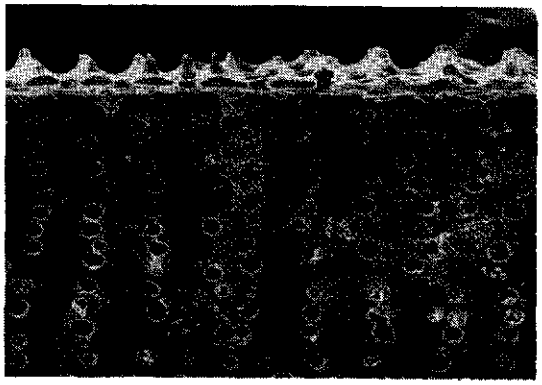

Figure 2: Only the phytomelan layer of Compositae fruit remains in the fossil record (x 540) (Wijninga 1996) (SEM)

Table 2: Chemical treatments of *Gasteria verrucosa* seeds, and the influence on the seed coat after 48 h.

chemical	influence	remarks
NaOH (conc.) + $KMnO_4$	-	aril is partly solved
NaOH (conc.)	-	
H_2O_2 + $KMnO_4$	-	
H_2O_2	-	the aril clears and endosperm disappears
Hexane	-	
Dichloromethane	-	
Hexane/Dichloromethane mixture	-	
Propionic acid	-	
H_2SO_4 (conc.)	-	seed dissolves; agressive
Wiesner mix	+	Dafert and Miklauz (1912); dissolves cell walls, but keeps phytomelan anatomically intact
96% ethanol	-	
96% acetic acid	-	
aceton	-	
$NaHClO_3$	±	Clears seed. Seed remains intact but is a bit jelly-like. Phytomelan is still brittle. Clearing with NaHClO3 gives no additional information on the chemical structure, because this solution clears every single structure in plant tissue. It is a very rough and non-selective method.

verrucosa (Asparagales, Asphodelaceae) and the fruit of *Arnica montana* (Compositae) is shown after treatment with the Wiesner mix. In the *Gasteria verrucosa* seed coat the phytomelan is present as a tertiary cell wall (Wittich & Graven 1995). In the fruit of Compositae phytomelan is present as an excretion at the outer tangential side of the sclerotic fiber bundles and fills the intercellular spaces. The sclerenchymatic layer of *Arnica montana* and *Helianthus annuus* first excretes a clear substance which then starts to become brown. Finally it indurates and becomes almost black. This process just outside the cell wall is comparable with the visible phytomelan synthesis in the seed coat of Asparagales. This is the phytomelan which remains in the fossil record (Fig. 2).

Histochemistry

Staining with the histochemicals tested (Table 3), indicate the presence of catecholic phenols at the start of phytomelan synthesis. Fast Red GG Salt and toluidine blue stained low molecular weight phenols red and greenish, respectively, whereas the nitroso reaction indicated the presence of catecholic phenols (Fig. 4). After full development of the phytomelan only a black layer was visible, making observation of color reactions on this wall impossible.

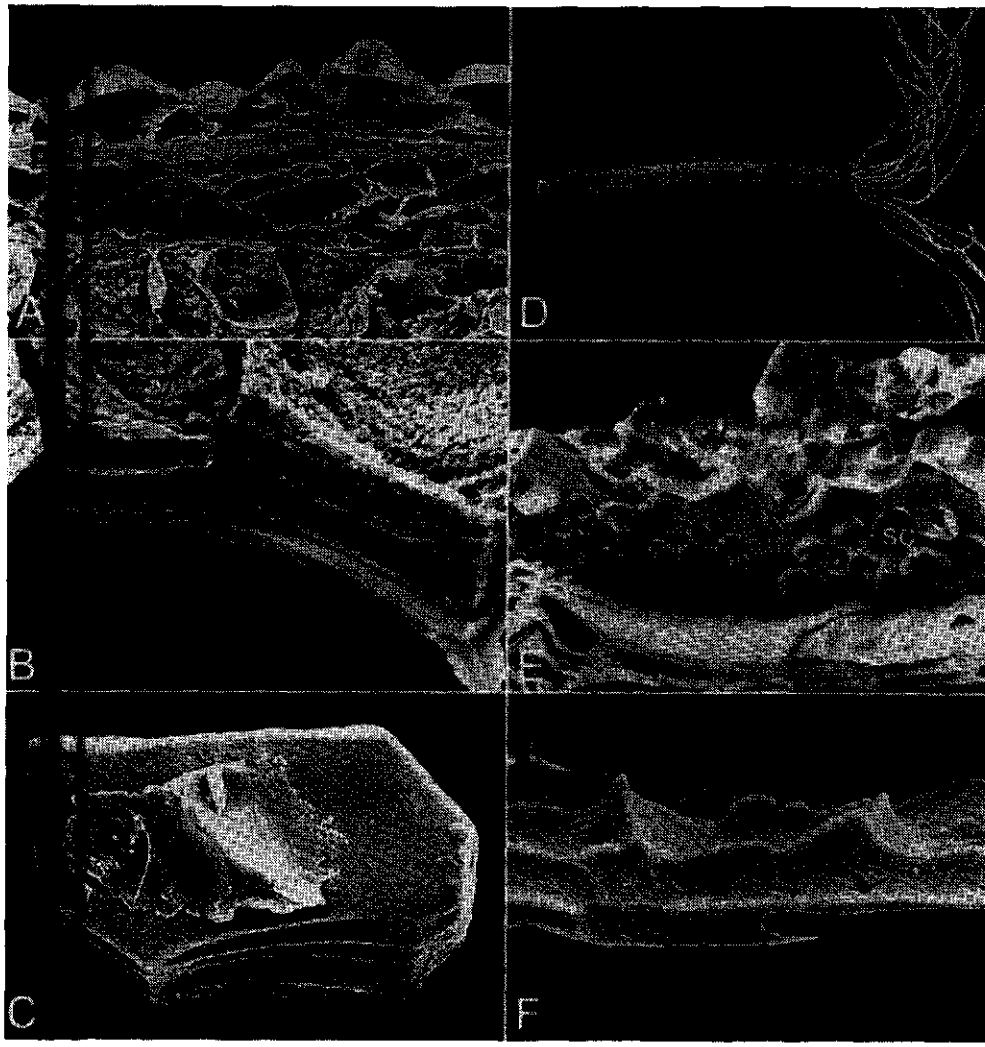

Figure 3: (SEM) **A-C** *Gasteria verrucosa*. **A** Section of mature seed *pm* phytomelan (exotesta); *en* endosperm; *ar* arillus (x 425). **B** Remains of a seed after treatment wit Wiesner mix (x 4200). **C** Almost every structure is biodegradated except blocks of phytomelan (x 3500). **D-F** *Arnica montana* **D** Fruit (x 15). **E** Transverse section of fruit wall, *pm* phytomelan, *sc* sclerenchymatic layer (x 875) **F** Phytomelan layer after chemical degradation of the fruit. (x 3025).

Table 3: Histochemical tests on phenolics in different stages of phytomelan development in the seed coat of *Gasteria verrucosa.*

stain	specificity	color reaction	reference	stage of phytomelan synthesis			
				no color	light brown	brown	dark brown
1 % ferric chloride in 0,1 N HCl	hydrolysable tannins	blue/blue-green	Reeve, (1951); Jensen, (1962)	-	-	-	-
2 % vanillin in conc. HCL	catechins	red	Morris and Robbins, (1992)	-	-	-	-
0, 3 % MBTH in 25 % ammonia	catecholic residues	red	Kalyani and Nellaiappan, (1989)	red	red	?	?
0,5 % 2,6 dichloro-quinone-4-chloro-imine in 95 % ethanol	polyphenols	blue/various colors	Gibbs, (1927); Mace, (1963); Gahan, (1984)	-	-	-	-
1 % DMB in 95 % ethanol	catechine and proanthocyanidins	bright red	Mace and Howell, (1974)	-	-	-	-
10 % vanillin in absolute ethanol	catechin/leuco-anthocyanidins	red	Blunden *et al.*, (1966)	-	-	-	-
2 % ferric chloride in 95 % ethanol	hydrolysable tannins	blue/blue green	Reeve, (1951); Jensen, (1962); Mace, (1963)	-	-	-	-
2 % ferric sulfate in formalin/water	hydrolysable tannins	blue/blue green	Reeve, (1951); Jensen, (1962); Mace, (1963)	-	-	-	-
Fast Red GG Salt	low molecular weight phenols	divers	Akin *et al.*, (1990)	red	red	red	?
p-nitroaniline	low molecular weight phenols (acids, aldehydes and esters), lignin extracts, polyphenols	divers	Akin *et al.*, (1990)	-	-	-	-
toluidine blue	polyphenols	turquoise-green/ blue green	Feder and O'Brien (1968)	green-blue[1]	-	-	-
Resorcine	callose	blue	Krisnamurthy (1988)	blue[1]	-	-	-

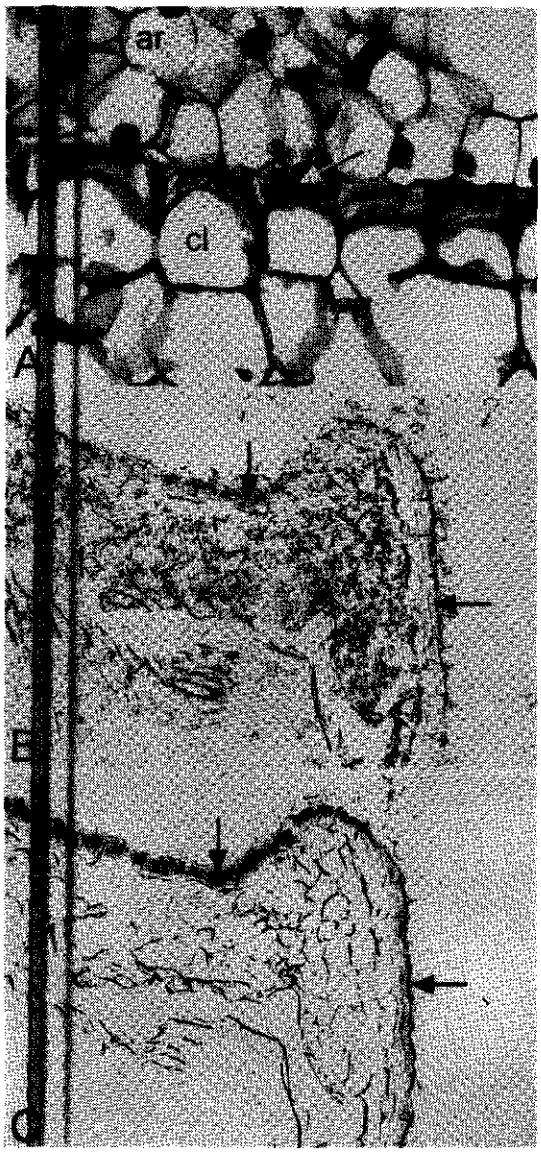

Figure 4: (LM) **A** Toluidine blue stains the tertiary cell wall green at the start of phytomelan synthesis, indicating the presence of phenolics (Wittich & Graven 1995). *ar* aril, *cl* cell lumen (x 560). **B** Early phytomelan synthesis before staining (arrows) **C** Staining by the nitroso reaction of the tertiary cell wall (arrows). (B and C x 140).

PyMS

In source pyrolysis mass spectrometry (PyMS) is a relative simple and fast method to obtain information on the chemical components of plant tissue at the molecular level (Boon 1989).

PyMS showed peaks with masses *m/z* 94, 110, and 126, during the onset of the third stage of development of the exotesta of the seed of *Gasteria verrucosa*. These peaks indicate the presence of catechol, one of the fragments of vegetable polyphenols (Graven *et al.* 1995, 1998), as they appeared in a late stage of the temperature ramp. Nicolaus (1968) also obtained catechol by means of alkali fusion out of several phytomelan containing seeds and seeds of other taxa. Although alkali fusion is a very rough degradation reaction and does not elucidate the chemical structure of phytomelan, it gave an indication about one of the components of phytomelan. From these analyses and from the histochemical tests it can be concluded that catechol is one of the precursors of phytomelan.

In all cases that phytomelan was isolated from mature seeds by using the Wiesner mix, and analyzed by pyrolysis mass spectrometry, only a very low signal for pyrolysis polysaccharide fragments and a very high disturbing signal of sulphur, originating from the

Wiesner mix, was detected. Sulphur was not present in non-treated phytomelan as shown in PyMS measurements and by X-ray analysis and was impossible to remove by extensive washing. Although the phytomelan stuck to the insertions probe, it is not clear whether the Wiesner-mixture made any changes the macromolecular composition of the phytomelan, it was decided to isolate the exotesta for further experiments without any chemical treatment. However, in the interpretation of the results it has to be taken into account that there may be some interference of primary and secondary cell wall polysaccharides, since it is impossible to isolate the tertiary walls of the exotesta without any other wall material. Further PyMS resulted in a mass spectrum with only a very low signal for polysaccharides. These polysaccharides were identified as cellulose fragments (Pouwels & Boon 1990), originating from the primary and secondary wall. The phytomelan itself was not pyrolyzed and stuck to the insertion probe of the mass spectrometer after running the experiments. This leads to the conclusion that phytomelan is a heat resistant, very condensed, probably ether bound, aromatic polymer.

X-Ray

Thin layer Röntgen diffraction analyses on the isolated phytomelan layer showed that the phytomelan of *Gasteria verrucosa* was not crystalline and did not contain anorganic constituents (not shown).

SEM with energy dispersive X-ray analysis on several developing stages also showed that specific signals for anorganic elements could not be detected in the phytomelan layer of the studied phytomelan containing taxa. The analysis showed only weak standard peaks for P, S, Cl, K and Ca in the secondary walls (not shown). These elements occur always in the secondary cell walls of seed coats, and are normally not specific present in one layer. The phytomelan and the phytomelan precursors did not contain specific anorganic elements and showed an organic character.

FTIR and ^{13}C NMR

Due to the chemical inertness of the phytomelan, non-destructive spectroscopic methods as FTIR and ^{13}C NMR can provide an insight in the functional groups and types of bonds present in the phytomelan itself.

Isolated phytomelan of the seed coat of *Gasteria verrucosa* and *Chlorophytum amairiense* was analyzed with FTIR. The samples gave the appearance of a brown black cellular material in a transparent matrix. The FTIR analysis gave voids and irregularities in the spectrum, which all contributed to a noise as a certain blunt appearance in the peaks. The experiments indicated the presence of an aromatic structure. In the lower area of the spectrum (not shown) no conclusion could be drawn on substituted groups due to the presence of only one peak at 730 cm^{-1}, which might be $-(CH_2)_4-$. High peaks appearing at 1700-1500 cm^{-1} could be assigned to C=C and

C=O stretching frequencies. Furthermore, there was much interference of the primary and secondary wall polysaccharides.

The first ^{13}C NMR direct measurements (HP-DEC) on the phytomelan samples of *Gasteria verrucosa* with proton coupling with a rf-field of 43 kHz, a relaxation delay of 10 s and spinner velocity of about 8 kHz (JBOF0510.002), as shown in figure 5, gave the resonances which are summarized in table 4. The spectrum was fitted to the program WINFIT and showed that the aromatic part of the spectrum (92 till 158 ppm) contained 75% of the total intensity. Figure 5 also shows the CP-MAS spectrum at a rf-field of about 50 kHz, a relaxation delay of 4 s and a mixing time of 3 ms. It is remarkable that the resolution of CP-MAS spectrum was significant better then the HP-DEC spectrum. This is probably due to the presence of coaled material in the phytomelan structure which does not appear in the CP-MAS spectrum because of an absence of protons in the surroundings of the C-atoms. In the CP-MAS spectrum also more peaks were found then in the HP-DEC spectrum. This could be due to a to short repetition times in case of the HP-DEC measurement, because the ^{13}C relaxation time of the

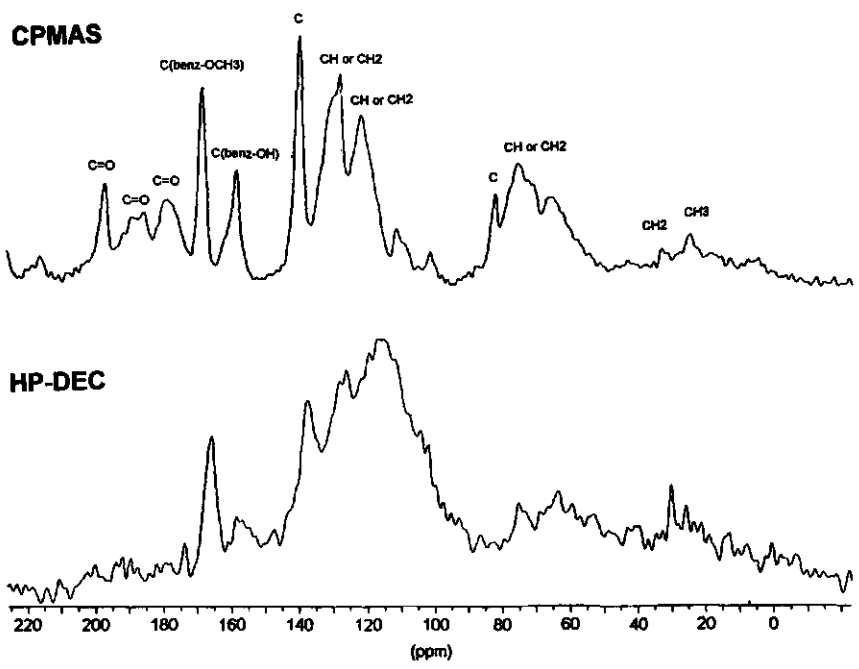

Figure 5: CP-MAS spectrum of phytomelan (7 kHz spinning), and HP-DEC spectrum of phytomelan (8 kHz spinning).

C=O groups are probably longer. In case of cross polarization the repetition time depends on the relaxation time of the protons. This relaxation time is in general shorter then for ^{13}C. Most of the resonances of the cellulose came from the secondary walls, and were hidden under the spinning side bands of the aromatic fractions. For the identification of the peaks more additional information was required. These were obtained by further experiments and comparison with other commercially available compounds, which gave more information on the possible composition of the phytomelan.

Table 4: Summary of ^{13}C resonances in ppm and percentages corresponding with the direct measurement with proton coupling as shown in figure 5

^{13}C Resonances ppm	Integral %
166.6	6.7
157.6	2.0
137.8	6.6
127.9	10.6
119.2	6.5
118.5	31.3
113.6	11.0
104.8	8.0
74.8	1.5
63.1	14.0
30.2	1.0

Catechin, one of the monomeric constituents of tannins, yielded catechol as the single degradation product, when it was subjected to the same degradation conditions as vegetable polyphenols (Galetti & Reeves 1992). Also phytomelan may be tannin-like, since it results also into catechol as final degradation product (Nicolaus 1968). Three commercially available standard products, catechin, ellagic acid and tannic acid (Fig. 6) were compared with phytomelan by analyzing them on the AM-500 in the Doty Probe with a rf-field of 43 kHz with different spinning velocities. Table 5 shows a summary of the isotropic values of the different structures in comparison to the phytomelan. From these results can be conclude that phytomelan is a more complex structure then those three controls, but it also shows some resemblance.

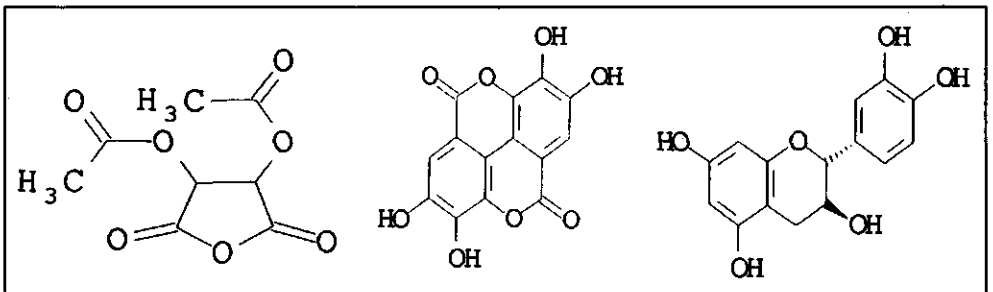

Figure 6: Standard chemical structures.

Table 5: Isotropic chemical shifts of standard structures measured with CP-MAS NMR,and phytomelan measured with CP-MAS NMR and HP-DEC NMR. Resonances in ppm.

Tannic acid CP-MAS	Catechin hydrate CP-MAS	Ellagic acid CP-MAS	Phytomelan CP-MAS	Phytomelan HP-DEC
			197.4	
			187.2	
			179.1	
169.9			168.8	166.8
		162.2		
	156.0		158.9	157.8
146.0	147.0	149.0		
140.0			140.1	137.8
	131.0		130.1	127.9
121.0	121.0		120.9	119.2/118.5
113.0		113.0/109.0	110.5	104.8
	97.0		101.5	104.8
			82.5	
76.0			76.0	74.8
	67.0		66.7	63.1
	31.0		32.4	30.2
			25.3	
			17.6	
			6.2	

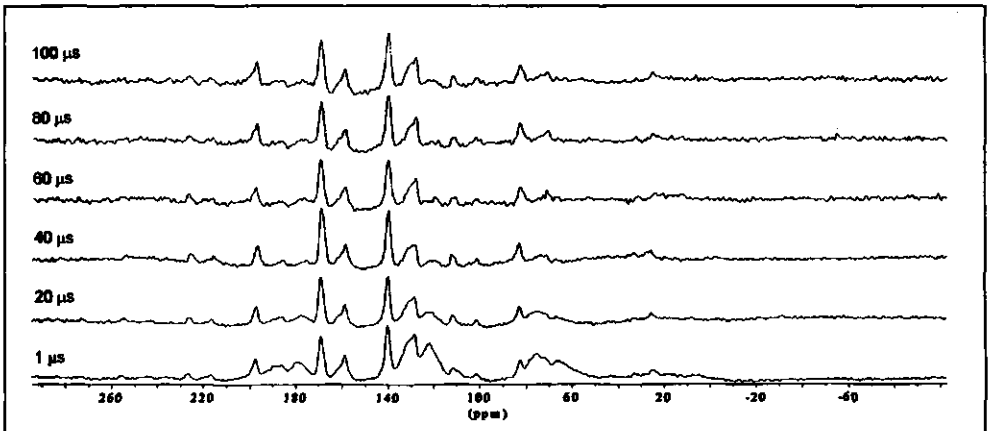

Figure 7: Dipolar Dephasing experiments on phytomelan.

CP-MAS

Furthermore, the *Gasteria verrucosa* phytomelan was analyzed using the Dipolar Dephasing technique combined with CP-MAS. With this technique a distinction can be made between C-atoms with a strong dipolar interaction as the CH and the CH_2 group, C-atoms with an average dipolar interaction as the CH_3 group, and C-atoms with no dipolar interaction as a non-protonized C-atom. For this dipolar dephasing, times were used of 1 μs, 20 μs, 40 μs, 60 μs, 80 μs, and 100 μs, respectively. Due to these different dipolar dephasing times, the intensity of the C-atoms with a strong dipolar interaction will disappear during the dipolar dephasing times. In other words, the intensity of a CH group or a CH_2 group will become weaker. The spectra of these experiments are shown in figure 7. The kind of C-atoms present in the phytomelan could be extrapolated from the results of these Dipolar Dephasing experiments and with the help of ^{13}C chemical shift tables. In table 6 the NMR peaks for the two outmost dipolar dephasing times are quantified, namely 1 μs and 100 μs. Only from these Dipolar Dephasing experiments, the identification of the groups resulted in a structure for phytomelan of 2,4,-di-methoxy-phlor-acetophenon (Fig. 8). This structure of 2,4,-di-methoxy-phlor-acetophenon is mainly based on the structural elements and the dipolar dephasing results. According to Wagner *et al.* (1976) resonances of C-atom 2 and 4 are around 166 ppm and not protonized. Furthermore, these authors concluded that C-atom 6 at 162.7 ppm, is not protonized, and can be compared with the resonance at 158.9 ppm in the case of phytomelan.

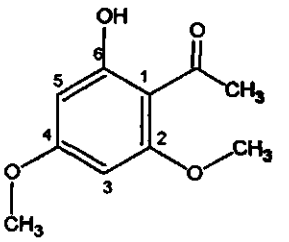

Figure 8: Structure of 2,4-di-methoxy phloracetatophenon.

1. 105.4 (102.8)	4. 166.0 (166.5)
2. 165.8 (162.4)	5. 93.5 (93.7)
3. 90.5 (92.4)	6. 162.7 (157.8)

Cross-Polarization is extremely sensitive for the spinning velocities. Especially at high velocities (higher then 7kHz) diminishes the efficiency which can be abolished by Variable Amplitude Cross-Polarization. On the DMX-300, a measurement was conducted with VACP (Variable Amplitude Cross Polarization) in order to get a better resolution while using a higher rf-field and higher spinning velocities. The results of this spectrum with a 100 kHz rf- field and a spinning velocity of 9 kHz are shown in figure 9.

Since the resolution of the spectrum did not increase, which could be due to the mobility of the phytomelan, other conditions as different temperatures and other rf-fields were used to conduct the measurement. A spectrum was recorded at a Te=223K and a rf-field of 50 kHz and for comparison at a Te=298K and a rf-field of 50 kHz. The results of the chemical shifts are listed in table 7. The spectrum measured at Te=223K had a better resolution, especially in the aliphatic area of 0 till 100 ppm. From the spectra, measured on the DMX-300 (Fig. 9) can

Table 6: Quantitative results of NMR Dipolar Dephasing experiments.

Nr.	1 µs DD		100 µsDD		Group
	Chemical shift	Integral %	Chemical shift	Integral %	
1	6.2	0.7	6.2	1.0	CH_3
2	17.6	1.8	17.6	3.3	CH_3
3	25.3	2.1	25.3	3.7	CH_3
4	32.4	1.1			CH or CH_2
5	66.7	14.4	71.3	2.7	CH or CH_2
6	76.0	7.1	76.0	3.0	CH or CH_2
7	82.5	1.9	82.5	4.4	C
8	101.5	0.5	101.5	2.3	C
9	110.7	2.7	111.5	2.9	
10	120.9	12.3	120.7	3.0	CH or CH_2
			128.0	2.1	
11	130.1	18.8	130.4	11.0	CH or CH_2
12	140.1	8.1	140.1	14.5	C
13	158.9	4.4	159.4	10.4	C(ϕ-OH)
14	168.8	6.5	168.8	16.0	C(ϕ-OCH_3)
15	179.1	6.4	175.2	8.4	C=O
16	187.2	6.2	187.8	3.8	C=O
17	197.4	5.0	197.9	7.5	C=O

be concluded that the spectral resolution was worse then expected. The influence of the mobility of the molecules in the phytomelan is an important factor, as was concluded from the point of the T-depending results.

Reference products

A literature survey of phenolic compounds present in plants, comparable with phytomelan, resulted in comparable spectra of green tea phenols (Davis *et al.* 1996) and flavanoids (Pomilio *et al.* 1977). Table 8 shows the chemical shifts of the green tea phenols (Fig. 10) extrapolated from the spectra found in literature and compared with the shift values found for phytomelan. The green tea polyphenol C-atom 2 (Table 8) could be related to the phytomelan peak at 82.5 ppm (Table 6), which is ascribed to a catechin-like structure. However, to the green tea C-atom 2 a proton is attached (Fig. 10), what is in contradiction with the results of the Dipolar-Dephasing experiments on phytomelan. Therefor the resemblance of the green tea C-atom 2 shift with the phytomelan shift is indicated by the symbol ± (Table 8). The green tea C-atom 3 has a resonance frequency at 69.3-70.5 ppm, and in the Dipolar-Dephasing experiments of phytomelan, a CH or CH_2 group was found at 66.7- 71.3 ppm. C-atom 4 of

Table 7: Chemical shift values (ppm) of phytomelan measured on a DMX-300 and a AM-500 via Cross Polarisation.

	DMX-300				AM-500
Resonance	vacp (100kHz) TE=298K s.s.=9kHz	vacp (100kHz) TE=298K s.s.=12kHz	cp (50kHz) TE=223K s.s.=7kHz	cp (50kHz) TE=298K s.s.=7kHz	cp (50kHz) TE=298K s.s.=7kHz
					6.2
1	16.03	13.6	13.5	15.0	
2	24.1	19.3	19.3	18.0	17.6
3		28.6	24.7	24.0	25.3
	30.8		30.0	32.2	
4	37.9	38.9	38.9	43.0	32.4
	46.5		53.0	57.3	
5	62.6	62.2	62.0	64.2	66.7
6	74.3	71.6	71.5	72.0	76.0
7	82.4	83.5	83.5	83.6	82.5
8	107.5	104.7	104.7	103.9	101.5
					110.5
9	116.1	115.0	115.0	115.4	
				118.4	120.9
				124.9	
10		128.0	128.0	129.0	130.1
	132.8		131.6	136.6	140.1
11	153.0	152.3	152.3		
12	161.2	160.1	160.1		158.9
					168.8
13	175.1	174.0	174.0	174.0	179.1
14	183.3	185.4	185.0		187.2
					197.4

green tea showed a relative good resemblance with the value found at 32.4 ppm of phytomelan. Also the resonance frequency at 100.7 ppm of the green tea C-atom 4a can be found in the spectrum of phytomelan, whereas C-atom 6 and 8 of the green tea polyphenol are not present in the spectrum of phytomelan. The resonances of the green tea C-atom 5 and 7 are comparable with the earlier proposed structure for phytomelan of the 2,4-dimethoxy-phlor-acetophenon (Fig. 8). Green tea C atom 1' and 4', of R=G and R'=OH, respectively, have a resonance frequency of about 130 ppm. However, this does not fit with the conclusion from the Dipolar Dephasing experiments where phytomelan C1' and C4' pointed out to be a CH or CH_2 group. In the phytomelan three other components are present, whereof two do not decrease in intensity, during the experiments (Fig. 7). This leads to the conclusion that at least two of the three phytomelan C-atoms have non-protonized sites. The green tea C-atom 6' with a resonance frequency of about 120 ppm was also found in the phytomelan experimental spectra. The Dipolar Dephasing experiment of phytomelan showed that this is a CH_2 or a CH group. It seems less probable that a C-atom is present in phytomelan analogue to the green tea

C-atom 1''. C-atom 2'' of green tea is a CH group of an aromatic ring and also present in the phytomelan spectrum. At a resonance of about 146 ppm green tea C-atom 3'' is situated as a quaternary C-atom. This seems not to be present in phytomelan, whereas C-atom 4'', positioned at about 139 ppm, was found present in the phytomelan. The resonance of phytomelan at 168.8 ppm can be ascribed to a CO group.

Summarizing the above results, it can be concluded that the structure of phytomelan matches highly with compound 3, 4, 7, 8 and 10 of the tea polyphenol. But since phytomelan is a polymerized product, the resonances differs on those sites were polymerization took place.

Wagner *et al.* (1976) and Pomilio *et al.* (1977) measured a great number of flavanoids with ^{13}C NMR. There is a lot of similarity between these flavanoids and phytomelan when the chemical shifts are compared. Table 9 shows this comparison of the chemical shifts of four those flavanoids (Fig. 11) with the chemical shift values of phytomelan. The exact presence or the absence of a particular shift is marked with a + or -, respectively. Flavanoid structure 8a and 8b (Fig. 11) showed the highest correlation with phytomelan.

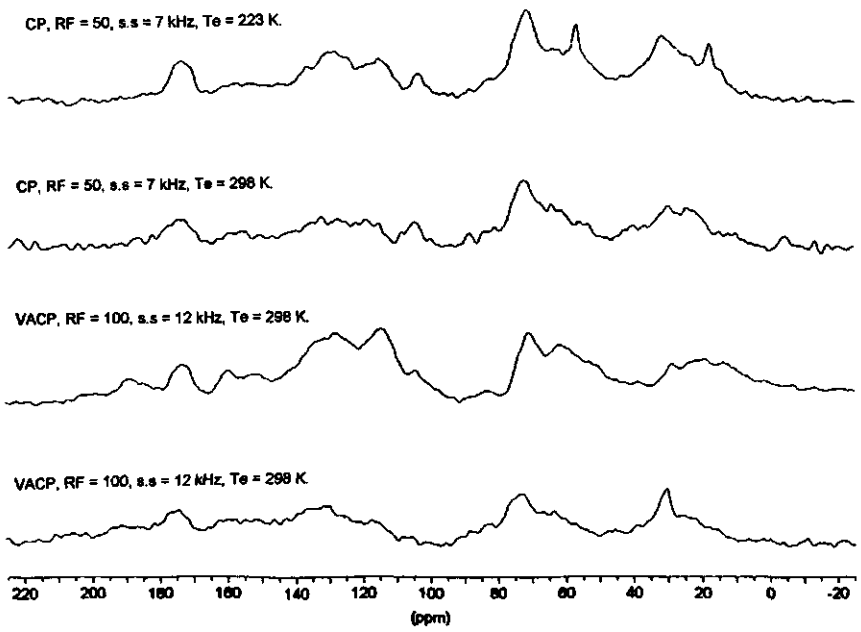

Figure 9: CP experiments of phytomelan using different conditions on DMX-300.

Table 8: Comparison of chemical shifts of green tea phenols, according to the compounds as shown in figure 10, and phytomelan. + = the resonance is present in phytomelan; ± = the resonance has a maximum difference of 1,5 ppm with the comparable resonance in phytomelan; - = not present in the phytomelan.

C-atom	Comp. 3	Comp. 4	Comp. 5	Comp. 8	Comp. 10	Presence in phytomelan				
						3	4	5	8	10
2	78.80	78.64	78.11	78.10	78.01	±	±	±	±	±
3	70.46	70.36	69.36	69.28	69.83	–	–	±	±	±
4	24.20	23.58	26.23	26.64	26.36	+	±	+	+	+
4a	99.24	99.14	99.03	99.04	98.99	±	±	±	±	±
6	96.47	96.40	96.56	96.54	96.50	–	–	–	–	–
8	95.61	95.57	95.87	95.87	95.79	–	–	–	–	–
5	157.25	157.23	157.50	157.46	157.45	±	±	±	±	±
7	158.08	158.02	157.81	157.78	157.88	+	+	+	+	+
8a	156.32	156.02	157.14	157.12	157.06	±	±	±	±	±
1'	131.47	130.95	131.42	130.77	130.85	+	+	+	+	+
2'	114.30	106.20	114.95	106.81	106.69	–	–	–	–	–
3'	145.82	146.57	145.60	146.27	146.35	–	–	–	–	–
4'	145.89	133.37	145.53	133.17	133.17	–	±	–	±	±
5'	115.99		115.67			–		–		
6'	119.13		119.25			+		+		
1"	121.80	121.80	121.87	121.92	121.81	+	+	+	+	+
2"	109.98	109.99	109.99	110.04	106.00	+	+	+	+	+
3"	146.00	146.03	145.94	145.09	148.47	–	–	–	–	–
4"	138.93	138.97	138.83	138.79	139.80	+	+	+	+	+
5"	-				145.79					–
6"	-				111.67					±
CO	166.04	166.15	166.04	166.07	166.16	±	±	±	±	±
O-Me	-	-		-	56.60	–				–

Concluding remarks

The above described results still do not allow unequivocally the determination of the structure of phytomelan exactly. However, it is clear that phytomelan shows much resemblance with catechin-like structures, as shown in figure 10, and flavanoid-like compounds as shown in figure 11. Also from the experiments conducted on the AM-500, which showed that 75% of the C-atoms is aromatic, can be concluded that the phytomelan has a comparable structure as green tea polyphenols and flavanoids. The ultrastructural composition of the *Gasteria verrucosa* phytomelan is already shown to consist of 15 nm units (Wittich & Graven 1998).

Catechol seems to be one of the precursors of the phytomelan, but the exact way of synthesis and possible enzymes involved in the process are not yet agreed upon. On the other hand, during the phytomelan synthesis an electron-dense border was found around the growing phytomelan globules (Wittich & Graven 1998). This is probably the location where catechol is converted into phytomelan.

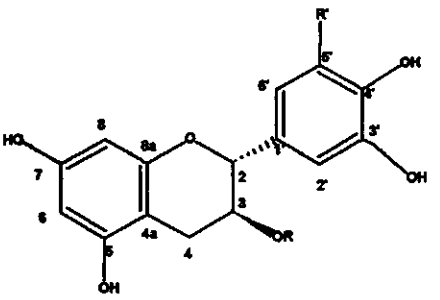

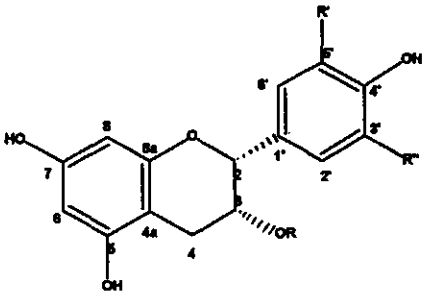

Compound 1	R=H	R'=H		epiafzelechin
Compound 2	R=H	R'=OH		catechin
Compound 3	R=G	R'=H		*epicatechin*
Compound 4	R=G	R'=OH		gallocatechin
Compound 5	R=H	R'=H	R''=OH	epigallocatechin
Compound 6	R=H	R'=OH	R''=OH	catechin-3-O-gallate
Compound 7	R=G	R'=H	R''=OH	epicatechin-3-O-gallate
Compound 8	R=G	R'=OH	R''=OH	gallocatechincatechin-3-O-gallate
Compound 9	R=H	R'=H	R''=H	epigallocatechin-3-O-gallate
Compound 10	R=GMe	R'=OH	R''=O	epigallocatechin-3-O-(3'-O-methyl-gallate)

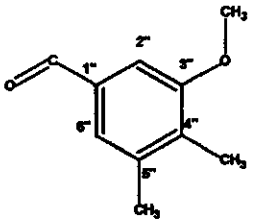

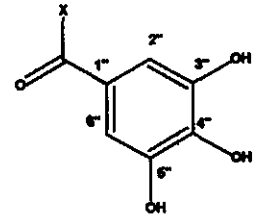

Figure 10: Cis and trans structures of green tea polyphenols.

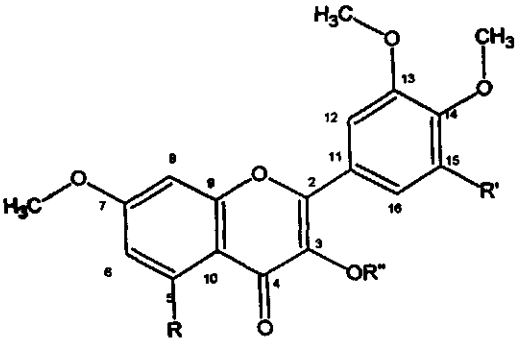

1. (= 4a)	R=OCH_3	R'=H	R''=H
2. (= 4b)	R=OCH_3	R'=H	R''=$COCH_3$
3. (= 8a)	R=H	R'=OCH_3	R''=H
4. (= 8b)	R=H	R'=OCH_3	R''=$COCH_3$

Figure 11: Four structures of flavanoids according to Wagner *et al.* (1976) and Pomilio *et al* (1977).

Table 9: Comparison of the chemical shift of natural flavanoids with phytomelan, as shown in figure 11. + = the resonance is present in phytomelan; ± = the resonance has a maximum difference of 1,5 ppm with the comparable resonance in phytomelan; - = not present in the phytomelan.

C-atom	4a	4b	8a	8b	Presence in phytomelan			
					4a	4b	8a	8b
2	150.2	152.2	153.3	155.6	±	+	+	±
3	137.5	133.7	137.8	133.3	+	+	+	+
4	171.6	168.1	172.7	167.9	±	+	+	+
5	158.7	159.1	126.5	127.3	+	+	±	+
6	95.5	95.9	114.7	114.7	-	-	+	+
7	164.2	164.2	164.4	164.3	-	-	-	-
8	92.3	92.6	100.1	100.1	-	-	±	±
9	160.4	161.5	157.2	157.1	+	+	±	±
10	106.1	108.8	114.7	117.3	±	±	±	±
11	123.7	122.4	126.8	125.0	±	±	±	±
12	110.3	110.8	105.7	105.8	+	+	+	+
13	148.7	148.8	153.3	153.2	-	-	+	+
14	148.6	148.8	140.2	140.6	-	-	+	+
15	110.8	111.5	153.3	153.2	+	+	+	+
16	120.5	121.6	105.7	105.8	+	+	±	±

The control reaction of the PATAg staining technique (without the peroxidase reaction) shows staining of the globules in TEM, indicating the presence of aldehyde groups in or at the globules (Wittich & Graven 1998). These aldehyde groups are relatively easily oxidized and play a role in the polymerization of the monomeric phytomelan units, resulting in the growing and fusing globules.

Tannins, as well as phytomelan, are present in dead cells (Swain 1965; Wittich & Graven 1995, 1998). Condensed or nonhydrolyzable tannins are often formed by the condensation of two or more molecules of flavan-3-ols, such as catechin.

It is assumed that phytomelan has the same protective function as condensed tannins in the seed coat, because related taxa without phytomelan often have condensed tannins instead. They may have lost the use of condensed tannins during evolution (Huber 1969). Phytomelan is chemically inert, and thus can offer effective protection or mechanical strength to seeds (Netolitzky 1926; Dahlgren and Rasmussen 1983). Netolitzky (1926) mentions the possibility of a light protective function in those seeds with phytomelan, whereas other pigmented layers of other taxa are more often situated in deeper layers of the seed coat. In the case of the family of the Asphodelaceae, the aril than offers even a double filter against light.

Many tannins are able to inhibit the growth of fungi, due to there toxicity, and they may be responsible for the resistance of plants to infection (Swain 1965). Phytomelan seems to have a same function. Catechol as precursor of phytomelan is also toxic. Catechol from the red onion

tunic stops fungal spore germination (Willemse, personal communication). Seeds of *Gasteria verrucosa* and *Chlorophytum amairiense*, *Cordyline haageana* and *Dianella caerulia* germinated easily, in a non-sterile and humid atmosphere, without the appearance of insects, fungi or other pathogens. But the phytomelan layer does not function solely as a mechanical barrier of the seed to prevent pathogen invasion, because there seems to be a possibility for microbial and fungal invasion. Experiments with imbibition of Gasteria verrucosa seeds in an eosin solution, as a 'tracer' (not shown), showed an easy access of the dye via a micropylar opening, while the exotesta of phytomelan showed no dye penetration.

This study brought us closer to the structure of phytomelan of *Gasteria verrucosa*, but it also appeared to be very difficult to analyze its chemical structure with modern analytical techniques. In the Asparagales and Compositae phytomelan is known to be present whereas in other taxa phytomelan might be present but not been detected. Further experiments have to be conducted whether phytomelan has the same composition in all related taxa.

ACKNOWLEDGEMENTS

The authors wish to thank Jaap Boon, Chris de Koster and Michel Willemse for the valuable discussions, Nora Devente for her technical assistance, and the SON National HF-NMR Facility Nijmegen for the NMR measurements. The study was partly supported by the Life Science Foundation (SLW) which is subsidized by the Netherlands Organization for Scientific Research (NWO).

REFERENCES

Akin DE, RD Hartley, WH Morrison III and DS Himmelsbach (1990) Diazonium compounds localize grass cell wall phenolics: relation to wall digestibility. Crop Sci 30: 985-989

Blunden G, SB Challen and B Jacques (1966) Accumulation of anthoxanthins and amino acids in leaf galls of *Salix fragilis* L. Nature 212: 514-516

Boon JJ (1989) An introduction to pyrolysis mass spectrometry of lignocellulosic material: case study on barley straw. In: Physicochemical characterization of plant residues for industrial and feed use. Chesson A and ER Ørskov (eds), Elsevier Applied Science, London: 24-45

Dafert FW (1932) Phytomelane. In: Handbuch der Pflanzenanalyse 2. Klein G (ed): 286-292

Dafert FW and R Miklauz (1912) Einführung des Namens Phytomelan. In: Untersuchungen über die Kohle ähnlich Masse der Kompositen. Hanausek F (ed), Denkschr. Akad. Wiss. Wien Math Naturw Kl 87: 143-152

Dahlgren RMT and HT Clifford (1982) The monocotyledons. A comparative study. Academic Press, London

Dahlgren RMT and FN Rasmussen (1983) Monocotyledon evolution characters and phylogenetic estimation. In: Evolutionary biology, vol 16. Hecht MK, B Wallace and GT Prance (eds), Plenum Publishing Corporation: 255-395

Dahlgren RMT, HT Clifford and PF Yeo (1985) The families of the monocotyledons: structure, evolution and taxonomy. Springer Verlag, Berlin, Heidelberg, New York, Tokyo.

Davis AL, Y Cai, AP Davies and JR Lewis (1996) ^{1}H and ^{13}C NMR assignments of some green tea polyphenols. Magn Reson Chem 34: 887-890

Feder N and TP O'Brien (1968) Plant microtechnique: some principles and new methods. Am J Bot 55: 123-142

Gahan PB (1984) Plant histochemistry and cytochemistry. An introduction. Academic Press, London

Galetti GC and JB Reeves (1992) Pyrolysis/gas chromatograph/ion-trapdetection of polyphenols (vegetable tannins): preliminary results. Org Mass Spec 27: 226-230.

Gerlach D (1969) Botanische Mikrotechnik. Ein Einfuhrung. Georg Thieme Verlag, Stuttgart

Gibbs HD (1927) Phenol test III. The indophenol test. J Biol Chem 72: 649-664

Graven P, CG Koster, JJ Boon and F Bouman (1996) Structure and macromolecular composition of the seed coat of the Musaceae. Ann Bot 77: 105-122

Graven P, CG Koster, JJ Boon and F Bouman (1997) Functional aspects of mature seed coat of the Cannaceae. Pl Syst Evol 205: 223-240

Hanausek TF (1902) Zur Entwicklung des Perikarps von *Helianthus annuus*. Ber Dtsch Bot Ges 20: 449-454

Hanausek TF (1907) Die Kohleschicht in Perikarp der Kompositen. Sitz Ber Akad Wiss Wien 116: 1-30

Hanausek TF (1908a) Ueber das Perikarp von *Humea elegans* Sm. Ber Dtsch Bot Ges 26: 292-298

Hanausek TF (1908b) Neue Mitteilungen über die sogenannte Kohleschicht der Kompositen. Wiesner Festschrift, Wien: 139-150

Hanausek TF (1911a) Ueber das Perikarp und das Perikarp-Sekret der Gattug *Carthamus*. Ber Dtsch Bot Ges 29: 13-18

Hanausek TF (1911b) Zur Kenntnis der Verbreitung der Phytomelane. Ber Dtsch Bot Ges 29: 558-562

Hanausek TF (1912) Untersuchungen über die Kohlenschicht ähnliche Masse der Kompositen. Denkschr Akad Wiss Wien 87: 94-141

Hanausek TF (1913) Ueber ein neues Vorkommen von Phytomelan. Arch Chem Mikrosk 6: 294

Hegnauer R (1962-1990) Chemotaxonomy der Pflanzen. vol 1-9. Birkhäuser Verlag, Basel

Huber H (1969) Die Samenmerkmale und Verwandschaftsverhältnisse der Liliifloren. Mitt Bot München 8: 219-538

Jensen WA (1962) Botanical histochemistry. Freeman, San Francisco.

Kalyani R and K Nellaiappan (1989) A new technique for staining catecholic residues in biological samples. Stain Technology 64: 15-18

Krisnamurthy KV (1988) Methods in plant histochemistry. Chetput, Madras, Visnawathan.

Lohde G (1875) Uber die Entwicklungsgeschichte und den Bau einige Samenschale. Schenk Leursens Mittel Gesamt Geb Bot. 2, 1875; auch Diss Leipzig, 1874

Mace ME and CR Howell (1974) Histochemistry and identification of condensed tannin precursors in roots of cotton seedlings. Can J Bot 52: 2423-2426

Mace ME (1963) Histochemical localization of phenols in healthy and diseased tomato roots. Phytopathology 16: 915-925

Morris P and MP Robbins (1992) Condensed tannin formation by *Agrobacterium rhizogenes* transformed root and shoot organ cultures of *Lotus corniculatus*. J Exp Bot 43: 221-231

Netolitzky F (1926) Anatomie der Angiospermen-Samen. Handbuch der Pflanzen Anatomie. Band X (K. Linsbauer). Verlag von Gebrüder Borntraeger, Berlin.

Nicolaus RA (1968) Melanins. Hermann, Paris.

Pomilio A, B Ellmann, K Künstler, G Schilling and K Weinges (1977) 13C-NMR-spektroskopische Untersuchungen an Flavanoiden. Liebigs Ann. Chem. 1977: 588-596

Pouwels AD and JJ Boon (1990) Analysis of beech wood samples, its milled wood lignin and polysaccharide fractions by Curie-point and platinum filament pyrolysis mass spectrometry. J Anal Appl Pyrolysis 17: 97-126

Reeve R (1951) Histochemical tests for polyphenols in plant tissues. Stain Technol 26: 91-96

Robbins WW and HA Borthwick (1925) Development of the seeds of *Asparagus officinalis*. Bot Gaz 80: 426-438

Rode WW (1913) Schutzeinrichtung von Früchten und Samen gegen Einwirkung fließenden Meerwassers. Diss Göttingen.

Swain T (1965) The tannins. In: Plant biochemistry. Bonner J and Varner JE (eds), Academic Press, New York: 552-580

Takhtajan A (1985) Anatomia seminum comparativa. Tomus 1. Liliopsida seu Monocotyledons. Leninpoli, Nauka.

Vries MA de (1948) Over de vorming van Phytomelaan bij *Tagetes patula* L. en enige andere Composieten. Diss, Leiden. H. Buurman, Leiden.

Wagner H, VM Chari and J Sonnenbichler (1976) ^{13}C-NMR-Spektren natürlich vorkommender Flavanoide. Tetrahedron Lett. 21: 1799-1802

Wiesner J (1867) Einleitung in die technische Mikroskopie. Wien.

Wijninga VM (1996) Paleobotany and palynology of neogene sediments of the high plain of Bogotá (Columbia). PhD thesis, University of Amsterdam, Amsterdam.

Wittich PE and P Graven (1995) Histochemical study of the development of the phytomelan layer in the seed coat of *Gasteria verrucosa* (Mill.) H. Duval. Protoplasma 187: 72-78

Wittich PE and P Graven (1998) Callose deposition and breakdown, followed by phytomelan synthesis in the seed coat of *Gasteria verrucosa* (Mill.) H. Duval. Protoplasma 201: 221-230.

Wunderlich R (1937) Zur vergleichende Embryologie der Liliaceae-Scilloideae. Flora 132: 48-90

Chapter

The study of carbohydrate transport and distribution in developing ovules and seeds

P.E. Wittich

Summary. Carbohydrates are transported into the seed via the phloem. At the end of the phloem they are unloaded and transported symplastically and/or apoplastically to the cells where they are utilized.

The transport and distribution of carbohydrates in developing seeds can be studied in many different ways. One method is to visualize the transport by using tracers which show symplastic or apoplastic transport. The problem however is that one type of tracers, the dye tracers, do not show the actual sucrose transport. An other type of tracers is radioactively labelled carbohydrates. However, the disadvantage of these tracers is that during fixation and embedding of the material the soluble sugars will be rinsed away and only the incorporated sugars will be detected. Another approach to study the distribution of carbohydrates are the sink strength studies. By demonstrating the break down capacity of sucrose by cells and tissues (*viz.* differences in sink strength), an indication can be given where most sugars will be transported to in the seed, *i.e.*, to the cells/tissues with the highest sink strength.

Both approaches can be used to complement each other in the study of transport and distribution of carbohydrates as long as there is no adequate, real time carbohydrate monitoring system available.

INTRODUCTION

Most ovules and seeds are true sinks because they do not synthesize their own sucrose, they are completely dependent on sucrose supplied via the phloem. Photosynthetic activity which is found in embryos of *Brassica napus* (Eastmond *et al.* 1996) and the pericarp of cereal grains, with the exception of maize (Duffus 1992), seems only to function in the re-fixation of respiratory carbon dioxide.

The phloem terminates in the chalaza, nucellus or integuments, where sucrose will be unloaded from sieve elements. The phloem unloading is generally symplastic, and the sucrose is distributed further symplastically into the growing sporophytic tissues. However, the developing gametophyte, the embryo sac, and later the endosperm and embryo, are genomically different organisms, and symplastically isolated from the sporophytic tissues (Fig.1). To pass this symplastic barrier, sucrose has to be unloaded into the apoplast between sporophytic tissue and developing gametophyte, embryo and endosperm (Fig.2A). This apoplast may consist of an extracellular space like that found in wheat grains (Wang *et al.* 1994), or only of the cell wall matrix as shown around the embryo sac of *Gasteria* ovules (this thesis Chapter 4). In this apoplast sucrose may be hydrolyzed into glucose and fructose by invertase activity, and after further transport the carbohydrates will be loaded into the symplast of the gametophyte, and later the embryo and endosperm (Fig.2A). The unloading into the apoplast may be simple, or facilitated diffusion, or energy coupled, while sugar uptake into the gametophyte, and later the embryo and endosperm, is expected to be mediated by symporters (Patrick 1997). In the following paragraphs different methods are discussed which are developed during the last decades to study carbohydrate transport in plant tissues.

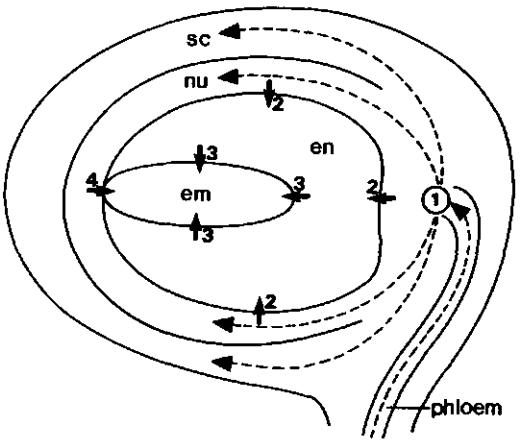

Figure 1 Symplastic and apoplastic sucrose transport steps in the seed. Between the three organisms in the seed (sporophytic tissue, endosperm, and embryo) no symplastic contacts exist, making an apoplastic step in the sucrose transport pathway necessary. Within the tissues most of the transport is symplastic, but apoplastic transport also occurs. **(1)** Symplastic unloading of sucrose from phloem into nucellus (*nu*) and seed coat (*sc*). **(2)** Apoplastic step between nucellus and endosperm (*en*), **(3)** between endosperm and embryo (*em*), and **(4)** between nucellus and embryo (via suspensor during early stages).

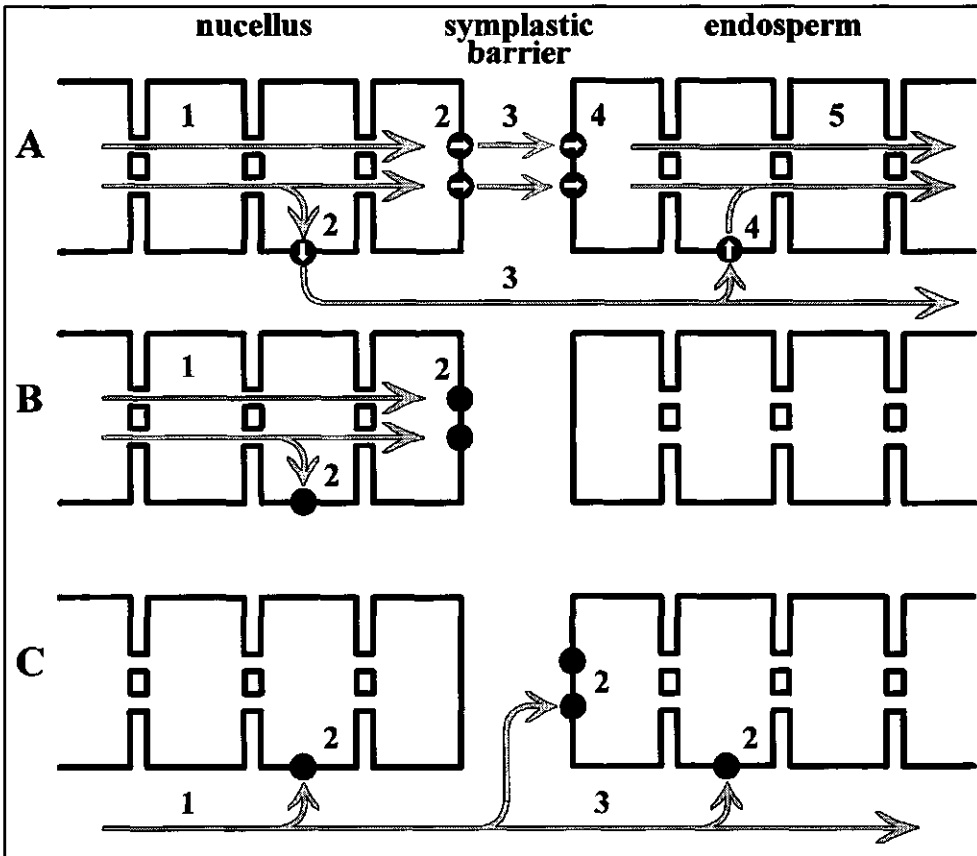

Figure 2 The transport of sucrose and tracers from the nucellus into endosperm (or into embryo), crossing a symplastic barrier. These tissues are not symplastically connected. Within the endosperm carbohydrates can be transported further via plasmodesmata (symplastic connections), as well as via the apoplast.

A Transport of sucrose. (1) Diffusion through the symplast of nucellus, (2) unloading into the apoplast, (3) apoplastic diffusion and often invertase hydrolization, (4) loading into symplast, (5) symplastic diffusion through endosperm / embryo.

B Transport of symplastic tracer. (1) Diffusion through the symplast of the nucellus, (2) no unloading into the apoplast, resulting in an accumulation of the tracer.

C Transport of apoplastic tracer. (1) Diffusion through the apoplast of the nucellus, (2) no loading into the symplast of nucellus and embryo/endosperm, resulting in further diffusion into the endosperm / embryo tissues (3).

TRACER STUDIES

To study the distribution routes of carbohydrates in seeds and other plant tissues many researchers use tracers in the form of dyes (Oparka 1991) or radioactive labelled sugars (Roeb and Fisher 1991).

Dyes are available which can be used specifically for either apoplastic transport, such as Prussian blue (Brady and Combs 1988), lucifer yellow (Wang and Fisher 1994), and sulphorhodamine G (Canny 1986), or symplastic transport, such as carboxyfluorescein (Wang and Fisher 1994), and also lucifer yellow CH (Oparka and Prior 1988). Other available dyes can permeate membranes and thus will be transported via both pathways. Import of the dye into the plant tissue is often performed via a cut-surface of a stem, or gently abraded leaf (see for methods Patrick *et al.* 1995). Hence, the uptake of a dye is via the apoplast and may be followed by loading into the cell symplast, while also further apoplastic transport will take place. Microinjection of a dye into the symplast prevents this apoplastic transport, but is technically difficult to apply on developing seeds and can only be used for studying short distance transport.

In general, sugars are expected to be transported symplastically through the phloem from the funicle into the nucellus, unloaded via transporters into the apoplast between nucellus and gametophytic tissues, and imported via transporters into the gametophytic tissue symplast from where further symplastic transport will take place through the tissue (as described for *Gasteria* and maize in this thesis) (Fig.2A). Symplastic dyes will also be transported to the symplastic barrier between nucellus and endosperm via the phloem and symplastic routes in the funicle and nucellus, but there the transport will be terminated since the tracers cannot pass the plasma membrane (Fig.2B). Thus, these dyes will only show their own transport pathway through the tissues, and will not visualize the transport pathway of carbohydrates, as sucrose, in the ovule or seed. A second aspect restricts the value of the tracer method as a way to visualize sucrose transport: unlike the tracer diffusion, the diffusive sucrose transport will be enhanced by the activity of sucrose synthase, invertase, and membrane transporters. These activities create a steeper sucrose gradient, enhancing diffusion of sucrose towards the sucrose converting cells.

Apoplastic dyes will reach the developing gametophytic tissues via the apoplast of the funicle and nucellus. For these dyes there is no barrier between those tissues, thus diffusion via the apoplast continues (Fig.2C).

Since membrane permeable dye tracers also can not demonstrate the actual sucrose transport pathway, dye tracers were not considered to be relevant for showing such carbohydrate transport in this thesis. However, the symplastic and apoplastic tracers can be used to demonstrate symplastic and apoplastic barriers, respectively, and symplastic dyes can be used to assess plasmodesmal exclusion limits (Wang and Fisher 1994, Kempers and Van Bel 1998).

Other tracers used for carbohydrate transport are radioactively labelled tracers. The method of feeding $^{14}CO_2$ to plants, followed by microautoradiography, seems not suitable to study sucrose transport since the radioactive carbon can be metabolized into other products than sucrose (Felker and Shannon 1979). A second method is to feed ^{14}C-sugars to plant ovules (Griffith *et al.* 1987). Besides the problem of getting the labelled sucrose only via the phloem into the ovule like is postulated to occur *in vivo*, and not also via the apoplast by uptake through the cut surface of the stem or placental tissues, the question rises what the results will reveal on tissue or cellular level. Most of the soluble products (like sucrose) cannot be fixed chemically, and thus will be rinsed away during the embedding procedure prior to microautoradiography. The results will only show the pathway where sucrose is utilized for the production of insoluble products like starch and cell walls. Such a problem might be solved in part by using freeze fixation and freeze substitution techniques as performed by Patrick *et al.* (1995). However, special requirements are needed for freeze substitution of radioactive plant material, and reliable localization results are uncertain since during the liquid phase of the embedding procedure radioactive sugars might dislocate. For the reasons described above it did not seem to be appropriate to use radioactively labelled sugars as tracers in ovules and seeds for structural analysis.

However, in numerous studies tracers are used in combination with other techniques to demonstrate potential transport pathways and barriers in sectioned plant material, or to detect macro-distribution patterns as in the 'empty seed coat technique' (Grusak and Minchin 1988, and references herein). In combination with the tracers, membrane inhibitors are used to deduce the cellular site of membrane exchange to and from the seed apoplast (Wang *et al* 1995a). The membrane transporters are recently localized immunocytochemically in *Vicia faba* seeds (Harrington *et al.* 1997), but can also be localized by using sulfhydryl-binding fluorescent dyes (Wang *et al.* 1995a). Heavy metal precipitation is used to indicate H^+-ATPase activity, a marker for carrier-mediated sucrose efflux (McDonald *et al.* 1996, Wang *et al.* 1995a). Plasmodesmal rupture is used in combination with tracer techniques to deduce symplastic transport routes (Wang *et al.* 1995b).

SINK STRENGTH STUDIES:

A different approach to study transport routes and carbohydrate distribution in plant tissues is to demonstrate the sink strength of cells and tissues.

Sucrose synthase and invertase are considered to be indicators for sink strength (Ho *et al.* 1991, Sung *et al.* 1989, 1994). By showing their activity on sections using enzyme histochemical techniques, it is possible to identify cells and tissues with high, low, or no

capacity to utilize sucrose. High enzyme activity implies high utilization of sucrose, and thus a decrease in sucrose concentration which enhances a diffusive transport to these sucrose-consuming cells. As a consequence there will be more sucrose transport from the phloem to tissues with high enzyme activity (high sink strength) than to tissues with low enzyme activity (low sink strength). Hence, monitoring the sucrose utilization capacity together with structural indications for symplastic and apoplastic barriers, loading and unloading, as is attempted in this study, may give an indication on the preferential sucrose transport pathways over cells and tissues.

Besides the theory of sink metabolism and compartmentation controlling sugar transport, it is also postulated that sink-located transfer and transport processes (membrane porters and channels, turgor, relative conductance of apo- and symplastic transport paths) regulate assimilate partitioning (Patrick 1997, Weber *et al.* 1997). Although these latter transport regulating processes are likely to play a role in the sugar transport, sucrose breakdown is presumed in this study to be the main controlling factor for diffusive sugar transport in ovules and seeds, and used to localize the destination of potential sucrose transport pathways.

Methods are available to determine the enzyme activity of extracted enzymes from dissected tissues by spectrophotometry. However, these methods cannot distinguish differences in enzyme activity between cells. For this reason, these techniques were further adapted to be applied on sections of plant material (enzyme histochemistry), thus making it possible to visualize the enzyme activity per cell (this thesis Chapter 2 - 5).

The technique of enzyme histochemistry is applicable on most plant tissues, and shows the activity of all isoforms of an enzyme for a certain condition. The sensitivity of the technique depends on the enzyme that is studied. It was shown that in the case of invertase the histochemical localization was less sensitive than the immunocytochemical localization in which the enzyme was detected by antibodies. These results may be explained by inactivity or very low concentration of invertase. However, in the case of sucrose synthase, the histochemical assay showed enzyme activity where immunochemistry could not detect the presence of the enzymes, indicating high activity of a low amount of sucrose synthase.

Using only immunocytochemical detection methods to detect sucrose synthase and invertase in order to localize sinks, has its restrictions. Besides the fact that antibodies only show the presence of the enzymes and not their activity, antibodies can be very isoform specific. Often antibodies are used which are raised against proteins of different plant species than the plant which is being studied, as in this thesis. Consequently, not all enzyme isoforms may be localized and some sinks may not be identified.

A combination of the techniques showing enzyme activity by enzyme histochemistry, and enzyme presence by immunocytochemistry, will also demonstrate that enzymes which are

shown to be present do not necessarily have to be metabolically active. Invertase activity for instance, can be involved in wound response (Matsushita and Uritani 1974). Thus, immunolocalization can give additional information on the localization of enzyme isoforms and a potential activity, while enzyme histochemistry demonstrates the actual activity of cells and tissues. The amount of actual activity will be an indication for the sink strength of the cell or tissue, hence, an indication for the distribution of sucrose over the cells and tissues.
Enzyme histochemistry and immunocytochemistry will give indirect information about symplastic or apoplastic transport. But activity of invertase in the cell walls may indicate that there is a need for sucrose, and therefore a transport into, or through the apoplast. Symplastic activity of sucrose synthase and invertase may point to a need for symplastic transport. Tracer studies and localization of membrane transport can be used to complement these enzyme localization studies to show diffusion pathways, and symplastic and apoplastic transport barriers. Nevertheless, from both approaches a carbohydrate transport pathway can be postulated, however, until now the real transport could not be visualized. Perhaps in the future advanced NMR techniques with a sufficient resolution on cellular level will become available to follow the pathway of selected carbohydrates.

ACKNOWLEDGEMENTS

I would like to thank JW Patrick, AAM van Lammeren, CJ Keijzer and MTM Willemse for their valuable contributions and critically reading this manuscript, DY Foreman for revising the English style of the manuscript, and AB Haasdijk for the drawing.

REFERENCES

Brady T and SH Combs (1988) The suspensor is a major route of nutrients into proembryo, globular and heart stage *Phaseolus vulgaris* embryos. In: Sexual reproduction in higher plants. Cresti M, P Gori and E Pachini (eds). Springer-Verlag, Heidelberg: 419-424

Canny MJ (1986) Water pathways in wheat leaves. III. The passage of the mestome sheath and the function of the suberised lamellae. Physiol Plant 66: 637-647

Duffus CM (1992) Control of grain growth and development. In: Fruit and seed production. Aspects of development, environmental physiology and ecology. Marshall C and J Grace (eds) Soc Exp Biol, Seminar Series 47: 125-149

Eastmond P, L Kolacna and S Rawsthorne (1996) Photosynthesis by developing embryos of oilseed rape (*Brassica napus* L.). J Exp Bot 47: 1763-1769

Felker FC and JC Shannon (1980) Movement of ^{14}C-labeled assimilates into kernels of *Zea mays* L. III. An anatomical examination and microautoradiographic study of assimilate transfer. Plant Physiol 65: 864-870

Griffith SM, RJ Jones and ML Brenner (1987) *In vitro* sugar transport in *Zea mays* L. kernels. I. Characteristics of sugar absorption and metabolism by developing maize endosperm. Plant Physiol 84: 467-471

Harrington GN, VR Franceschi, CE Offler, JW Partick, M Tegeder, WB Frommer, JF Harper and WD Hitz (1997)Cell specific expression of three genes involved in plasma membrane sucrose transport in developing *Vicia faba* seed. Protoplasma 197: 160-173

Ho LC, A Lecharny and J Willenbrink (1991). Sucrose cleavage in relation to import and metabolism of sugars in sink organs. In: Recent advances in phloem transport and assimilate compartmentation. JL Bonnemain, S Delrot, WJ Lucas and J Dainty (eds.). Ouest editions, Nantes: 178-186

Kempers R and AJE van Bel (1997) Symplasmic connections between sieve element and companion cell in the stem phloem of *Vicia faba* have a molecular exclusion limit of at least 10 kDa. Planta 201: 195-201

Matsushita K and I Uritani (1974) Change in invertase activity of sweet potato in response to wounding and purification and properties of its invertases. Plant Physiol 54: 60-66

McDonald R, S Fieuw and JW Patrick (1996) Sugar uptake by the dermal transfer cells of developing cotyledons of *Vicia faba* L. mechanism of energy coupling. Planta 198: 502-509

Oparka KJ (1991) Uptake and compartmentation of fluorescent probes by plant cells. J Exp Bot 42: 565-579

Oparka KJ and DAM Prior (1988) Movement of Lucifer Yellow CH in potato tuber storage tissues: A comparison of symplastic and apoplastic transport. Planta 176: 533-540

Patrick JW (1997) Phloem unloading: sieve element unloading and post-sieve element transport. Annu Rev Plant Physiol Plant Mol Biol 48: 191-222

Patrick JW, CE Offler and X-D Wang (1995) Cellular pathway of photosynthate transport in coats of developing seed of *Vicia faba* L. and *Phaseolus vulgaris* L. I. Extend of transport through the coat symplast. J Exp Bot 46: 35-47

Roeb GW and DB Fisher (19..) Some in vivo tracer techniques for studying transport. In: Recent advances in phloem transport and assimilate compartmentation. Bonnemain JL, S Delrot, WJ Lucas and J Dainty (eds). Oest Editions, Nantes: 309-316

Sung S-JS, D-P Xu and CC Black (1989) Identification of actively filling sucrose sinks. Plant Physiol 89: 1117-1121

Sung SS, WJ Sheih, DR Geiger and CC Black (1994) Growth, sucrose synthase, and invertase activities of developing *Phaseolus vulgaris* L. fruits. Plant Cell Env 17: 419-426

Wang N and DB Fisher (1994) The use of fluorescent tracers to characterize the port-phloem transport pathway in maternal tissues of developing wheat grains. Plant Physiol 104: 17-27

Wang HL, CE Offler, JW Patrick and TD Ugalde (1994) The cellular pathway of photosynthate transfer in the developing wheat grain. I. Delineation of a potential transfer pathway using fluorescent dyes. Plant Cell Env 17: 257-266

Wang X-D, G Harrington, JW Patrick, CE Offler and S Fieuw (1995a) Cellular pathway of photosynthate transport in coats of developing seed of *Vicia faba* L. and *Phaseolus vulgaris* L. II Principal cellular site(s) of efflux. J Exp Bot 46: 49-63

Wang HL, JW Patrick, CE Offler and X-D Wang (1995b) The cellular pathway of photosynthate transfer in the developing wheat grain. III. A structural analysis and physiological studies of the pathway from the endosperm cavity to the starchy endosperm. Plant Cell Env 18: 389-407

Weber H, L Borisjuk, and U Wobus (1997) Sugar import and metabolism during seed development. Trends in Plant Science 2: 169-174

Chapter

10

Seed development and carbohydrates: general discussion

P.E. Wittich

Summary. In this chapter the different aspects of seed development in relation to carbohydrate transport are discussed. First, a résumé is given of the results on sink localizations in seeds by focusing on the activity of the sucrose degrading enzymes sucrose synthase and invertase, and the impact of the activity of these enzymes on carbohydrate transport is discussed. Second, the outcome of sink localization studies on developing maize and *Gasteria* seeds are reviewed in the scope of carbohydrate distribution. In the third part, correlations found between carbohydrate distribution and seed development will be projected into a model for angiosperm ovule and seed development. Also the development of the phytomelan layer in the seed coat of *Gasteria* will be put into this perspective.

SINKS DURING OVULE AND SEED DEVELOPMENT

The present study on sugar transport in ovules and seeds is based on a few hypotheses. The main hypothesis is that the two known sucrose degrading enzymes, sucrose synthase and invertase, can be used as indicators for the sink strength of cells and/or tissues. Every cell within a tissue of an ovule or seed can be seen as a unique unit. Every unit uses sucrose, which is transported to it via the neighbouring cells. Consequently, every cell is a sink with its own sink strength. Using immunocytochemistry and the activities of sucrose synthase and invertase to show their presence *in situ* gives a good impression of cells in which sucrose conversion occurs. Additionally, these techniques can be used during ovule and seed development to identify cells and tissues to which sucrose is transported. A prerequisite is that there is a good sucrose supply via the phloem towards the developing ovules and seeds, which seems to be the case under the optimal plant growth conditions used in this study. Secondly, it is hypothesized that transport of sucrose through the ovular tissues (after unloading from the phloem) is primarily by diffusion. Pressure driven flow is considered to be a less predominant factor in the sugar transport since in the cases studied here the developing ovules and seeds grow in a humid atmosphere, protected by carpels and leaves. Hence, they will not loose much water to evaporation. It is thought that within tissues the main transport route is symplastic, and therefore plasmodesmata may have a regulating function in solute transport. However, in this thesis this aspect is not considered to be limiting for carbohydrate transport.

Also the membrane passage of carbohydrates into and out of the apoplast between sporophytically and gametophytically derived tissues are considered not to be limiting steps for seed development under the optimal plant culturing conditions.

Sucrose synthase as indicator for sink strength:

Sucrose synthase catalyses the reaction: sucrose + UDP $\rightleftharpoons$ UDP-glucose + fructose. In maize and *Gasteria* the cytoplasmic sucrose synthase was found to function at three different levels: (1) The enzyme was found to function in cell and tissue growth in both carpels of maize (Chapter 2 and 3), and nucellus, integuments, endosperm and arillus of *Gasteria* (Chapter 4 and 5). (2) Cytoplasmic sucrose synthase activity was found to be correlated with cell maintenance in maize (Chapter 2 and 3) and *Gasteria* (Chapter 4 and 5). (3) Enzyme activity was shown to be related with the synthesis of storage products; that is starch synthesis in the maize endosperm (Chapter 2 and 3), protein synthesis in the endosperm of *Gasteria* (Chapter 5) and aleurone layer of maize (Chapter 2 and 3), and callose synthesis in the outer integument of *Gasteria* before the moment of phytomelan synthesis (Chapter 6). The membrane-associated form of sucrose synthase was only detected by immunocytochemistry, and was correlated with cell wall synthesis.

The conversion and utilization of sucrose can generate transport of sucrose to the cells with sucrose synthase activity, since breakdown of sucrose will create a sucrose gradient. The enzyme activity assay can indicate the preferential direction of the sucrose transport *in vivo*, because the *in situ* localization of sucrose synthase activity can be used to distinguish cells in ovules and seeds with different sink strengths.

From the data on the localization of cytoplasmic sucrose synthase in developing seeds of *Gasteria* (Chapter 5) it is concluded that sucrose synthase activity is correlated with the developmental sequence of the seed tissues; first there is a high activity localized in the growing arillus and integuments, then in the seed coat during the formation of the phytomelan layer, followed by a localization of high activity correlated with the development of the embryo and endosperm, and finally high sucrose synthase activity only in the storage product synthesizing endosperm. Deducing from these experiments in which sucrose synthase activity was used as an indicator for sink strength, it seems that the *Gasteria* plant possesses a dynamic carbohydrate distribution network for the successive steps in seed development. Also maize seed development seems to follow a comparable pattern of sucrose distribution. After fertilization sucrose synthase activity was found in the carpels, integuments and nucellus. But during the following days this activity diminished and the developing endosperm started to absorb most of the imported sucrose. The embryo started growing faster after the endosperm began to accumulate carbohydrates in the form of starch in its apical cells.

Invertase as indicator for sink strength:

The second indicator for sink strength is the activity of the enzyme invertase, which catalyses the reaction: sucrose ⟶ glucose + fructose.

In this study it is suggested that soluble (cytoplasmic/vacuolar) invertase is involved in the synthesis of storage products due to a correlation between invertase activity and the synthesis of lipids in *Gasteria* seeds (Chapter 5), and between invertase activity and the glucose accumulation in *Gasteria* ovules around the time of fertilization (Chapter 4 and 5). The activity of these soluble invertases is in its function comparable to the cytoplasmic sucrose synthase. Immunolabelling on maize kernels showed the presence of an invertase protein in the aleurone layer, but enzyme histochemistry techniques detected no invertase activity in this layer that stores mainly proteins. This invertase might become activated during imbibition or the activity could not be detected by the assay (Chapter 3).

Invertase is also found predominantly in the apoplast of tissues bordering a symplastic barrier (cell wall bound invertase): in the basal maize endosperm and pedicel (Chapter 3), and in the nucellus around the endosperm of *Gasteria* (Chapter 5). The transport of carbohydrates to the pedicel and nucellar tissues is symplastic, but here the carbohydrates are unloaded into the

apoplast. This unloading may be by facilitated diffusion via a transport protein, as is suggested for wheat nucellar unloading (Wang and Fisher 1995) and maize pedicel unloading (Shannon *et al.* 1986). Apoplastic, cell wall bound invertase activity creates a sucrose gradient in the apoplast by converting the sucrose into glucose and fructose, thus enhancing the unloading from the symplast into the apoplast, and consequently the symplastic diffusion of sucrose to those sucrose unloading cells. The breakdown products are transported through the apoplast by diffusion, and transported into the symplast of the embryo sac, embryo, or endosperm. In maize this import is likely to be a diffusion process in the case of glucose and fructose transport, while sucrose is imported actively (Griffith *et al.* 1987). In the symplast resynthesis of sucrose may take place, a conversion that will enhance symplastic monosaccharide import. Sucrose can be transported further via a new diffusion gradient to cells where it is being utilized (Figure 1).

The results in this study from maize seed development (Chapter 3) show that the cell wall bound invertase is active in the basal endosperm relatively far from the symplastic barrier between endosperm transfer cells and sporophytic tissue. This presence of invertase activity suggests that there is apoplastic sucrose transport far into the endosperm without hydrolyzation, and it may also imply that not much sucrose can escape the hydrolyzing activity of the invertase in the basal endosperm. This can also be interpreted that sucrose will not be imported into the symplast of the endosperm cells, but that sucrose has to be hydrolyzed first. Disaccharide transporters may not be active or may even be absent in these maize endosperm cells. For maize embryos it is shown that the uptake of monosaccharides from the apoplast into the symplast of the embryo occurs faster compared to the uptake of sucrose (Griffith *et al.* 1987, Humphreys 1978).

The apoplastic, cell wall bound invertase activity between sporophyte and gametophyte derived organisms seems to function as a driving force that works together in a series of similar driving forces (sucrose synthesizing and degrading enzymes, symporters and antiporters) to supply the symplastically isolated tissues (endosperm and embryo) with sufficient carbohydrates by creating diffusion gradients (Fig.1). However, not all plants show invertase activity between the apoplast of sporophytic tissue and gametophytically derived tissues to enhance carbohydrate transport. In legumes for instance, sucrose is not hydrolyzed prior to uptake into the cotyledons (Thorne 1985), but in these cases sucrose transport is enhanced by energy mediated sucrose symporters (Harrington *et al.* 1997).

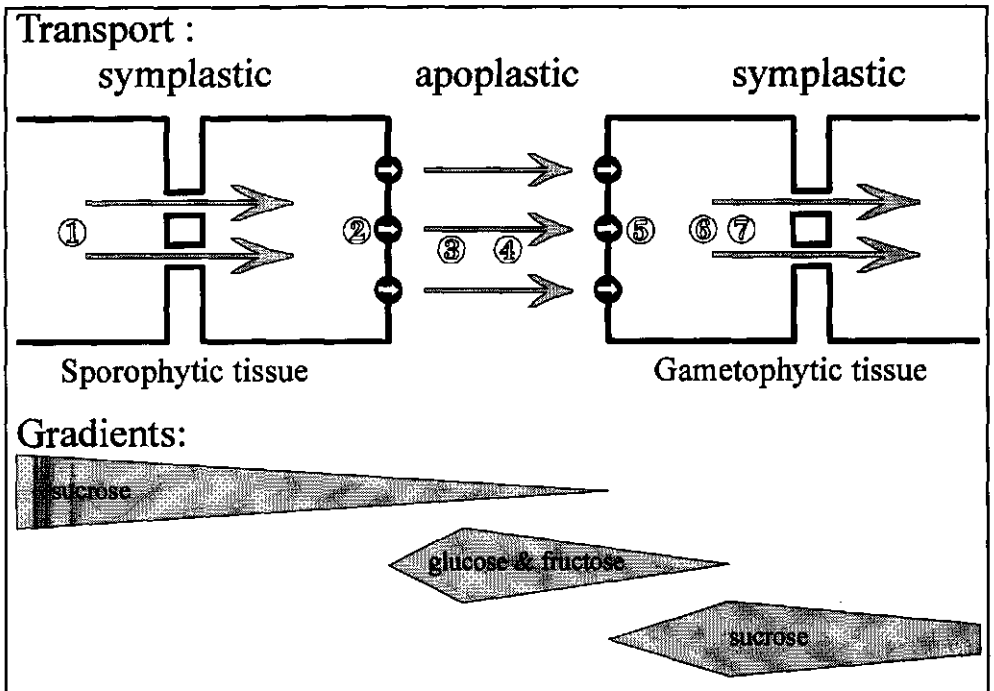

Figure 1: Carbohydrate gradients function as driving forces

Sucrose is transported symplastically through the sporophytic tissue (1) and via facilitated diffusion through the membrane (2) into the apoplast between sporophytic tissue and gametophytic derived tissue (3). In this apoplast sucrose is hydrolyzed by invertase (4) into glucose and fructose, resulting in a low sucrose concentration and high glucose and fructose concentrations. The monosaccharides will be transported into the gametophytic derived tissues (embryo sac, embryo or endosperm) via membrane transport (5), after which resynthesis of sucrose takes place by the activity of sucrose phosphate synthase (SPS) and other enzymes (6), resulting in a low monosaccharide concentration and a high sucrose gradient. Sucrose will diffuse further symplastically (7) via a gradient which is created by the utilization of sucrose in remote cells. The activity of invertase, SPS, and enzymes involved in the sucrose utilization enhance respectively a sucrose, glucose and fructose, and again a sucrose gradient, and thus the diffusive transport of these carbohydrates, *viz.*,. the enzymes function as driving forces for diffusive carbohydrate transport.

seems plausible that there is enhanced nutrient uptake by the chalazal chamber of helobial endosperm. These nutrients will be transported symplastically to the micropylar endosperm cells.

In maize the integuments do not form a seed coat but degenerate during endosperm development. Only the carpel grows further to envelope the expanding nucellus and endosperm. Initially the endosperm grows at the cost of the nucellus. A function of these extra layers of nucellus (the crassinucellate type) may be sought in the predetermination of seed shape. The nucellus already expands the ovule, after which the endosperm replaces the nucellus. Thus, the first stage of seed development in which carbohydrates are invested into the sporophytic tissue is followed now by the second stage, *i.e.* increased growth of the endosperm. The endosperm is cellular from the beginning, and may determine the final size of the seed. After complete degeneration of the nucellus the supply of nutrients to the endosperm only seems to take place via the apoplast at the basal part of the kernel (chalazal part), since many specialized transfer cells are found here. The developing seed transports the bulk of imported sucrose first to the tissues which are the most remote from the importing basal endosperm cells, where storage takes place in the form of starch (third developmental stage). This use of enhanced diffusion gradients seems an economical means of carbohydrate transport for growth and storage, since in this case of maize seed development the import of nutrients takes place at only the basal side of the tissue.

The symplastically isolated embryo in both *Gasteria* and maize starts to develop faster during the third stage of seed development when the seed coat is formed and the endosperm starts to synthesize storage products. Advanced development of the endosperm seems to be a prerequisite for starting embryo development. Before that time, the endosperm was probably a stronger sink than the embryo, and prior to this endosperm development the seed coat was the strongest sink. In the case of *Gasteria*, a strong sink capacity of the seed coat may prevent development of the endosperm during the first stage of seed development, by not passing enough nutrients into the connecting apoplast. After complete cellularization of the endosperm, both, embryo and endosperm, seem to be strong sinks, capable to obtain enough nutrients for their growth and storage.

PERSPECTIVES

Aspects of seed development

Seed, and diaspores are units of dispersal. The state of embryo/endosperm development in mature seeds can be correlated with the seed germination, the structure of the seed coat with protection, and the shape of the seed or position of the seed in the fruit carpel with the

mechanism of dispersal. Irrespective of the state of development of embryo, endosperm, and seed coat at the time of dispersal, the embryo must undergo further development into a seedling and eventually produce its own offspring. A pattern in (angiosperm) seed development can be deduced using the results described in this thesis for maize and *Gasteria*, and the development of seeds of other plants (Boesewinkel and Bouman 1984, Borisjuk *et al.* 1995, Jacobsen 1984, Johri *et al.* 1992). The sequence of investing carbohydrates (energy) in ovule development, followed by seed coat development, endosperm development, embryo development, and synthesis of storage products, prior to desiccation and dispersal, can be distinguished in many types of seed development. This results in a model of carbohydrate investment during angiosperm seed development as presented in Figure 3.

In this model different moments of dispersal are correlated with carbohydrate investment. It shows that the differentiation of sporophytic tissue, endosperm, and embryo, is related with the moment that the plant finishes investing carbohydrates into the developing seed. This model of carbohydrate investment is supported by some general features of angiosperm seed development: Boesewinkel and Bouman (1984) state that when the endosperm or perisperm is scanty or absent in mature seeds, only the embryo contains storage products. After fertilization these ex-endospermous seeds show growth of the ovule, followed by growth of the endosperm and then the embryo. During its growth the embryo consumes the endosperm completely. Also in endospermous seeds the endosperm grows ahead of the embryo, but the endosperm is not completely consumed by the developing embryo prior to germination. Failure of endosperm development results in this case in abortion or defective seeds (Boesewinkel and Bouman 1984). In the case of plants with an incompletely developed embryo in the seed, the embryo develops further only after hydration (Jacobsen 1984).

In Figure 4 the carbohydrate distribution model for seeds is applied to the development of broad bean seeds (embryo with storage, exendospermous), maize and *Gasteria* seeds (endospermous), and orchid seeds (almost no embryo and endosperm development). It will be interesting to study the distribution of sucrose and other carbohydrates in the differentiating seed tissues of other plants to ascertain if the investment of carbohydrates into the developing seed follows the general pattern. The model also gives a perspective on the energy needed after imbibition to develop a seedling, correlated to the developmental stage of a mature seed (investment in embryo and endosperm development), as well as on the external conditions needed for further seedling development after dispersal.

This sequence of carbohydrate distribution during seed development in angiosperms may apply also to seed development of gymnosperms and prespermaphytes. These groups of plants show different moments of fertilization compared to the angiosperm, and after fertilization they all lack a resting phase in the embryo development (Favre-Duchartre 1984). Most

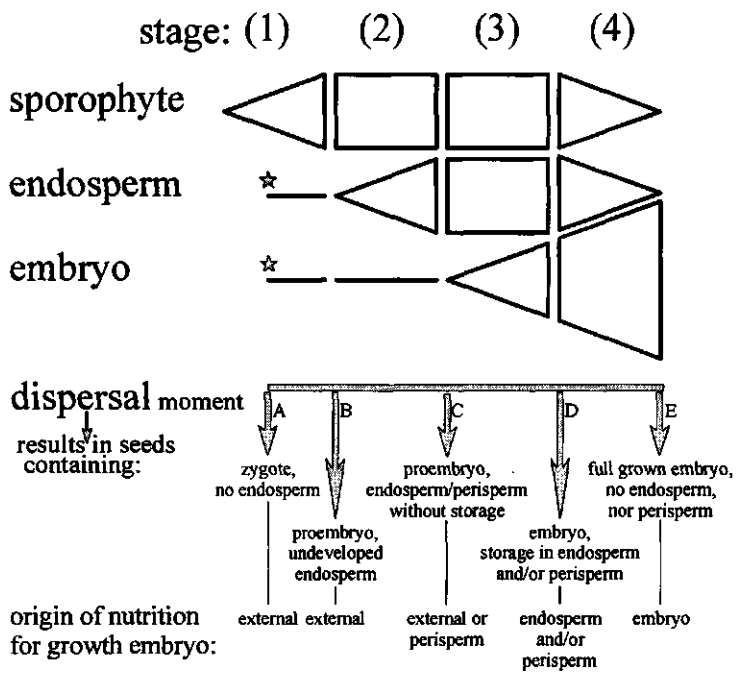

LEGENDS

Carbohydrate investment in tissue growth.

Possible carbohydrate investment in tissue differentiation or cell maintenance.

Tissue degeneration and possible carbohydrate investment in non degenerating parts (maintenance, storage).

No strong tissue growth.

☆ Fertilization.

Figure 3: Model for carbohydrate distribution during seed development after double fertilization.

Figure 3

During *stage 1* the sporophytic tissue develops and the embryo sac is formed. Almost all carbohydrates are invested in the growth of the sporophyte, growth mainly by cell divisions and a little in the developing gametophyte. After double fertilization (of egg cell and central cell) the zygote and endosperm stay in a relatively dormant stage and the sporophytic tissue consumes most carbohydrates. The developing sporophytic tissue determines the seed volume, forms the seed coat, and in some cases it stores nutrients for vector transport.

In *stage 2* carbohydrates are invested into the endosperm which starts to grow either coenocytic or by cellularization. The sporophytic tissue needs carbohydrates for further differentiation and might become partly degenerated by the enlarging endosperm. The zygote remains in a dormant stage.

In *stage 3* the volume of the endosperm is maximal and the zygote starts to develop into an embryo. Carbohydrates for embryo growth may partly come from the endosperm, but also from the sporophytic tissue. In the endosperm carbohydrates are used for differentiation (mainly storage product synthesis) but this may also occur in the perisperm. The sporophytic tissue is completed, and may degenerate or persists. In the latter case only some carbohydrates are used for cell maintenance.

In *stage 4* sporophytic tissue and endosperm will largely degenerate, while carbohydrates from these tissues will be used for further development of the embryo. Exceptions of sporophytic (starch) degeneration might be found in plant species with edible parts for the distributor, like in a sacrotesta of Magnolia seeds and some elaisomes of ant-distributed seeds (F. Bouman, personal communication). At the end of stage 4 the embryo is a complete seedling with well developed root, shoot and leaves, and has enough storage products. It might only require water to germinate.

During the development according this model, various moments can be found where plants stop to invest carbohydrates into their seeds. These seeds are described as "mature", but do not contain an embryo that can grow out as a seedling without carbon supplies from storage within the seed (endosperm or sporophytic tissue), or from external sources. Examples of different moments of dispersal are indicated in the figure by A till E, but also other intermediate moments are likely to exist.

At dispersal moment A (during *stage 1*) only fertilization and some sporophytic tissue development took place. The zygote has to develop further into a complete seedling by using external carbohydrates since there is no sufficient carbohydrate storage. At dispersal moment B (end of *stage 1*) the embryo has developed into a proembryo and still needs external carbohydrates since there is no sufficient carbohydrate storage in the sporophytic tissue to develop into a complete seedling.

At dispersal moment C (end of *stage 2*) endosperm has developed but does not contain carbohydrate storage products for the incomplete embryo to grow. Storage products might be present in the perisperm for embryo development after dispersal, otherwise the embryo is dependent on external carbohydrates to develop into a seedling.

At dispersal moment D (end of *stage 3*) the endosperm and/or the sporophyte have stored carbohydrates for further embryo development after dispersal into a seedling.

At dispersal moment E (end of *stage 4*) the embryo is fully developed and after dispersal it needs only water to develop into a seedling. There is no storage anymore in sporophytic tissue, nor in the endosperm, but only in the embryo itself.

advanced gymnosperms have a small female gametophyte at the moment of (usually single) fertilization. During embryogenesis further development of the haploid endosperm takes place, however, more rapidly than embryo development. In primitive gymnosperms the endosperm growth take place before fertilization, but storage of nutrients in the endosperm is initiated when embryogenesis begins. In prespermaphytes the (primary) endosperm development, including the storage phase, is before fertilization (Favre-Duchartre 1984). Following the angiosperm carbohydrate distribution model, fertilization in prespermaphytes occurs relatively late during their endosperm development, and is immediately followed by carbohydrate investment in the embryo.

Figure 4

(1) After fertilization, plants like broad bean continue developing their seed coat *(stage 1)* before they start expanding the endosperm *(stage 2)*. The embryo increases its growth after the endosperm *(stage 3)* and grows partly at the cost of the latter (Borisjuk *et al.* 1995). This results in a complete seedling *(stage 4)* filled with storage products, which only needs water to germinate after dispersal. During endosperm and embryo growth the seed coat persists, having a function in transport of nutrients to the endosperm and embryo. Probably the only energy invested in this tissue is for cell maintenance.

(2) Maize seed development starts with carpel, integument and nucellus development. After fertilization the nucellus continues expanding while integuments and carpel cytoplasm degenerates *(stage 1)*. Embryo development increases as the endosperm starts storing starch and proteins *(stage 3)*. This embryo development is at the cost of the endosperm (Chapter 2 and 3). At dispersal *(during stage 4)* the embryo is fully developed but lacks enough carbohydrates to grow out as a seedling. The nutrients stored in the endosperm will become the source for further embryo development.

(3) After double fertilization in *Gasteria* the plants directs its carbohydrate sources to develop the arillus and phytomelan layer. During this stage the endosperm nuclei divide, but the endosperm stays coenocytic *(stage 1)*. After finishing the seed coat most carbohydrates are used for cellularization of the endosperm *(stage 2)*. During the storage phase of the endosperm *(stage 3)* the embryo increases its growth, partly at the cost of the endosperm. During this stage, degeneration of the seed coat cytoplasm and most of the nucellus takes place. At dispersal *(during stage 4)* the embryo has to continue its growth to become a complete seedling. Storage lipids and proteins in the embryo itself and from the endosperm supply the required energy.

(4) Orchids only develop their sporophytic ovular tissue often after pollination, but mostly only until fertilization *(stage 1)*. After single or double fertilization the endosperm does not develop further than a coenocytic stage and is ruminate *(stage 2)*. In many species the embryo remains undifferentiated (Johri *et al.* 1992). Having only the seed coat and sometimes perispermous storage products, the embryo has to develop into a seedling *(stage 3 and 4)* with the supply of external nutrients. Some orchids use carbohydrates which are set free by saprophytic fungi (Natesh and Rau 1984).

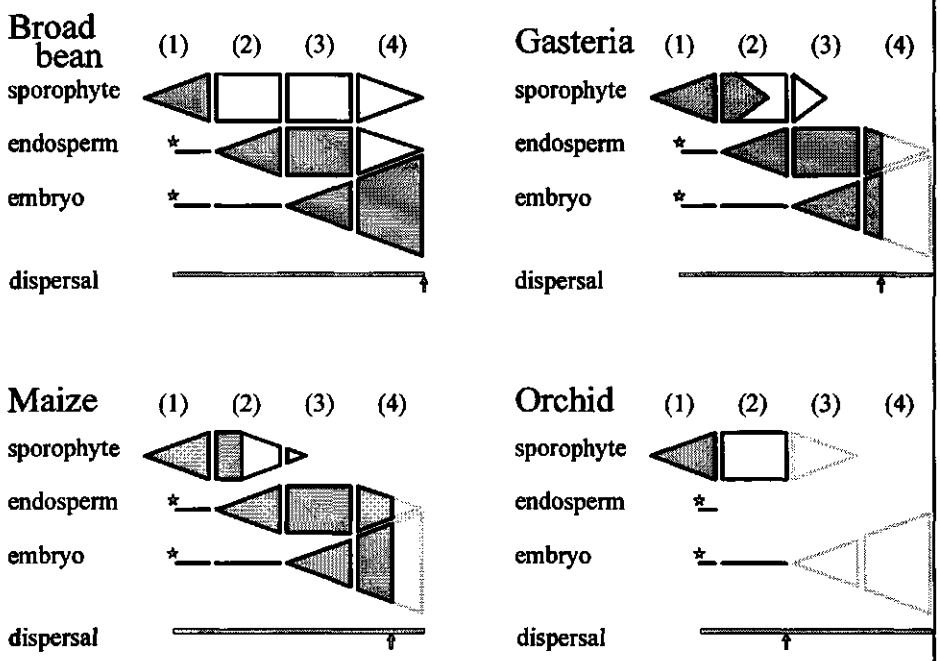

LEGENDS

High carbohydrate investment by the plant, mainly for growth and storage.

Low carbohydrate investment, mainly for maintenance.

Further tissue development after dispersal.

Tissue growth.

Tissue differentiation and maintenance.

Tissue degeneration.

No abundant tissue growth.

Fertilization.

Moment of dispersal.

Figure 4: Examples of carbohydrate distribution during seed development.

Phytomelan development

One of the main distribution sites of sucrose during seed development in *Gasteria* is the outer epidermis of the outer integument were phytomelan is synthesized. During the development of the phytomelan layer in these integumental cells the main stream of sucrose seems to go specifically to this cell layer. Once the phytomelan layer is almost completed, the endosperm cellularizes and starts to receive most of the imported sucrose.

The development of the phytomelan can be divided into three phases (Chapter 6 and 7). During the first stage a block of callose is deposited between plasma membrane and outer tangential secondary wall. Callose is a polymer of glucose, synthesized from UDP-glucose by callose synthase at the plasma membrane. The UDP-glucose is supplied by the activity of sucrose synthase, the latter in cytoplasmic form or in a membrane-associated form (Amor *et al.* 1995), although neither the presence, nor the activity of the latter form could clearly be demonstrated in these cells by immunocytochemical and enzyme histochemical methods. These techniques did show an abundant presence and activity of the cytosolic sucrose synthase during callose synthesis, creating a declining sucrose gradient, and therefore sucrose transport towards these cells.

During the second stage the callose block is broken down, probably into glucose monomers and polymers, while in the third stage phytomelan is synthesized in the by the callose created lumen. Thus, the block of callose seems to function as mould for the phytomelan, determining the size of the phytomelan block. It has never been considered before that callose can function in determining the shape and size of a wall. The closest related function known of callose seems to be around the developing pollen grains, when the exine is formed. During exine development a function of the callose is considered to be a mould for the basal exine pattern (Willemse 1971). The function of callose as temporary storage of carbohydrates is mentioned by other authors to be around the tetrad cells during micro and megasporogenesis (Keijzer and Willemse 1988). However, in these and other studies only the synthesis and disappearance of callose was demonstrated, while it was only assumed that its breakdown products were consumed by the developing cells. In the case of phytomelan synthesis there is a stronger indication that the callose breakdown products from the mould, being glucose or glucose polymers, are used for the synthesis of phytomelan and/or the new cellulose layer between callose and plasma membrane. The electron microscopy results show the dissolving callose and growing phytomelan globules in the lumen with dissolved carbohydrates. Phytomelan synthesis can be distinguished at the border of these growing globules.

The presence of a relative large block of callose prior to phytomelan synthesis is interesting for further studies on callose synthesis and degradation. Most studies on this subject have been carried out on relatively small callose plugs or thin callose layers, like around plasmodesmata,

sieve plates, in cotton hairs, microspore tetrads, or pollen tubes (Stone and Clarke 1992, and references here in).

The presented ultrastructural and chemical study of the phytomelan could be very useful for plant taxonomy. Phytomelan is used as a general taxonomic character, but it is very likely that its chemical composition among the species, taxa or families is different. Also the pattern of deposition is probably different in these groups since drawings of the *Asparagus officinalis* seed coat made by Robbins and Borthwick (1925) show phytomelan blocks in cells, while drawings of *Muscari commosum* and *M. racemosum* by Wunderlich (1937) show a phytomelan layer covering the integumental cells like a cuticle. To obtain more knowledge about different forms of phytomelan, techniques as described in this study have to be applied to other phytomelan containing plants.

In the context of seed development and dispersal the mechanical-protective function of the phytomelan in the seed coat is worth studying. The phytomelan is also thought to be involved in chemical protection of the seed.

The study of phytomelan development gives new insights in the development of complex polymers. Remarkable is the synthesis in globular aggregates, not showing any gradient in the apoplastic space, while cell walls usually develop in layers. More knowledge on the synthesis pathway may be important for the chemical industry, in order to produce complex artificial polymers which may be useful because of a high temperature and chemical resistance (like phytomelan itself).

Concluding remarks

The carbohydrate distribution in the developing seeds follows a pattern. Carbohydrates are directed first to the developing seed coat, then to the endosperm, and finally to the embryo. The supply of carbohydrates might determine the final seed configuration.

ACKNOWLEDGEMENTS

I would like to thank J van Dongen, F Bouman, CJ Keijzer, AAM van Lammeren and MTM Willemse for their discussions, DY Foreman for revising the English style of the manuscript, and AB Haasdijk for the drawing.

REFERENCES

Amor Y, CH Haigler, S Johnson, M Wainscott and DP Delmer (1995) A membrane-associated from sucrose synthase and its potential role in synthesis of cellulose and callose in plants. Proc Natl Acad Sci USA 92: 9353-9357

Boesewinkel and Bouman (1984) The seed: structure. In: Embryology of angiosperms. BM Johri (ed), Springer-Verlag, Berlin: 567-610

Borisjuk L, H Weber, R Panitz, R Manteuffel and U Wobus (1995) Embryogenesis of *Vicia faba* L.: histodifferentiation in relation to starch and storage protein synthesis. J Plant Physiol 147: 203-218

Favre-Duchartre M (1984) Homologies and phylogenie. In: Embryology of angiosperms. BM Johri (ed), Springer-Verlag, Berlin: 697-734

Griffith SM, RJ Jones and ML Brenner (1987) In vitro sugar transport in Zea mays L. kernels. II. Characteristics of sugar absorption and metabolism by isolated developing embryos. Plant Physiol 84: 472-475

Harrington GN, VR Franceschi, CE Offler, JW Patrick, M Tegeder, WB Frommer, JF Harper and WD Hitz (1997) Cell specific expression of three genes involved in plasma membrane sucrose transport in developing *Vicia faba* seed. Protoplasma 197: 160-173

Humphreys T (1978) A model for sucrose transport in the maize scutellum. Phytochem. 17: 679-684

Jacobsen JV (1984) The seed: Germination. In: Embryology of angiosperms. BM Johri (ed), Springer-Verlag, Berlin: 611-646

Johri BM, KB Ambegaokar and PS Srivastava (1992) Comparative embryology of angiosperms. Springer-Verlag, Berlin

Keijzer CJ and Willemse MTM (1988) Tissue interactions in the developing locule of *Gasteria verrucosa* during microsporogenesis. Acta Bot. Neerl. 37: 493-508

Natesh S and MA Rau (1984) The embryo. In: Embryology of angiosperms. BM Johri (ed), Springer-Verlag, Berlin: 377-443

Pate JS and BES Gunning (1972) Transfer cells. Ann Rev Plant Physiol 23: 173-196

Robbins WW and Borthwick HA (1925) Development of the seed of *Asparagus officinalis*. Bot. Gaz. 80: 426-438

Shannon JC, GA Porter and DP Knievel (1986) Phloem unloading and transfer of sugars into developing corn endosperm. In: Cronshaw J, WJ Lucas and RT Giaquinta (eds) Plant biology. vol 1: Phloem Transport. Alan RR. Liss, New York: 265-277

Stone BA and AE Clarke (1992) The biology of (1,3)-β-glucans. La Trobe University Press, La Trobe

Thorne JH (1985) Phloem unloading of C and N assimilates in developing seeds. Ann Rev Plant Physiol 36: 317-343

Wang and Fisher (1995) Sucrose release into the endosperm cavity of wheat grains apparently occurs by facilitated diffusion across the nucellar cell membranes. Plant Physiol 109: 579-585

Willemse MTM (1971) Morphological and quantitative changes in the population of cell organelles during microsporogenesis of *Pinus sylvestris* L. III. Morphological changes during the tetrad stage and in the young microspore. A quantitative approach to the changes in the population of cell organelles. Acta Bot. Neerl. 20: 498-523

Wunderlich R (1937) Zur vergleichenden Embryologie der Liliaceae - Scilloideae. Flora 132: 48-90

SUMMARY

Seeds assure the plant the onset of a next generation and a way of dispersal. They consist of endosperm and an embryo (originating from gametophytic tissue), enveloped by a seed coat (sporophytic tissue). Plants generate different types of seeds. For instance, the endosperm may either be consumed by the embryo during seed development or retained for use by the embryo during germination. Differences in timing of endosperm digestion can be illustrated with broad bean (*Vicia faba*) and *Gasteria verrucosa*. Broad bean forms seeds in which the endosperm has been consumed by the fully developed embryo, while the embryo of *Gasteria* is less developed and surrounded by a large amount of endosperm for use during germination.

An important factor in seed development is the distribution, storage, and utilization of carbohydrates, since carbohydrates are a major source of energy for cell growth. In this thesis the carbohydrate distribution is studied in developing ovules and seeds of maize (*Zea mays*) and *Gasteria*, by identifying the cells and tissues in which sucrose is degraded. Sucrose is the main carbohydrate supplied by these plants in the developing seeds. The sucrose degrading activity of the enzymes sucrose synthase and invertase indicates the destination of the sucrose transport (Chapters 9 and 10). Immunocytochemical and histochemical techniques are used for the localization of these enzymes *in situ*.

The results obtained in this study on maize (Chapter 2 and 3) and *Gasteria* seed development (Chapters 4 and 5) show a general pattern of carbohydrate transport. First, the greatest amount of carbohydrates is applied for the development of the seed coat and nucellus (sporophytic tissues). An example of such a carbohydrate consuming process is the deposition of phytomelan in the seed coat of *Gasteria*. Phytomelan is a black cell wall component and chemically very inert. Histochemical and electron microscopy observations (Chapters 6 and 7) show that callose forms a mould for the deposition of phytomelan. The breakdown products of callose (glucose monomers and polymers) seem to be used for the synthesis of the phytomelan. Chemical analysis reveals that phytomelan is a complex polyphenolic polymer, and not a melanin (Chapter 8). Second, carbohydrate transport to the sporophytic tissues is followed by transport of most carbohydrates into the endosperm. These carbohydrates will be used for endosperm growth and for storage. Finally the main carbohydrate flow will go to the embryo. The pattern of carbohydrate usage observed in maize and *Gasteria* was used to generate a general model for angiosperm seed development (Chapter 10). The model explains differences between seeds by relating carbohydrate distribution during seed development to the timing of seed dispersal.

SAMENVATTING

Zaden verzekeren de plant van het begin van een nieuwe generatie en een manier van verspreiding. Ze bestaan uit endosperm en embryo (afkomstig van gametofytisch weefsel), omhuld door een zaadhuid (sporofytisch weefsel). Planten ontwikkelen verschillende typen zaden. Het endosperm kan bijvoorbeeld verbruikt worden door het embryo gedurende de zaad ontwikkeling, of het wordt bewaard voor het embryo tijdens de kieming. Verschillen in het moment van endospermafbraak kan aan de hand van tuinboon (*Vicia faba*) en *Gasteria verrucosa* worden geïllustreerd. Tuinboon vormt zaden waarbij het endosperm is verbruikt door het volledig ontwikkelde embryo. Het *Gasteria* embryo daarentegen is minder ontwikkeld en ingebed in een grote hoeveelheid endosperm dat bij de kieming gebruikt wordt.
Een belangrijke factor in zaadontwikkeling is de distributie, opslag en het gebruik van koolhydraten, want koolhydraten zijn een belangrijke energiebron voor celgroei. In dit proefschrift is de koolhydraatdistributie bestudeerd in ontwikkelende zaadbeginsels en zaden van maïs (*Zea mays*) en *Gasteria* door cellen en weefsels te identificeren waar sucrose wordt afgebroken. Sucrose is het voornaamste koolhydraat dat door deze planten wordt geleverd aan ontwikkelende zaden. De sucrose-afbrekende activiteit van de enzymen sucrose synthase en invertase geeft de bestemming van het sucrosetransport aan (Hoofdstuk 9 en 10). Immuno-cytochemische en histochemische technieken zijn gebruikt voor de enzymlocalizatie *in situ*.
De in deze studie verkregen resultaten m.b.t. maïs (Hoofdstuk 2 en 3) en *Gasteria* zaad ontwikkeling (Hoofstuk 4 en 5) geven een algemeen patroon van koolhydraattransport. Eerst wordt de grootste hoeveelheid koolhydraten gebruikt voor de ontwikkeling van de zaadhuid en nucellus (sporofytische weefsels). Een voorbeeld van een dergelijk koolhydraatverbruikend proces is de afzetting van phytomelan in de zaadhuid van *Gasteria*. Phytomelan is een zwarte celwandcomponent en chemisch zeer inert. Histochemische en elektronenmicroscopische waarnemingen (Hoofdstuk 6 en 7) laten zien dat callose een mal vormt voor de afzeting van phytomelan. De afbraakproducten van callose (glucose monomeren en polymeren) lijken te worden gebruikt voor de synthese van het phytomelan. Uit chemische analyse blijkt dat phytomelan een complex polyfenolisch polymeer is, en niet een melanine (Hoofdstuk 8). Na het koolhydraat transport ten behoeve van het sporofytisch weefsel vindt aansluitend transport van de meeste koolhydraten naar het endosperm plaats. Deze koolhydraten zullen worden gebruikt voor endospermgroei en opslag. Tenslotte gaat de voornaamste koolhydraat-stroom naar het embryo. Het patroon van koolhydraatgebruik, zoals gevonden in maïs en *Gasteria*, is aangewend om een model te genereren voor zaadontwikkeling in angiospermen (Hoofdstuk 10). Het model verklaart verschillen tussen zaden door een verband te leggen tussen koolhydraatdistributie tijdens zaadontwikkeling en het moment van zaadverspreiding.

NAWOORD

Nu ik aan het eind gekomen ben van het schrijven van dit proefschrift wil ik enkele mensen noemen die ik dankbaar ben voor hun steun en bijdragen aan dit proefschrift.
Als eerste wil ik mijn promotor en direkte begeleider in dit onderzoek bedanken, Michiel Willemse. Hij gaf me de tijd om te groeien in het onderzoek en de ruimte om het project in de richting te sturen die mij het best leek. Van Michiel en de co-promotoren Koos Keijzer en André van Lammeren heb ik de vele facetten van het wetenschappelijk onderzoek geleerd. De waardevolle discussies met bovengenoemde personen hebben dit proefschift zijn uiteindelijke vorm gegeven.
De inbreng van Dick Vreugdenhil was onontbeerlijk voor de ontwikkeling van de histochemische detectie methode van sucrose synthase activiteit. Een gezamelijk artikel was het gevolg. Via Dick is Joost van Dongen tijdens zijn afstudeerproject komen werken aan de verbetering en verdere toepassing van de enzym assay.
Met mijn goede vriend, Peter Graven, had ik een zeer bijzondere samenwerking. Discussiëren over het werk in De Vlaamsche Reus is eigenlijk "not done", maar die ene avond dat we dat toch deden heeft uiteindelijk wel geleid tot drie hoofdstukken over phytomelan!
Een deel van de tekst is door Daphne Foreman gecontroleerd op het gebruik van de Engelse taal. Ik hoop dat ze straks ook mijn Nederlandse teksten zal kunnen en willen nakijken.
Het digitaal-fotografische onderdeel van dit proefschrift is uitgevoerd door Sijbout Massalt. Heel wat uurtjes hebben we achter zijn computer zitten werken aan de fotoplaten. De zeer geslaagde tekeningen in de verschillende hoofdstukken zijn het creatieve werk van Allex Haasdijk en Paul van Snippenburg.
Zonder planten zou ik geen onderzoek hebben kunnen uitvoeren. Gerrit van Geerenstein en Leen Peterse zijn de personen die met hun goede zorg de *Gasteria* en maïs planten lieten groeien en bloeien, waarna ik vervolgens de bloemen en vruchten in plakjes kon snijden.
Alle collega's van de vakgroep hebben zo hun bijdrage in de totstandkoming van dit werk geleverd via discussies, experimenten, karweitjes, of de lunchpauzes in het Kopshuis. Ik zal ze niet allemaal bij naam gaan noemen, maar wel de drie promovendi die zo ongeveer gelijk met mij opwerkte: Folbert Bronsema, Marja Thijssen en Kees Straatman. Gezamelijk hebben we gewerkt voor onze belangen als Assistent In Opleiding (AIO) en daarnaast hebben we in onze vrije tijd veel gezellige uurtjes samen doorgebracht. Vijf jaar deel ik nu met Kees kamer 007, de zorg om onze planten, de vele stapels papier op onze tafels en de beslommeringen van de dag. Helaas komt daar nu wegens zijn vertrek snel een einde aan.
Peter Witte (ja u leest het goed) was voor dit proefschrift op een heel andere manier belangrijk. Het is namelijk een groot plezier om met hem te reizen, te ontspannen en van zijn kookkunsten te genieten.
Tenslotte wil ik de twee belangrijkste mensen in mijn leven noemen, mijn vader en moeder, Bert en Tineke Wittich. Hun steun en vertrouwen hebben mij gebracht tot dit moment, de voltooiing van dit proefschrift. Ik ben ze daarvoor heel erg dankbaar.

Peter.

CURRICULUM VITAE

Peter Egbertus Wittich was born on December 9, 1965 in Wageningen, The Netherlands. In 1985 he obtained his VWO-B certificate from the Christelijk Lyceum Veenendaal, and started the same year with the study Plant Breeding at the Wageningen Agricultural University. He did one thesis project at the Department of Phytopathology, and two at the Department of Plant Cytology and Morphology. Furthermore, he spent a practical training period at the Department of Botany of the University of Reading, England, which was funded by the European Erasmus-program. In September 1991 he graduated at the Wageningen Agricultural University.
In January 1992 he started with his Ph.D. research on the carbohydrate distribution in developing seeds at the Department of Plant Cytology and Morphology, Wageningen Agricultural University, of which the results are discussed in this thesis. This research was embedded in the Graduate School Experimental Plant Sciences. For two years he was the president of the student council of this graduate school.
In November 1996 he started with a three year project on the regulation of ovule and embryo development, at the Department of Plant Cytology and Morphology, Wageningen Agricultural University. This project is part of the European Plant Embryogenesis Network, a joined project of European laboratories and companies, financed by the European Community.

Peter Egbertus Wittich werd op 9 december 1965 geboren te Wageningen. In 1985 behaalde hij het diploma VWO-B aan het Christelijk Lyceum Veenendaal, en hij begon dat zelfde jaar de studie Plantenveredeling aan de Landbouwuniversiteit Wageningen. Hij deed één afstudeervak bij de vakgroep Fytopathologie, en twee bij de vakgroep Plantencytologie en -morfologie. Verder heeft hij een stage gevolgd bij de afdeling 'Botany' van de Universiteit van Reading, Engeland, dat door het Europese Erasmus-programma werd gefinancierd. In september 1991 studeerde hij af aan de Landbouwuniversiteit Wageningen.
In januari 1992 begon hij zijn promotieonderzoek naar de verdeling van koolhydraten in ontwikkelende zaden bij de vakgroep Plantencytologie en -morfologie van de Landbouw-universiteit Wageningen, waarvan de resultaten zijn besproken in dit proefschrift. Dit promotieonderzoek was onderdeel van de onderzoekschool Experimentele Plantenweten-schappen. Twee jaar was hij voorzitter van de AIO-raad van deze onderzoekschool.
In november 1996 begon hij met een driejarig onderzoek naar de regulatie van zaadbeginsel- en embryo-ontwikkeling bij de vakgroep Plantencytologie en -morfologie van de Landbouwuniversiteit Wageningen. Dit project is onderdeel van het Europese Plant Embryogenese Netwerk, een samenwerkingsverband van europese laboratoria en bedrijven, gefinancierd door de Europese Gemeenschap.

PUBLICATIONS

Papers

Wittich PE and P Graven (1995) Histochemical study of the development of the phytomelan layer in the seed coat of *Gasteria verrucosa* (Mill.) H. Duval. Protoplasma 187: 72-78

Colombo L, J Franken, AR van der Krol, PE Wittich, HJM Dons and GC Angenent (1997) Downregulation of ovule-specific MADS box genes from petunia results in maternally controlled defects in seed development. Plant Cell 9: 703-715.

Wittich PE and P Graven (1998). Callose deposition and breakdown, followed by phytomelan synthesis in the seed coat of *Gasteria verrucosa* (Mill.) H. Duval. Protoplasma 201: 221-230

Willemse MTM and PE Wittich.(1998) Pollination and fertilization in *Gasteria verrucosa* (Mill.) H. Duval: Interaction between pollen tube and ovary. In: Reproductive Biology '96 Conference Book. In press.

Wittich PE and D Vreugdenhil (1998). Localization of sucrose synthase activity in developing maize kernels by *in situ* enzyme histochemistry. J Exp Bot In press.

Colombo L, G Marziani, S Masierol, P Wittich, RB Schmidt, MS Gorla and M Pé (1998) *BRANCHED SILKLESS* mediates the transition from spikelet to floral meristem during *Zea mays* development. Plant Journal, submitted.

Dornelas MC, P Wittich, I von Recklinghausen, A van Lammeren and M Kreis (1998) Characterization of three novel members of the *Arabidopsis SHAGGY*-realted protein kinase (*ASK*) multigene family. Plant Journal, submitted.

Graven P, PE Wittich, F Bouman, G Nachtegaal and APM Kentgens (1998) Characterization of phytomelan in the seed coat of *Gasteria verrucosa* (Mill.) H. Duval. New Phytologist, To be submitted.

Wittich PE (1998) Carbohydrates in developing ovules and seeds of *Gasteria verrucosa* (Mill.) H. Duval: sucrose synthase and invertase localization and activity. In preparation.

Abstracts

Wittich PE and Graven P (1994) The origin of an exotestal phytomelan layer in the seed coat of *Gasteria verrucosa*. Poster presentation. Frontiers in sexual plant reproduction research. 13th International congress on sexual plant reproduction. Vienna, Austria, 10-14 July 1994: 136

Graven P and Wittich PE (1995) Macromolecular composition and development of phytomelan in seed coats. Oral presentation. 12. Symposium Morphologie, Anatomie und Systematik. Johannes Gutenberg Universität Mainz, 7-10 March 1995: 32

Graven P and PE Wittich (1995) Phytomelan, a chemical approach of an exotestal cell wall polymer. Poster presentation. 7th Cell wall meeting. Santiago de Compostela, Spain, 25-29 October 1995: 203

Wittich PE (1995) Histochemical localization of sucrose synthase and invertase activity in developing ovules. Poster presentation. International conference on the transport of photoassimilates. Canterbury, United Kingdom, 13-17 August 1995: 32

Wittich PE and P Graven (1995) The origin of phytomelan, a cell wall polymer in the seed coat of *Gasteria verrucosa*. Oral presentation. 7th Cell wall meeting. Santiago de Compostela, Spain, 25-29 October 1995: 202

Wittich PE and P Graven (1995) The origin of an exotestal phytomelan layer in the seed coat of *Gasteria verrucosa*. Poster presentation. Combined meeting of the Royal Dutch Botanical Society (KNBV) section for plant physiology and the SLW section for experimental plant science on 28 October 1994. Acta Bot Neerl 44: 286

Graven P and PE Wittich (1996) What is the cell wall polymer phytomelan? A chemical approach. Oral presentation. Meeting of the Royal Dutch Botanical Society (KNBV) section for plant morphology on 24 November 1995. Acta Bot Neerl 45: 413-414

Wittich PE (1996) Carbohydrate distribution in developing ovules. Poster presentation. 14th International congress of sexual plant reproduction. Lorne, Australia, 18-23 February 1996:134

Wittich PE and P Graven (1996) Histochemistry and ultrastructural development of phytomelan in the seed coat of *Gasteria verrucosa*. Oral presentation. Meeting of the Royal Dutch Botanical Society (KNBV) section for plant morphology on 24 November 1995 Acta Bot Neerl 45: 414

Wittich PE and MTM Willemse (1996) Carbohydrate distribution in developing ovules of *Gasteria* and maize. Poster presentation. Reproductive Biology 96, International conference. Royal Botanic Gardens, Kew, United Kingdom, 1-5 September 1996: 60

Colombo L, J Franken, S van de Krol, P Wittich, M van Lookeren Campagne and G Angenent (1997) Downregulation of ovule-specific MADS box genes from petunia results in maternally controlled defects in seed development. Poster presentation. 5th international congress of plant molecular biology. Singapore, 21-27 September 1997: 407

Colombo L, G Marziani, S Masiero, P Wittich, MS Gorla and ME Pé (1997) The transition from inflorescence to floral meristem in *Zea mays* is differentially controlled in the tassel and in the ear. Poster presentation. 5th international congress of plant molecular biology. Singapore, 21-27 September 1997: 406

Wittich PE (1997) Localization and function of sucrose synthase and invertase during maize kernel development. Oral presenttion. Meeting of the Royal Dutch Botanical Society (KNBV) section for plant morphology, anatomy and cytology, and section for fertilization research in plants on 27 September 1996. Acta Bot Neerl 46: 227-228